

MODELLING THE EFFECTS OF LOGGING
ON THE WATER BALANCE
OF A TROPICAL RAIN FOREST
A STUDY IN GUYANA

TROPENBOS SERIES 6

The Tropenbos series presents the results of studies and research activities related to the conservation and wise utilization of forest lands in the humid tropics. The series continues and integrates the former Tropenbos Scientific and Technical Series. The studies published in this series have been carried out within the international Tropenbos programme. Occasionally, this series may present the results of other studies which contribute to the objectives of the Tropenbos programme.

CIP-DATA KONINKLIJKE BIBLIOTHEEK, DEN HAAG

Jetten, Victor Gerlof

Modelling the effects of logging on the water balance of a tropical rain forest : a study in Guyana / Victor Gerlof Jetten. - Wageningen : The Tropenbos Foundation. - III. - (Tropenbos Series ; 6)

Thesis Universiteit Utrecht. - With ref. - With summary in Dutch.

ISBN 90-5113-018-X

Subject Headings: tropical rain forests ; Guyana / hydrology.

© Stichting Tropenbos

All rights reserved. No part of this publication, apart from bibliographic, brief quotations in critical reviews, may be reproduced, re-recorded or published in any form including photocopy, microform, electronic or electromagnetic record, without written permission.

Cover design: Diamond Communication.

Printed by: Veenman Drukkers, Wageningen.

Cover photo: The Essequibo river (photo by Victor Jetten).

MODELLING THE EFFECTS OF LOGGING
ON THE WATER BALANCE
OF A TROPICAL RAIN FOREST

A STUDY IN GUYANA

MODELLERING VAN DE EFFECTEN VAN HOUTKAP
OP DE WATERBALANS
VAN EEN TROPISCH REGENWOUD

EEN STUDIE IN GUYANA

(met een samenvatting in het Nederlands)

PROEFSCHRIFT

TER VERKRIJGING VAN DE GRAAD VAN DOCTOR
AAN DE UNIVERSITEIT UTRECHT, OP GEZAG VAN DE
RECTOR MAGNIFICUS PROF. DR. J.A. VAN GINKEL,
INGEVOLGE HET BESLUIT VAN HET COLLEGE VAN DEKANEN
IN HET OPENBAAR TE VERDEDIGEN OP
MAANDAG 13 JUNI 1994 DES MORGENS TE 10.30 UUR

DOOR

VICTOR GERLOF JETTEN

GEBOREN OP 10 JANUARI 1962 TE VEGHEL

Promotor: Prof. Dr. P.A. Burrough
Faculteit der Ruimtelijke wetenschappen, Universiteit Utrecht
Copromotor: Dr. H.Th. Riezebos
Faculteit der Ruimtelijke wetenschappen, Universiteit Utrecht



Universiteit Utrecht



The investigations reported in this thesis were carried out at the Tropenbos Programme Guyana, 12E Garnettstreet, Campbelville, Georgetown, Guyana and the Department of Physical Geography, Faculty of Geographical Sciences, Utrecht University, P.O.Box 80.115, 3508 TC Utrecht, The Netherlands.

*Green in nature is one thing, green in literature another.
Nature and letters seem to have a natural antipathy;
bring them together and they tear each other to pieces.
[...] Moreover, nature has a few tricks of her own.*

from: "Orlando" by Virginia Woolf

*I have heard a saying that Mabura is not the end of the world,
but that you can see it from there. I may add that this is not true,
the trees block your view! Ironically, and in a different sense,
you may see it when those same trees disappear.*

CONTENTS

LIST OF FIGURES	xi
LIST OF TABLES	xiii
ACKNOWLEDGEMENTS	xvi
1 INTRODUCTION	
1.1 The tropical rain forest	1
1.2 Use and management, the Tropebos Programme in Guyana	1
1.3 Research Aims	3
2 THE MABURA HILL RESEARCH AREA	
2.1 The research area	6
2.2 Geological history	8
2.3 Soils	10
2.4 Climate	14
3 USING SPATIAL ANALYSIS TO COMPARE PATTERNS IN RAIN FOREST WITH ECOLOGICAL GRADIENTS	
3.1 Introduction	22
3.2 Methodology	23
3.2.1 Study site	23
3.2.2 Soils and topography	24
3.2.3 Forest types	26
3.2.1 Theory of fuzzy k-means clustering (FKM)	26
3.2.3 Spatial analysis	28
3.3 Results and interpretation	28
3.3.1 Relation of TWINSPAN forest types with soils and drainage	28
3.3.2 Fuzzy clustering	31
3.3.3 Comparison of FKM forest types with soils and hydrology	34
3.3.4 Interpolation of DECORANA results	35
3.4 Discussion and conclusions	37
4 MODELLING THE ONE DIMENSIONAL WATER BALANCE	
4.1 The hydrological framework	39
4.2 The SOAP water balance model	41
4.3 The <i>Soil</i> subsystem	43
4.3.1 Principles of one dimensional flow	43
4.3.2 Numerical solution of the flow equation	44
4.3.3 Modelling the $k(h)$ and $\theta(h)$ relationships	46
4.3.4 Upper boundary conditions	47
4.3.5 Lower boundary conditions	48

4.4	The <i>Canopy</i> subsystem	48
4.4.1	Canopy structure	48
4.4.2	Interception and throughfall	50
4.4.3	Micro climate and transpiration	50
4.4.4	Root structure	53
4.4.4	Uptake from the root zone	55
5	SPATIAL VARIABILITY OF INFILTRATION AND RELATED SOIL PROPERTIES	
5.1	Introduction	57
5.2	Methodology	58
5.2.1	Spatial variability	58
5.2.2	Sample design	58
5.2.3	Data preparation	60
5.3	Results	61
5.3.1	Differences in infiltration between the soil types	61
5.3.2	Differences in spatial structure between soil types	63
5.4	Sources of variation: regression analysis or spatial structure	64
5.4.1	Laterite	65
5.4.2	White Sands	67
5.4.3	Brown Sands	67
5.4.4	The effect of the regression model on the spatial variance	68
5.5	Conclusions	69
6	INTERCEPTION AND THROUGHFALL: MODELLING THE CANOPY WATER BALANCE	
6.1	Introduction	70
6.2	Methodology	71
6.2.1	The RUTTER model	71
6.2.2	Experimental design	72
6.2.2	Calculation of model parameters	74
6.3	Results	75
6.3.1	Comparison of forest type interception	75
6.3.2	Derivation of model the parameters	76
6.3.3	Simulation with the RUTTER model	78
6.3.4	Sensitivity analysis	80
6.4	The CASCADE model	80
6.4.1	Evaporation and drainage in the layered canopy	81
6.4.2	Results	84
6.5	Discussion and conclusions	84
7	OVERLAND FLOW UNDER UNDISTURBED FOREST	
7.1	Introduction	86
7.2	Methodology	87
7.2.1	Throughflow theory	87
7.2.1	Overland flow theory	87
7.2.2	The experimental setup	88

7.3	Results	90
7.3.1	The field experiment	90
7.3.2	The flow tests: surface runoff as litter throughflow	93
7.3.3	The flow tests: surface runoff as overland flow	97
7.4	Discussion and conclusions	101
8	THE VERTICAL WATER BALANCE OF UNDISTURBED FOREST	
8.1	Introduction	103
8.2	Methodology	104
8.2.1	Field data	104
8.2.2	Microclimate in the canopy	105
8.2.3	Soil properties	105
8.3	Results	106
8.3.1	Microclimate	106
8.3.2	Mixed forest on Ferralic Arenosols (the gap experiments)	108
8.3.3	Mixed forest on Haplic Ferralsols (the runoff experiments)	111
8.4	Annual fluctuations of the water balance for three environments	113
8.5	Discussion	118
8.6	Conclusions	121
9	THE IMPACT OF LOGGING ON SOIL HYDROLOGICAL PROPERTIES	
9.1	Introduction	122
9.2	Impact of skidding on the topsoil	122
9.3	Methodology	124
9.4	Results	124
9.4.1	Texture and structure of undisturbed topsoil	124
9.4.2	Saturated hydraulic conductivity, porosity and bulk density	125
9.4.3	Water retention and hydraulic conductivity	128
9.5	Discussion and conclusions	131
10	THE VERTICAL WATER BALANCE OF A GAP	
10.1	Introduction	133
10.2	Methodology	134
10.2.1	The gap experiment	134
10.2.2	Microclimate on the gaps	135
10.2.3	Seedling cover	136
10.2.4	Simulations with SOAP	138
10.3	Results of the gap experiments	138
10.3.1	Microclimate	138
10.3.2	Skid trails	139
10.3.3	Crown zone	142
10.3.4	Undisturbed zone	145
10.3.5	Differences between gaps and zones	148
10.4	Annual fluctuations of the water balance for gaps on 3 soil types	149
10.5	Comparing gap and forest	153
10.6	Conclusions	156

11 THE IMPACT OF LOW INTENSITY LOGGING ON THE WATER BALANCE OF A SMALL CATCHMENT	
11.1 Introduction	157
11.2 Methodology	158
11.2.1 The experimental catchment, topography and soils	158
11.2.2 Hydrological measurements	161
11.2.3 The logging experiment	162
11.3 Results	163
11.3.1 Discharge	163
11.3.2 Groundwater fluctuations	167
11.3.3 Surface runoff	170
11.3.4 Annual water balance before and after logging	170
11.4 Comparison of low intensity logging with heavy disturbance in French Guyana	174
11.5 Discussion and conclusions	175
SUMMARY AND CONCLUSIONS	178
SAMENVATTING EN CONCLUSIES	184
REFERENCES	189
CURRICULUM VITAE	196

FIGURES

- 2.1 Tropenbos Ecological Reserve with infrastructure and locations of the main experiments in the water balance research (see text).
- 2.2 Main landscape types in Guyana.
- 2.3 Schematic representation of the landscape formation of the Tropenbos Ecological Reserve, which is situated on the boundary of the White Sands Plateau and the Pre-Cambrian Lowlands.
- 2.4 Digital soil map of Tropenbos Ecological Reserve, According to the FAO classification.
- 2.5 Monthly rainfall and potential evaporation in Mabura.
- 2.6 Annual rainfall distributed over 24 hours.
- 2.7 Mean, minimum and maximum daily course for each month in 1992 for a) incoming shortwave radiation (R_{in}) from 0.3 to 3 μm ; b) air temperature (temp) in $^{\circ}\text{C}$; c) relative humidity (RH) in %; d) wind speed (wind) in m/s and e) potential evaporation (PE) in mm/h.
- 3.1 Basic environmental information of the Waraputa area. The maps are raster maps with a 50x50 m cell size. a) Soil map with FAO classification; b) Texture map based on clay percentage; c) Drainage classes; d) Upstream elements (see text for explanation).
- 3.2 Mean species abundance for each forest type (based on 252 plots). For abbreviations see text.
- 3.3 Sample design of 252 plots with the 5 main forest types (see text).
- 3.4 Relative frequency of occurrence of the 5 forest types on a) the 6 soil types and b) the 4 drainage classes (based on 252 plots).
- 3.5 a) Mean species composition in Dry Evergreen Forest, Mixed Forest and Wet Forest based on the TWINSpan clustering; b) The cluster centres given by the FKM clustering. The Y-axis shows the mean abundance class that is used in TWINSpan and FKM (see text).
- 3.6 Interpolated memberships of the 3 forest types: a) Dry Evergreen Forest; b) Mixed Forest and c) Wet Forest. d) Maximum membership to any forest type (maximum of a to c). The isolines represent combinations of soil properties and drainage (explained in section 3.3.3).
- 3.7 Frequency diagram of the memberships of all cells of the "maximum membership map" (figure 3.6d).
- 3.8 Average membership of the 3 forest types on each of the 6 soil types.
- 3.9 Interpolated DCA scores of a) first axis and b) second axis. Isolines are based on a) clay content with 2.5% interval, and b) a selection of loamy soils on the water divide (see also figure 3.6b).
- 4.1 The rain forest hydrological cycle (adapted from Douglas, 1977 in Bruijnzeel, 1990).
- 4.2 Flow diagram of the SOAP water balance model.
- 4.3 The flow domain with the actual pressure heads (h) and the shape function with which h is estimated.
- 4.4 Cumulative Leaf Area ($\text{m}^2\cdot\text{m}^{-2}$) for Mixed forest near Manaus (data from Roberts et al., 1993).
- 4.5 Linear relations of bulk stomatal conductivity (g_s in $\text{mm}\cdot\text{s}^{-1}$) and vapour pressure deficit (δe in Pa) for different levels of incoming radiation (R_{in} in $\text{W}\cdot\text{m}^{-2}$). Each line represents an increase in radiation of $100 \text{ W}\cdot\text{m}^{-2}$. Adapted from data of Roberts et al. (1990, 1993), see text.
- 4.6 Root distribution to a depth of 100 cm, as weight (in $\text{g}\cdot\text{kg}^{-1}$ soil) on the left and relative to the total root mass (in %) on the right: a) Dry Evergreen forest on Albic Arenosols ($n=10$), and b) Mixed forest on Ferralic Arenosols ($n=7$). Bars represent 1 standard deviation (data from Prinsen and Straatsma, 1992).
- 4.7 Variation of root length per volume of fine earth (in dm/liter) with depth, from the surface to the first impenetrable layer in an Albic Arenosol and a Haplic Ferralsol (after data from Eernisse, 1993).
- 4.8 Uptake reduction term $\alpha(h)$ as a function of pressure head.
- 5.1 Sample design in the catchment of the Tropenbos Ecological Reserve and main physiographic units.
- 5.2 Cumulative relative variance in relation to sampling distance for infiltration rate (IR) and sorptivity (SP) in the three physiographic units.
- 5.3 Cumulative relative variance of measured and modelled infiltration rate (IR) and sorptivity (SP).
- 6.1 Schematic representation of the Rutter interception model (see text for explanation of the sym-

- bols).
- 6.2 Frequency distributions of the gauge catch expressed as a fraction of the gross rainfall, for Dry Evergreen Forest (left) and for Mixed Forest (right).
 - 6.3 Derivation of the saturation storage capacity S from rainfall (P) and troughfall (T). See text for explanation of the regression lines. The lower graph is an enlargement of the first part of the upper graph.
 - 6.4 Results of the simulation of the DA series with the Rutter model. The line is a quadratic regression equation of the measured datapoints
 - 6.5 Cumulative frequency distribution of daily rainfall of period in which the DA series were measured.
 - 6.6 a) Sensitivity of simulated interception percentage to changes of the saturation storage capacity (S) and the potential evaporation (PE). b) Results of the simulation using a saturation storage capacity of 1.35 mm, 1.5 times larger than the original value of 0.89 mm. Original simulated values and the regression line through the measured data are also shown.
 - 6.7 Schematic representation of the CASCADE interception model (see text for explanation of the symbols).
 - 6.8 Change in canopy storage C from 0:00 h on 7/1/1992 to 23:50 h on 11/1/1992. The top graph shows the potential evaporation in mm/hr and the rainfall in mm per 10 min intervals. The bottom graph shows the actual canopy storage C , where the storage of the CASCADE model is the sum of the storage of each layer.
 - 6.9 Results of the simulation of the DA series with the CASCADE model, compared to the measured values.
 - 7.1 Experimental setup for flow tests on large soil samples (for the abbreviations see text).
 - 7.2 Runoff-throughfall relations at five small forest plots for throughfall amount less than 50 mm. The regression coefficients of the lines are given in table 7.1.
 - 7.3 Simulated pressure head at the surface of plot A and the measured runoff events.
 - 7.4 Lateral conductivity (K_{lat} in m/day) at 6 slope angles for all samples. a) with litter thickness d (cm), b) with constant head h_1 (cm) and c) with the ratio of h_1/d .
 - 7.5 Box-whisker diagrams of lateral conductivity (K_{lat} in m/day) and Runoff % of all soil samples at 6 slope angles.
 - 7.6 Relations between Runoff (%) and lateral conductivity (K_{lat} in m/day) at 6 slope angles (graphs a to f). Regression coefficients for the first part, and the maximum K with which the regression analysis was done are given in table 7.2
 - 7.7 Reynolds number in relation to h_1/d ratio for the EC tests of all samples at three slope angles. Grey shades indicate the slope angle.
 - 7.8 Mean velocity (V_{mean} in m/day) calculated with the EC tests and corresponding Reynolds number. Grey shades indicate litter thickness d (cm).
 - 7.9 Box-whisker diagram of mean velocity calculated with the EC tests for each slope angle.
 - 7.10 Fastest velocity (V_{fast} in m/day) calculated with the EC tests and corresponding Reynolds number. Grey shades indicate litter thickness d (cm).
 - 7.11 Darcy-Weisbach friction factor f corresponding with V_{main} . Grey shades indicate litter thickness d (cm).
 - 8.1 Temperature ($^{\circ}C$) and relative humidity (%) measured below the canopy on a clear sunny day (27 March 1992) and a cloudy rainy day (8 April 1992). Weather station readings of temperature, relative humidity and incoming radiation are added.
 - 8.2 Measurements and simulation of the matric potential in a Ferralic Arenosol under Mixed Forest, at three depths (from top to bottom). This page shows the dry period in 1992, the next page shows the wet period in 1993. On the right y-axis the fluxes in $mm \cdot d^{-1}$ are given.
 - 8.3 Response time of the soil for a 42 mm rainstorm on 8 March 1992. The horizontal bars at the top of the graph indicate the amount of time needed for the rainstorm to reach 30 cm, 70 cm and 120 cm.
 - 8.4 Measured and simulated matric potentials in a Haplic ferralsol under Mixed Forest in 1992 on a) 20 cm depth and b) 50 cm depth.
 - 8.5 Model results for Ferralic Arenosols under Mixed Forest (all fluxes are in mm/day): P = rainfall; ET = total evapotranspiration (dotted line) and transpiration (solid line); pF = average pF values at 10 cm and 100 cm depth; Per = percolation.

- 8.6 The simulated daily matric potentials (pF values at 1200h) at 10 cm depth and 100 cm depth, in the three soil types ARa, ARo and FRh. The solid lines represent the avg soil properties, the dotted lines represent +std and -std.
- 8.7 Summary of the water fluxes in percentage of rainfall over a 346 day period. The soils are arranged in order of a decreasing permeability from left (ARa+std) to right (FRh-std, see text for explanation of abbreviations). Ei = interception, U = uptake, Es = soil evaporation, Per = percolation, Ro = surface runoff, Moist = soil moisture change.
- 9.1 Change of Ks, θ_s and Bd with depth in a Haplic Acrisol, under forest, at a gap and at a market.
- 9.2 Moisture retention curves of the topsoil of the 4 soil types, in undisturbed and disturbed situations.
- 9.3 Hydraulic conductivity curves of the topsoil of the 4 soil types, in undisturbed and disturbed situations.
- 10.1 Increase in Leaf Area Index on two gaps in the La Selva Reserve in Costa Rica (Parker, 1985).
- 10.2 Increase in leaf surface with seedling height for two pioneer species (left) and two climax species (right) (Raaymakers, unpublished data).
- 10.3 Increase in root mass with seedling height for two pioneer species (left) and two climax species (right) (Raaymakers, unpublished data).
- 10.4 Temperature (Temp) and relative humidity (RH) on two days on the large gap (LG) and small gap (SG). Weather station data (Meteo) of temperature, relative humidity and radiation (Rin) have been added.
- 10.5 Skid trail: measured and simulated matric potentials at 3 depths (top to bottom) in the dry season of 1992 (this page) and the wet season of 1993 (next page).
- 10.6 Crown zone: measured and simulated matric potentials at 3 depths (top to bottom) in the dry season of 1992 (this page) and the wet season of 1993 (next page).
- 10.7 Undisturbed zone: measured and simulated matric potentials at 3 depths (top to bottom) in the dry season of 1992 (this page) and the wet season of 1993 (next page).
- 10.8 Annual variation in daily fluxes (in mm/day) on a gap on a Ferralic Arenosol. P = rainfall, ET = evapotranspiration (dotted line), T = transpiration (solid line), pF = average pF values at 10 cm and 100 cm depth, Per = percolation.
- 10.9 Daily values of matric potential at 1200 h for three soils at 10 cm depth and 100 cm depth). The solid line is the gap average (1/3 compacted, 2/3 uncompacted top soil), the upper and lower dotted lines are the minimum and maximum midday potentials.
- 10.10 Summary of annual simulation in percentage of rainfall. Avg = average calculated from 1/3 compacted and 2/3 non-compacted topsoil, min = least permeable compacted topsoil (skid trail), max = most permeable undisturbed soil (crown zone). Es = soil evaporation, U = uptake, Ei = interception evaporation, Per = percolation, Ro = surface runoff and Moist = soil moisture change.
- 10.11 Simulation of fluxes as percentage of rainfall, related to a linear increase in LAI. The period covers 2 years, LAI = 0 in October 1991 and LAI = 2.3 in October 1993. Left end bar is undisturbed forest situation (LAI = 6.3).
- 11.1 Derivatives of the digital elevation model of the experimental catchment and the main soil types (note that north is downward): a) Upstream Elements, b) Slope map (%), c) Soil types, and d) Skid trails.
- 11.2 Topographic map with the locations of the weir and piezometers.
- 11.3 Cumulative frequency of a) rainstorm volumes (P in mm) relative to the total amount of rainfall, b) stormflow volumes (Qp in mm) relative to the total amount of stormflow.
- 11.4 Double logarithmic regression of rainfall (P in mm) and stormflow event (Qp in mm): a) before logging, n = 90 and $R^2 = 0.7112$, and b) after logging, n = 60 and $R^2 = 0.7234$.
- 11.5 30-day total discharge (Q), peakflow (Qp) and rainfall (P) (both in mm) during the entire measurement period.
- 11.6 Total discharge in 5 day totals and running average of the 5-day totals of rainfall (both in mm).

- The thick line at the top of the graph shows the periods in which the datalogger was operative.
- 11.7 Groundwater fluctuations (in m) relative to the streambed for the entire measurement period: a) piezometers in sandy soil types (ARa and ARo), and b) piezometers in loamy soil types (FRh and ACh).
 - 11.8 Mean groundwater levels relative to the streambed for two periods of more or less equal length, before and after logging.
 - 11.9 Difference in storage (in mm) between two moments in time 1 year apart, for 4 dates spread evenly throughout the period.
 - 12.1 Comparison of the vertical water balance of undisturbed forest, a gap immediately after logging, and a gap one year after logging. All water fluxes are given as a percentage of the annual rainfall (approximately 2700 mm).

TABLES

- 2.1 Variables measured and instruments used at the Mabura Hill Weather Station and with height of measurements.
- 2.2 Monthly rainfall of Mabura and Great Falls (9 years) and Georgetown (30 years).
- 2.3 Penman Potential Evaporation (PE) for Mabura and Georgetown.
- 2.4 Parameters of the 5th degree polynomial used to estimate the daily course of the meteorological variables.
- 4.1 Vertical structure of the canopy used in the SOAP model.
- 5.1 Variables examined for the regression model.
- 5.2 Basic statistics of the variables and correlations with infiltration rate (corIR) and sorptivity (corSP).
- 5.3 Results of the Nested Analysis of Variance (the cumulative relative variance at the highest level is always 100%).
- 5.4 Results of the regression analysis. R^2 -change is the increase in explained variance contributed by each independent variable.
- 5.5 Spatial variance in relation to several sample distances.
- 6.1 Saturation storage capacity S (in mm) of various tropical forests.
- 7.1 Regression coefficients for runoff (mm) and throughfall (mm), for throughfall amounts larger than 10 mm.
- 7.2 Regression coefficients for runoff (%) and Klat (m/day) in the range of Klat from 0 to Kmax.
- 7.3 Darcy-Weisbach friction factors for various types of surface conditions.
- 8.1 Soil properties used in the simulations with SOAP, avg = average values, +std = average values + 1 standard deviation, -std = average values - 1 standard deviation.
- 8.2 Cumulative values of fluxes on ARa under DEF based on simulation of 346 days, fluxes are in mm and percentages are relative to rainfall. P = rainfall, Ei = interception, Th = throughfall, Ro = runoff, I = infiltration, U = uptake, Es = soil evaporation, Per = percolation, Moist = change of soil moisture storage, ET = actual evapotranspiration (sum of Ei, U and Es), PET = potential evapotranspiration, TimePond = ponding time (min), havg = average yearly pressure head (cm), hwet is the average wet season pressure head, hdry = average dry season pressure head.
- 8.3 Cumulative values of fluxes on ARo under MF based on simulation of 346 days, fluxes are in mm and percentages are relative to rainfall. The abbreviations are explained in table 8.2.
- 8.4 Cumulative values of fluxes on FRh under MF based on simulation of 346 days, fluxes are in mm and percentages are relative to rainfall. The abbreviations are explained in table 8.2.
- 9.1 Average texture of the topsoil of the Albic and Ferralic Arenosols, the Haplic Ferralsols and the Haplic Acrisols in the Mabura area (data from Rotmans, 1993)
- 9.2 Soil properties of Albic Arenosols under forest (undisturbed) and on skid trails (disturbed), F values give the result of the ANOVA between the two situations.
- 9.3 Soil properties of Ferralic Arenosols under forest (undisturbed) and on skid trails (disturbed), F values give the result of the ANOVA between the two situations.
- 9.4 Soil properties of Haplic Ferralsols under forest (undisturbed) and on skid trails (disturbed), F

- values give the result of the ANOVA between the two situations.
- 9.5 Soil properties of Haplic Acrisols under forest, on a gap (not on skid trails) and on a market. Codes for ANOVA F-values: FG = forest vs. gap; FM = forest vs. market; GM = gap vs. market.
 - 9.6 Van Genuchten parameters for all soils under forest (*und*) and on a skid trail (*dis*). Codes for ANOVA F-values of ACh: FG = forest vs. gap; FM = forest vs. market; GM = gap vs. market.
 - 10.1 Partitioning of rainfall on the large gap and in the adjacent forest in 2 seasons. Simulation of the 1993 gap data with restoring plant cover or without plants.
 - 10.2 Cumulative values of fluxes on ARa in a gap, based on simulation of 365 days, fluxes are in mm and percentages are relative to rainfall. P = rainfall, Ei = interception evaporation, Th = throughfall, Ro = runoff, I = infiltration, U = uptake, Es = soil evaporation, Per = percolation, Moist = change of soil moisture storage, ET = actual evapotranspiration (sum of Ei, U and Es), PET = potential evapotranspiration, TimePond = ponding time (min), havg = average yearly pressure head (cm), hwet is the average wet season pressure head, hdry = average dry season pressure head.
 - 10.3 Cumulative values of fluxes on ARo in a gap, based on simulation of 365 days, fluxes are in mm and percentages are relative to rainfall. The abbreviations are explained in table 10.2.
 - 10.4 Cumulative values of fluxes on FRh in a gap based on simulation of 365 days, fluxes are in mm and percentages are relative to rainfall. The abbreviations are explained in table 10.2.
 - 11.2 Annual catchment water balance before logging. "Estimated" is the discharge calculated from the rainfall with the method explained in the text, "Measured" is the discharge at the weir. P = rainfall, ET = evapotranspiration, Q = total discharge, Qp = peakflow, Qb = baseflow (all in 1000 m³).
 - 11.3 Annual water balance after logging. "Estimated" is the discharge calculated from the rainfall with the method explained in the text, "Measured" is the discharge at the weir. P = rainfall, ET = evapotranspiration, Q = total discharge, Qp = peakflow, Qb = baseflow (all in 1000 m³). Days 174-223 of 1993 are excluded from the calculations, see text.
 - 11.4 Percentage increase in discharge as a result of a change in land use (Fritsch, 1990), for 8 catchments of 1 - 2 ha in size. All catchments are situated in the Crique Délice catchment in French Guyana, listed in table 11.5. The "fallow" period in which the soils were bare lasted 6 months to 1 year, the "growth" period is given in years. Clearing method: T = Tyre, C = Caterpillar, Man = Manual clearing.
 - 11.5 A selection water balance studies of small and medium sized catchments under tropical rainforest. P = annual rainfall; Q = total discharge; Qp = stormflow; Perc = deep percolation; ET = total evapotranspiration; Store = catchment storage

ACKNOWLEDGEMENTS

Environmental studies, and in particular geographical research, are often carried out in different parts of the world. This means that you are a guest, a guest in a country, in a village and also at institutes and companies that aid you in your efforts. Without the help and consent of a great many Guyanese people I could never have done this study. What do they get in return? Well, I hope that some of the data and knowledge compiled in this book will be of use to them.

Here is a list of everyone I would like to thank and I hope that I didn't make any "serious bad" mistakes by omitting people who helped me:

- Peter Burrough, the travelling wonder doctor whose powerful GIS potions are a cure for (almost) everything. His enthusiasm was very inspiring and helpful in times when the research threatened to stagnate. Special thanks to Hans "papa" Riezebos for his help and support, not only on a professional but also on a personal level.
- Ben ter Welle, Location Coordinator of the Guyana programme, for finding solutions to everything.
- George Walcott and Indarjit "Charlie" Ramdass for their continuous support of the Tropenbos Programme and the other members of the National Committee.
- The indestructible Zab Khan for sharing his field experience and his knowledge about the soils of Guyana, and the staff of the National Agricultural Research Institute.
- The staff of Demerara Woods Ltd. and later of Demerara Timbers Ltd, and of Boskalis for their invaluable logistical support to the Tropenbos Programme.
- Leonnard Wong Kam for his never ceasing friendship and assistance (if his skills are a family trade, one of his forefathers must have invented the wheel), and Sandra Mohabeer for preventing me from becoming an absolute barbarian and keeping me informed about life in Mabura. Through them I would like to thank the people of Mabura.
- Hans and Petra for making me feel welcome in Guyana, especially the first time I arrived. I fondly (yet somewhat vaguely) remember the Mabura Velvet Hammer and other killer cocktails. Hans, I hope that you finally will get your globe to rotate, I know how it feels when these things keep eluding you. Leo and Jet for always making room for me in that tiny house. And of course Roderick (mr. Pringles), René, Carmen, David, Allison, Peter, Marcel, Caroline, Dorinne and Renske for their friendship, their team spirit, sharing books, meals and for organizing swimming trips at the end of the day.
- Leo for continuing my experiments while I was in the Netherlands and for letting me use valuable parts of his dataset. Without him I couldn't have pulled this off.
- Sampurno Bruijnzeel and Koos Verstraten for discussions and criticism.
- Dennis, Collin, Oswald en others of the field staff, for helping us with the tedious filed experiments at ungodly hours.
- Frans and Janine (whose samples I managed to f... up several times, forgive me!), Ruud and Robbert (who managed to kill a respectable amount of animals), Geert and Gert, Nienke and Sandra, Hein and Jannie, Karel and Joel, Arjen and Dany for gathering information and contributing substantially to this research, and

- of course Nienke for her help in continuing the field experiments.
- Mrs. Sybil Stewart, Mrs. Joan Watson and Mr. D.E. "Harry" Hariprasad for their management in every way of the Tropenbos Office in Garnettstreet, and thanks to our neighbours for introducing me to life in Guyana (at all hours).
 - My present and former colleagues (de zgn. "vage kennissen") at the Geography Department in Utrecht for their willingness to listen to these endless stories about the rain forest and for fondly remembered pizza dinners: Steven, Ad, Cees, Jan, Ernst-Jan, Jos, Willem, Lodewijk, Gerard, Theo, Edzer, Mark, Maarten, Thijs, Jaap, Hans, Aart and Torbjörn.
 - The staff at the Herbarium for making me feel welcome in the higher regions of the 2nd floor and for their logistical support.
 - Cees, Bas and Theo for their technical assistance, Celia, Heleen and Charlotte for layout assistance and Jaque and Mr. Bosma for reproducing the draft manuscript.
 - Nelleke Bouwma and Guus Asten of the Medical Department of the university for giving me a few "shots" every time I went to the bush.
 - The Tropenbos Foundation for making this research possible.
 - The Faculty of Geographical Sciences for continuation of my job as a researcher.

First and last, I would like to thank my parents Gerrit and Truus who always support me regardless of the choices I make in life, René and Malou who made me realise the importance of a family and Christine who is a kindred spirit. And finally Nanda, Jan Willem, Janine, Prisca and Steven for keeping me firmly based in Utrecht.

Victor Jetten

1 INTRODUCTION

1.1 Tropical rain forest

Someone who enters the rain forest for the first time receives two immediate impressions: everything within viewing range (which is about 20 meters) seems like chaos with an abundance of detail, while at the same time there is a notion that in a spatial sense it goes on forever (at least to our limited perception). Indeed rain forests belong to the richest ecosystems on earth, certainly with respect to the large number of plant and animal species. This immense variability results from the fact that the rain forest is a very dynamic system. At a macro scale there is evidence of areal expansion and reduction caused by climatic changes in the past (Riezebos, 1979), at a medium scale disturbances are caused by environmental hazards such as landslides, climatic events or flooding (Ter Steege, 1993), while at a micro scale trees die and create gaps (about 1% annually). This results in an environment which, although strikingly similar in physiognomy and functioning (Oldeman, 1987), experiences a large variability in stages of development, species composition and structural components, and in the processes between these components (Sombroek, 1987). This variability is often referred to in terms of a "mosaic pattern" (Whitmore, 1990), which is helpful to understand the processes of regeneration and development (from gap to forest), but it also suggests a clearly defined spatial pattern. At a macro scale there may be very sharp landscape boundaries, which in Guyana for instance are caused by geological history (Barron, 1986), but within these units it is probably better to use the concept of a spatial continuum with considerable changes over short distances.

The notion of mosaics or any form of classification are simply a way of bringing order into chaos and depend very much on the framework of the research. A hydrologist will see a different pattern than someone studying population dynamics. From a hydrological point of view the water flows between various components of the forest and the components themselves are equally important: the concept of a highly variable continuum relates very well to the dynamic aspects of the water balance. The large spatial variability however, prevents the selection of a single "typical" or "representative" research location, because it does not exist. Therefore it is necessary to quantify the variability and assess the range of possible water flows within a type of landscape. This is extremely difficult, because we are not only dealing with soil properties and drainage network, but also with the structure and physiology of a wide variety of plant species.

1.2 Use and management: the Tropenbos programme in Guyana

Tropical rain forests and the land they occupy have been used for centuries, but the present rates of forest disturbance are very much higher than has ever been known before. Use and misuse of forest is a hot issue and much has been written on the subject (e.g. Werger, 1992; Bruijnzeel, 1990; Van Beusekom et al., 1987). However

there is little consensus on the extent of tropical forest disappearing each year. According to the FAO there were 1200 million ha of closed tropical forest in 1982 (Luning, 1987). Estimates suggest that some 20 million ha are altered annually, 11 million ha of which are converted to other kinds of land use and 4.5 million ha are degraded by selective logging (Marshall, 1992). It is clear however that the forests are "mined", only 0.1% of the remaining forest was under some form of management in 1989 and 3% set aside for conservation (Holmberg et al., 1991 in Marshall, 1992). Research of the past 25 years has made it clear that the forest itself is probably one of the most suitable types of land use for the area it occupies. The soils covered by rain forest in South America and Africa are hardly suitable for agriculture and a change in land use is almost always for the worst, certainly on the long term. Therefore there is need for the implementation of management systems that are based on sustainable forest use. While increasing the knowledge and understanding of the rain forest ecosystem, scientific research can be helpful in adapting a management system to a specific area, and analyzing the consequences. Meanwhile the actual implementation of management systems is not so much hampered by lack of knowledge but by political constraints.

The Dutch Tropenbos Foundation was established to generate tools for policy makers and managers for conservation and to promote wise use of the tropical rain forest (Tropenbos, 1990). Under its supervision, the governments of Guyana and the Netherlands have been cooperating in a research programme that started in 1989. The research has been concentrated in the interior of Guyana, some 235 km south of the capital Georgetown on the concession of Demerara Timbers Ltd. A wide range of projects was formulated:

- an inventory and description of valuable timber species;
- an inventory of soils of the concession;
- water balance and the effects of logging (this research);
- nutrient cycling and the effects of logging;
- population structure and dynamics, seed dynamics and reproduction strategies;
- growth in relation to environmental constraints;
- logging intensity studies and the implementation of a certain management system;
- the effects of logging on bio-diversity.

Initially, the projects focused on the undisturbed ecosystem, in order to analyze and describe the reference situation against which the impact of logging must be evaluated. The effects of logging depend of course on the intensity of timber extraction, and the kind of logging operations that are practised in Guyana.

Compared to other countries with tropical rain forest, the annual rate of deforestation in Guyana is negligible (Luning, 1987). Logging is practised in an area parallel to the coast, south of the White Sand Plateau (see chapter 2, and Ter Steege, 1993). Several species are logged commercially, but there is a strong emphasis towards one species (Greenheart or *Chlorocardium rodiei*¹), which accounts for 45% of all harvested timber (Ter Steege, 1993). Thus the logging is often classified as "selecti-

¹ In this thesis the Latin names of the species are given only. A full list of species and authorities can be found in Ter Steege (1990), Ter Steege and Persaud (1991) and Mennega et al. (1988).

ve logging", which implies a low intensity of extraction. Although Greenheart constitutes 0.5 - 1.5% of the country's standing stock of timber, in areas where Greenheart occurs logging may be quite severe. With mainly Greenheart (and a few other species) as the most valuable source of timber, the research objective in Guyana has become to define a logging intensity that is low enough for the ecosystem to retain all its functions as a forest, while at the same time being economically feasible.

1.3 Objectives and approach

Apart from the timber industry there is hardly any pressure on the Guyanese forest. The country has a population of approximately 800,000 which live mainly on the coastal plain, where all the agricultural activities are concentrated. Since the only other important activities in the interior are gold mining and gold dredging in the main rivers, the population density there is very low. This means that the impact of logging is not evaluated in terms of how it affects the living environment for the people, but solely in terms of the impact on the forest ecosystem itself.

The central research objective of the study presented in this thesis is: "the assessment of the water balance of undisturbed rain forest and the impact of disturbance caused by low intensity commercial timber extraction". The fact that the Tropenbos research in Guyana focuses on the forest ecosystem is particularly true for this research: the changes in the water balance brought about by logging are usually evaluated in terms of: suitability for agriculture or livestock keeping, drinking water supply, hydro-electricity, flooding, erosion, siltation of rivers etc. In this study none of these issues are important and the water balance of the partially logged forest is evaluated against the undisturbed ecosystem.

It was mentioned above that several landscape types occur in Guyana (Daniels and Hons, 1984) with distinctly different combinations of forest types and soil types. The impact of logging on the hydrology may vary with the hydrological characteristics of these combinations. Not all combinations could be studied: the selection is based on silvicultural, scientific and practical criteria. Tropenbos is obviously interested in those forest types in which commercial tree species occur and logging takes place: Mixed Forest where Greenheart is logged and to a lesser extent Dry Evergreen Forest where Wallaba is extracted. However, the exact location of the research is based on scientific criteria, which dictate for instance the sampling strategies and the type of equipment used. Practical constraints are that the research area is accessible and infrastructural facilities are present. The combination of forest and soil type on which the water balance research focused were: Dry Evergreen Forest on Arenosols and Mixed Forest on Arenosols and Ferralsols. A third combination of interest to Tropenbos is Mixed Forest on lateritic soils. However, areas with this combination were poorly accessible at the start of this research and are hydrologically very difficult to analyze. The water balance of lateritic soils is very different and the findings presented in this thesis cannot be extrapolated to these areas.

Ter Steege et al. (1993, see also Ter Steege, 1993) show that the tree species composition of Dry Evergreen Forest and Mixed Forest is strongly related to the soil type and hydrology. This leads to the first research question:

- 1) To what extent are the spatial patterns of the forest types related to the patterns of the soil types, and is there a combination of soil hydrological properties that explains the spatial variation in species composition? Two other aspects are very important: a) are the "forest types" the result of imposing a rigid classification on a continuous forest or are there actually sharp spatial boundaries, and b) which is the best method to investigate this? These questions are addressed in chapter 3.

The Tropenbos Programme in Guyana emphasises the impact of logging on the functioning of the forest ecosystem itself. Therefore both the ecosystem components and the processes between the components were studied. This is where the spatial variability of the components of the tropical rain forest becomes important. From a hydrological point of view the spatial variability expresses itself in canopy structure and structure of the root system, physiological properties of the plants, soil structure, hydraulic conductivity and water retention capacity of the various layers, relief and surface drainage pattern. This leads to the second research question:

- 2) What is the spatial variability of the hydrological properties of the specific combinations of forest type and soil type, and is it feasible to map the spatial patterns? This question is addressed in chapter 5.

As water moves from the top of the canopy along various flow paths to the creek, the water fluxes are altered in size and temporal variation. Of these fluxes only the rainfall, the canopy drainage and the stream discharge can be measured directly (although on a micro scale it is also possible to measure certain fluxes inside a plant). This means that most of the fluxes have to be calculated from changes in the water content of the ecosystem components. This was done by the construction of a one dimensional water balance model in which all vertical water fluxes are quantified with a high temporal resolution (the model is described in chapter 4). This leads to the third and fourth research questions:

- 3) Can the model be calibrated and does it give an adequate analysis of the temporal variation of the water fluxes when compared to other studies?
- 4) Given that the model is a successful tool, how does the spatial variation of the hydrological properties affect the water balance? These questions are addressed in chapters 6 and 8.

Although the soils are very permeable (Jetten et al., 1993) and most of the water movement in the soils is vertical (Daniel and Hons, 1984), there is evidence of overland flow under natural forest. This leads to the fifth research question:

- 5) What is the nature of the processes that lead to overland flow, how much overland flow is generated and where does it occur? This question is addressed in chapter 7.

In low intensity logging a series of gaps are created in the forest by the removal of the timber trees. To reach these trees a series of access trails are created that link the locations where the actual logging takes place to the timber storage areas and permanent roads. This leads to the sixth research question:

- 6) To what extent are the soil structure, water retention capacity and hydraulic conductivity of the main soil types altered by the activity of heavy machinery? This question is addressed in chapter 9.

Thus the logging creates heavily disturbed areas in an otherwise undisturbed forest. From a sustainable yield point of view the forest has to be able to regenerate on the gaps and tracks, while at the same time the disturbance must not be too great to "unbalance" the forest ecosystem (the forest must still remain a forest). Therefore the impact of logging on the water balance is studied both at the level of a single gap and at the level of a catchment. Within the gap the vegetation and soils are disturbed to different degrees. This leads to the seventh research question:

- 7) Compared to the pristine forest, what is the change in temporal and spatial variation of the water fluxes after the gap is created and how does the water balance develop in time? This question is addressed in chapter 10.

At a catchment level the discharge and groundwater fluctuations are considered to be the variables that integrate the vertical and lateral water movement inside the catchment. It is assumed that when logging takes place in the catchment these same variables integrate the effect of the disturbance on the surrounding forest. For this purpose a small catchment was selected in which the discharge and groundwater fluctuations were monitored before and after logging. This leads to the final research question:

- 8) What is the size and nature of the impact of low intensity logging on the water balance of a small catchment, and is it possible to define an acceptable level of disturbance? This question is addressed in chapter 11.

The summary and conclusions are presented in chapter 12.

2 THE MABURA HILL AREA

2.1 Research locations

The research activities of the Tropenbos project take place in the vicinity of the Mabura township, approximately 235 km south of the capital Georgetown, between the Demerara and Essequibo rivers (see figures 2.1 and 2.2). The township is located on the northern boundary of the concession of Demerara Timbers Ltd. (DTL), the largest timber company operating in the area. Some 20 km south of Mabura, Tropenbos has established an ecological reserve of 900 ha. On the southern boundary of the Reserve a fully equipped field station was built where most of the experiments involving undisturbed forest took place. Parts of the water balance research that involved logging activities were carried out at other locations.

Three general inventories were done to gather background information on soil types and forest types. First, a soil map was made of the 20 km² catchment of the Tropenbos Ecological Reserve (see below). Second, the relations between spatial patterns of soil types and forest types were analyzed, using a tree inventory by DTL of a small watershed in the "Waraputa Compartment", which is a section of the concession located some 20 km west of the Tropenbos Reserve (see chapter 3). Third, the spatial variability of soil hydrological properties was investigated (see chapter 5).

To quantify parts of the water balance of undisturbed forest, a number of experiments were done, the locations of which are shown in figure 2.1. Atmospheric input and output of the water balance were measured with a meteorological station set up on a medium sized clearing at the northern boundary of the Tropenbos Reserve. About 1 km south of the weather station, two 1 ha plots were demarcated in two different forest types where throughfall was measured (chapter 6). In between these plots and the weather station a first order catchment was selected, in which surface runoff was measured on 5 small plots (chapter 7), as well as the temporal change of the topsoil moisture content (chapter 8).

Near the south west corner of the Reserve, two gaps of different size were created as part of the Nutrient Balance project of the Tropenbos Programme. This was done to investigate the relations between gap size and nutrient dynamics (Brouwer, in prep). Among other things, changes in soil moisture content were monitored on the gaps and in the forest. These data are used in a comparison of the vertical water balance of disturbed and undisturbed forest (chapters 8 and 10).

Approximately 2 km to the north of the weather station a 6 ha first order catchment was selected for a logging experiment. Topography and soils were mapped and discharge and groundwater levels were monitored first for a period of 1 year. DTL logged the catchment in October 1992 after which monitoring was continued for another year (chapter 11). Soil properties of disturbed locations were measured here and compared with those of undisturbed locations (chapter 9).

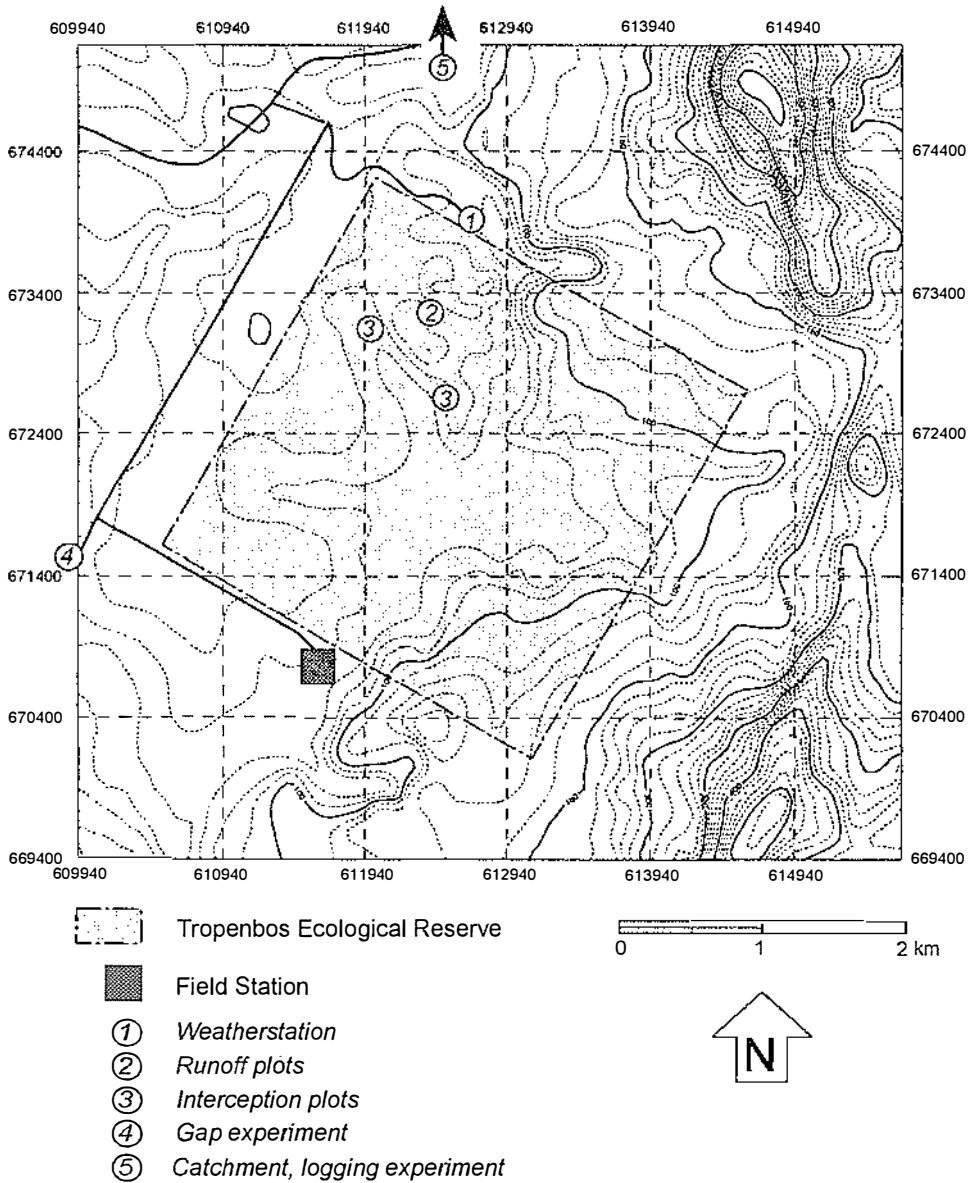


Figure 2.1 Tropenbos Ecological Reserve with infrastructure and locations of the main experiments in the water balance research (see text).

2.2 Geological history

The research area lies on the boundary between two of the four major landscape types of Guyana, each of which has its own ecosystem with a typical combination of topography, soils and vegetation. These four are the Pre-Cambrian Lowlands, the Pakaraima Mountains, the White Sand Plateau and the Coastal Plain. The differences between the landscape types find their origin in the geological history of the region. The brief outline of the geology and geomorphology given below is based on FAO (1965), Daniel and Hons (1984), Khan et al.(1980), Barron (1986), Khan and Jetten (1993) and Eernisse (1991).

Most of the geological formations in Guyana date from the Pre-Cambrian. They are known as the "crystalline basement complex rocks" (figure 2.2) that are part of the Guiana Shield which underlies most of the country. Generally the crystalline basement complex consists of granites, gneiss, amphibolites, rhyolites and quartzites and a variety of metamorphic rocks of both sedimentary and volcanic origin. It can be divided into two regions: the early formations (2700 million years BP) are exposed in the southern half of the country in the Rupununi Savannah and the Kanuku mountains; the late formations (2200 million years BP) are exposed in the north west of the country in the Cuyuni-Mazaruni area.

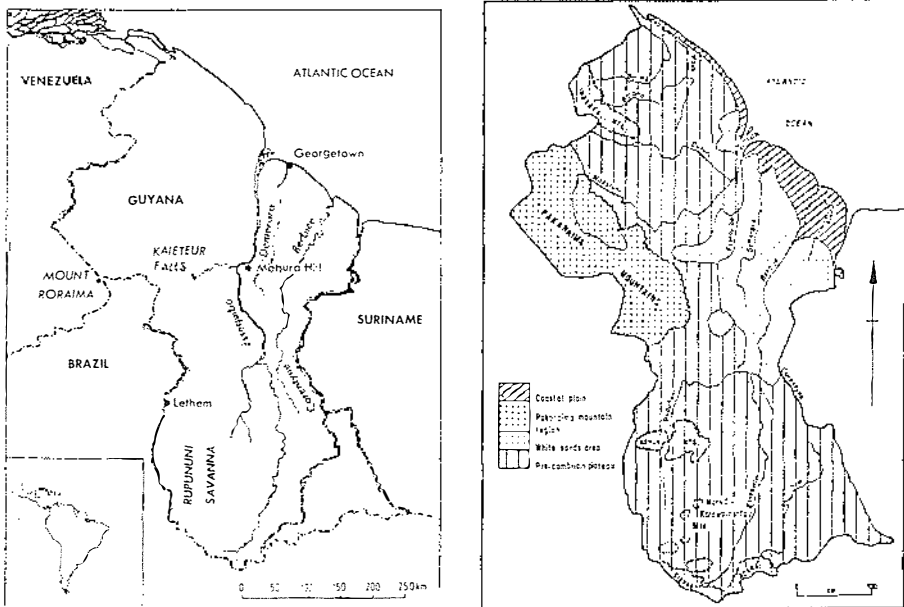


Figure 2.2 Main landscape types in Guyana.

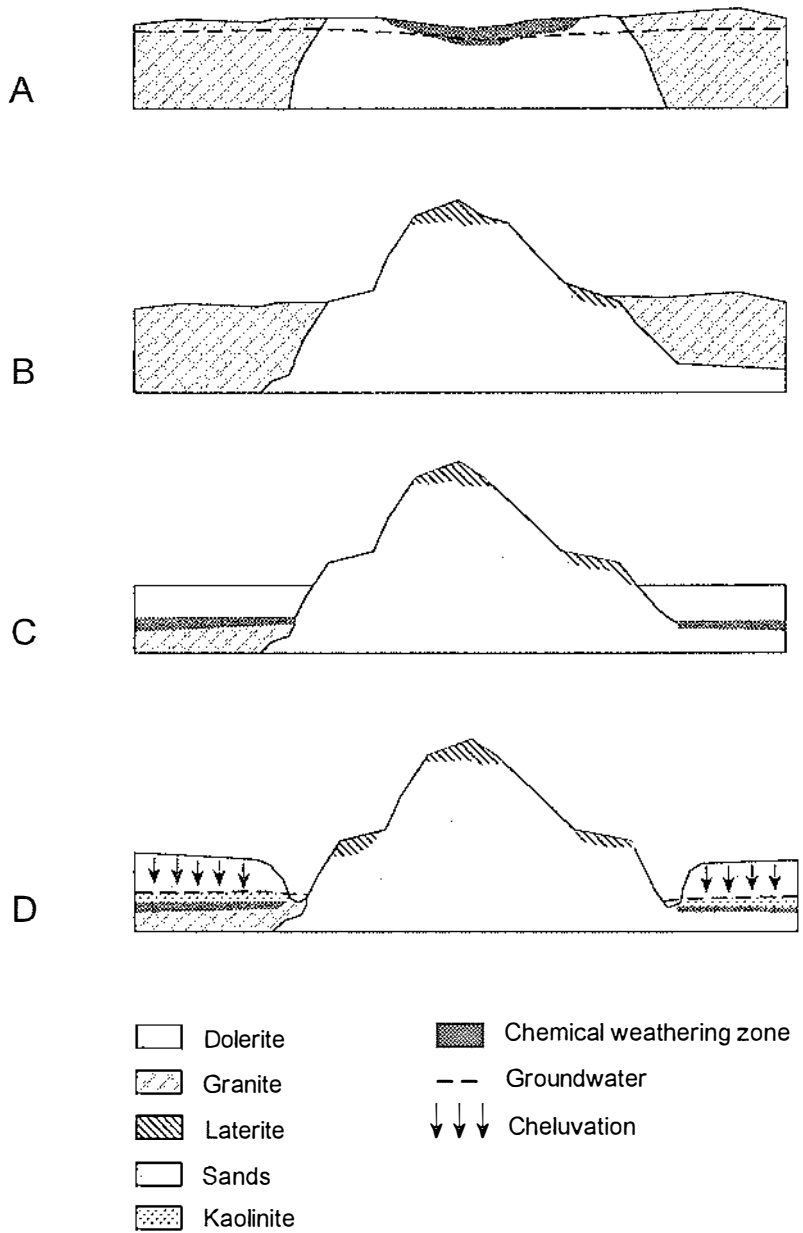


Figure 2.3

Schematic representation of the landscape formation of the Tropicbos Ecological Reserve, which is situated on the boundary of the White Sands Plateau and the Pre-Cambrian Lowlands.

In the western part of the country, known as the Pakaraima mountain region, the crystalline basement complex was lifted after which a prolonged period of denudation took place. Thick layers of sediments formed the basis of quartzitic sandstones, interbedded with conglomerates and thin beds of shales and schists, which together form the Roraima Formation in the late Pre Cambrian. After this denudation period the area was lifted again and at the same time gabbro intrusions formed massive sills that can be dated to 1600 to 1800 million years BP. The area was subjected to block faulting which enabled the sills to attain considerable thickness and size. Because of the intrusions the sedimentary rocks are partly metamorphic. Differential weathering and the coverage of large areas with relatively hard metamorphic rocks, resulted in a landscape of table mountains and cuestas, whereas large parts of the sandstones have been eroded. Outside the mountain region, dolerite dykes associated with the Roraima Formation were formed. The ridge east and south of the Mabura township is formed from such a dyke. The combination of crystalline basement rocks and intrusions is known as the Pre-Cambrian Plateau (see figure 2.2).

In the late Pliocene to early Pleistocene the crust was subsiding and thick sand layers, known as the Berbice Formation, were deposited in the slowly sinking basin. The mineral composition suggests that the bulk of the deposits (mainly quartz rich sand) was derived from the Roraima Formation. The basin may be part of the Berbice-Corentyne geosyncline which has its axis in the Berbice river area, where the sediments reach a thickness of nearly 2000 m. Subsequently the area was lifted and tilted towards the coast, which caused part of the sandy deposits to be eroded again, leaving the crystalline basement rocks exposed. At present the remains are known as the White Sand Plateau, located in the north east of the country and wedging out in the interior towards the Pakaraima Mountains. The tilting probably caused some major changes in the drainage system of Guyana, with the upper reaches of the Berbice becoming part of the Essequibo river system, which is now the largest in the country. During the Holocene a narrow Coastal Plain was formed.

2.3 Soils

The Tropenbos Reserve borders on the White Sands Plateau where it wedges out against a dolerite intrusion in the crystalline basement complex. The intrusion forms a row of sharp crested hills in the present day landscape. The main creek in the reserve forms the boundary between the two areas. In figure 2.3 a tentative explanation is given of the landscape formation, which may explain the sharp landscape boundaries and typical relief forms that are found in the Tropenbos Ecological Reserve and the catchment of the logging experiment.

The landscape may have gone through a series of 4 stages. After the formation of the crystalline basement complex with dolerite intrusions, a long period of weathering followed. Because these rocks are rich in quartz, kaolinite is one of the main weathering products, although ferralitisation takes place as well. In the low wet areas the sesquioxides accumulated and plinthite was formed. When the groundwater level dropped (e.g. by a lowering of the erosion base) the plinthite irreversibly hardened and laterite was formed. Because of the strong resistance against erosion of

the thick laterite crust, relief inversion took place. This cycle of laterite formation and relief inversion may have repeated itself several times. In the Pleistocene the sands of the Berbice Formation were deposited against the dolerite ridges. These sediments are very permeable and most of the infiltrating water moves vertically down. On the dolerite a groundwater table occurred and kaolinite and saprolite were formed by chemical weathering of the parent material. At the same time cheluvation of the sands caused the formation of a thick bleached E-horizon. In the humid tropical environment the organic matter was removed completely from the soil, because of decomposition and/or lateral transport. Clay illuvation did take place on top of the weathered dolerite.

Thus over large areas a relatively thin white kaolinite layer can be found under the sands, which forms the basis for the groundwater body at present. Since the laterite has a strong resistance against erosion, the sharp boundaries between the sandy and lateritic soils stay intact. On the boundary, the sands are eroded and often the dolerite is exposed in the stream channels. Perpendicular to the main creek in the Tropenbos Ecological Reserve groundwater emerges on top of the kaolinite layer and headward erosion takes place, sometimes with removal of the kaolinite. Thus, although the sands are very permeable, steep gullies are formed. In the gully heads the kaolinite layer ensures wet conditions and swamps are formed. The combination of flat water divides with steep bottom slopes, and swamps in the gully heads is often found in the area.

Based on the FAO classification system, 12 soil types are recognized in the Tropenbos Reserve (see figure 2.4). On the west side of the main creek, sands and sandy loams are found which are classified as Arenosols and Ferralsols. On the east side clayey soils with thick laterite layers and laterite gravel beds occur, classified as Plinthosols. In the swamps and valley floor Histosols and Fluvisols occur. Because the various experiments of the water balance research all occurred on the sandy and loamy soils, the Plinthosols are not discussed here. They have not yet been fully mapped in the Tropenbos Ecological Reserve and are shown in figure 2.4 as a single map unit. For more information the reader is referred to Pulles et al. (in prep.), Driessen and Dudal (1989), FAO (1988), Brinkman (1979) and Sánchez (1976). Seven soil types are distinguished in the study area according to the FAO classification (the name used in the Guyanese classification system is given between brackets¹).

ARa - Albic Arenosols (Tiwivid Sand, unit 700):

The White Sand Plateau consists for more than 86% of quartz with a texture of medium sand, very little silt and no clay. Intense and prolonged dissociation of weatherable minerals and translocation of weathering products through the process of cheluvation, have resulted in a deep white E-horizon (Driessen and Dudal, 1989). The A-horizon may consist of greyish brown sand with evenly mixed organic matter,

¹ It should be noted that as more information became available the classification for some of the soils changed. In earlier papers and Tropenbos reports Haplic Arenosols are used instead of Albic Arenosols, and Acrisols were classified as Lixisols. A soil inventory of the concession is expected to be finished in 1994 and some of the soils will probably be reclassified again.

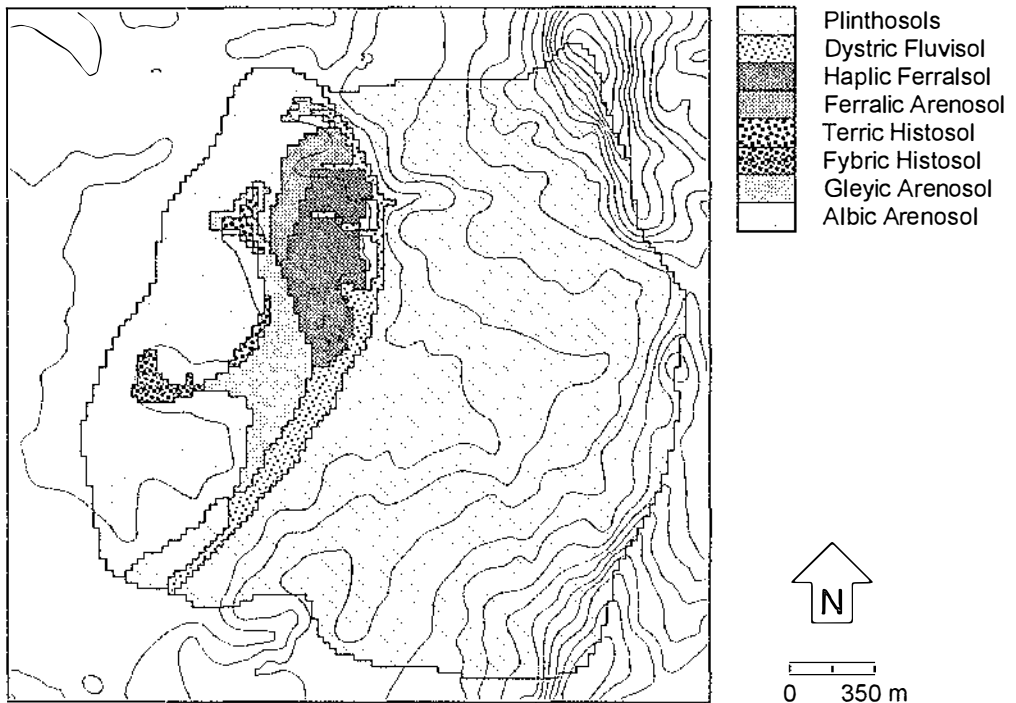


Figure 2.4 Digital soil map of Tropenbos Ecological Reserve, According to the FAO classification.

or the organic matter is present in small distinct particles giving the soil a "pepper and salt" appearance. Sometimes the texture changes to coarse sand below several meters and the colour becomes light grey. Similar soils are found in the Sanderij belt in Surinam, and in French Guyana and Venezuela where they are known as Giant Podzols (Ahmad, 1989). In the research area Albic Arenosols have a pH between 4 and 4.5 and both CEC and total bases that are about 1.5 meq/100g.

ARg - Gleyic Arenosols (Ituni Sand, unit 701):

The upper part of the soil is similar to the Albic Arenosols but a very dark brown to black, very dense sandy layer occurs within 1 meter of the surface. Below this layer one can often find a white kaolinitic clay layer. Both layers are virtually impermeable and a perching or permanent groundwater table causes a reduced environment. From field observations it seems that this layer stretches out over large areas beneath the Albic Arenosols but only on the lower slopes it occurs near the surface, where it causes a change in classification from Albic to Gleyic Arenosols. According to Khan et al. (1980) the black pan may be a result of lateral movement of water with a high content of soluble organic acids, which precipitate as organic complexes and chelates with aluminum and iron. Although the organic matter content of the pan is somewhat higher, the acidity, total bases and CEC in the rest of the soil are similar to the Albic Arenosol.

ARo - Ferralic Arenosols (Tabela Sand, unit 800):

These soils have a sand to loamy sand texture. Because of the dark brown A-horizon over a yellowish to reddish brown C-horizon, this soil type is a member of the "Brown Sands" group in Guyana. The Ferralic Arenosols also consist mainly of quartz sand but the higher clay and silt content may have prevented extensive podzolization. These soils are often found adjacent to the Albic Arenosols with very sharp lateral boundaries (changes from a typical ARo to a typical ARa may occur within 10 m). In the research area they are always found in a sequence from the loamier Brown Sands (see below) to the White Sands, indicating that the Ferralic Arenosols were possibly formed during the deposition of the Berbice Formation as a mixture of sediments with the weathering material formed in situ on the granite. On the other hand, the variation in texture could also be a result of sedimentation in a different environment. Acidity is high (pH 4-4.5) and total bases and CEC are about 6 meq/100g in the topsoil to less than 2 meq/100g below.

FRh - Haplic Ferralsols (Kasarama Loamy Sand, unit 810):

The soil has a dark brown loamy sand A-horizon over a strong brown to yellowish brown sandy loam B and C-horizons and is also a member of the Brown Sands group. In the area the soil can be more than 5 m deep with weathered rock at the lower boundary. Intensive ferralitisation of the crystalline basement complex rocks has resulted in a relative accumulation of resistant primary minerals and formation of kaolinite and iron oxides and hydroxides (hematite and goethite). Because the parent material is rich in quartz the ferralitisation process is slow and kaolinite is formed rather than aluminum hydroxide (gibbsite). However on the intrusions the parent material is mainly dolerite which has a lower quartz content, causing a more intensive ferralitisation process with the possible presence of gibbsite. The iron oxides are strong binding agents which form very stable micro aggregates in the soil. Acidity can be very low (pH < 4) and because of the higher clay content the total bases and CEC can be between 2 and 6 meq/100g over the whole profile.

ACh - Haplic Acrisols (Ebini Sandy Loam, unit 820):

This type of Brown Sands soil has a clay illuvation horizon. The dark brown sandy loam A horizon overlies a strong yellowish red sandy clay loam to sandy clay B-horizon. The accumulation of clay and the presence of an E-horizon are not always clear in the area. Apart from clay movement, ferralitisation is an important process and iron oxides and kaolinite clay predominate. Because the CEC is very low (4-6 meq/100g) the base saturation is more than 60% and the soils should, strictly speaking, be classified as a Haplic Lixisol. However, from the general description and occurrence of these soils given by Driessen and Dudal (1989) a classification as Haplic Acrisol (base saturation less than 50%) seems more appropriate. This soil type does not occur in the Tropenbos Ecological Reserve but it is found in the Waraputa Compartment (see chapter 3) as well as in the experimental catchment (see chapter 11).

Fld - Dystric Fluvisols (Mixed Alluvial, unit 366; Barima Silt Loam, unit 370):

These weakly developed soils consist of recent deposits in floodplains and can have any texture from sand to silty clay. Colours vary from yellowish brown to light grey. The sedimentation processes may cause stratification. They are subject to

flooding several times a year and the topsoil is rich in organic matter. Acidity is high (pH 3.1-4.5) and CEC is variable (1.8 to 6.3 meq/100g).

HSs/HSf - Terric and Fybric Histosols (Lama Muck, Anira Peat, unit 60 and 20):

Dark grey to black sandy soils rich in partly decomposed organic matter. They are formed in small swamps in gully heads and along the floodplain, and are inundated most of the year. They have a high acidity (pH 3.1-3.5) and a low CEC (2.5 - 5.1 meq/100g).

2.4 Climate

The Mabura Hill Weather Station has been operating since January 1991 and is located at a clearing in the forest of approximately 50x50 metres, at the northern boundary of the Reserve (coordinates 5°11'7" north and 58°43'36" west). Rainfall is measured in 5 minute totals with a tipping bucket rain gauge, with a accuracy of 0.2 mm/tip. Wind speed, pressure, temperature, relative humidity and incoming short wave radiation (0.3-3 μm) are measured every 10 minutes and each hour the average of these ten minute readings is recorded. The instruments are listed in table 2.1. The wind speed is measured at 10 m height while part of the gap is surrounded by forest that is higher. Thus the fetch requirements are only partly met. This has been taken into account with the calculation of the Penman potential evaporation. Due to damage and malfunctioning lapses occur in the measurements and the monthly values presented here are calculated from the remaining days in a month. The climatic variables measured are used to calculate the potential evaporation from an open water body, using the well known formula designed by Penman (see e.g. Ward and Robinson, 1990). An additional non-automatic rainfall gauge was installed at the field station (3 km to the south) to measure the daily rainfall.

Table 2.1 Variables measured and instruments used at the Mabura Hill Weather Station and with height of measurements

<i>Variable</i>		<i>Instrument</i>	<i>Height of measurement</i>
P	Rainfall	Campbell ARG100 tipping bucket	0.8 m
Wind	Wind speed	Vector Instruments A100 anemometer	10.0 m
p	Air pressure	Druck PDCR 830 pressure transducer	3.5 m
RH	Relative Humidity	Rotronic YA-100 air probe	3.5 m
T	Temperature	Rotronic YA-100 air probe	3.5 m
Rin	Radiation	Solar Radiation Instruments SRI-5 (0.3-3 μm)	0.8 m
Datalogger	Campbell CR10		

Seasonal change in Guyana is related to north-south movements of the Inter Tropical Convergence Zone (ITCZ) which influences mainly rainfall annual rainfall distribution. A long wet season occurs from May to August and a short wet season from December to February. The remaining periods are dryer with October generally being the driest month. In November a thermic low pressure area starts to develop in the Amazon Basin which causes air masses to flow into the basin, thus diminis-

hing the effect of normal air convergence in the ITCZ. Therefore the December wet season is less pronounced. Rainfall distribution in Guyana is also strongly affected by the Pakaraima mountains. Because easterly winds prevail, orographic uplift and condensation of the air on the eastern side of the mountains cause a high annual rainfall of 4400 mm. The annual rainfall decreases to 1700 mm towards the east of the country, as west Surinam lies on the leeward side of the Wilhelmina Mountains. The Mabura area lies immediately north-east of the Pakaraima mountains and has an annual rainfall of approximately 2700 mm. This is the annual mean precipitation measured at the Great Falls weather station located approximately 20 km east of Mabura, which was operational from 1965 to 1973. Table 2.2 gives the monthly rainfall of the Mabura Hill Weather Station, compared to Great Falls and Georgetown. In general 1992 can be described as a relatively dry year, because of the low rainfall in January, March and June, whereas 1991 and 1993 were average years.

Table 2.2 Monthly rainfall of Mabura and Great Falls (9 years) and Georgetown (30 years).

	1991	1992	1993	Great Falls	Georgetown
Jan	-	139	186	236	251
Feb	-	234	191	135	122
Mar	-	126	272	159	113
Apr	230	196	216	168	178
May	235	315	387	324	296
Jun	367	237	362	392	346
Jul	422	455	338	363	281
Aug	255	261	232	305	185
Sep	241	92	97	174	88
Oct	107	85	122	108	98
Nov	109	227	206	126	147
Dec	197	149	198	207	313
Total	2163	2515	2730.	2697	2418

The atmospheric variables recorded at the weather station were used to calculate Penman potential evaporation (PET, the equations are given in chapter 5). The PET given here is calculated with the weather station parameters (i.e. corresponding to the micro climate prevailing at the weather station clearing). Therefore it differs from the PET calculated for a forest stand (see chapter 8) which is based on the canopy micro climate. The net radiation contributing to evaporation was calculated with an albedo of 0.13 and a cloudiness of 0.55 (Ter Steege, 1993). The aerodynamic factor was calculated with a vegetation height of 5 m, corresponding to the height of the shrub on two sides of the clearing. Unfortunately the fetch requirements are not met as the other side of the clearing was bounded with forest of some 25 m high. Nevertheless with these factors the annual potential evaporation, which amounts to 1350 to 12500 mm, correspond fairly well with values found by other researchers. For instance Poels (1984) gives a mean Pan evaporation of 1579 mm (over 4 years) at Tonka in northern Surinam, Fritch (1990) reports a mean Penman PE of 1565 mm for northern French Guyana, in an area with a higher annual

precipitation. Other values for that area range from 1440 to 1528 mm, but these are calculated with a catchment water balance (Bruynzeel, 1990; Fritch, 1990). Shuttleworth (1988) reports a value of 1311 mm at the Ducke Reserve in Brazil, but this figure represents the actual forest evaporation. The Penman ET for that area is 1573 mm (Goeas Ribeiro and Villa Nova, in Fritch, 1990). In a review Bruynzeel (1990) arrives at an average ET of 1430 mm using the values of 11 research locations.

The monthly potential evaporation is given in table 2.3. It follows the trend in radiation: October has the highest PE in all three years while lowest PEs are generally in wetter months such as May, June and August. Months with a very high rainfall (such as July 1992) have a PE higher than the adjacent months, possibly because an increase in rainfall generates atmospheric turbulence. Thus a higher aerodynamic evaporation is calculated which diminishes the effect of increased cloudiness. The start of the dry season is sometimes delayed, as can be seen in figure 2.5, where PE exceeds P in October and November in 1991, while in the other years September and October are the driest months.

Table 2.3 Penman Potential Evaporation (PE) for Mabura and Georgetown.

	1991	1992	1993	G'Town
Jan	132	104	118	133
Feb	137	95	105	121
Mar	139	124	99	140
Apr	135	111	126	142
May	124	126	115	149
Jun	105	111	103	144
Jul	115	124	112	149
Aug	109	118	125	152
Sep	121	125	112	149
Oct	166	139	120	150
Nov	127	101	115	143
Dec	106	116	103	137
Total	1516	1377	1333	1709

The distribution of rainfall over the day is shown in figure 2.6. Most rain falls in the late afternoon and early evening, related to instability of the atmosphere caused by irradiation. The effect may be enhanced by the vicinity of the Mabura ridge, a row of hills running north-south at a distance of 3 km, which will probably influence air movement. Because of the daily distribution the rain that is intercepted by the forest canopy will evaporate the next day, which adds to the high early morning humidity. The spatial variation of rainfall is probably quite large. Rainfall measured during the interception experiment (see chapter 6) on plots about 1 km from the weather station was not significantly different. However, the differences between daily totals measured at the field station (distance 3 km) and at the weather station were usually much larger. This indicates that individual storms rarely cover a surface larger than 2-3 km².

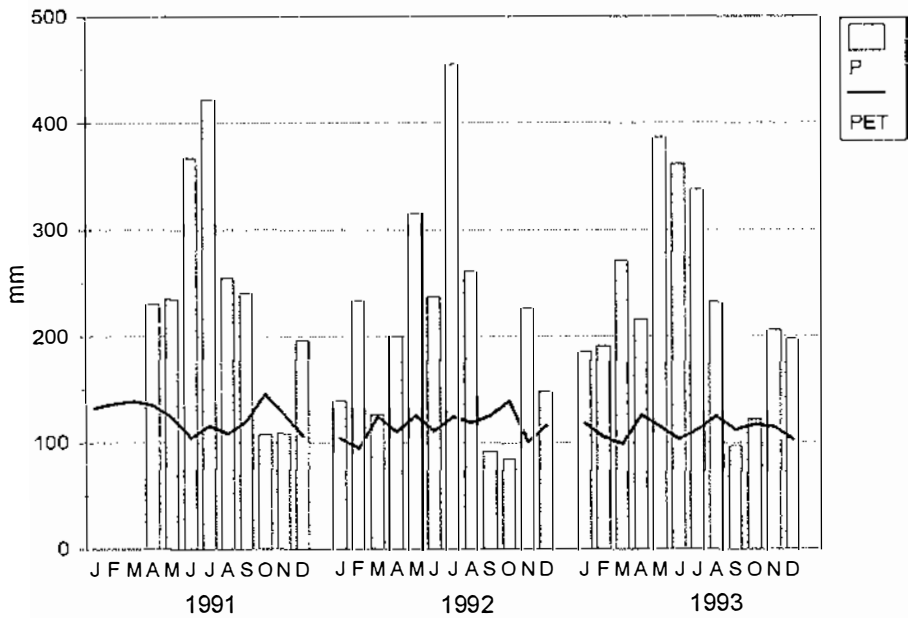


Figure 2.5 Monthly rainfall and potential evaporation in Mabura.

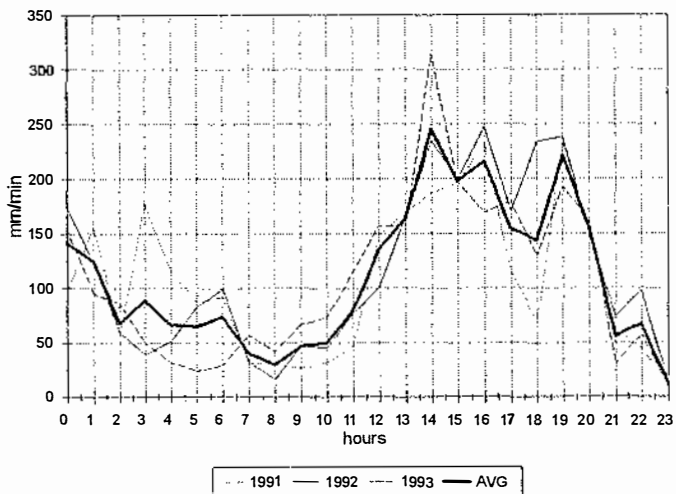


Figure 2.6 Annual rainfall distributed over 24 hours.

For all atmospheric variables measured at the weather station the diurnal variation is much larger than the annual variation, as is common for the humid tropics. As an example the mean, minimum and maximum daily course calculated for each month in 1992 is shown in figure 2.7 a to e. Other years show a similar distribution.

Mean incoming short wave radiation (0.3-3 μm) is between 550 and 650 W/m^2 at 2 p.m. while maximum values frequently exceed 800 W/m^2 . Radiation levels in 1992 were lower than in the other years: the yearly mean value at 2 p.m. was 675 W/m^2 as opposed to 710 W/m^2 in 1991 and 720 W/m^2 in 1993. The biannual peak in radiation caused by the yearly course of the sun is not very distinct, only the maximum radiation values have a vague bimodal shape. The total radiation per day varies from 11.3 to 14.2 MJ/m^2 for February and May respectively. This is only 30% to 40 % of the theoretical radiation levels calculated for the top of the atmosphere which range from 32.9 to 37.4 $\text{MJ}/\text{m}^2/\text{day}$, which gives an idea of the transmission of the atmosphere. In a literature review, Ter Steege (1994) reports on average 50% to 80% transmission, although values as low as 40% transmission were measured for the humid tropics.

Both temperature and relative humidity are strongly related to the radiation and show a similar course. While the annual variation in mean temperature is only about 2 $^{\circ}\text{C}$, the daily variation is about 6 $^{\circ}\text{C}$. Warmest months are September and October, coldest are January and February. Lowest temperatures are always recorded at 7 am (17 $^{\circ}\text{C}$ lowest in 3 years), highest temperatures at 2 pm (37.5 $^{\circ}\text{C}$ highest in 3 years). Relative humidity is the reciprocal of the temperature graph, with a lowest mean value of 60% in October and highest mean value of 75 % in February. However values as low as 45 % humidity have been measured.

Although the course of wind speed (at 10 m height) is somewhat erratic, it shows a clear daily variation from 0.05 m/s just before sunrise to over 0.6 m/s in the afternoon. It increases again from 0.1 to 0.25 in the evening, probably due to an increased rainfall in those hours. Maximum values often exceed 1 m/s at noon. The resulting Penman Potential Evaporation is dominated by the radiation which determines the daily course, with a small variation caused by the wind superimposed on it. Because of the wind there is some night time evaporation but on average this is very small. On average 70% of the potential evaporation is contributed by the radiation component. The PE is highest around 2 pm, varying from 0.55 mm/h in February to 0.85 mm/h in October. In fact the annual variation is quite small with daily totals vary from 1.5 to 6 mm in any season.

These variables are used in the water balance model to calculate potential and actual evapotranspiration (see chapter 4). At periods where one or more of the instruments were malfunctioning, the variable had to be estimated. Normally a simple sine curve is used to represent the daily course of the sun and the other variables are assumed to have the same variation. However, the curves in figure 2.7 are more "bell-shaped" than sinusoidal. To obtain a good estimation of a variable the following procedure was followed. The mean daily course of 1992 was calculated and a curve was fitted through the mean hourly values. A 5th degree polynomial gave the best fit. Table 2.4 gives the polynomial parameters and the variable (V_{ref}) with which the

daily course is calculated:

$$V = V_{ref} * (a + bt + ct^2 + dt^3 + et^4 + ft^5) \quad (2.1)$$

in which t is the time of day in hours. The radiation (Rin) is set to zero between 1800h and 600h.

Table 2.4 Parameters of the 5th degree polynomial used to estimate the daily course of the meteorological variables.

V_{ref}	a	b	c	d	e	f
RH-max	0.9411	0	0.0075	-0.0020	0.00014	-2.8E-06
Temp-avg	0.9260	0	-0.0076	0.0019	-0.00013	2.7E-06
Wind-avg	0.8327	-0.4284	0.0755	0	-0.00038	1.1E-05
Rin-max	1.6419	0	-0.2021	0.0402	-0.00269	5.9E-05

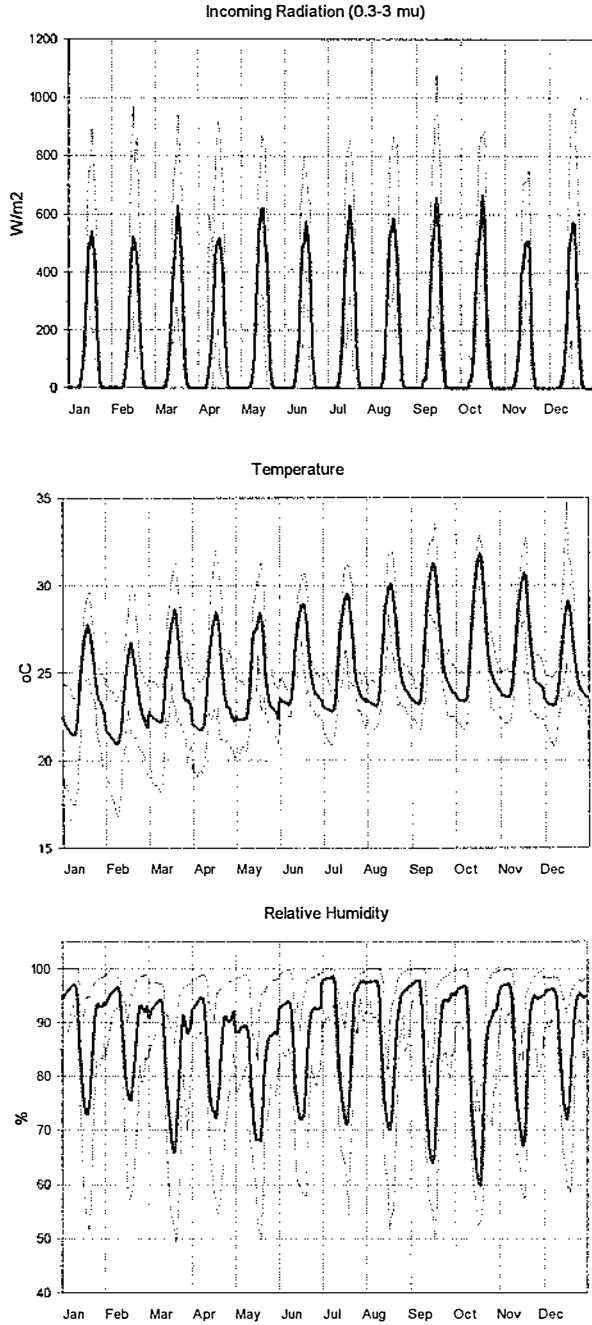


Figure 2.7

Mean (thick line), minimum and maximum (dotted lines) daily course for each month in 1992 of: a) incoming shortwave radiation (R_{in}) from 0.3 to 3 μm ; b) air temperature (temp) in $^{\circ}\text{C}$; c) relative humidity (RH) in %; d) wind speed (wind) in m/s and e) potential evaporation (PE) in mm/h.

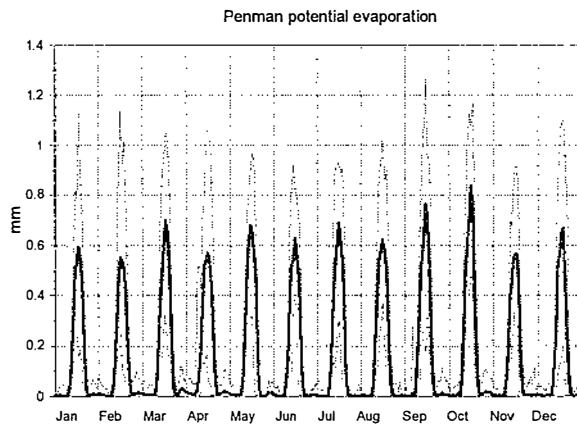
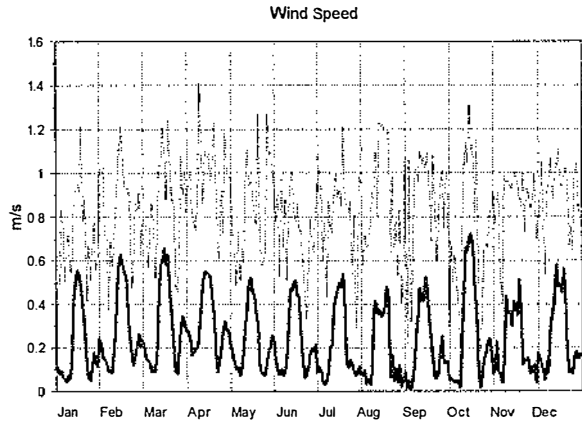


Figure 2.7

Continued.

3 USING SPATIAL ANALYSIS TO COMPARE PATTERNS IN RAIN FOREST WITH ECOLOGICAL GRADIENTS

3.1 Introduction

Analysing a complex plant community such as the lowland rainforest of central Guyana is often done with a detailed inventory of a few plots. The aim of an inventory is to reduce the complexity of the rain forest to a limited number of groups that can be defined in terms of species composition. One of the methods to achieve this is to perform a cluster analysis in order to detect groups of associated species. Also there is often an implicit assumption that under natural conditions there are distinct relations between species composition and ecological conditions, which are described for instance by the soil type, relief, drainage or soil fertility status. Correspondence analysis is one of the most frequently used methods to test this assumption. It was applied successfully for instance to relate topography and topographic disturbance to tree patterns in Puerto Rico (Basnet, 1992), to relate forest type patterns to rainfall distribution in Ivory Coast (Van Rompaaij, 1993), forest types and soil patterns in Australia (Burrough et al., 1977) and vegetation patterns in Oak forest with soil chemistry in North Carolina (Reed et al., 1993).

Species distribution and abundance can be seen as spatial attributes: if a statistical analysis produces groups of species it is often assumed that these groups form contiguous units in the research area. The ecological conditions with which the groups may be associated have a spatial distribution as well. When looking for relations between vegetation and ecological conditions another assumption is made, namely that the two have the same level of spatial resolution, and that both can be mapped coherently at the same scale. Nevertheless the spatial aspects of species distribution in relation to ecological conditions have only recently been considered in vegetation analysis. In a study in the North Carolina woodlands, Reed et al. (1993) emphasized the importance of the scale of observation in relation to the scale of environmental processes which are correlated with the vegetation (in their case the soil chemistry).

To map both vegetation and environment at adequate scales demands a certain support. On the one hand the species diversity of the rain forest induces a certain plot size, which is often large plots (in the order of one to several hectares), but also transects and grids have been used (Williams et al., 1968; Basnet, 1992). On the other hand however, a plot design that enables the study of inter-species association may include a wide range of ecological conditions and it may not provide useful information on relations between species composition and ecological gradients. First soil samples and auger holes have only a very limited size compared to one or more trees. Second, soil types, hydrological properties and relief characteristics may have a spatial variation that can be described at several scales (Oliver & Webster, 1990). Jetten et al. (1993) showed that a different sample supports are needed to map hydrological properties in different soil types in central Guyana (see also chapter 5).

Apart from problems of plot design in relation to spatial variation, there is the problem of how to analyze the variation in species composition accurately. Belbin and McDonald (1993) cite several researchers who suggest that the distribution of species form a continuum along an environmental gradient. They argue that well-defined crisp clusters ("natural groups") may not exist and one can always find a sample with an intermediate composition. If clusters are found in the dataset they could be considered the result of inadequate sampling. Consequently it is unrealistic to force conditions of discreteness and non-overlap on the data, it would be better to use methods that work with continuous variation in both the data and in the geographical space. There are several alternatives to discrete multivariate classification that can be used when variation in data and geographical space is both continuous and overlapping. Fuzzy k-means clustering methods (FKM) allocate individuals to overlapping clusters: an individual is not assigned uniquely to a given cluster but given a value that reflects the degree of membership to that cluster (Vriend et al., 1988; Van Gaans and Burrough, 1993; Triantafilis and McBratney, 1993; Odeh et al., 1992 a,b; De Gruijter and McBratney, 1988). If the coordinates of the plots are known, the spatial variation of the memberships can be mapped.

An alternative to "crisp" or "fuzzy" classification is to perform a multivariate analysis such as correspondence analysis on the species or site data to reduce the data to a limited number of independent dimensions. Each dimension may reflect a particular aspect of the ecological variation in the area, allowing the gradual variation in species composition to be related to the variation of ecological controls. Again, using the geographical location of the plots, the values (or scores) of the plots in the new dimensions can be mapped.

In this chapter crisp classification, fuzzy classification and correspondence analysis are compared, to see which of these methods is best suited to describe the rain forest, in terms of the spatial variation in species composition in relation to soil types and hydrology. To achieve this a tree inventory of an area west of the Tropenbos Ecological Reserve was used. The inventory was done on a regular grid which enabled mapping of the classes, the class memberships and the scores, and comparison with soil types and hydrological information in a Geographical Information System (GIS).

3.2 Methodology

3.2.1 Study site

This study is based on a tree inventory of a 480 ha area in the Waraputa Compartment of the DTL concession, some 20 km west of the Tropenbos Ecological Reserve. The inventory was later updated in this research. In total 252 plots of 0.05 ha were selected on a grid of roughly 100 x 100 m (the sample design is shown in figure 3.3). All trees with a diameter at breast height (DBH) larger than 20 cm were identified. At each plot, species composition, basal area, general relief characteristics and texture class of the topsoil were noted.

In a previous study Ter Steege (1993, see also Ter Steege et al., 1993) analysed this dataset with a divisive clustering and a correspondence analysis. They used the programmes TWINSpan and DECORANA which are designed by Hill (1979 a, b). A detailed explanation of the methods used in the programmes is beyond the scope of this chapter, and an extensive description can be found in Jongman et al. (1987), see also Belbin and McDonald (1993) and Van Groenewoud (1992). The results of TWINSpan and DECORANA are used directly in this chapter and compared with Fuzzy k-means clustering. Since the latter method is relatively new it is explained briefly below.

3.2.2 Soils and topography

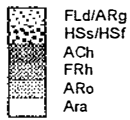
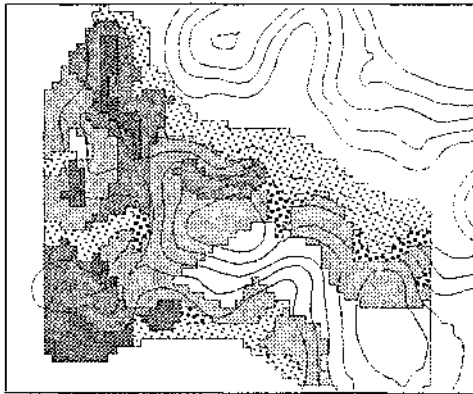
On the basis of the same grid used in the tree inventory, 120 evenly distributed locations were selected where soil auger observations were done to a depth of 120 cm. For each soil horizon texture, colour and consistence were noted, as well as the drainage class, based on the Guidelines for Soil Description (FAO, 1977). From these soil augerings, field observations and a topographical map 1:50,000 a soil map was made at a scale of 1:25,000. In order to avoid defining soil boundaries on the basis of vegetation boundaries, which would confuse the comparison of soil and vegetation patterns, air photo interpretation was not used. The following soil types were found (see chapter 2 for a description):

- Albic Arenosols (ARa)
- Ferralic Arenosols (ARo)
- Haplic Ferralsols (FRh)
- Haplic Acrisols (ACh)
- Dystric Fluvisols and Gleyic Arenosols (FLd and ARg)
- Terric and Fybric Histosols (HSs and HSf)

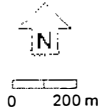
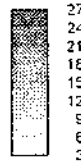
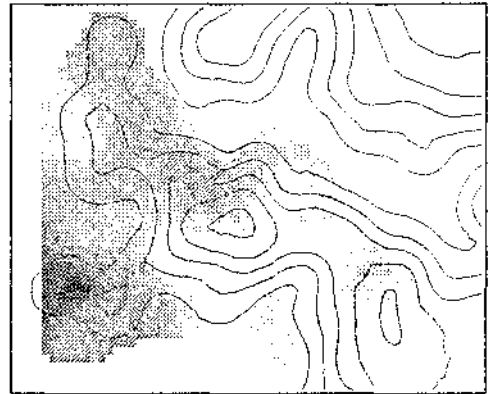
The soil map (figure 3.1a) shows that the Arenosols occur in the central and south eastern part, and the Ferralsols and Acrisols in the western part of the area. To the north and south narrow strips of Fluvisols can be found. Only the larger areas with Histosols are shown as some of the swamps were too small to appear on the map. Isolated patches of Gleyic Arenosols were found but no attempt was made to separate them spatially from the Fluvisols because of insufficient information.

The texture map, i.e. the clay content of the B-horizon, is shown in figure 3.1b. As the silt content of all soils is rather low, the clay content alone represents the texture well. The clay content was not analyzed but was based on the average value belonging to the texture class that was allocated in the field. A map of the drainage classes was made based on the 120 augerings (figure 3.1c). The drainage pattern was derived from the digital elevation model by calculating for each grid cell the number of grid cells that are upstream of that location (see below). This results in an "upstream element" map and can be used to define watershed boundaries and potential drainage ways (figure 3.1d).

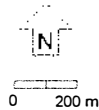
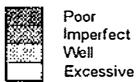
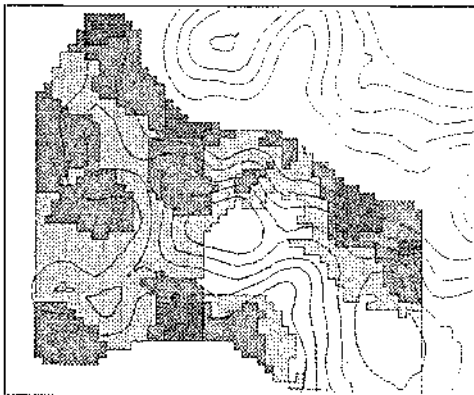
Soil Types



Texture (clay %)



Drainage classes



Upstream elements

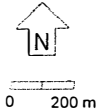
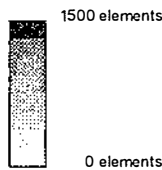
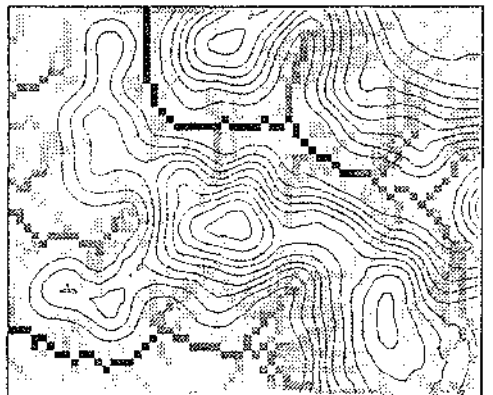


Figure 3.1

Basic environmental information of the Waraputa area. The maps are raster maps with a 50x50 m cell size. a) Soil map with FAO classification; b) Texture map based on clay percentage; c) Drainage classes; d) Upstream elements (see text for explanation).

3.2.3 Forest types

On the 252 plots, a 111 different species of trees with a DBH larger than 20 cm were found in a total of 2952 individuals. The floristic composition of the area is described in detail by Ter Steege (1993), who gives a full list of species and authorities. Seven species have a very high abundance: 68% of all individuals are accounted for by *Eperua rubiginosa* (25.0%), *Dycimbe altsonii* (16.2%), *Eperua grandiflora* (8.1%), *Eperua falcata* (6.4%), *Eschweilera sagotiana* (6.3%), *Chlorocardium rodiei* (5.4 %) and *Mora gonggrijpii* (2.8%). Together they make up 76% of the total basal area.

The cluster analysis with TWINSpan resulted in 8 clusters, based on species with more than 10 individuals. TWINSpan does not use the species count directly but reclassifies the dataset into 6 logarithmic abundance classes (with 1, 2, 3-4, 5-8, 9-16 and > 16 individuals). Also a correspondence analysis was done with DECORANA using both reciprocal averaging and detrended correspondence analysis (Jongman et al., 1987), which showed that there existed a strong relation between species composition and a gradient from sandy soils in the east of the area, to loamy soils in the west. Based on these analyses, and earlier definitions of vegetation types of the region, Ter Steege et al. (1993) distinguished 5 main forest types:

- **Dry Evergreen Forest (DEF)** on excessively drained Albic Arenosols, dominant species are *Eperua falcata* and *Eperua grandiflora*. Other common species are *Tovomitia* sp., *Swartzia* sp., *Aspidosperma excelsum* and *Catostemma fragrans*. *Ormosia coutinhoi* is found near the borders with wetter areas.
- **Mixed Forest on poorly drained soils (MFpd)** often found in wetter areas such as creek heads and valleys on Ferralic Arenosols and Haplic Ferralsols. Dominant species are *Eperua rubiginosa*. Co-dominant are *Eschweilera sagotiana*, *Chlorocardium rodiei* and *Mora gonggrijpii*.
- **Mixed Forest on well drained soils (MFwd)** often found in dryer areas on the watersheds, on Ferralic Arenosols and Haplic Ferralsols. Dominant species are *Chlorocardium rodiei*, *Eschweilera sagotiana* and *Dycimbe altsonii*.
- **Palm-swamp Forest (PSF)** on Histosols, dominant species are *Eperua rubiginosa* and *Dycimbe altsonii*. Other common species are *Eperua falcata*, *Diospiros ierensis*, *Jessenia bataua*, *Tabebuia insignis*, *Trypanthera lancifolia*, *Symphonia globulifera* and *Couratari* cf. *gloriosa*.
- **Creek Forest (CF)** on Fluvisols and Gleyic Arenosols, dominant species are *Eperua falcata* and *Catostemma* sp. Other common species are *Eperua rubiginosa*, *Chamaecrista adiantifolia* and *Diospiros ierensis*.

3.2.4 Theory of fuzzy k-means clustering (FKM)

Conventional k-means clustering is an iterative partitioning of cases among sub-groups or clusters whereby the maximum distance of a case to its cluster centre is minimized (Vriend et al., 1988). Cases are unambiguously allocated to only one cluster based on the chance that this is the most likely configuration. The influence of cases that might belong to two or more clusters or none of the clusters is large on

the cluster they are assigned to and nil on the other clusters, which distorts the representation of the data. Using the concept of fuzziness, as introduced by Zadeh (1965), Bezdek et al. (1981) designed a fuzzy k-means cluster method (FKM) that allowed for some "fuzziness" or "vagueness" in the description of the cluster model (the method is also known as Fuzzy *c*-means clustering). The emphasis is put on how much a case and a cluster are alike, rather than looking for the largest chance that a case belongs to a cluster. In fuzzy models, similarity is indicated by a continuous membership function that ranges between zero (completely different) to one (exactly the same). The memberships of a case to all clusters sum up to unity. The reader is referred to Burrough (1989), Burrough et al. (1992), Van Gaans and Burrough (1993), Vriend et al. (1988), Triantafilis and McBratney (1993) and De Gruijter and McBratney (1988) for a comprehensive description of fuzzy mathematics and its application in soil science and soil chemistry, and to Moraczewski (1993) for its application in phytosociology.

The algorithms used to define the cluster centres and case memberships are defined as follows. Suppose that there are *n* cases (index *i*), *m* variables (index *j*) and *c* clusters (index *k*). The cluster centre *C_c* for the *k*th cluster, is then calculated from all individuals *x_{ij}* by (Vriend et al., 1988):

$$C_{c_{kj}} = \frac{\sum_{i=1}^n (u_{ik})^q x_{ij}}{\sum_{i=1}^n (u_{ik})^q} \quad i=1..n; j=1..m; k=1..c \quad (3.1)$$

with the membership *u_{ik}* of case *i* to cluster *k* calculated with some measure of distance to the cluster centre *d_{ik}*:

$$u_{ik} = \frac{(d_{ik}^2)^{-1/(q-1)}}{\sum_{k'=1}^c (d_{ik'}^2)^{-1/(q-1)}} \quad k'=1..c \quad (3.2)$$

The exponent *q* determines the extent of membership sharing between fuzzy clusters (Bezdek et al., 1981). There is no physical meaning to *q*. If *q* = 1 the fuzzy clustering converges to a normal k-means clustering, whereas if *q* becomes +∞ there is extreme fuzziness and all cluster centres converge to the overall centre of the data cloud. Several measures of distance *d_{ik}* from a case to a cluster centre in the data space are available. One can use simply the Euclidian distance:

$$d_{ik}^2 = \sum_{j=1}^m (x_{ij} - C_{c_{kj}})^2 \quad (3.3)$$

Other distance measures are the Diagonal distance, in which case attributes are scaled to have equal variance, or the Mahalanobis distance, in which case not only differences in variance but also correlations between variables are used (De Gruijter and McBratney, 1988). These distance measures can be used if the variables have a

different order of magnitude. As this was not the case in this study (the species abundances are of the same magnitude), ordinary Euclidian distance was used.

Although the species abundances in this study are more or less log-normally distributed, but at the same time many plots also have abundances of zero for most of the rarer species, a log transformation was not done. Instead the same 6 abundance classes were used as in the TWINSpan clustering: the data were classified in classes with 1, 2, 3-4, 5-8, 9-16 and > 16 individuals (see above).

In both conventional and fuzzy clustering the number of clusters to be created is predefined. Several numbers of clusters have to be tried or a suitable number selected on basis of a priori knowledge. The user has to decide on the best number of clusters, based on the cluster contents and the number of iterations required. In this study the forest types defined by (Ter Steege et al., 1993; Ter Steege, 1993) were used as a starting point.

3.2.5 Spatial analysis

The plot design enabled mapping of all the variables involved. Continuous maps were made of the FKM cluster memberships as well as of the DECORANA axis scores using Ordinary Kriging as spatial interpolation technique. It is beyond the scope of this chapter to describe in detail the spatial interpolation procedure and extensive literature can be found on the subject (Isaaks and Srivastava, 1989; Webster and Oliver, 1990; Burrough, 1986). The memberships are scaled between 0 and 1 and not normally distributed. Therefore they were transformed with a logit function, and the resulting maps were retransformed.

All maps were constructed and analyzed with the PCRASTER geographical information system (Wesseling et al., 1993; Pebesma, 1993). Discrete maps were made of the soil types and soil properties and a drainage pattern map was created from the digital elevation model of the area with the WATERSHED programme (Van Deursen, 1992). For every grid cell this programme searches for the cell that drains towards it. In an iterative procedure artificial obstructions are bypassed and each cell receives a value corresponding to the number of cells upstream of it (a so called upstream element map is constructed). Thus the outlet of the catchment has a value corresponding to the size of the catchment (e.g. the value 1500 in figure 3.1d). All maps presented here have a resolution of 50 x 50 metres.

3.3 Results and interpretation

3.3.1 Relation of TWINSpan forest types with soils and drainage

From the definitions given above and the average forest type composition given in figure 3.2, it seems that the forest types are all based primarily on the dominant 7 species and the reasons for classification, i.e. the species on which the clusters are defined, are quite clear. In this dataset however, the absence of one or two species

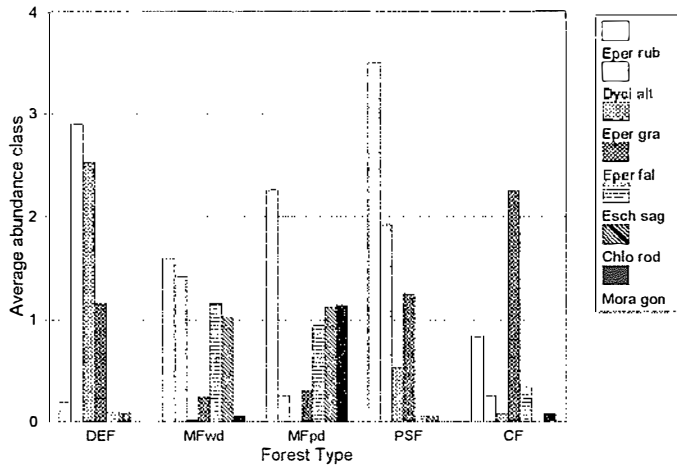


Figure 3.2 Mean species abundance for each forest type (based on 252 plots). For abbreviations see text.

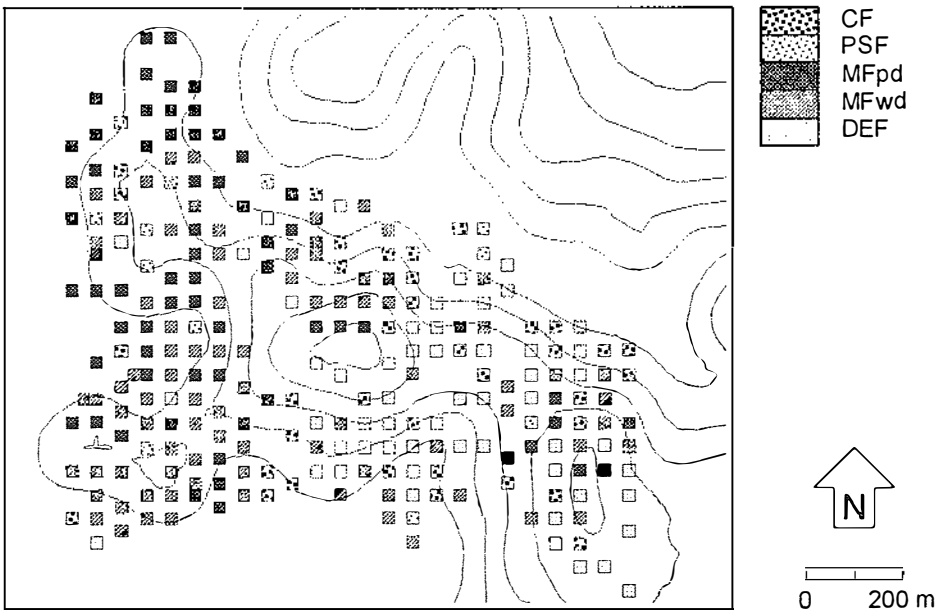


Figure 3.3 Sample design of 252 plots with the 5 main forest types (see text).

defines the forest type rather than a typical and singular species composition. Thus with the spatial variation in abundance of a species the forest types alternate from place to place and a map of the forest types shows an alternating classification from location to location which is difficult to interpret (see figure 3.3). Although there are some contiguous areas where a single forest type is present (e.g. patches of DEF in the centre and south east, and patches of Mixed forest in the south west), the classification alternates over short distances and a coherent forest type map could not be made.

The names and descriptions of the forest types suggest a strong relation with soil and hydrology. Figure 3.4a shows the frequency of occurrence of a forest type on a soil type. Almost all forest types appear on every soil type. Nevertheless there are some preferences: Dry Evergreen Forest is associated strongly with the Albic Arenosols although it also occurs on Histosols and Fluvisols. The Mixed forest types have a strong preference for Ferralic Arenosols, Haplic Ferralsols and Haplic Acrisols, with MFpd occurring more on the loamy FRh and ACh. Apparently there is a slight preference of MFpd for FRh and MFwd for ACh, which is contrary to what was expected because the Acrisols have a weakly developed clay illuvation B-horizon and are usually less well drained than the Ferralsols. However depending on the actual location in the field both soils can be imperfectly or well drained. Palm Swamp Forest and Creek Forest both have a weak preference for Histosols and Fluvisols, but these soil types are not differentiating factors to distinguish between PSF and CF. Figure 3.4b shows the frequency of occurrence of a forest type on a soil with a given drainage class. Again there are preferences with DEF mainly on excessively drained soils and the "wet" forest types PSF and CF occurring mostly on poorly drained soils, but there is no indication that drainage is a differentiating factor to distinguish the Mixed Forest types.

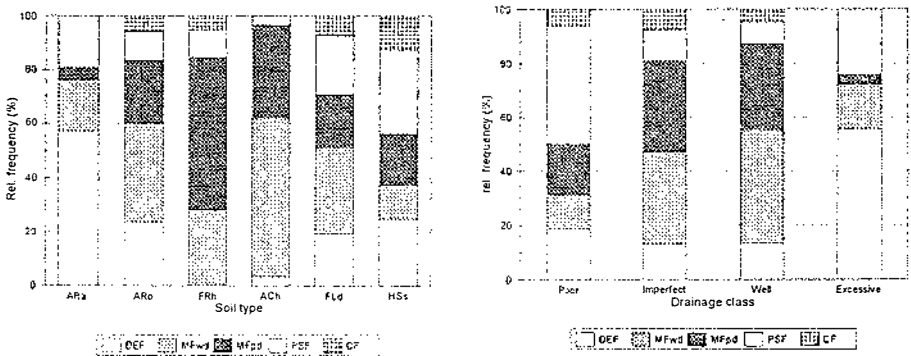


Figure 3.4 Relative frequency of occurrence of the 5 forest types on a) the 6 soil types and b) the 4 drainage classes (based on 252 plots).

Thus the forest types are based on the species composition alone, and there is only a weak relation with soils or drainage classes, contrary to what the names suggest. The names are probably based on the preferred habitat of some of the indicator species. For instance *M. gonggrijpii* generally prefers wetter sites than *D. altsonii* (Ter Steege, 1993), which are the main species on which Poorly drained and Well

drained Mixed Forest are separated. However the other species may have their own environmental preferences. Also *E. rubiginosa* is abundant in both the MF types, while it occurs throughout the study area with the exception of water divides. Thus both MF types contain this species which confuses an interpretation based on environment.

3.3.2 Fuzzy clustering

Fuzzy k-means clustering was done using a computer program developed by Bezdek and modified by Van Gaans and Vriend (1988). The same dataset as in the TWINS-SPAN analysis was used, with a reclassification into abundance classes (see above). A value of $q=1.5$ gave the best results. Clustering was very consistent: various runs with the program using different species as a starting point for the iterations gave virtually the same cluster centroid composition.

Up to 5 different clusters could be distinguished, six or more caused a repetition of clusters. This supports in fact the decision to define 5 forest types out of 8 TWINS-SPAN clusters by Ter Steege et al. (1993). However the species composition of the clusters was quite different from that of the forest types, in particular for *E. rubiginosa*, which is the most abundant species. The first division in TWINS-SPAN was not based on this species, so that it occurred in both branches. However, FKM places all plots with a large abundance of *E. rubiginosa* in one cluster. Also the 5 forest types are not very well related to soil type or drainage class, so that they cannot be distinguished on the basis of environment. On the other hand, the spatial relation between forest types and environmental factors, and the methods to analyze this, are the goal of this study. Therefore it was decided to distinguish only three broad forest types: Dry Evergreen Forest (DEF), Mixed Forest (MF, consisting of the forest types "well drained" and "poorly drained" Mixed Forest) and a group which is called Wet Forest (WF) in this study, which represents both PSF and CF.

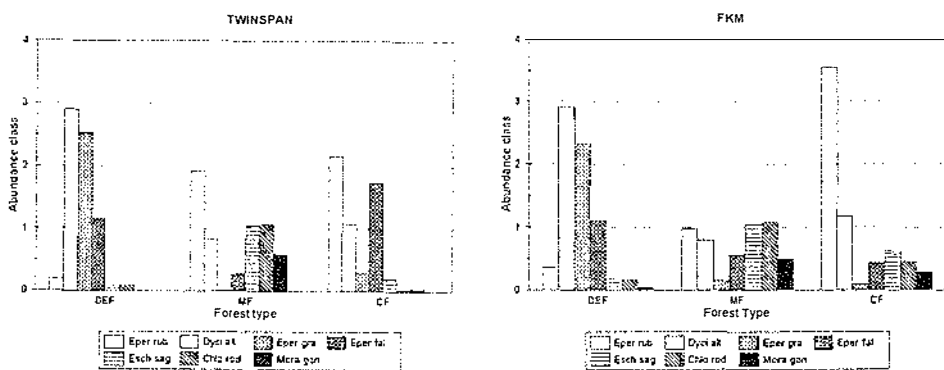
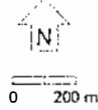
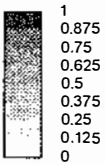
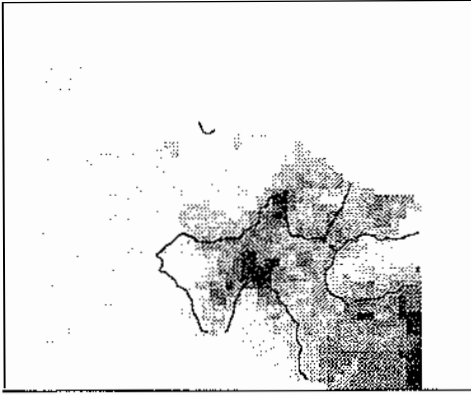
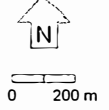
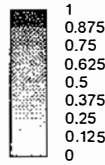
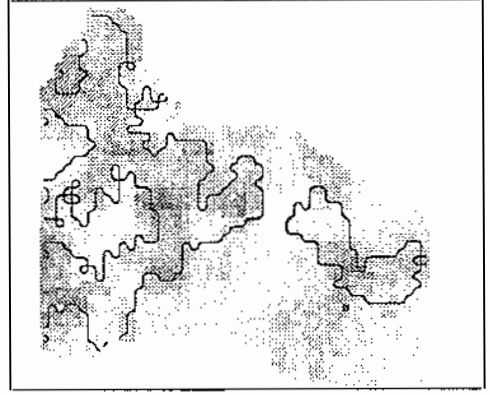


Figure 3.5 a) Mean species composition in Dry Evergreen Forest, Mixed Forest and Wet Forest based on the TWINS-SPAN clustering; b) The cluster centres given by the FKM clustering. The Y-axis shows the mean abundance class that is used in TWINS-SPAN and FKM (see text).

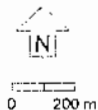
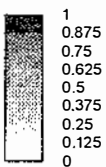
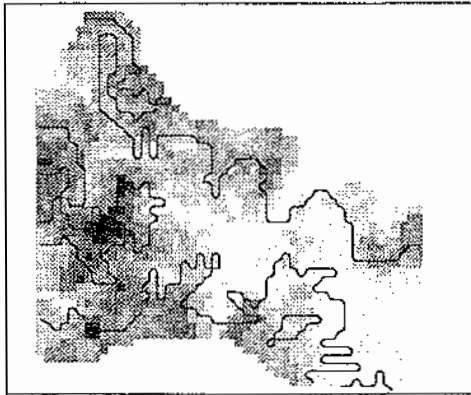
FKM membership to Dry Evergreen Forest



FKM membership to Mixed Forest



FKM membership to "Wet" Fores



Maximum FKM membership of 3 clusters

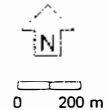
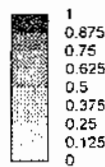
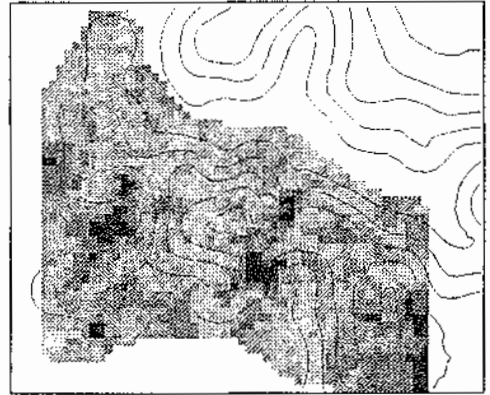


Figure 3.6

Interpolated memberships of the 3 forest types: a) Dry Evergreen Forest; b) Mixed Forest and c) Wet Forest. d) Maximum membership to any forest type (maximum of a to c). The isolines represent maximum combinations of soil properties and drainage (explained in section 3.3.3).

Figure 3.5 shows the average plot composition of these 3 forest types for both cluster methods. In case of the TWINSpan clustering the forest type composition is calculated from the mean abundance class of a species. In case of FKM the plot composition in figure 3.5b is the cluster centre given by the FKM programme, which can also be seen as a representation of the average plot composition. Dry Evergreen Forest and Mixed Forest are similar, whereas *Eperua rubiginosa* is associated more with Wet Forest in the FKM clustering than in TWINSpan. However, other species mentioned in the forest definition (such as *Tabebuia insignis*, *Chamaecrista adiantifolia* and *Diospyros ierensis*) also occur in the third cluster defined by FKM indicating that this cluster can be identified as Wet Forest.

To investigate the spatial variability of the FKM forest types in the area, maps were made of the memberships. Figures 3.6a to 3.6c show that DEF is spatially well defined with large contiguous areas in the south-east and cells with memberships above 0.9. Mixed Forest is less well defined with maximum memberships around 0.75, and only a small area with memberships above 0.5. Wet Forest is better defined with large contiguous areas in the west and south-west and memberships above 0.9. Figure 3.6d shows the maximum membership to any of the forest types. It seems that large areas do not belong clearly to any of the forest types. This is made clear by a frequency diagram in figure 3.7 of all cell values in figure 3.3d: more than half of the cells have a membership of less than 0.6. (note that, because of the interpolation and retransformation, a few cells have a maximum membership of less than 0.33 which is not possible). Thus even if three broad forest types are distinguished that have a clearly defined species composition, contiguous areas where these forest types occur are hard to find in reality. There are actually several well defined areas with a continuous change in between.

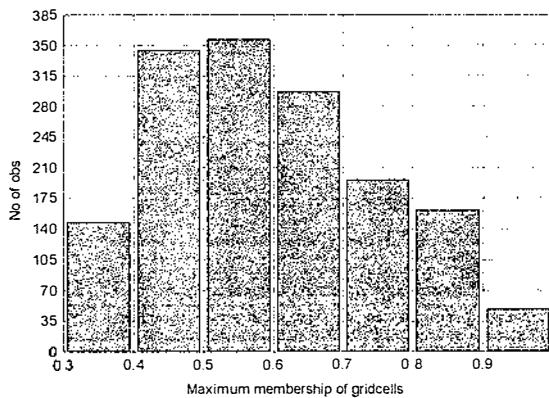


Figure 3.7 Frequency diagram of the memberships of all cells of in the "maximum membership map" (figure 3.6d).

3.3.3 Comparison of the FKM forest types with soils and hydrology

The FKM clusters are not restricted to a given soil type (figure 3.8). However, there is some relation with soil type in the sense that DEF has a preference with ARa and very low memberships on the loamy soils (FRh and ACh). Wet forest has a preference for these loamy soils. The membership to WF is even slightly larger than on the Fluvisols and Histosols. Average membership to Mixed Forest is very low for all soil types. The reason for these preferences can be found in the species composition: the separation of MF is based on the abundance of *C. rodiei*, *E. sagotiana* and *M. gonggrijpii*, which occur also in the Wet Forest cluster. In the latter *E. rubiginosa* dominates which is species with the highest abundance and widespread throughout the area (Ter Steege, 1993).

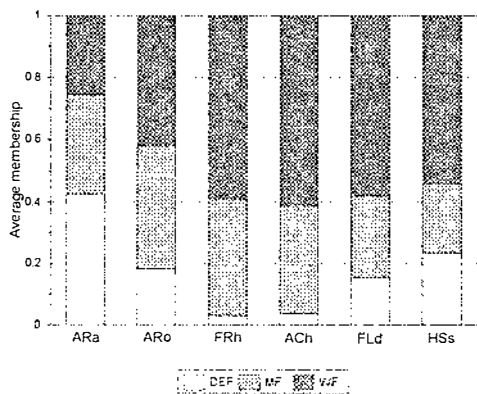


Figure 3.8 Average membership of the 3 forest types on each of the 6 soil types.

Comparing the spatial distribution of the membership values (in figure 3.6) to the soil map (in figure 3.1a) gives an idea where the maximum memberships occur. Highest values for DEF are found on ARa in the south east and also on the Fluvisols in the north east. Highest MF memberships are found on isolated areas of ARo, FRh and ACh. Wet Forest has no preference for any soil type (except that it does not occur on ARa) but occurs in lower wet areas. Because the area the formed mainly by a process of headward erosion by the creeks, wetter areas can be found on any of the soil types. Also the wet clusters may actually appear on Histosols areas, of which were often too small to be mapped at this scale.

Clearly soil types can only explain the membership patterns in the sense that a forest type is absent on a given soil type, in stead of preferring one. Soils are classified mainly on pedogenetic aspects and soil properties such as texture and drainage can vary within a soil type. Therefore the texture, the drainage class and the surface drainage maps (figures 3.1b to d) are included in the spatial analysis of the forest type patterns. The best combinations of these factors that coincide with the spatial distribution of the memberships, are included in the membership maps as isolines (the black lines in figures 3.6a to 3.6c).

Dry Evergreen Forest is strongly related to a sandy texture which includes both the ARa area and some of the areas on FLd in the north east (the line in figure 3.6a is the 5% clay isoline). Although part of the sandy area certainly has low values for DEF membership, the reverse holds true in the sense that all high DEF membership areas are contained within the 5% clay isoline. The fact that the drainage for ARa is excessive and for FLd is poor is not a contradiction, because the dominant species within DEF (*E. grandiflora* and *E. falcata*) can occur on a wide variety of soils and tolerate a wide range of drainage situations (Ter Steege, 1990, 1993).

The spatial pattern for Mixed Forest seems to follow the water divide between the two creeks. Selecting from the upstream element map (figure 3.1d) all cells with less than 4 upstream elements results in a map of the water divide. If this map is combined with the loamy soil types (ARo, FRh and ACh) the resulting area envelops the areas with a high MF membership values quite well. This selection can be interpreted in hydrological sense as an area which is well but not excessively drained while at the same time having a sufficient water holding capacity of the root zone. This is the preferred habitat of the three dominating species *E. sagotiana*, *C. rodiei*, and *M. gonggrijpii*, whereby the latter two species are often found on a gradient from dry to wet (Ter Steege, 1993).

Although spatial distribution of Wet Forest is related to wet areas, these areas are rather difficult to select from the maps because many factors determine if an area is wet (relief, drainage, flooding frequency). Nevertheless an area can be selected that envelops more or less the cells with higher memberships. It is based on a selection of cells which surround the drainage channels (in this case more than 6 upstream elements), combined with the Fluvisols, Histosols and Acrisols, which are soils that either have a poor drainage, a high flooding frequency or a large water holding capacity.

3.3.4 Interpolation of DECORANA results

Often the relation between species abundance and environment is studied with correspondence analysis. Ter Steege et al. (1993) analyzed this dataset with DECORANA. Using reciprocal averaging, they found two ecological gradients that were strongly related to the species composition of the forest types. Scores along the first axis were related to a division in two broad soil type groups, namely the Arenosols on the one hand and the Ferralsols and Acrisols on the other hand. The second axis scores were related to a hydrological gradient within these soil types, which could be a result of the soil properties: there is a very large difference between the soils in terms of water retention capacity, infiltration and drainage characteristics (Jetten et al., 1993). However the hydrology is also strongly related to the relief, as the groundwater table is very deep on the water divide and near the surface in the floodplains.

This interpretation is supported by a spatial interpretation of the axes scores. Figure 3.9a and b show the maps of the scores for axes 1 and 2, which explained respectively 43% and 25% of the variance. The correspondence of the first axis scores with the texture map is striking, the isolines in fig 3.5a are texture contours with a 2.5%

clay content interval. The high scores are found on the soils where clay is almost absent, i.e. on ARa and parts of FLd in the west. Low scores are found on soils with a high clay content, especially ACh in western part of the area. Moreover, the scores follow a gradient in texture within the ARO and FRh, which are soil types that contain a variety of texture classes, from loamy sands to sandy clay loams. However, because the clay content is only an estimation from hand determined classes, a further quantitative analysis is beyond the scope of this study. The second axis compares well with the same selection as was used for Mixed Forest, consisting of a combination of loamy soils (ARo, FRh and ACh) on the water divide (areas with few upstream elements). Thus the high scores are found on the water divide and become lower towards the valley floor (with exception of the very sandy areas which are covered by the first axis).

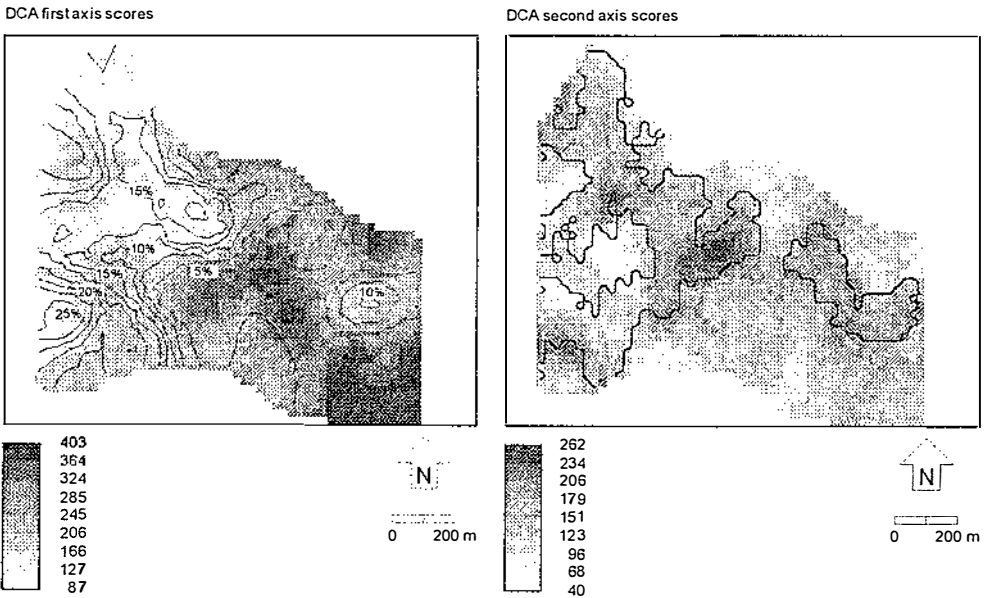


Figure 3.9 Interpolated DCA scores of a) first axis and b) second axis. Isolines are based on a) clay content with 2.5% interval, and b) a selection of loamy soils on the water divide (see also figure 3.6b).

In order to make the maps, Detrended Correspondence Analysis (DCA) was used rather than reciprocal averaging (RA), because with DCA the spatial structure for the second axis was much clearer. The reason for this can be found in the regionalized variables theory: the spatial variation can be mapped adequately only if it is random, i.e. if a possible trend has been removed from the dataset (see also chapter 5). Because the second axis has a parabolic distortion of the scores when using RA (Jongman et al., 1987), there is a definite second order trend which is removed in DCA. Thus although as a scattergram of the plot scores this dataset is better

interpretable using RA (Ter Steege et al., 1993), the DCA scores have to be used to retain the spatial information.

When quantitative environmental data are available it is possible to analyze the scores by means of a regression analysis. However, if the environmental data are only qualitative or classified as in this study, analysis is limited to a visual interpretation of the scattergram of the first against the second axis scores. Although the general conclusions made by Ter Steege et al. (1993) are obviously correct, the GIS greatly enhances the possibilities to explore the data.

3.4 Discussion and conclusions

Some criticism of TWINSpan has been voiced lately, because the method may dichotomise at an inappropriate point along the first axis if the primary gradient is not well defined or if more gradients exist perpendicular to the first (Belbin and McDonald, 1993; Van Groenewoud 1992). However the CA scores maps show a clear relation between variation in the vegetation composition and an east-west texture gradient in the area, with a less clearly defined hydrological gradient from the watershed to the valley floor.

Using TWINSpan yielded 5 groups that were based on only 7 species that dominate the clustering. The indicator species on which the divisions are based are clear and are confirmed with field observations (Ter Steege et al., 1993). On the other hand the fact that the clustering is based on the absence of one or two species, rather than on a clear association of species, is also a drawback. In combination with the small plot size and the need to cover a large area, the spatial variation of these indicator species result in an alternating classification from place to place. This can be dealt with in two ways. Either one accepts a division in 3 broad groups, i.e. Dry Evergreen Forest, Mixed Forest and a "wet" forest type, with local dominance of certain species, or one uses a method such as FKM clustering to show the gradual changes in species composition.

However, retaining information on gradual changes during the clustering process, also gives you more information to deal with. The results are based on multivariate analysis which is more difficult to interpret, especially at locations which do not strictly belong to any cluster. Also FKM clustering is probably influenced by the plot size. On a small plot only a few individuals of a different forest type will cause a low membership. The spatial interpolation adds an uncertainty to the memberships (usually of a known size), and because of the smoothing effects of the interpolation the maps do not add to unity at all locations, nor is the maximum membership always larger than 0.33 (which should be the case with 3 clusters).

The poor results obtained by comparing clusters with soil types is probably not only a result of the fuzziness of the clusters, but also of the quality of the soil map. In the introduction the importance of a correct sample support was mentioned, which applies also to this study. Firstly a crisp classification is used to define the soils while many soil properties behave in a continuous way. Soil boundaries are usually

based on the notion that each soil class can be identified by a central concept, and that sharp boundaries exist between the classes (Burrough, 1989). In reality soils often show a continuous spatial variation and the concept of fuzziness has also been applied successfully in soil classification (see for instance Odeh et al., 1992a, 1992b; Triantafilis and McBratney, 1993; McBratney and De Gruijter, 1990, 1991). However, to achieve this quantitative soil data are needed while here only qualitative field observations were available. Secondly, airphotos can be used to improve the accuracy of the soil map. Because the airphotos were deliberately not used here, the soil sampling was done on a regular grid, which induces a certain level of accuracy. For instance some patches of Histosols were too small to appear on the map. Thirdly a spatial analysis of soil hydrological properties in the Tropenbos Ecological Reserve showed that most properties can be mapped accurately only if the sample points are less than 50 m apart (Jetten et al, 1993). Thus the sample distance in this study (which is 100 meters at its smallest) is inadequate to map spatial variability of hydrological properties.

The results of this investigation with FKM suggest that it is sensible to regard species abundance as a spatial variable, which yields three main, but overlapping forest types: Dry Evergreen Forest, Mixed Forest and Wet Forest (forest on flood plains and swamps). It appears that half of the study area does not belong to any of these 3 forest types for more than 60%. There are several contiguous areas with high memberships but in between there are gradual changes. In general there is a large spatial variability within each forest type. The membership patterns could be matched with a combination of soil types, texture and surface drainage network in a GIS. There appeared to be a strong association between membership patterns, an east-west texture gradient and a hydrological gradient from the water divide to the valley floor.

Spatial interpolation of the DCA scores supported the conclusions from the FKM analysis. Maps of the first and second axis scores were matched with a texture map and a map showing a combination of soil types with drainage pattern, respectively. The mapping of the FKM memberships or the DCA scores both enhance the possibilities for exploratory data analysis, especially when the environmental data are not quantitative. Both methods have their advantages, the first because there is still a clear link between the clusters and the species composition, the second because the DCA gives extra statistical information (such as the explained variance).

4 MODELLING THE ONE DIMENSIONAL WATER BALANCE

4.1 The hydrological framework

A brief outline of the rain forest hydrological cycle is given to define the parts of the water balance and the symbols with which they are indicated. This description is adapted from Bruijnzeel (1989; see also Bruijnzeel, 1990). In subsequent chapters these definitions and symbols are maintained.

Rain is the principle input of forests in the humid tropics, with the exception of forests in coastal fog belts or cloud forests in high mountainous terrain. Figure 4.1 shows the main water fluxes of the lowland tropical rain forest in Guyana. A small part of the rainfall reaches the forest floor. This is referred to as "direct" or "free" throughfall. Of the rainfall that strikes the vegetation, part is intercepted by the canopy and evaporates from the leaves during and after the rainstorm. Most of the water will move downward in the canopy and falls from the leaves to the forest floor. A small part runs via branches and stems downward and is referred to as stemflow. The total of direct throughfall, crown drip and stemflow is referred to as throughfall in this study. The processes involved in interception are described and modelled in chapter 6. The evaporation of intercepted water is often referred to as interception loss, as the water does not become available to the plant for transpiration (Ward and Robinson, 1990). However, when the leaves are covered with a water film this affects the transpiration as the energy needed for transpiration is consumed by the evaporation process. The principles used in the model described in this chapter are discussed below.

The throughfall is intercepted by the litter layer which determines the flow path to reach the stream channel. A small part moves laterally through the litter if the soil is nearly saturated, depending on the conductivity of the litter, the conductivity of the soil and the form of the terrain. The process of surface runoff is described in chapter 7. The remainder of the water infiltrates and moves downward in the soil. There it is partly taken up by the plants as transpiration. The amount of uptake depends on the extent to which the atmospheric demand is modified by the canopy. Transpiration was not measured in this research, but it is modelled with the principles explained in this chapter. Water that moves downward in the soil is generally called percolation. In this research the term percolation is used to indicate the water that has moved below the root zone and is not available for uptake. The speed and quantity of percolation depends on the soil and on its moisture content. The vertical water balance from the top of the canopy to below the root zone is described and modelled in chapter 8. It is assumed that the lateral throughflow above the groundwater is negligible. When the water reaches the groundwater body, it moves laterally towards the stream channel. There it emerges as streamflow. The streamflow or discharge can be separated into a groundwater component known as baseflow and a surface runoff component known as stormflow. The discharge and stormflow of a small catchment are discussed in chapter 11.

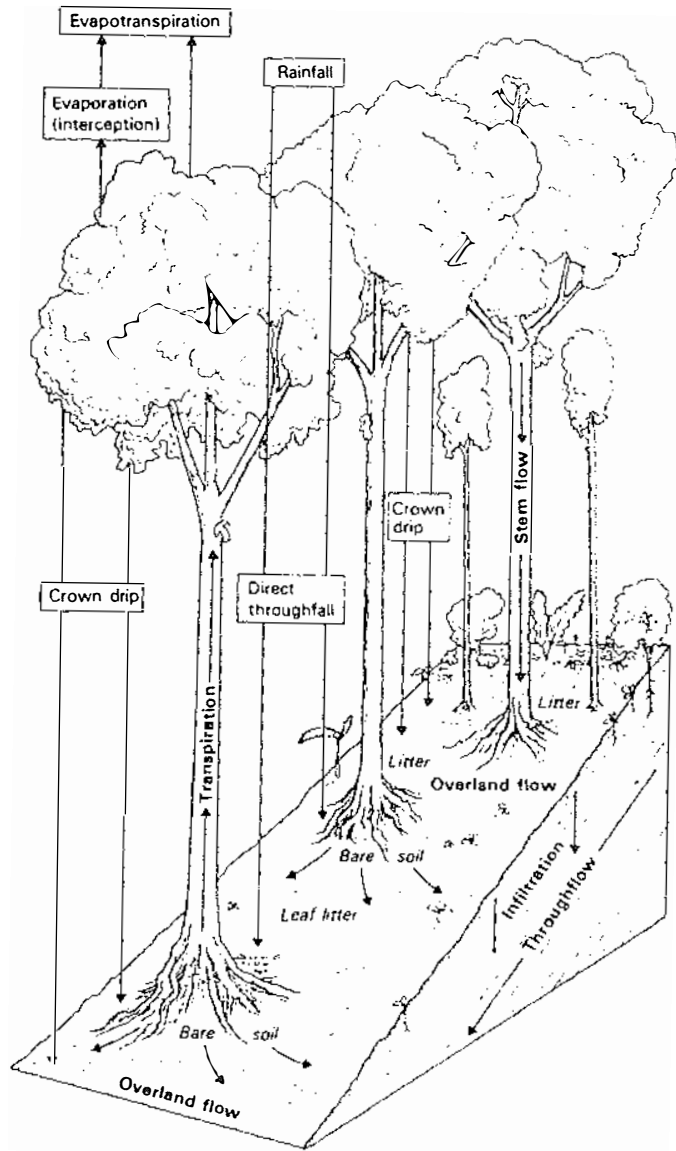


Figure 4.1 The rain forest hydrological cycle (adapted from Douglas, 1977 in Bruijnzeel, 1990).

4.2 The SOAP water balance model

There are many water balance models exist, which have been calibrated for various environments and situations. Most of them are coupled to growth of rainfed or irrigated crops and grasslands, or to land degradation and erosion. They range in complexity from simple empirical relations to energy balance models that are based as much as possible on physical laws. Most models operate in the grey area between empirical and entirely physical, because at the scale of operation processes have to be lumped. For instance one can model the transpiration of a single leaf, but transpiration of a plant or a group of plants is too complicated and often "representative" bulk values for leaf distribution, conductivity etc. are used. The same goes for water flow in the soil which is very difficult to model in more than one dimension, or even in one dimension while fully retaining variability of soil properties. Well known one dimensional water balance and crop growth models are SWATRE and derivations (Feddes et al., 1978), GAPS (Riha, 1990), WOFOST (Van Keulen and Wolf, 1986), whereas GIS based distributed erosion models are for instance ANSWERS (Beasley et al., 1980; De Roo, 1992), LISEM (De Roo et al., 1994).

In forest research that includes the one dimensional water balance, the emphasis is usually put usually on the above ground water fluxes, i.e. interception, evaporation and transpiration. Examples of such water balance studies in temperate forests are Draaiers (1993) who investigated atmospheric deposition and acid rain, Dolman (1987) and Bouten (1992) who emphasised interception and transpiration. Sellers and Lockwood (1981) couple a multi layer vegetation model to the soil water balance, which is modelled as a single container. The SWIF model, Soil Water in Forested Ecosystems (Bouten, 1992), is probably one of the most extensive models in forest water balance research to date, designed in a research programme of the effects of acidification of the forest in the Netherlands. It couples a finite difference solution of the soil water balance to extensive transpiration and interception modelling. Unfortunately SWIF was not available at the time this research was carried out.

In modelling of the tropical rain forest water balance the emphasis is put on transpiration, such as in the research of Shuttleworth et al. (1984) and Roberts et al. (1993) who designed the CLATTER model based on data of the Reserva Ducke near Manaus, or on photosynthesis and respiration, such as in the research of Allen and Lemon (1976) in Costa Rica, or nutrient balance research such as done by Stoorvogel (1994) in Ivory Coast. The latter research resulted in the model DYNAMITE (Noij et al., 1993) which was also developed as part of the Tropenbos Programme. However, DYNAMITE emphasises the nutrient balance while the hydrological part is greatly simplified and based on monthly data. So it is not suitable for modelling the effects of low intensity logging in the Mabura research area.

When this research started, no forest water balance model was readily available, so parts of other models were combined in a PASCAL computer program. The resulting model is called SOAP: SOil Atmosphere Plant model. The idea of constructing a new model was not to add yet another one to the list, but to retain full flexibility and compatibility with the type of data measured in the Tropenbos research in Guyana.

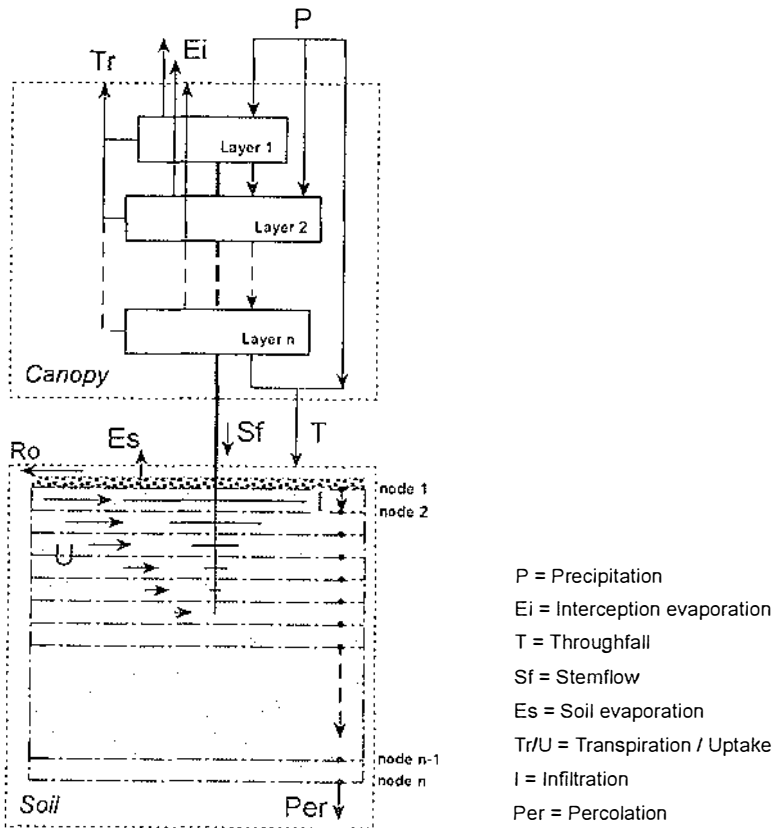


Figure 4.2 Flow diagram of the SOAP water balance model.

Figure 4.2 gives a flow diagram of SOAP with the symbols for the water fluxes. It is identical to the conceptual framework of the rain forest (see above). There are two subsystems, the above ground water balance which is indicated with the term "canopy", and the below ground water balance which is indicated with the term "soil". These subsystems are both divided into a number of layers and nodes for which the temporal change in water content is calculated. The modelling techniques with which this is done are explained below. The *Soil*-subsystem forms the basis of the model and it is described first.

4.3 The *Soil* subsystem

4.3.1 Principles of one dimensional flow

Water flows in unsaturated soil in response to a difference in potential (Ψ). In a situation where there is no overburden pressure on the soil, no external gas pressure and the osmotic pressure of the water is negligible, the two main potentials are the matric potential (ψ_m) which arises from local interactions between the water and the soil matrix, and the gravitational potential (ψ_g). The mass conservation law states that a change in water content (θ) with time on a particular location in the soil equals the change in water flux (Q) on that location. A source or sink term (S) is added to include addition or extraction of water to or from the system (e.g. by irrigation or plant uptake):

$$\frac{d\theta}{dt} = \frac{dQ}{dz} + S \quad (4.1)$$

The flux can be described by Darcy's law, which in its one-dimensional form for vertical flow is written as:

$$Q = K \frac{\delta \Psi}{\delta z} \quad (4.2)$$

where K is the hydraulic conductivity. Expressing the potentials in terms of head, the matric potential is translated to a (negative) pressure head or suction head h (with dimension L) and gravitational potential is written as elevation z relative to the surface (with dimension L). The hydraulic conductivity $k(h)$ is a non-linear function of the pressure head (LT^{-1}). A negative sign indicates a direction upwards:

$$q = -k(h) \cdot \frac{\delta(h - z)}{\delta z} = -k(h) \left(\frac{\delta h}{\delta z} - 1 \right) \quad (4.3)$$

Combining equations 4.1 and 4.3 and introducing the differential soil water capacity $C(h)$ (which equals $\delta\theta/\delta h$), the well known Richard equation is obtained:

$$C(h) \frac{\delta h}{\delta t} = \frac{\delta}{\delta z} \left[-k(h) \left(\frac{\delta h}{\delta z} - 1 \right) \right] - S \quad (4.4)$$

In the forest water balance S represents water extraction by plants only and is therefore negative. It is expressed as volume of water extracted from a unit volume of soil per unit of time (T^{-1}). Equation 4.4 has the advantage of being applicable to the entire flow domain, including saturated and partially saturated flow. Furthermore the use of h instead of θ as the dependent variable enables the calculation of flow problems in a layered soil, because h remains continuous at the layer boundaries.

4.3.2 Numerical solution of the flow equation

The partial differential flow equation is highly non-linear because both hydraulic conductivity and pressure head depend on water content. Closed form analytical solutions are only possible under for simplified flow cases under restricted conditions (Richter, 1990). A numerical solution must be applied to the flow problem whereby a discretization scheme is applied to the soil depth-time domain. A system of nodal points is superimposed on this domain and combined with boundary conditions to obtain a set of linear algebraic equations that can be solved by various methods. Best known are finite difference and finite element techniques (Feddes et al., 1988; Laible et al., 1984).

The reasons for choosing between a finite difference method or a finite element method is rather arbitrary. Both methods are able to address a wide range of flow problems, ranging from rapid changing boundary conditions under infiltration, to fluctuating groundwater tables on less permeable layers. Finite difference methods are the most frequently used and well documented (Richter, 1990; Feddes et al., 1988; Campbell, 1988). However, for a stable system there either is a strict relation between the distance between the nodes and the size of the time step (in case of an explicit solution), or calculation times are longer (in case of an implicit solution, Richter, 1990). On the other hand solutions based on FEM are usually very fast. Calculation speed becomes important when the water balance is calculated for long periods of time rather than for single rainstorms. Also in the case of distributed modelling, when the flow problem has to be solved for many landscape elements (such as in a system of grid cells), speed is essential.

In a complex landscape many different hydrological situations occur: spatial variation of soil properties, moisture conditions, presence of groundwater and influence of different vegetation types. Within an area that is ecologically more or less similar a model should be able to handle all the hydrological situations that may occur. Moreover, the changes in soil hydrology caused by forest exploitation vary from insignificant to extreme, from very lightly disturbed to a non-forest situation. A robust model is needed that is able to handle such a wide variety of circumstances. As Feddes et al. (1988) state, finite element methods are capable of solving complex flow geometries, nonlinear and time-independent boundary conditions, while they possess a high flexibility in following rapid soil water movement. Thus, considering calculation speed and the complexity of a tropical rain forest system, The water balance model used in this research is based on a finite element solution.

The infiltration module is based on a finite element solution designed by Van Genuchten (1987), see also Neuman et al. (1974). He developed a model for irrigation purposes with special emphasis on solute transport and crop water use. This model was modified by Dirksen et al. (1993) to include hysteresis, while modifying some of the iteration procedures. The result is a very robust and fast model, of which the iteration scheme was used directly in SOAP. However, several modifications were made to adapt the model to a forest environment. In particular a transpiration and interception model were added, while the top boundary conditions were modified to make the rainfall or throughfall input more easy.

The full numerical implementation of the FEM scheme used in SOAP will not be repeated here. A comprehensive explanation is given by Van Genuchten (1987), and also by Neuman et al. (1974) and Bruch (1975). Principles of finite element simulation can be found in Pinder and Gray (1977) and examples for groundwater and surface hydrology in Laible et al. (1984). In principle the soil profile is divided into a series of equally sized layers (or elements). Nodes are allocated along the boundaries between the layers and a system of linear equations is designed to estimate the pressure head (see figure 4.3). For each time step the linear equations approximate the actual pressure head as a function of depth and time $h(z,t)$. Thus each node is defined by has two linear functions that represent the line to the node above and the line to the node below. These functions can be used to solve the Richard's equation which for the system of nodes has the form (Feddes et al., 1988):

$$[A]\{h\} + [B]\frac{d\{h\}}{dt} + \{F\} = 0 \tag{4.5}$$

where:

- [A] = tridiagonal conductivity matrix
- [B] = tridiagonal differential moisture capacity matrix
- {h} = pressure head vector
- {F} = combination of gravity term, sink term and boundary conditions vectors

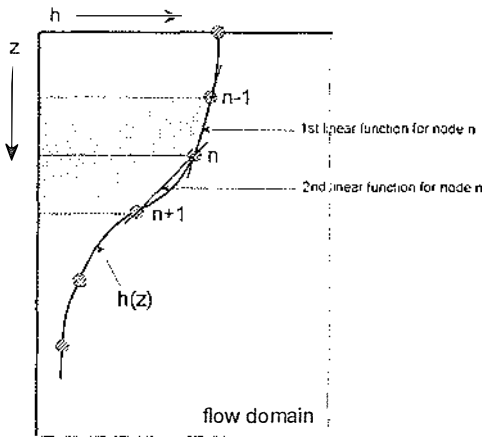


Figure 4.3 The flow domain with the actual pressure heads (h) and the shape function with which h is estimated.

Equation 4.5 is solved by discretization of the time domain and replacing $d\{h\}/dt$ by its finite difference form $(\{h\}^{t+\Delta t} - \{h\}^t)/\Delta t$. A fully implicit scheme with Gaussian elimination is used to solve it at half the time step ($t+0.5\Delta t$) to prevent unwanted oscillations. The error, i.e. the difference between $\{h\}$ of two subsequent iteration steps, is calculated by the difference between the integral of $h(z,t)$. Because $h(z,t)$ is approximated by linear functions, the integral can be simply estimated with the Trapezoidal rule or Simpson's rule.

SOAP uses a variable time step so that the number of iterations is minimal. At the beginning of the time step $h^{t+\Delta t}$ is estimated by linear extrapolation from the previous suction head h^t and that before $h^{t-\Delta t}$. The differential moisture capacity and hydraulic conductivity are calculated from the average of h^t and $h^{t+\Delta t}$ to provide a stable solution. If the difference between h^t and $h^{t+\Delta t}$ is large enough the capacity can be calculated directly from $(\theta^{t+\Delta t}-\theta^t)/(h^{t+\Delta t}-h^t)$, else it is calculated with an analytical function. The hydraulic conductivity is also calculated with an analytical function. The functions are based on the $k(h)$ and $\theta(h)$ relationships defined by Van Genuchten (1980).

4.3.3 Modelling the $k(h)$ and $\theta(h)$ relationships

The relations between suction head h , water content θ and hydraulic conductivity k can be derived from measurements and interpolation. Another possibility is to use mathematical functions for $\theta(h)$ and $k(h)$. Two types of functions are used most frequently (Hendrickx, 1990). Brooks & Corey (1966) (in Campbell, 1988) used a power function to describe the relative water content Se :

$$Se = 1 \quad h \geq h_b$$

$$Se = \frac{\theta - \theta_r}{\theta_s - \theta_r} = (h/h_b)^{-\beta} \quad h < h_b \quad (4.6)$$

where:

- θ_r = residual water content
- θ_s = saturated water content
- h_b = pressure head at air entry
- β = soil related empirical parameter

The discontinuity of the function above a pressure head at air entry point ($h \geq h_b$) is a disadvantage (Hendrickx, 1990) because it may prevent rapid convergence of the numerical solution when parts of the soil are close to saturation. Diekkrüger (1992) compared the function values with measurements and found that the differences were unacceptable if the soil was near saturation or very dry, particularly for sandy soils. He obtained better results by using the function designed by Van Genuchten (1980):

$$Se = [1 + (a|h|)^n]^{-m} \quad (4.7)$$

where a , n and m are parameters that determine the shape of the water retention curve. Furthermore it appears that $m = 1-1/n$ (Mualem, 1976). Thus there are two parameters to be fitted from water retention values. Unfortunately the residual water content θ_r is ill defined. Either the water content of a "very dry" soil is measured (e.g. wilting point) or 5% to 10% of θ_s is taken.

Based on research by Mualem (1976) and equation 4.7, Van Genuchten (1980) designed a similar function for the relative hydraulic conductivity Kr :

$$Kr = k_s Se^\gamma [1 - (1 - Se^{1/m})^m]^2 \quad (4.8)$$

where k_s is the saturated hydraulic conductivity and γ is an empirical parameter. For In this research γ is set to 0.5 (Hendrickx, 1990), while n and a are determined from the moisture retention curve $\theta(h)$ by using a non-linear fitting algorithm. For example the software package CSS-Statistica offers a non-linear fitting module which can handle user-defined functions and several fitting methods.

4.3.4 Upper boundary conditions

Upper boundary conditions are the incoming throughfall flux and the outgoing transpiration and soil evaporation flux. In both cases the potential fluxes are calculated first in the *Canopy* subsystem, after which they are modified in the *Soil* subsystem. If throughfall and evapotranspiration are smaller than the maximum possible flux across the soil surface, the top node is adjusted to these fluxes. On the other hand if these fluxes are too large the maximum possible fluxes and applied.

The throughfall flux is simply added as source term to the first node before the new pressure heads are calculated. If the throughfall is smaller than the maximum possible flux, the actual flux is set equal to the throughfall. If it is larger, ponding occurs and surface storage is allowed to built up. Water in excess of that storage is removed instantly from the *Soil* subsystem as lateral runoff. When ponding occurs the pressure head at the top node $h(z=0,t)$ is set equal to the depth of ponding and the actual infiltration flux across the upper boundary is calculated from the potentials at the first two nodes. The procedures followed to calculate actual transpiration are explained below in the *Canopy* subsystem.

The evaporation of the soil surface is on the one hand limited by the atmospheric demand, on the other hand by the ability of the soil matrix to transport water. Following the method proposed by Feddes et al. 1976) two fluxes are calculated based on the Penman-Monteith potential evaporation and on the soil water potential. The actual evaporation is set to the minimum of these fluxes and the potential of the top node is corrected accordingly. Because the wind speed is nil at the forest floor, the atmospheric potential evaporation (PE_{atm}) at that level is determined only by the net radiation that reaches the surface, and a simplified version of the Penman-Monteith equation can be used:

$$E_{atm} = \frac{\Delta Rn}{L(\Delta + \gamma)} e^{(-k LAI)} \quad (4.9)$$

in which Rn is the net radiation above the canopy ($W.m^{-2}$), Δ is the change of saturation vapour pressure with air temperature ($Pa.K^{-1}$), γ is the psychrometric constant ($Pa.K^{-1}$), L is the latent heat of vaporization ($J.kg^{-1}$), LAI is the canopy leaf area index ($m^2.m^{-2}$) and k is the radiation extinction factor (-).

The maximum evaporation flux determined by the soil is calculated from equilibrium conditions between soil water and atmospheric vapour (Feddes et al., 1988):

$$h_{atm} = \frac{RT}{Mg} \ln(f) \quad (4.10)$$

where:

- R = universal gas constant (Jmol⁻¹K⁻¹)
- T = absolute temperature (K)
- M = molecular weight of water (kg mol⁻¹)
- f = relative air humidity (-)
- g = gravity acceleration (m.s⁻²)

The head h_{atm} is the suction head equivalent of the atmosphere. The maximum flux PE_{soil} corresponding to this equilibrium is calculated from the average h of the first element (at a depth of 0.5dz) and the geometric mean of the conductivities (Feddes et al., 1978):

$$PE_{soil} = -\sqrt{(k_{atm})^2(k_{1/2})^2} \left[\frac{(h_{1/2} - h_{atm})}{0.5 dz} - 1 \right] \quad (4.11)$$

The actual soil evaporation (E_s) is the smallest of PE_{atm} and PE_{soil} . In case PE_{soil} is the smallest the potential of the top node is set to h_{atm} . The evaporation is added to the first node as sink term.

4.3.5 Lower boundary conditions

At the lower boundary of the *soil* subsystem, either free drainage is assumed, calculated from the matric potentials of the last nodes, or a groundwater level is present, which fluctuates according to incoming flux from the node above. If the pressure head at a node becomes positive it is set to zero. A flux out of the system has to be applied to the bottom of the groundwater body to prevent the soil profile from gradually filling up is long periods of time are simulated. This flux is stationary as SOAP is not able to calculate a lateral flux from spatial differences in hydraulic potential. It should have a size that represents adequately a lateral flow of groundwater and it assures a fall of the groundwater table if the influx from above stops. However, simulation with a groundwater table were not done in this research and this procedure is not further tested or developed.

4.4 The *Canopy* subsystem

4.4.1 Canopy structure

In order to simulate the microclimate from the top of the canopy to the forest floor, as well as simulate the interception processes, a vertical representation of the canopy structure is needed. The canopy is divided into a number of layers (see figure 4.4) that each functions as a container in which water is stored and from which evaporation and transpiration take place. The size of each layer is determined by the vertical leaf area distribution. Roberts et al. (1993) give vertical leaf area distributions derived from their own data, from Klinge et al. (1976) and from McWilliam et al. (1993). Figure 4.4 shows the change of cumulative leaf area with height, for a canopy of approximately 35 m high. All values come from Mixed forest in the vicinity of the Reserva Ducke near Manaus (Brazil). The graphs are quite similar

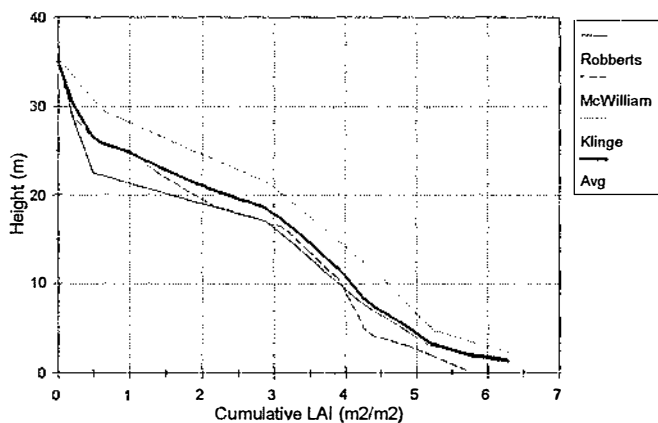


Figure 4.4 Cumulative Leaf Area ($m^2 \cdot m^{-2}$) for Mixed forest near Manaus (data from Roberts et al., 1993).

with the bulk of the leaf mass occurring between 15 and 25 m and an increase near the surface probably related to a dense understorey of seedlings. Table 4.1 shows the average values derived from figure 4.4 used in this study. The layers are defined in such a way that the layer LAI does not exceed $1 m^2 \cdot m^{-2}$ because of the simulation of the interception processes (see chapter 6). The cumulative LAI, including the understorey, is $6.3 m^2 \cdot m^{-2}$. Unfortunately there are no data available for the vertical leaf distribution in Dry Evergreen forest. However, it appears that the interception characteristics (see chapter 6) for both forest types are not significantly different, and the same distribution as for Mixed forest is used in the simulations.

Table 4.1 Vertical structure of the canopy used in the SOAP model

Layer #	Height (m)	LAI m^2/m^2	LAI-cum m^2/m^2
1	35.0	0.25	0.25
2	27.0	0.30	0.55
3	24.0	0.72	1.27
4	20.5	0.85	2.12
5	17.5	0.95	3.07
6	15.0	0.40	3.47
7	12.0	0.50	3.97
8	8.5	0.30	4.27
9	4.5	0.50	4.77
10	3.0	0.70	5.47
11	1.0	0.90	6.37
12	0	0	6.37

4.4.2 Interception and throughfall

A separate module of SOAP deals with the interception and evaporation of water by the forest canopy. It is based on an extension of the model designed by Rutter et al. (1975) and described in detail in chapter 6. The temporal change in water storage of each of the canopy layers is calculated with the layer drainage and evaporation. Thus, in addition to the layer LAI, canopy storage and drainage parameters are needed in SOAP. The evaporation of intercepted water is based on the Penman-Monteith potential evaporation (PE), calculated from the micro climate inside the canopy. The procedures are similar to the calculation of potential transpiration described below. The canopy water balance leads to an estimation of the fraction of each layer that is wet during and after a rainstorm. This canopy wetness fraction influences stomatal behaviour and therefore the transpiration (see below).

4.4.3 Micro climate and transpiration

Transpiration of a crop is often modelled with bulk values that represent the micro climate surrounding the crop. In case of forest however, the micro climate is influenced considerably by the plant structure, and vice versa the stomatal activity is influenced by the micro climate. Therefore atmospheric circumstances inside the canopy have to be determined. To achieve this the canopy is divided into a number of layers with a known leaf area index L . The potential transpiration T is calculated for each layer i with the Penman-Monteith equation (Roberts et al., 1993):

$$T_i = \frac{\Delta_i(Rn_i - Rn_{i-1}) + \rho c_p (\delta e_i) g_{ai}}{L(\Delta_i + \gamma(1 + g_{ai}/g_{ci})} \quad (4.12)$$

in which Δ_i is change of saturation vapour pressure with air temperature (Pa.K^{-1}), Rn is the net radiation absorbed by the layer (W.m^{-2}), ρ and c_p are the air density (kg.m^{-3}) and specific heat of the air ($\text{J.kg}^{-1}.\text{K}^{-1}$), δe_i is the saturation vapour pressure deficit (Pa), γ is the psychrometric constant (Pa.K^{-1}), L is the latent heat of vaporization (J.kg^{-1}) and g_a and g_c are respectively aerodynamic and canopy conductance (m.s^{-1}).

Radiation extinction in the canopy is calculated with an exponential extinction curve relative to the cumulative leaf area (Goudriaan, 1977; Ross, 1976; Roberts et al. 1993):

$$Rn_i = Rn_0 \exp(-k \sum_{j=1}^i L_j) \quad (4.13)$$

An extinction factor $k = 0.6$ is used here (Roberts et al., 1993). The net radiation is the difference between the absorbed short wave radiation and the outgoing long wave radiation. The latter is calculated from the temperature of the leaves which for simplicity are assumed to be at air temperature. The absorbed shortwave radiation depends on the albedo which is about 0.11 to 0.15 for Mixed forest in the Amazon (Shuttleworth, 1984), while Pinker et al. (1980) measured albedos between 0.10 and 0.18 for Dry Evergreen Forest in Thailand. The albedo depends on the season and time of day but an average value of 0.12 is used here for both forest types.

The main role of wind in microclimate is the acceleration of air turbulence, which controls the rate of exchange of heat, water vapour, carbon dioxide etc. in the atmosphere by eddy diffusion. Wind speed is drastically reduced inside dense plant communities due to the resistance of plant shoots. Vertical mixing within the community space is generally inactive, and temporal variations of microclimate conditions under the canopy tend to be less than those outside the canopy space (Kira and Yoda, 1989). Thus, to calculate the second term in equation 4.12, vertical profiles of temperature, humidity and wind speed have to be assumed.

Temperature and humidity profiles are constantly changing because of heating up of the air and tree surface inside the canopy and photosynthetic activity (Allen and Lemon, 1976). However, it is beyond the scope of this study to model the complete energy balance on the level of individual leaves. Roberts et al. (1993) compared estimates of the transpiration calculated with a energy balance model and calculated with a constant temperature based on the temperature measured above the canopy. The latter overestimated the transpiration. To avoid this a simple temperature gradient is used here: because little radiation finds its way to the surface the temperature is assumed to remain fairly constant, and the mean daily temperature is used as an estimate of the forest floor temperature. A linear interpolation simply divides the temperatures between this daily average at the soil surface and the ambient air temperature at the top of the canopy. The relative humidity is interpolated in the same way.

The aerodynamic conductance g_a is calculated from the wind speed $u(z)$ and the friction velocity u_* , both in $m \cdot s^{-1}$ (Thom, 1976):

$$g_a = \frac{u_*^2}{u(z)} \quad (4.14)$$

Thus also a vertical wind profile has to be constructed. Because of the friction of the earths surface, the wind speed increases in a logarithmic fashion with height (Thom, 1976):

$$u(z) = \frac{u_*}{k} \ln\left(\frac{z-d}{z_0}\right) \quad (4.15)$$

in which the Von Karman constant $k = 0.41$, and d and z_0 are respectively surface roughness height and zero plane displacement (m) calculated as 0.75 and 0.1 of the vegetation height h (Rutter et al., 1975). In this research the wind speed above the canopy (assumed to have a height of 35 m) was not measured. Therefore the wind speed measured at the weather station is extrapolated with the weather station values for d and z_0 to the arbitrary height of 50 m. Using again equation 4.15 but with the forest stand values of d and z_0 , this extrapolated wind speed was recalculated to the wind speed at the top of the canopy ($u(h)$). To calculate the vertical wind profile in the canopy, the following equation is used (Thom, 1976):

$$u(z) = u(h) e^{-3(1-z/h)} \quad (4.16)$$

To calculate g_a for each canopy layer the parameters d and z_0 inside the canopy are needed. However, Shuttleworth et al. (1984) measured friction velocities u_* along a vertical profile in the rain forest near Manaus and found a linear relation u_* and $u(z)$. With it he obtained an average value for $(z-d)/z_0$ of 10.4. Using this value in equation 4.15, the aerodynamic conductance in equation 4.14 simplifies to $g_a = u(z)/32.6$. This relation together with equation 4.16 are used in SOAP to calculate g_a .

The canopy conductance g_c is a bulk value of the stomatal conductance and is calculated by multiplying the stomatal conductance g_s with the leaf area of a canopy layer. Stomata react to incident radiation and air humidity. However the relation between radiation, vapour pressure deficit and g_s is not straight forward and a set of empirical regression equations are used to estimate g_s . Roberts et al. (1990, 1993) did extensive measurements on g_s in the Reserva Ducke near Manaus (Brazil). They found that the relation between g_s and specific humidity was negatively linear whereas the relation with incoming radiation was non-linear and difficult to define. Consequently they define a series of regression equations for various radiation levels and for several species which varied in height (from emergent species to understorey species). Based on these results a set of linear equations were defined for various levels of radiation. It should be noted that the specific humidity was recalculated to vapour pressure deficit and stomatal conductance was recalculated from $\text{mol.m}^{-2}.\text{s}^{-1}$, to mm.s^{-1} , using a conversion factor of 0.406 based on average air temperature and pressure (Percy et al., 1989). Figure 4.5 shows the regression equations for radiation levels ranging from 1000 to 200 W.m^{-2} and vapour pressure deficits ranging from 0 to 2000 Pa.

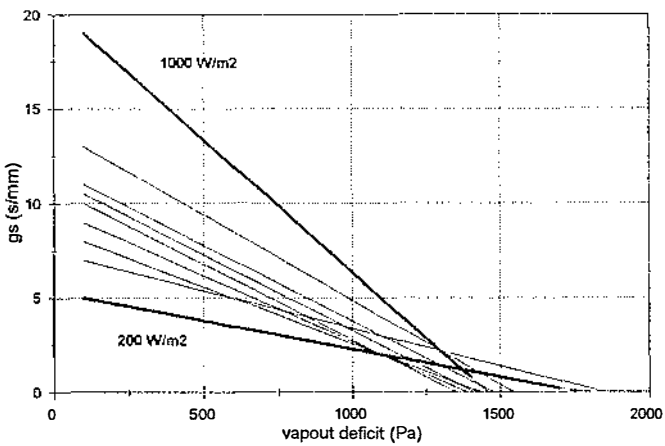


Figure 4.5 Linear relations of bulk stomatal conductivity (g_s in mm.s^{-1}) and vapour pressure deficit (δe in Pa) for different levels of incoming radiation (R_{in} in W.m^{-2}). Each line represents an increase in radiation of 100 W.m^{-2} . Adapted from data of Roberts et al. (1990, 1993), see text.

With the methods described above the potential transpiration is calculated. The actual transpiration may be lower mainly because of several reasons: first if the canopy is wet the stomata in contact with the water are closed, second the energy that is used to evaporate intercepted water from the leaves is not available for transpiration and third, if the soil is very dry the uptake is reduced. Most tree species have much more stomata on the lower than on the upper side of a leaf. Roberts et al. (1990) found ratios between stomatal conductance between upper and lower side ranging from 10/90 to 25/75. Given these ratios it is assumed in SOAP that 15% of the transpiration comes from the upper side of the leaves and 85% from the lower sides. If the upper sides are partly or completely wet after a rainstorm, the upper side transpiration is reduced with the wetted fraction of the canopy. This fraction is calculated for each canopy layer by the interception model, as well as the amount of water that evaporates from each canopy layer (see chapter 6). This evaporation flux is subtracted from the potential transpiration to arrive at the actual "water demand" of the plant. The influence of the soil moisture status on the actual transpiration is discussed in the next section.

4.4.4 Root structure

The actual transpiration equals the amount of water taken from the root zone according to the relative vertical distribution of the roots. Figure 4.6 shows the fine root distribution (roots smaller than 1.5 cm diameter) for Dry Evergreen forest on ARa and Mixed forest on FRh (Prinsen and Straatsma, 1992). All samples were taken at some distance from the trees. The root densities are expressed in g/kg soil (left hand graphs). Since SOAP uses a relative root distribution, the root mass distribution relative to the total of the first 100 cm were calculated (right hand graphs).

Eernisse (1993) measured the root distribution in two profile pits in ARa and FRh (figure 4.7). Samples were taken to a depth of the first impermeable layer, i.e. kaolinite layer at a depth of 3.95 m for ARa, and weathered bedrock at a depth of 2.75 m for FRh. It appeared in both soil types a few roots occurred very deep. In case of FRh these were mostly fine roots below 1.5 m, which are probably related to the availability of nutrients in the weathering zone. In ARa however, thick roots were common in the entire profile, although in terms of the total root mass it was only a small fraction. These larger roots are important for the uptake of water, and the fact that they reach the impermeable kaolinite layer in ARa, which often has a groundwater table on top of it (see also chapter 2), indicates that moisture stress may occur in these soil types. Unfortunately it is difficult to incorporate the thicker roots in SOAP because it is not known what the relation is between the amount of water they extract from the soil and their mass relative to the total root mass. In theory the uptake of water could be linked to the root water potential and the dimensions (radius and length), estimating a contact zone of the root in the soil and a potential gradient. However, in view of the lack of data a simpler extraction model was chosen, and the uptake is related to the vertical root mass distribution given in figure 4.6.

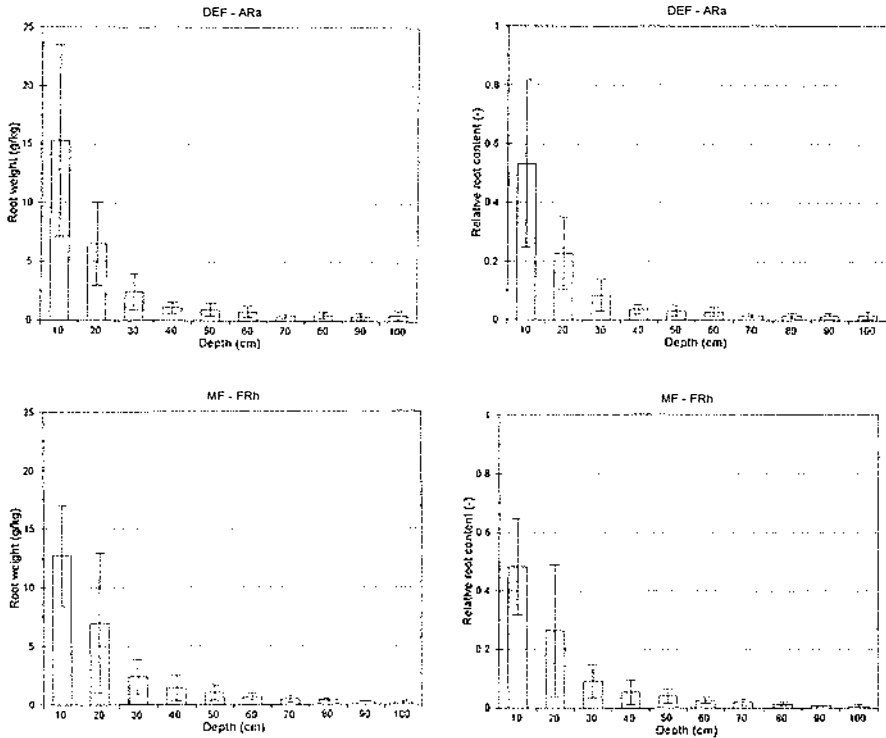


Figure 4.6 Root distribution to a depth of 100 cm, as weight (in g.kg^{-1} soil) on the left and relative to the total root mass (in %) on the right: a) Dry Evergreen forest on Albic Arenosols ($n=10$), and b) Mixed forest on Ferralic Arenosols ($n=7$). Bars represent 1 standard deviation (data from Prinsen and Straatsma, 1992).

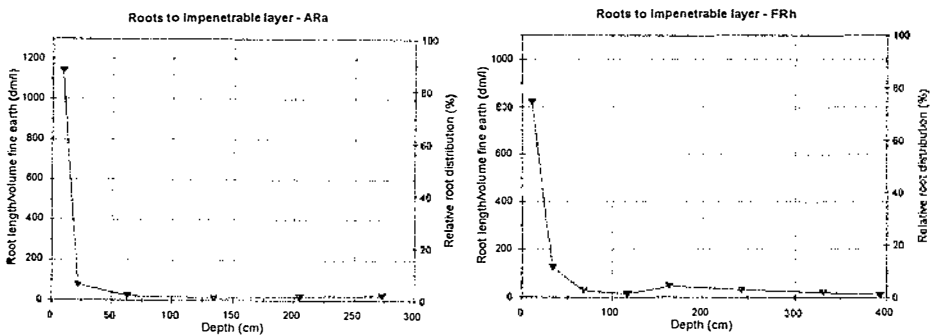


Figure 4.7 Variation of root length per volume of fine earth (in dm/liter) with depth, from the surface to the first impenetrable layer in an Albic Arenosol and a Haplic Ferralsol (after data from Eernisse, 1993).

4.4.5 Uptake from the root zone

The integrated value of the transpiration of all the canopy layers forms the potential plant uptake. The atmospheric demand creates a series of hydraulic potentials in the plant from leaves to roots. A review of the principles of water extraction by roots and models used to calculate the water extraction is given by Molz (1981). Most models are based on the difference in pressure head between the root and the surrounding soil, the hydraulic conductivity and a factor describing the distribution of the roots with depth. To calculate the water exchange surface one has to know not only the fraction of roots at a certain depth (usually root length per unit of soil volume) but also the size distribution of active roots. This information is not available for a complex plant community such as the tropical rain forest. Therefore a simpler approach is taken for the root extraction in this model (Feddes et al., 1978; Van Genuchten, 1987; Molz, 1981):

$$S(h) = r(z) \alpha(h) T_p \quad (4.17)$$

which calculates the actual uptake $S(h)$ (s^{-1}) from potential transpiration T_p ($m \cdot s^{-1}$), a root distribution function with depth $r(z)$ (m^{-1}) and a dimensionless uptake reduction factor related to the pressure head $\alpha(h)$.

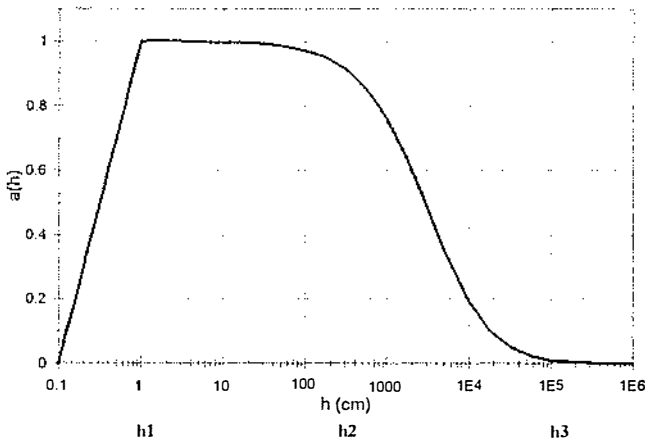


Figure 4.8 Uptake reduction term $\alpha(h)$ as a function of pressure head.

Figure 4.8 shows a graph of $\alpha(h)$ in which Between saturated conditions and a point h_1 , deficient aeration conditions exist and the uptake is reduced. This "anerobiosis" point is hard to define and depends both on the plant and the soil properties. Feddes et al. (1978) relates the reduced uptake to a reduced oxygen diffusion rate which corresponds for most plants to a fraction of gas filled pores of less than $0.05 \text{ cm}^3 \cdot \text{cm}^{-3}$ for loamy soils. In the second interval, from the pressure heads h_1 to h_2 , the uptake is not reduced and equals the potential transpiration rate. In the third interval, for pressure heads between h_2 and h_3 , water stress causes a reduced

uptake. The value of h_2 is not fixed but depends on the potential transpiration. Feddes et al. (1988) give values between -500 cm and -1000 cm for a potential transpiration rate between respectively 5 mm.day⁻¹ and 1 mm.day⁻¹ for most crops. For pressure heads lower than h_3 uptake is nil. Medina (1983) reviews leaf osmotic pressures and finds an average value of -10000 for rain forest on lateritic soils to -12000 cm for forest on sandy podzolic soils. The wilting point h_3 is lower than that and a value of -16000 cm is mostly used for crops. The shape of $\alpha(h)$ can be described with several equations. SOAP uses the continuous function (Van Genuchten, 1987):

$$\alpha(h) = \frac{1}{1 + (h/h_{50})^{1.5}} \quad (4.18)$$

in which h_{50} is the pressure head at which the extraction rate is reduced by 50%, for which a value of $h = -3200$ cm is used (pF 3.5).

The actual transpiration $\alpha(h)T_p$ is extracted from the root zone according to the root distribution with the depth $r(z)$. Therefore $r(z)$ is recalculated relative to the total root content, so that the sum over all the layers equals 1. The root distribution is then expressed in a fraction per layer thickness (m⁻¹). The transpiration is taken as sink term from each soil layer according to the relative root content of the layer (e.g. a layer with 32% of the roots will provide 32% of the transpiration). Thus the actual units in which the root density is measured are not important.

5 SPATIAL VARIABILITY OF INFILTRATION AND RELATED SOIL PROPERTIES

5.1 Introduction

In the previous chapters it was shown that several distinctly different "landscape types" occur in the Tropenbos Ecological Reserve and the surrounding area. The differences between these units can be attributed for a large part to the soil hydrological properties. Thus, it may be expected that the water balance is also different, depending on the influence of the soil properties on the water fluxes. This influence can be direct, such as in the case of saturated hydraulic conductivity and porosity which, together with the actual soil moisture content, determine the water fluxes. It can also be indirect, such as with texture and root content, which determines for a large part the soil structure, porosity, aggregate stability, risk of surface sealing etc. If one has determined which properties dominate the water balance within a unit, it is obviously important to obtain representative values.

How to obtain these values? Representative means that a value for the mean of the unit has to be found and that the variation has to be quantified. There are several ways to quantify the areal mean (Brus, 1993; De Gruijter and Ter Braak, 1990, 1993). One can assume that a representative location can be selected from experience and that the samples taken from the soil profile provide accurate values of the areal means. On the other hand one can assume that the properties are spatially correlated stochastic variables and try to define a model that describes the spatial variability. With the right sampling design the property can be mapped. If the spatial correlation cannot be found or quantified at the scale of observation, the samples can be processed in a traditional statistical way and the property mean and variance can be calculated. If the latter is the case it is imperative that the sample locations are randomly selected (Brus, 1993).

Given that the variability of the properties is known, the variability of the water fluxes is not easily assessed. When for instance a model is used to calculate the water fluxes, for which a set of soil properties are used as input parameters, the variability of the model results will be a result of the way the errors are propagated in the model (Heuvelink, 1993). At the time this study was done a practical tool for error propagation was not yet available. Therefore a crude method was used. In this chapter the levels of variance associated with these two approaches are compared to see in what way the spatial variability differs. A simple parametric model is used, based on multiple regression between infiltration measurements and soil properties. This serves two purposes: i) a regression model allows for the inclusion of the complete set of soil properties thought to be relevant, and ii) regression analysis enables a detailed assessment of the errors involved. The spatial variability of both the measured infiltration and the model infiltration are compared.

Thus, the study presented in this chapter has two objectives: is it feasible to quantify and map the spatial variability of the soil hydrological properties, and how is the variability altered in a simple parametric model.

5.2 Methodology

5.2.1 Spatial variability

Regionalized variables theory (Journel and Huijbregts, 1978; Webster and Oliver, 1990; Isaaks and Srivastava, 1989) assumes that a spatial variation of a variable $z(x)$ can be expressed as the sum of three components:

$$z(x) = m(x) + \epsilon'(x) + \epsilon'' \quad (5.1)$$

where:

- x = position given in two or three coordinates;
- $m(x)$ = structural component, i.e. a trend or a mean of an area;
- $\epsilon'(x)$ = stochastic component, i.e. spatially correlated random variation;
- ϵ'' = residual error component (noise), i.e. spatially uncorrelated random variation.

Spatial analysis of a variable involves the detection and subsequent removal of trends $m(x)$ in the dataset, after which the spatially correlated random variation $\epsilon'(x)$ can be described. The spatially uncorrelated random variation ϵ'' cannot be described or mapped (at least not at the same scale). The way the structural component $m(x)$ is analysed depends on its nature: $m(x)$ can be a gradual change in the study area or, in case of sharp landscape boundaries, it consists of different levels that are related to significantly different groups of the population.

A rough assessment of $\epsilon'(x)$ is possible with nested analysis of variance. Spatial variation can occur at scales that differ by several orders of magnitude simultaneously, since the physical processes that create this pattern of variation operate at different scales (Oliver and Webster, 1986). Nested analysis of variance aims at discovering these scales, i.e. the spatial level at which $\epsilon'(x)$ can be analysed best. The technique uses a hierarchical sampling scheme, consisting of a specified number of levels of distance (usually the distances differ in a logarithmic way). At the highest level a number of sites is chosen which cover the study area, and at lower levels a number of observations is added for each location in an identical way. The contribution in variance of each group of observations at a certain distance level to the total variance of the population is determined. In this way the sampling distance that is responsible for the largest increase in variance can be estimated. In fact it quantifies the variance of $\epsilon'(x)$ at fixed distances.

5.2.2 Sample design

The study was carried out in the catchment of the Tropenbos Ecological Reserve, which is about 20 km². The western half of the catchment is formed by the dissected White Sands plateau (called in this chapter physiographic unit "White Sands" or "WS"), consisting entirely of sandy Albic and Gleyic Arenosols, with minor inclusions of Histosols (see chapter 2). The eastern half is formed by a dolerite-granite intrusion in which lateritic crusts and gravel were formed, consisting of Xanthic Ferralsols and Plinthosols (physiographic unit "Laterite" or "LA"). The

lateritic soils are dominated by red clay loams and clays, with a high content of iron concretions. An intermediate position is taken by Ferralic Arenosols and Haplic Ferralsols (physiographic unit "Brown Sands - BS"), which are consist of deep yellowish brown loamy sands and sandy loams. The Fluvisols and Histosols along the river and in swamps represent only a small area, so only the three main physiographic units (LA, WS and BS) are compared here. In order to assess the spatial variability at several scales, it was decided to use a stratified random sampling design.

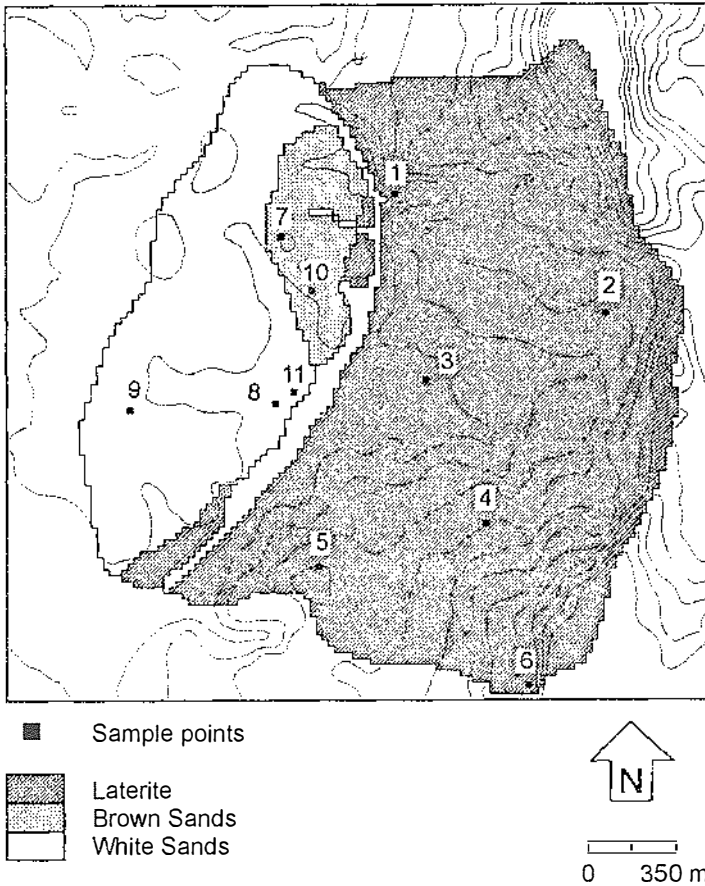


Figure 5.1 Sample design in the catchment of the Tropenbos Ecological Reserve and main physiographic units.

A sampling scheme with 9 evenly distributed clusters of 8 points chosen in a random direction was used (see figure 5.1). At the highest level the distance was roughly 1500 - 2000 meters. At lower levels the distances between the points were 2, 20, 200 meters apart, making a total of $9 \times 2 \times 2 \times 2 = 72$ observation sites. From field

observations it seemed that the soil characteristics of the physiographic units were indeed very different, as is suggested by the general descriptions of the soils in the region. However, the original sampling scheme had only 1 cluster in Brown Sands and 2 clusters in White Sands. Therefore a cluster was added to each of these units: clusters 10 and 11 raised the total to 88 observation sites. This decreased the maximum average distance for Brown Sands to approximately 1000 m.

At each location a ring infiltrometer test was performed, using a single ring of 30 cm diameter. From these tests the sorptivity (variable SP in table 5.1) and the constant infiltration rate at the end of the test (variable IR in table I, hereafter called "infiltration rate") were determined using the Philip's equation (Chow et al., 1984). Kopecki sample rings (100 cm³) were used to determine the variables listed in table I. In addition to that the textural composition of the topsoil was analysed.

Table 5.1 Variables examined for the regression model

<i>Code</i>	<i>Variable</i>	<i>units</i>
IR	Infiltration Rate	mm/min
SP	Sorptivity	mm/min ^{1/2}
KS	Saturated Hydraulic Conductivity	mm/min
BD	Bulkdensity	g/cm ³
PV	Pore volume	cm ³ /cm ³
IM	Initial Moisture Content	cm ³ /cm ³
RW	Root Weight	g/100cm ³
RV	Root Volume	-
CF	Coarse Fragments	-
SA	Sand Content	-
SI	Silt Content	-
CL	Clay Content	-
SD	Soil Depth	m

5.2.3 Data preparation

While reviewing the dataset it appeared that the data varied considerably for each of the three units (White Sands, Brown Sands and Laterite). In other words, the structural component $m(x)$ in equation 5.1 at the scale of the entire area is not a gradual trend. Rather it reflects the nature of sharp boundaries occurring in the landscape. Therefore $m(x)$ was investigated by cluster analysis. Clustering was done using two different techniques: firstly a hierarchical technique was used, so called tree joining, and secondly a partitive technique, the so called K-means clustering (Davis, 1986). The first technique separated the variables clearly into three groups, corresponding exactly with the physiographic units. The second technique yielded a similar separation except for an inclusion of three White Sands-samples in the Brown Sands unit. Variables responsible for the cluster separation were texture, soil depth and saturated hydraulic conductivity, in that order. The other variables contributed relatively little to the cluster analysis. Since clustering results in three distinct groups, the structural component $m(x)$ was accounted for by analysing the spatial

variability of the soil properties in each physiographic unit separately.

Measurements could not be done at some of the sample locations, e.g. some were located on hard bedrock, prohibiting texture analysis. Augering depth is limited for Laterite only and in the other physiographic units a depth of 120 cm was recorded (the length of the auger). Since the variance of soil depth could not be measured for WS and BS it has been excluded from further analysis of these units.

Most of the variables are expressed as a fraction or a percentage, confining the observed values clearly in the range of 0 - 100 %. Therefore they do not show a normal distribution, which is a prerequisite for most tests of statistical significance. In order to be able to evaluate the regression analysis, a transformation of the values was needed. Webster and Oliver (1990) suggest the use of a Logit transformation, which transforms the fraction p into a more or less normally distributed value p' :

$$p' = \ln\left(\frac{p}{1-p}\right) \quad (5.2)$$

5.3 Results

5.3.1 Differences in infiltration between the soil types

The average infiltration rates (IR) are very different: White Sands show values that are 2 times higher than those of Laterite, and 20 times higher than those of Brown Sands (see table 5.2). Almost none of the soil properties has a high correlation with IR. Only Laterite shows a clear positive correlation between IR and coarse fragments (CF) and bulk density (BD). Although the clay content of Laterite is highest (33%), the iron concretions apparently cause the soil to have large aggregates, macropores and fissures. In a shallow soil IR is slowed down once the wetting front reaches the impenetrable layer, which explains the high correlation between IR and soil depth (SD) in Laterite. The only other high correlation is between saturated hydraulic conductivity (KS) and IR in Brown Sands. Although one expects IR in White Sands to be very high because of the medium coarse sand, the variation in IR cannot be explained by texture alone. The correlation is somewhat better with initial moisture (IM). Mean root content of White Sands is highest, suggesting large macropores in the topsoil. However, one should be aware that at some places in the White Sands swampy conditions prevail, with accumulation of organic matter. The samples taken at these locations have a large mean root weight (RW) and root volume (RV), but field observations show that IR is low because of the relatively high organic matter content and wet conditions.

The three physiographic units show distinct differences in sorptivity (SP). In general SP seems to increase with increasing clay content: the White Sands unit has the lowest SP, Laterite the highest. Theoretically sorptivity reflects the start of the infiltration process when matric suction is the driving force. Since matric suction is low in the absence of clay and silt, this explains the low values found in the White

Table 5.2 Basic statistics of the variables and correlations with infiltration rate (*corIR*) and sorptivity (*corSP*).

<i>Soil</i>	<i>Var</i>	<i>n</i>	<i>min</i>	<i>max</i>	<i>mean</i>	<i>stdev</i>	<i>CV%</i>	<i>corIR</i>	<i>corSP</i>
LA	IR	17	0.910	43.140	11.171	11.360	102	1.00	0.63
WS		22	5.120	49.160	26.967	12.311	46	1.00	0.56
BS		15	0.080	3.850	1.221	1.224	100	1.00	0.12
LA	SP	18	0.230	5.960	2.391	1.451	61	0.63	1.00
WS		16	0.130	5.270	1.581	1.309	83	0.56	1.00
BS		14	0.170	4.950	1.933	1.370	71	0.12	1.00
LA	KS	40	0.000	49.770	18.616	4.527	24	0.34	0.25
WS		23	0.200	62.530	28.086	18.488	66	0.31	0.13
BS		15	0.030	9.600	2.329	2.533	109	0.66	0.05
LA	BD	42	0.710	1.950	1.454	0.329	23	0.70	0.53
WS		23	0.870	1.290	1.102	0.105	10	0.37	0.21
BS		16	0.990	1.500	1.282	0.136	11	-0.54	0.35
LA	PV	42	0.390	0.750	0.576	0.076	13	-0.33	-0.33
WS		23	0.460	0.720	0.580	0.060	10	-0.39	0.03
BS		16	0.460	0.620	0.539	0.038	7	0.46	-0.45
LA	IM	42	0.150	0.620	0.354	0.117	33	-0.24	-0.39
WS		23	0.110	0.700	0.254	0.149	59	-0.47	-0.48
BS		16	0.250	0.540	0.358	0.084	23	-0.15	0.07
LA	RW	41	0.000	2.500	0.929	0.622	67	-0.38	-0.32
WS		23	0.900	9.200	2.570	1.903	74	-0.20	-0.20
BS		16	0.300	1.900	1.006	0.514	51	0.31	-0.19
LA	RV	41	0.000	0.033	0.011	0.0075	68	-0.38	-0.30
WS		23	0.012	0.120	0.034	0.0254	74	-0.19	-0.20
BS		16	0.002	0.022	0.013	0.0060	48	0.37	-0.26
LA	CF	42	0.000	0.950	0.509	0.344	68	0.83	0.53
WS		23	-	-	-	-	-	-	-
BS		16	-	-	-	-	-	-	-
LA	SA	38	0.190	0.804	0.421	0.1730	41	0.29	-0.09
WS		23	0.821	0.980	0.894	0.0306	3	0.25	0.23
BS		16	0.350	0.787	0.665	0.1045	16	-0.24	0.20
LA	SI	38	0.125	0.420	0.247	0.0690	28	0.42	0.19
WS		23	0.020	0.141	0.105	0.0270	26	-0.11	-0.03
BS		16	0.069	0.224	0.142	0.0406	29	0.28	-0.06
LA	CL	38	0.000	0.672	0.333	0.0167	50	-0.39	-0.03
WS		23	-	-	-	-	-	-	-
BS		16	0.113	0.520	0.194	0.0929	48	0.12	-0.30
LA	SD	42	0.050	1.500	0.604	0.564	93	0.60	0.28
WS		23	-	-	-	-	-	-	-
BS		16	-	-	-	-	-	-	-

Sands unit. Nevertheless, the correlations between SP and the other variables are low. It seems that none of the independent variables gives a good representation of the upper root zone, which controls the start of the infiltration process.

It should be noted that the sample rings represent of course a smaller soil volume than is involved in the infiltration tests. Large roots and soil aggregates affect the latter, which shows in the coefficient of variation. The CV% also shows that whereas White Sands are more homogeneous than the other soils with respect to IR, BD and texture, this is not the case for the other variables, in particular for SP and IM.

From the above it can be concluded that the variation in IR and SP cannot be explained by any of the other variables by itself. Particularly texture, which is usually seen as a typical representative for all kinds of soil properties, cannot be used successfully to quantify infiltration.

5.3.2 Differences in spatial structure between soil types

Table 5.3 shows the increase in relative variance with sample distance, whereby the sample variance equals 100%. It is clear that the physiographic units differ considerably in the spatial variability. Properties of the Laterite unit seem to have a long distance variation, where most of the variance is included at a distance level of 200 m. On the other hand there is a high "noise" level. This corresponds well with the actual situation: large areas with "sheet laterite" (cemented layers) and gravel (iron concretions), alternate with unconsolidated clayey soil. Within these areas a large variability occurs due to the randomness of the lateritization process.

Table 5.3 Results of the Nested Analysis of Variance (the cumulative relative variance at the highest level is always 100%)

	<i>Laterite</i>			<i>White Sands</i>			<i>Brown Sands</i>		
	<i>2m</i>	<i>20m</i>	<i>200m</i>	<i>2m</i>	<i>20m</i>	<i>200m</i>	<i>2m</i>	<i>20m</i>	<i>200m</i>
IR	6.35	7.58	100.00	19.82	19.82	26.37	50.98	91.45	100.00
SP	44.58	95.98	95.98	45.77	93.10	93.10	100.00	100.00	100.00
KS	42.36	64.10	100.00	21.54	80.64	80.64	33.27	88.98	100.00
BD	81.75	81.75	97.19	19.65	94.76	94.76	18.06	21.89	100.00
PV	39.48	39.48	99.94	33.68	74.12	74.21	32.65	50.00	100.00
IM	62.27	62.27	78.27	3.20	4.65	68.02	14.19	15.97	100.00
RW	44.23	96.42	96.42	64.71	100.00	100.00	23.86	33.44	100.00
RV	46.79	95.12	95.12	50.47	100.00	100.00	12.32	19.47	100.00
CF	15.06	15.06	100.00	-	-	-	-	-	-
SA	25.04	25.04	91.68	24.80	32.00	100.00	49.41	52.87	100.00
SI	54.03	55.41	65.98	30.62	30.65	100.00	46.24	47.20	100.00
CL	16.56	16.56	100.00	-	-	-	84.86	84.89	100.00
SD	3.31	3.65	41.95	-	-	-	-	-	-

The supposedly homogeneous White Sands show a considerable increase of variance at the 20 m level for many properties (see table 5.3). Only texture, initial moisture content and infiltration rate vary at a larger distance. The large distance variation of IR can be explained by the fact that the permeability of White Sands is so high, that the infiltration rate is little affected by the other soil characteristics. The short distance variation of BD and PV are caused by the fact that the samples are taken at the surface. Thus, the variation is related to the rooting characteristics with which BD and PV have a high correlation (respectively 0.83 and 0.55).

All Brown Sands properties reach the maximum variance at the 200 m level (see table 5.3). In contrast with the White Sands, the rooting properties vary at a larger distance, whereas the texture shows a high short distance variation. Infiltration, sorptivity and hydraulic conductivity are clearly more affected by the latter, showing a high short distance variation.

5.4 Sources of variation: regression analysis or spatial structure

Since a simple correlation does not exist, it has been investigated whether a combination of variables explains the variation of IR and SP better. A stepwise multiple regression analysis provided a relation between infiltration rate (IR) and sorptivity (SP) and a combination of the other variables, for each physiographic unit. Independent variables were included, using an F test to determine how significant the contribution of a variable had to be in order to be added to the equation (the actual equations are not given here). The relative importance of each independent variable is given by its contribution to the explained variance R^2 . By manipulating the threshold F-value it is possible to include or exclude variables. In general as few variables as possible were included. There are two reasons for this: first, it is hardly useful to be able to model the infiltration process if many parameters are needed; second, adding a variable will always increase the explained variance because of the random error involved. The order in which the independent variables are included is maintained in table 5.4.

Figures 5.2a to 5.2f show the increase in relative variance with the logarithmic distance between the sample points. The straight lines between the points suggest a log-linear relationship between distance and variance. Although this may not be so it is the best guess with the information available. Two important distances of variation can be seen from the graphs. The distance belonging to a high variance just after a large increase in variance (e.g. 200 m points of variables CL, CF and IR in figure 5.2a), can be interpreted as the sampling distance at which the spatial variance of the sampled area is completely included with a minimum of sampling points. However, this sampling distance would give an inaccurate spatial representation of that variable. The distance belonging to a low variance just before a strong increase in variance (e.g. 20 m points of variables CL, CF and IR in figure 5.2a) indicates that sampling at this distance ensures an accurate spatial representation of that variable, but usually with a very large amount of sampling points in relation to the size of the study area. The optimum sampling distance is a balance between the number of

Table 5.4 Results of the regression analysis. R²-change is the increase in explained variance contributed by each independent variable

		<i>n</i>	<i>R</i>	<i>R</i> ²	<i>F</i>	<i>p</i>
<i>IR</i>	Laterite	15	0.920	0.846	20.120	0.000
	Ind. Var.	CF	BD	CL		
	R ² -change	0.656	0.099	0.090		
	White Sands	20	0.831	0.690	18.960	0.000
	Ind. Var.	IM	SA			
	R ² -change	0.449	0.242			
	Brown Sands	13	0.872	0.761	15.942	0.000
	Ind. Var.	SA	KS			
	R ² -change	0.385	0.373			
<i>SP</i>	Laterite	15	0.909	0.826	0.8538	0.003
	Ind. Var.	BD	RW	RV	KS	SD
	R ² -change	0.273	0.190	0.164	0.104	0.096
	White Sands	14	0.802	0.644	6.024	0.013
	Ind. Var.	PV	IM	BD		
	R ² -change	0.422	0.185	0.038		
	Brown Sands	14	0.678	0.460	4.691	0.033
	Ind. Var.	PV	SI			
	R ² -change	0.407	0.053			

sampling points and an acceptable level of variance. Sampling at a distance of about 100 m or higher is assumed to be feasible for an area with the size of the Tropenbos Reserve. Depending on the spatial structure of a variable this distance corresponds to a certain percentage of the sample variance, which can be read from figures 5.2a to 5.2f.

5.4.1 Laterite

The correlation coefficient (*R*) is fairly high for both *IR* and *SP* (table 5.4). *CF* contributes most to the goodness of fit (see R²-change in table 5.4), stressing the fact that the gravelly matrix of the lateritic soils is an important hydrological characteristic. Although *CL* does not increase R² much, the nested analysis of variance (figure 5.2.a) shows that the spatial scale of variation of *IR* resembles that of *CF* and *CL*. *BD* has a much higher "noise" fraction, but has large distance variability (close to 200 m) as well. In terms of optimal sampling distance there is no difference in sampling *IR* directly or sampling the independent variables.

Regression analysis for *SP* shows that *BD* and root characteristics contribute most to R². Apparently the matric suction is best represented by these variables. *SD* and *KS* increase R² only a little. Only the combination of five variables can predict *SP* satisfactorily. *SP* has a large short range variability and a high "noise" fraction (see

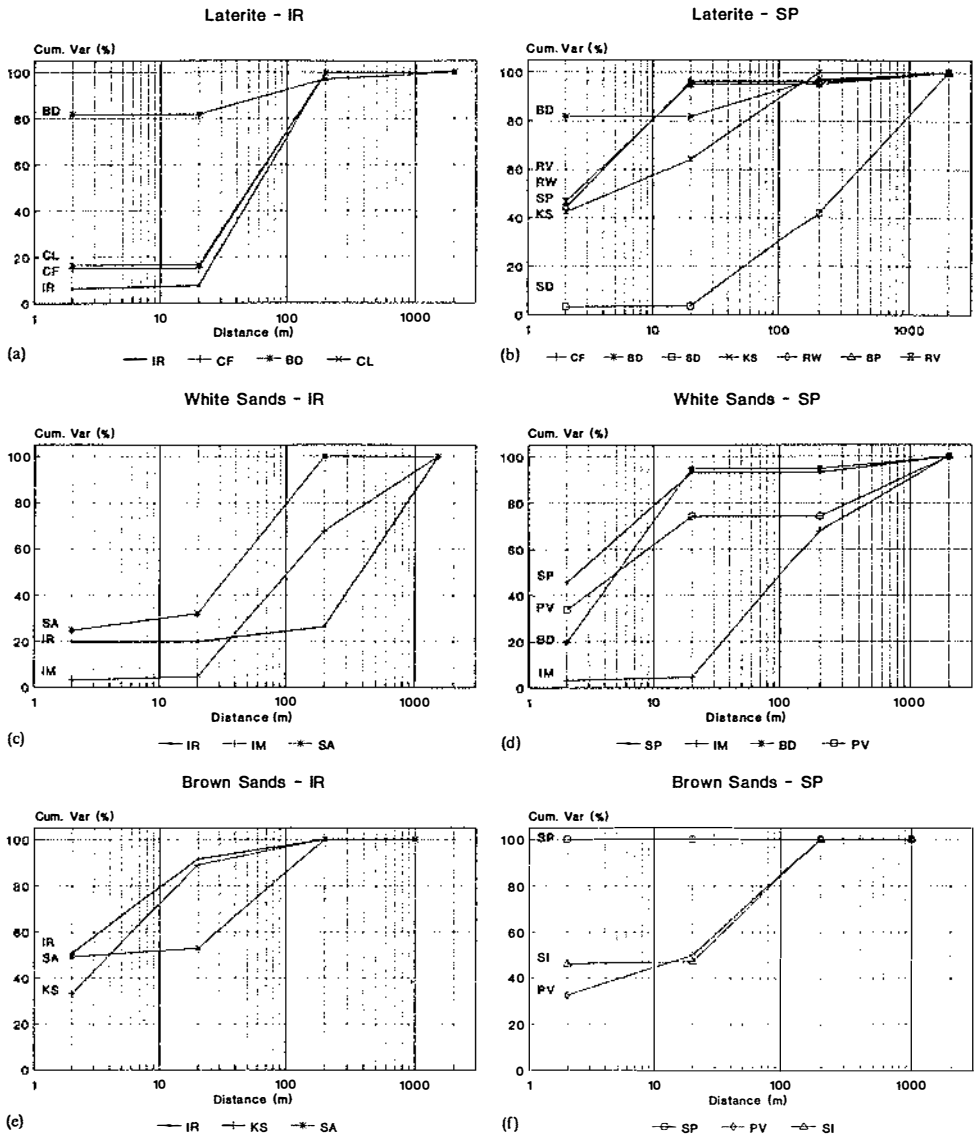


Figure 5.2 Cumulative relative variance in relation to sampling distance for infiltration rate (IR) and sorptivity (SP) in the three physiographic units

figure 5.2b). The independent variables differ considerably, with only the rooting characteristics resembling SP closely. To sample SP on a regular grid without loss of spatial information is not feasible, the number of sampling points needed is prohibitive (e.g. sampling every 10 m results in more than 160000 points for Laterite). Although the other variables can be sampled at a greater distance without loss of spatial information, there is a large short range variability for almost all regression variables. Hence, one has to accept the large variance when either calculating or measuring SP.

5.4.2 White Sands

IM and SA are clearly the factors governing IR in White Sands (table 5.4). However, the spatial structure of these variables differs clearly from IR: at the 200 m level almost all spatial variance is accounted for with IM and SA, while IR varies at a larger distance (see figure 5.2c). This indicates that calculating IR with a parametric model is not practical as it only increases the variance, it is better to measure the infiltration rate. The sampling distance can even be fairly large: e.g. 300 m and more.

IM has the highest correlation with SP and is included in the regression equation first, in the next step the explained variance is increased considerably when PV is added. Both can be seen as representing the matric suction: the higher the moisture content in the soil, the smaller the matric potential below the wetting front. Although BD adds only little to R^2 , both PV and BD resemble SP closely, with respectively 75% and 90% of the sample variance obtained at a distance of only 20 m, whereas IM varies at a larger distance (figure 5.2d). It is not feasible to map the SP. Spatial variability is so large at small distances, that adequate sampling is impossible. This does not improve if SP is calculated from other variables as they have the same spatial structure.

5.4.3 Brown Sands

Multiple regression for Brown Sands shows that IR is related to KS and SA. KS resembles IR spatially with a short distance variability, whereas SA has a medium distance spatial structure (see figure 5.2e). As described above the Brown Sands do not have a clear macro structure (see also chapter 9), and infiltration will probably be affected by a combination of short range distance variation and noise. Therefore the more "complex" variables (such as IR, SP and KS) have a short range variability, while the more "simple" variables (such as texture) have a medium range variability. In view of this, correlation between IR and KS is not surprising. When KS is left out of the regression, the results are poor: at least 4 independent variables are needed (BD dominating) to explain only 50% of the variance. Thus, mapping IR in Brown Sands is hardly feasible. Although SA can be sampled at a larger distance (100 m or less), the other variables have a large short range variability. Therefore, the total variance of IR will always be large.

Multiple regression for SP in Brown Sands is not feasible with the independent variables of this study. PV contributes considerably to the explained variance, but of

the other variables only SI increased R^2 with more than 0.05. Also spatially there is no relation between SP and other variables, since SP doesn't show any spatial structure at the distances at which it has been measured (figure 5.2f). In practice SP can be measured at any distance without gaining information about the spatial structure, as long as the number of samples is large enough for a sound statistical analysis.

5.4.4 The effect of the regression model on the spatial variance

A full analysis of the propagation of measurement errors in the regression equations was not done. To get some idea of the contribution of the model to the total variance, the infiltration rate IR and sorptivity SP were calculated with the regression equations, and model results were analysed with a nested analysis of variance. Figure 5.3 shows the increase in relative variance with sampling distance of the measured IR and SP (triangles) and the calculated IR and SP (squares). Above a distance of 20 metres there is no difference in the spatial structure of the measured or calculated IR. At a smaller distance the calculated IR has a somewhat lower variance than the measured IR for White Sands and Brown Sands. With SP there is hardly any difference between the spatial structure of the measured and calculated values, except for Brown Sands, for which the measured SP have a slightly lower relative variance. As a whole there is little difference between the measured and modelled IR and SP. The increase in variance with the sample distance is almost the same in all physiographic units.

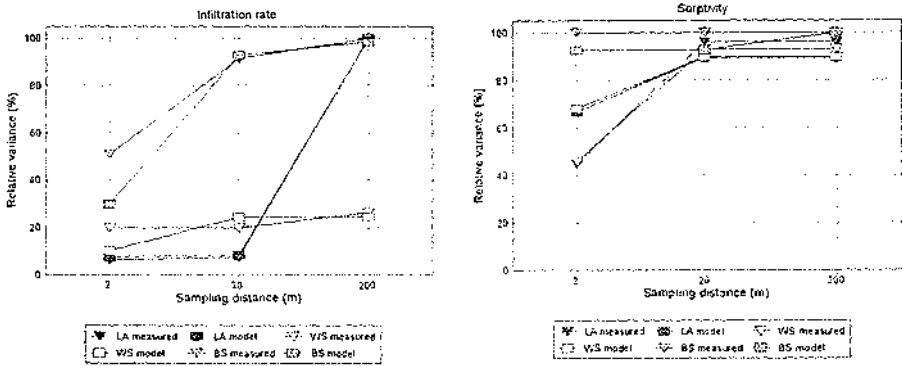


Figure 5.3 Cumulative relative variance of measured and modelled infiltration rate (IR) and sorptivity (SP).

In table 5.5 the variance of IR and SP is calculated for three arbitrary sampling distances. The size of the study area is approximately 20 km² which means that sampling at distances of 50, 100 and 200 m would result respectively in 8000, 2000

and 500 sample points. On Laterite, IR can be sampled at a reasonable distance (i.e. more than 50 m) only if a large variance is accepted, i.e. more than 80% of the sample variance. On White Sands the sample distance for IR can be increased without much loss of spatial information. On Brown Sands on the other hand, there is a high variance at any reasonable distance. The same goes for SP in any of the three physiographic units: variance levels of more than 90% of the sample variance have to be accepted.

Table 5.5 Spatial variance in relation to several sample distances

		<i>Sample var</i>	<i>50m</i>	<i>100m</i>	<i>200m</i>
IR	Laterite	129.05	57.49	93.269	129.05
	White sands	151.56	34.01	36.99	39.97
	Brown Sands	1.50	1.42	1.46	1.50
SP	Laterite	2.11	2.02	2.02	2.02
	White Sands	1.71	1.59	1.59	1.59
	Brown Sands	1.88	1.88	1.88	1.88

5.5 Conclusions

Almost all soil hydrological properties exhibit a large short range spatial variability. In the White Sands, properties such as bulk density, porosity, saturated hydraulic conductivity and rooting characteristics have a distance of variation around 20 m. Brown Sands have high noise levels (variation at a distance of less than 2 m) for almost all properties and spatial patterns which vary at distances of less than 20 m. There is no difference in variability of the infiltration process if it is measured directly, or if the process is modelled with the basic hydrological properties. In view of this it is not feasible to map any of the hydrological properties. The number of sample points required to represent the spatial structure adequately is prohibitive. Therefore, the best strategy is random sampling, to ensure that the values of the soil properties are good representatives of the areal mean and variance. The sampling scheme used here is random and the property means and variances can therefore be regarded as representative values.

Each of the three physiographic units has its own combination of variables that are related to infiltration. Also, there is a clear difference between infiltration rate and sorptivity. The infiltration rate is related to texture in combination with coarse fragment content, initial moisture content and saturated hydraulic conductivity for Laterite, White Sands and Brown Sands respectively. Sorptivity is related to pore volume and bulk density in combination with root activity and initial moisture content for Laterite and White Sands respectively. Sorptivity in Brown Sands cannot be modelled with a parametric model. The spatial structure of the modelled and measured infiltration rate and sorptivity is virtually the same.

6 INTERCEPTION AND THROUGHFALL: MODELLING THE CANOPY WATER BALANCE

6.1 Introduction

By its nature the tropical rain forest is an ecosystem where the vegetation has an enormous influence on the hydrological processes. The trees intercept most of the rainfall, a part of which evaporates, whereas the water flux that reaches the soil surface is determined both by the rainfall intensity and the drainage characteristics of the canopy. Therefore, when describing the water balance of a forested catchment, interception cannot be treated as a fraction that is simply subtracted from the rainfall, but the water fluxes associated with the wetting and drying processes have to be quantified. Contrary to the canopy wetting and drainage processes, for which only empirical models are available, evaporation of water on the canopy is well understood. It can be calculated as part of the energy balance of a plant, i.e. the exchange of momentum, radiation and water vapour between the canopy and the atmosphere. Good results have been obtained for monocultures with plants that are similar in size and structure and for which the model calculations for an individual plant are extrapolated (Goudriaan, 1977; Murphy and Knoerr, 1975; Sellers and Lockwood, 1981). Also the energy balance of a temperate coniferous forest has been modelled with success (Bouten, 1992). For a tropical rain forest environment, energy balance models have been applied in photosynthesis studies (e.g. Allan and Lemon, 1976) and micro climate studies (Shuttleworth et al., 1984; Roberts et al., 1993). From a scientific point of view these deterministic microclimate models are attractive as the water fluxes between the compartments are calculated in detail and the link with other physical models that describe e.g. the soil water and nutrient balance is feasible. However, in case of tropical rain forests with their large species abundance, extrapolation of the results found with one individual or even a particular species is nearly impossible because of the amount of data required.

Therefore a more empirical model such as the one designed by Rutter et al. (1971, 1975, 1977) is often used. The Rutter model offers several advantages: the input parameters are relatively easy to obtain from throughfall measurements and basic meteorological data, it uses stand characteristics rather than properties of individual plants and it calculates the water fluxes on a small time step basis, which makes it easy to link it to a vertical water balance model. In this chapter the interception and throughfall by the two main forest types, Dry Evergreen Forest and Mixed Forest, are first compared. The Rutter model was calibrated and tested for these forest types. Because it was designed originally for coniferous forest, it should in fact not be rigorously applied to tropical rain forest. In an attempt to give a more accurate description of the hydrological processes in the canopy, the Rutter model has been extended by incorporating canopy structure. In this extended model, named CASCADE, drainage and evaporation are calculated for a layered canopy, using virtually the same input parameters. The results of both models are compared to the measured throughfall.

6.2 Methodology

6.2.1 The Rutter Model

Rutter et al. (1971, 1975, 1977) designed an interception model for a Corsican Pine stand in Great Britain. The water balance for the canopy is calculated using empirical forest stand parameters and Penman potential evaporation obtained from the nearest meteorological station. The Rutter model has been adapted with success to other coniferous forest stands (Gash and Morton, 1978; Bouten, 1992), temperate deciduous forests (Rutter et al., 1975; DeWalle and Paulsell, 1969) and tropical rain forests (Lloyd et al., 1988).

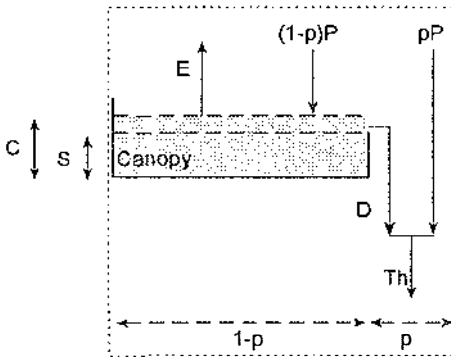


Figure 6.1 Schematic representation of the Rutter interception model (see text for explanation of the symbols).

The principles of the Rutter model are shown in figure 6.1. The water balance, i.e. the change in momentary storage (C) per unit area of a canopy, is calculated as the sum of the proportion of rainfall (P) that falls on the canopy and drainage (D) and evaporation of intercepted water (E_i) from the canopy:

$$dC/dt = (1-p-p_i)P - D - E_i \quad (6.1)$$

where C is in mm and the other variables in $\text{mm}\cdot\text{min}^{-1}$. The fraction of rainfall intercepted by the canopy is calculated as the difference between rainfall (P), the fraction of rainfall falling directly to the ground (p) and the fraction of the rainfall diverted to stemflow (p_i). Drainage from the canopy (also called "canopy drip", see chapter 4) is described with an exponential function (Lloyd et al., 1988):

$$\begin{aligned} D &= 0 & C < S \\ D &= D_0 e^{-b(C-S)} & C \geq S \end{aligned} \quad (6.2)$$

where S is the storage capacity (in mm), defined by Gash and Morton (1978) and Gash (1979) as the amount of water retained by the canopy when rainfall and throughfall have ceased and the canopy is saturated. The minimum drainage rate D_0

is the drainage rate when C equals S (in $\text{mm}\cdot\text{min}^{-1}$) and b is a dimensionless parameter. In the model, evaporation from a wet canopy surface is considered equal to the evaporation from an open water body. Therefore the potential evaporation (PE) can be used, calculated for the atmospheric conditions that prevail at the top of the canopy. In interception research the term potential evaporation is used to indicate the evaporation calculated with the Penman-Monteith formula while assuming that the bulk stomatal conductance g_c is infinitely large (Rutter et al., 1975). Furthermore the evaporation of intercepted water (E_i) is proportional to the wetted surface:

$$\begin{aligned} E_i &= PE \cdot C/S & C < S \\ E_i &= PE & C \geq S \end{aligned} \quad (6.3)$$

The throughfall (Th) is the sum of the direct throughfall and the canopy drainage:

$$Th = D + (p-pt) \cdot P \quad (6.4)$$

To calculate the stemflow (S_f) a function similar to equation 6.1 is used, where the depletion of the momentary trunk storage capacity (C_t) is compared to the trunk storage capacity (St). The excess water is completely diverted to stemflow at the end of each time step and the evaporation is taken as $0.02 \cdot PE$ (Gash et al., 1980). Following Gash et al. (1980) a numerical solution with a finite difference approximation of the change in water storage on the canopy (dC/dt) was programmed for this study. Gash et al. (1980) estimated that the difference between an analytical and numerical solution is acceptable if the integration time step is less than 2 minutes. Therefore a time step of 1 minute is used in the simulations.

6.2.2 Experimental design

The interception experiment was concentrated on two forest types: Dry Evergreen Forest and Mixed Forest. The species composition is described in chapter 3. Throughfall was measured at a 1 ha plot in each forest type (see figure 2.1 in chapter 2), which were located some 600m apart. On each of the plots 20 funnels were used, placed in a stratified random design (random placement of funnels in 20 out of 25 blocks of $20 \times 20\text{m}$). The steep angle funnels were 25 cm in diameter and put on top of 75cm high PVC containers with a content of approximately 5 litres, to avoid incoming splash from the ground. The rainfall was measured on small natural gaps adjacent to the plots, with a funnel attached to the top of a 12 m pole. A hose connected the funnel with a closed 5 l container on the ground. Although freely exposed to rainfall, these funnels were sheltered from the wind by the surrounding trees.

Throughfall was measured in two periods: from 1 October 1991 to 1 December 1991, and from 12 December 1991 to 14 February 1993. The first series was used for statistical analysis of interception of the two forest types, the second series was used to calibrate the Rutter model and derive the model parameters S , D_0 and b . In addition, stemflow measurements provided data to estimate pt and St , whereas p was derived from canopy photos (see below). Finally, the input data for the Rutter model, rainfall and potential evaporation, were taken from a weather station located approximately 1 km north of the plots.

Because the canopy structure is far from homogeneous, there is a large spatial variability in throughfall (Ford and Deans, 1978). Therefore many readings are needed to characterise and compare the interception of the forest types. According to Lloyd and Marques (1988) this can be achieved by relocating the gauges randomly after each rainstorm. The throughfall fraction of a gauge can then be seen as a measure of the canopy properties with regard to interception, and each reading can be treated as a separate measurement. During the first period of throughfall measurements this was done. From the rainstorms recorded 11 of varying size were selected in both forest types, giving a total of 213 and 220 readings for Dry Evergreen and Mixed Forest respectively. The selection was based on the fact that the rainstorms were the only one for that day and were separated from others by at least 24 hours to allow the canopy to dry completely. This dataset is called "single rainstorm" or SR-series.

Unfortunately logistical constraints made it impossible to maintain the random relocation of the funnels and each of the gauges was fixed at a randomly chosen position in the 20x20 m block. The containers were emptied every 3-14 days depending on the amount of rainfall. On a few occasions a number of large rainstorms followed each other within a day which caused the containers to overflow, leaving a total of 37 measured intervals for each plot. For each interval the mean daily throughfall was calculated (this dataset is called "daily average" series or DA-series).

Normally it should be possible to simulate the sequence of throughfall measurements throughout the whole period. However, the Rutter model uses rainfall intensities as input which are obtained from the weather station tipping bucket. Because this rainfall data record is not exactly the same as that of the plots, the simulation will always deviate from the measurements if compared directly. Thus, for instance, the throughfall cannot be compared chronologically, nor can a regression analysis of the simulated against the measured values be done. To overcome this problem, the simulation results are treated in the same way as the DA-series: the mean daily simulated interception is calculated for each of the measurement intervals. This leads to a total of 37 simulated values. The simulated and measured rainfall-interception graphs are then compared visually. Although this is a rather crude way to test a small scale interception model, it has the advantage that it can be easily seen for which range of interception values the model performs best.

However, a correction has to be made because the mean cannot be calculated by simply dividing the total interception with the length of the interval. The interception process (including the evaporation of intercepted water) continues until the moment when the canopy is completely dry. After that the process stops until the next rainstorm. The length of the period has to be adjusted for this excess time. For this purpose the assumption was made that it took on average 24 hours after a rainstorm for the canopy to dry completely. Any length of time after that moment until the next rainstorm was subtracted from the length of the measurement period.

The stemflow was recorded in the same period as the SR series. One small plot in each of the two forest types was demarcated and all trees above 10 cm DBH were

included in the stemflow measurements. The area covered by the crowns of these trees was approximately 100 m² for both plots. Plastic tubes were cut to obtain flexible drains, which were then glued to the bark. The tube spiraled two times around the stem (to ensure a complete catch of stemflow) and drained in a PVC container.

6.2.3 Calculation of model parameters

Following the method of Leyton (1967, in Rutter et al., 1971), the canopy storage capacity S is calculated from a regression analysis of the daily throughfall and rainfall measurements. When the actual amount of water on the canopy C is smaller than the canopy storage capacity S , only direct rainfall reaches the ground, i.e. $T_h = (p-pt)P$. When C is larger than S , both canopy drip and direct throughfall reach the ground, i.e. $T_h = (p-pt)P + D$. This produces an inflection point in the P-T graph. Linear regression lines through the values below and above this inflection point will give the value at which the canopy is just saturated: theoretically at this point the equality $T = P - S$ is valid. The lines should be drawn through the datapoints with maximum throughfall, as these represent data with nil evaporation.

On the Dry Evergreen and Mixed Forest plots the stemflow of 10 and 11 rainstorms were recorded respectively. The stem saturation storage S_t is derived in the same way as the canopy saturation storage S from these measurements, while the fraction pt (equation 6.1) is assumed to equal the average stemflow/rainfall ratio.

To determine the fraction of the rainfall reaching the surface (parameter p in equation 6.1), it is assumed that $p = 1 - fr$, where fr is simply the fraction of ground surface covered by the canopy. To calculate fr , black and white canopy photographs were taken from the part of the canopy directly above the funnel during the SR series measurements. In total 210 photographs were taken with a 50 mm lens to avoid distortion. The photographs were scanned with a resolution of 300 dots/inch and combined with a digital mask leaving a circle free in the centre. Thus a circular area, corresponding to approximately 60 m² on canopy level, was isolated on the photograph. It was assumed that the mean fraction of black and white pixels gives a good estimate of fr . To calculate the mean an arcsine transformation is used so that the sample distribution resembles a normal distribution.

The potential evaporation (PE) was calculated from weather station data of the same period. In chapter 4 the procedures are explained with which the weather station measurements (in particular the wind speed) are extrapolated to a height of 50 m, in order to calculate the PE at canopy level. Equation 4.12 gives the Penman-Monteith formula for a single canopy layer. When regarding the canopy as a single container and with the conductance determined by the aerodynamic conductance g_a only, equation 4.12 simplifies to (Thom, 1976):

$$PE = \frac{\Delta Rn + \rho C(\delta e)g_a}{\lambda(\gamma + \Delta)} \quad (6.5)$$

where Δ is the rate of increase with temperature of the saturated vapour pressure of

water at air temperature (in Pa.°C⁻¹); γ is the psychrometric constant (in Pa.°C⁻¹); λ is the latent heat of the vaporization of water (J.Kg⁻¹); R_n is net radiation (in W.m⁻²); ρ is air density (in Kg.m⁻³); C is the specific heat of the air (in J.Kg⁻¹.K⁻¹); δ is the vapour pressure deficit (Pa) and g_a is the aerodynamic conductance (in m.s⁻¹). The aerodynamic conductance is calculated with equations 4.14 and 4.15 in chapter 4.

6.3 Results

6.3.1 Comparison of forest type interception

To characterize and compare the interception of Dry Evergreen forest (DEF) and Mixed forest (MF), the SR-series were analyzed statistically. However, the data are positively skewed for both forest types, and following Lloyd and Marques (1988), the square root of the readings were taken to normalize the distributions. This gave slightly better distributions ($\chi^2 = 11.6^{**}$ for both forest types), and all statistics in this study were based on these transformations. The retransformed mean and standard error of the interception fractions are 0.222 ± 0.020 for DEF and 0.250 ± 0.024 for MF.

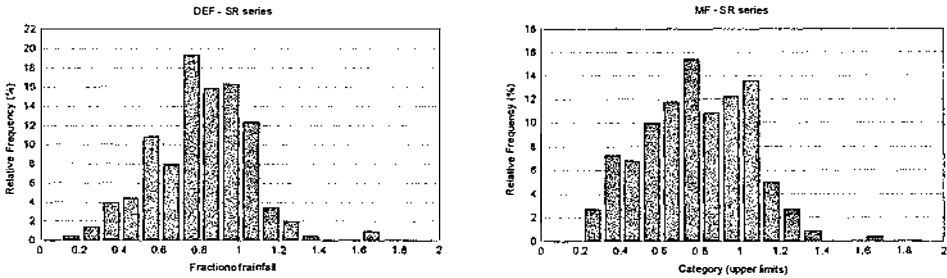


Figure 6.2 Frequency distributions of the throughfall expressed as a fraction of the rainfall, for Dry Evergreen Forest (left) and for Mixed Forest (right).

Looking at the frequency distribution of the throughfall as a fraction of the rainfall (figure 6.2), the two forest types seem somewhat different. In DEF 25% of the throughfall measurements are above gross rainfall which account for 29.5% of the total throughfall; in MF these values are 23% and 43% respectively. The large percentage of throughfall larger than rainfall is common for tropical rain forests, comparable values are found in the rain forest near Manaus by Lloyd and Marques (1988): 29% of their throughfall measurements were above rainfall accounting for 46% of the total amount. Fritsch (1990) reports throughfall values between 10 and 160% of the gross rainfall in a Mixed forest in French Guyana. The difference between DEF and MF could be an indication of differences in canopy structure which are reflected in the throughfall.

An ANOVA showed that the interception for both forest types was not significantly different ($F = 1.236$ n.s., $n = 443$). However, because the SR-series covered only a short period, the DA-series were analyzed as well. Because the gauges are not relocated a systematic error is introduced if all readings are treated as separate values. An estimate of this systematic error can be made from the SR series, using the method proposed by Lloyd and Marques (1988):

$$\sigma_n = \sigma_N(1 + \sqrt{N/n}) \tag{6.6}$$

where n is the number of samples (i.e. 20 gauges), N is the number of locations used in the sampling scheme (i.e. $N = 220$ random relocations) and σ_N is the standard error resulting from random relocations within this scheme (i.e. the standard errors given above). The resulting interception fractions and standard errors associated with the DA-series are: $I = 0.215 \pm 0.086$ for DEF and $I = 0.218 \pm 0.104$ for MF. Thus the standard errors have increased from 10% of the interception to almost 50%. This corresponds well research of Fritsch (1990) in French Guyana who calculated a systematic error of 0.108 for a scheme of 20 funnels. Nevertheless, using the mean of 20 gauges of one measurement as a characterization of the interception, an ANOVA showed that the forest types are also not significantly different ($F = 0.140$ n.s., $n = 72$) for the DA-series. In view of these results the forest types are considered not to be significantly different and a single set of stand parameters is derived from the DA-series of both DEF and MF to test the Rutter model.

6.3.2 Derivation of model the parameters

The saturation storage capacity S is one of the most important parameters of the model (Jackson, 1975). It is derived from a linear regression of the daily rainfall (P) and throughfall (T). In this analysis the mean daily values are used as the throughfall was not measured every day. Figure 6.3 shows that there is considerable scatter. The inflection point in figure 6.3b lies at $(P, T) = (3.04, 2.15)$ mm. This yields a canopy storage capacity of $S = P - T = 0.89$ mm. Because of the scatter, both regression lines can be made to vary without much difference in explained variance, and S varies accordingly from 0.7 to 1.2 mm. The slope of the lower regression line (the line derived from the white triangles in figure 6.3b) is 0.7 and should equal $p - pt$. However, it is much higher as $p - pt$ is 0.08 (see below), which indicates that datapoints with zero evaporation did not exist in the dataset. In spite of the uncertainty in the derivation of S , the value of 0.89 mm compares well with values found for tropical forests (see table 6.1).

Table 6.1 Saturation storage capacity S (in mm) of various tropical forests

<i>Reference</i>	<i>S (mm)</i>	<i>Location</i>
Jackson, 1975	0.89	Tanzania
Lloyd et al., 1988	0.74	Manaus, Brazil
Herwitz, 1985	0.26-0.99	Queensland, Australia
This study	0.89	Mabura, Guyana

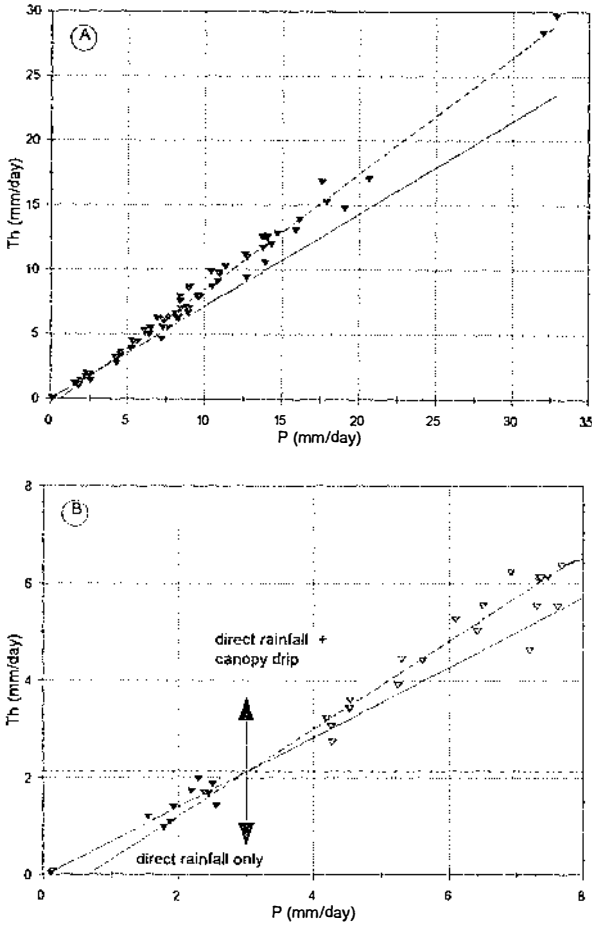


Figure 6.3 Derivation of the canopy storage capacity S from rainfall (P) and throughfall (Th). See text for explanation of the regression lines.

Contrary to the canopy storage capacity, the drainage parameters b and D_0 can only be assessed with measurements of throughfall at a sub-storm level. This has been done for a Corsican pine forest by Rutter et al. (1975) who found the values $D_0 = 0.002 \text{ mm}\cdot\text{min}^{-1}$ and $b = 3.89$. Under the assumption that differences in drainage between the forest under investigation and the Corsican pine forest are caused by a different canopy and not by the depth of water on the canopy, the drainage

parameters can be modified by using the difference in S (Rutter and Morton, 1977; Lloyd et al., 1988): $D_0 = 0.002 * S = 0.00178 \text{ mm} \cdot \text{min}^{-1}$ and $b = 3.89/S = 4.37$.

The stemflow measurements of the two forest types are not significantly different at a 5% level. Thus the fraction of rainfall diverted to stemflow (pt) is set equal to the mean of the total dataset: $pt = 0.0063 \pm 0.0027$. The trunk storage capacity is derived from the stemflow graph in a similar way as S, resulting in $St = 0.04 \text{ mm}$. A linear relation can be found between the stemflow and the rainfall:

$$Sf = 0.0086 * P - 0.0373 \quad n = 22, R^2 = 0.87 \quad (6.7)$$

Equation 6.7 is used to correct the mean rainfall of the DA-series, in order calculate the interception as the difference between rainfall, throughfall and stemflow:
 $I = P - Th - Sf$.

The cover fraction of the two forest types, calculated from the digital photographs, appears not to be significantly different at a 5% level. Therefore the re-transformed mean of the total data set was used in the model. Because the photographs distinguish between sky and non-sky only, the stemflow fraction is included in the non-sky pixel fraction. The sky-pixel fraction $fr = 0.93 (\pm 0.03) - 0.0063 = 0.92$. Thus the parameter p equals 0.08.

6.3.3 Simulation with the RUTTER model

Using the values for the parameters derived above and a 1 minute time step for the simulation, the Rutter model underestimates the total interception. Whereas the cumulative measured interception is 17.3% for DEF (393 mm of a rainfall total of 2276 mm) and 16.0% for MF (361 mm of a rainfall total of 2259 mm), the model estimates only 13.4% interception (313 mm of a rainfall total of 2333 mm) over the same period. However, in view of the large standard error associated with the DA-series, this difference may not be significant.

To interpret the model results a scatterplot of the daily rainfall against mean daily measured and simulated interception is shown in figure 6.4. The measured values consist of the mean daily interception of both forest types. Because the plots were located 600m apart and the rainfall distribution between the plots differed slightly, the mean interception of the plots were treated as separate measurements. The measured values show a wide scatter caused by factors such as antecedent canopy moisture content, rainstorm intensity and duration, evaporation rate and measurement errors, which result in a widely varying interception associated with the same rainfall (Jackson, 1975). The variation of simulated interception values clearly differs from the measured variation. Especially above a daily mean rainfall of approximately 10 mm the Rutter model seems to underestimate the interception considerably. Apparently the accumulated effect over the measurement period is an underestimation of the interception percentage of 3 - 4%. The long term effect depends on the rainfall frequency distribution of the research area. Figure 6.5 shows the cumulative frequency curve of the daily rainfall recorded at the weather station. About 30% of the rainfall falls on days with more than 10 mm. This means for this

area the Rutter model gives a reasonable estimate of the interception for 70% of the rainfall only. For instance Lloyd et al. (1988) found a small overestimation of the long term interception in an area near Manaus which has a similar annual rainfall. Clearly the model cannot be evaluated properly without a rainfall frequency distribution.

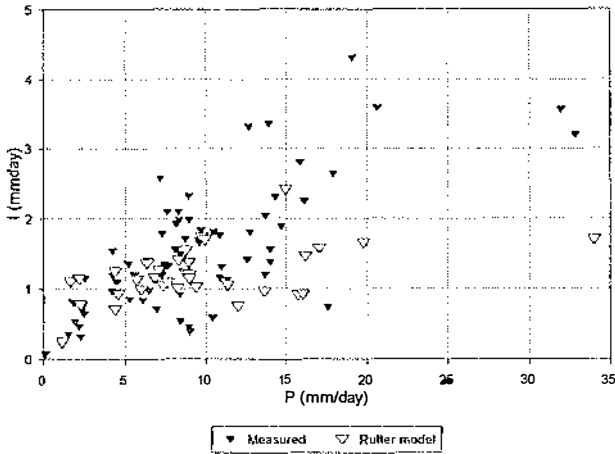


Figure 6.4 Results of the simulation of the DA series with the Rutter model.

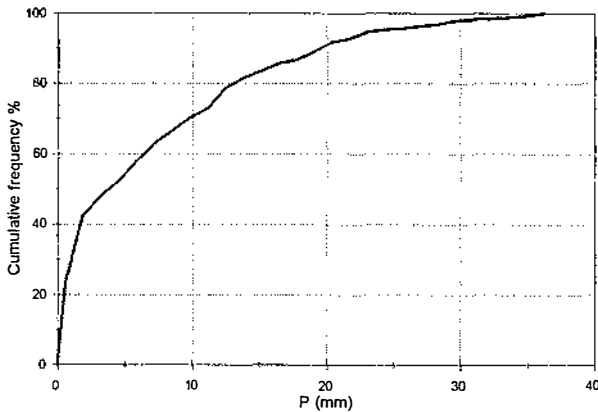


Figure 6.5 Cumulative frequency distribution of daily rainfall of period in which the DA series were measured.

6.3.4 Sensitivity analysis

Because the model parameters are also derived from the DA-series, they will have an error margin as well. Of the model parameters, the canopy storage capacity S is most likely to have a large error because of the wide scatter of points in the P-T

graph. Of the model variables, the extrapolation of potential evaporation to canopy level is most susceptible to errors because of the simplified way the wind profile is extrapolated and because of the assumption that the micro-climate above the canopy is similar to that of the weather station clearing. To test the sensitivity of the Rutter model the interception was calculated with both S and PE varying from -50% to +100% of the original value. The drainage parameters are dependent on S and were allowed to vary with it. The results of the sensitivity analysis are shown in figures 6.6a and b.

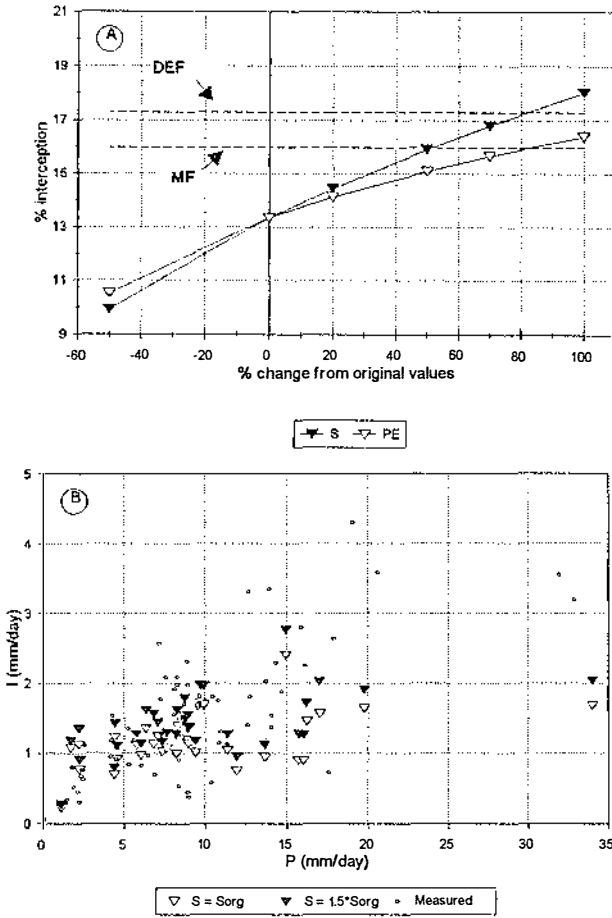


Figure 6.6 a) Sensitivity of simulated interception percentage to changes of the canopy storage capacity (S) and the potential evaporation (PE). b) Results of the simulation using a canopy storage capacity of 1.35 mm, as compared to the original value of 0.89 mm.

Increasing S by 50% and 100% of the original value of 0.89 mm brings the cumulative simulated and measured interception closer together. A similar result is achieved by increasing the evaporation with 100%. Nevertheless, these adjustments are very large: increasing S by 50% to 1.35 mm brings the value outside canopy storage capacities found by other researchers (see table 6.1). Also, a comparison of the simulated values of $S = 0.89$ mm and $S = 1.35$ mm, shows that interception is increased over the whole range of rainfall values, resulting in an overestimation in the low range while the high range is still severely underestimated (figure 6.6 b). Thus this not actually an improvement.

6.4 The CASCADE model

6.4.1 Evaporation and drainage in the layered canopy

In order to improve the performance of the Rutter model the interception should be increased for large rainstorms. To achieve this the model was extended with a layered representation of the canopy. The drainage and evaporation functions are modified accordingly, and the resulting model is termed the CASCADE model.

The vertical stratification described in chapter 4 (table 4.1 and figure 4.4) is used also in the CASCADE model. Evaporation and drainage depend on the amount of leaf surface in each layer. The evaporation of intercepted water from each canopy layer depends on the micro climate inside the canopy. In chapter 4, section 4.4.3, is explained how the micro climate is derived from the weather station measurements. In analogy with the Rutter model, the layer evaporation is based on the layer PE, calculated with equation 4.12 and using the aerodynamic conductance g_a only.

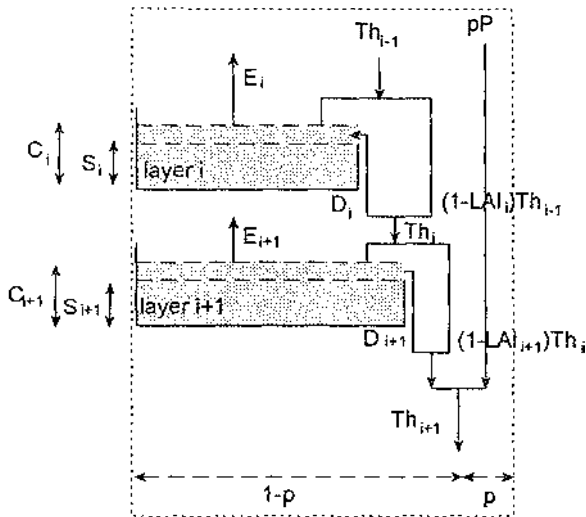


Figure 6.7 Schematic representation of the CASCADE interception model (see text for explanation of the symbols).

From figure 6.7 it can be seen that a small part of the water still reaches the forest floor as direct rainfall, which is calculated in the same way as in the Rutter model with the fraction p . In order to estimate the fraction of the rainfall that is intercepted by a layer i , the horizontal projection of the individual leaves has to be known. However, the average leaf angle distribution, and its horizontal projection, of the two forest types are unknown. Therefore, it is simply assumed that the fraction equals the LAI_i of a layer. Thus the change in the amount of water stored on the layer (dC_i/dt) depends on the amount of throughfall from the layer above (Th_{i-1}), the leaf area index LAI_i , the evaporation from the layer E_i and the drainage from the layer D_i . The throughfall of a layer is then the sum of the fraction of Th_{i-1} not retained by the layer and the drainage:

$$\frac{dC_i}{dt} = LAI_i(Th_{i-1}) - D_i - E_i \quad (6.8)$$

$$Th_i = (1 - LAI_i)Th_{i-1} + D_i$$

In analogy with Sellers and Lockwood (1981), the drainage parameters are derived by regarding each layer as a small canopy. This allows the layer storage capacity S_i and drainage parameters b_i and D_{0i} to be derived from the original parameter values measured by Rutter et al. (1975), using the same reasoning as above:

$$S_i = S \frac{LAI}{LAI_i} \quad (6.9)$$

$$b_i = 3.89/S_i$$

$$D_{0i} = 0.002S_i$$

6.4.2 Results

From figure 6.8, which shows 4 rainstorms during the first week of January 1992, it can be seen that a layered canopy has a buffering effect as a result of the change in drainage processes. At the start of each rainstorm more water is stored in the layered canopy of the CASCADE model (thin line) than in the single storage canopy of the Rutter model (thick line). The reason is that the sum of C_i does not equal C because the drainage of a layer is determined by the throughfall from the layer above. Thus the layers influence each other progressively as the water moves downward in the canopy. The canopy also dries out faster especially for the smaller rainstorms. The throughfall below the canopy consists only of the sum drainage of the last layer, the throughfall fraction of the layer above the last and the direct throughfall.

The accumulated effect is that the interception is considerably increased, for all rainfall amounts except the highest (figure 6.9). The overall interception calculated by the CASCADE model is very close to the measured interception: 16.4% (382 mm of a rainfall total of 2332 mm). The better performance of the model is also shown by the wider scatter of the points: whereas the Rutter model interception values lie in a relatively narrow band, the CASCADE model values are closer to the measured values between 5 and 20 mm of daily rainfall.

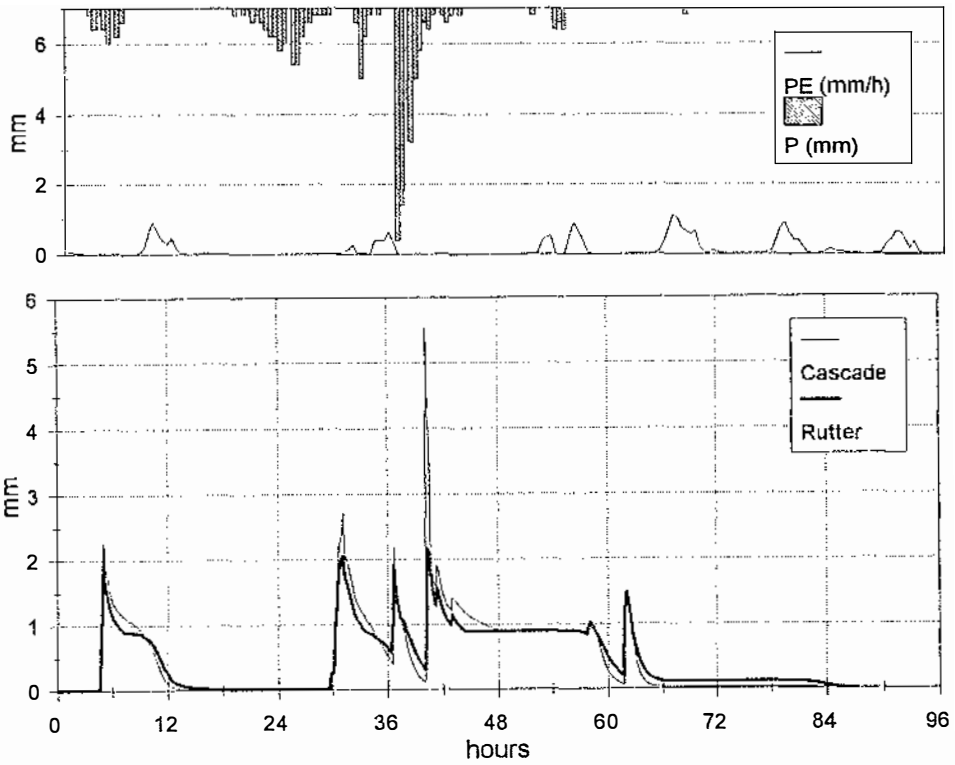


Figure 6.8 Top graph: potential evaporation (mm/h) and the rainfall (mm) in 10 min intervals. Bottom graph: change in canopy storage C from 0:00 h on 7/1/1992 to 23:50 h on 11/1/1992. C of the CASCADE model is calculated as the sum of C of each layer.

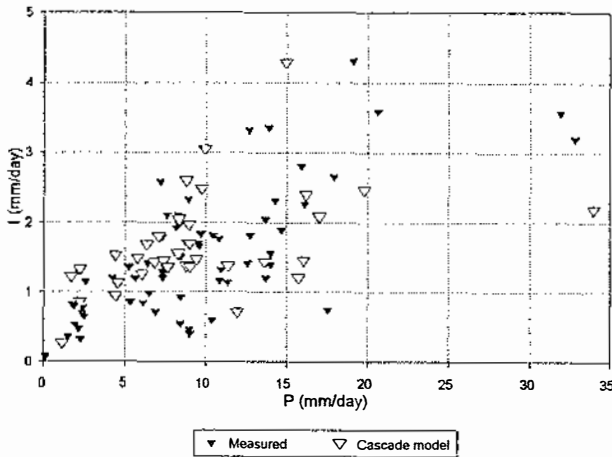


Figure 6.9 Results of the simulation of the DA series with the CASCADE model, compared to the measured values.

The dataset poses its constraints on the testing of the model. The fact that the funnels were not relocated induces a relatively large systematic error, which was estimated at almost half the interception fraction. Therefore a difference between measured and simulated interception in the order of 25%, could well be a result of uncertainty in the measurements and not of the model. Moreover, calculating average simulated interceptions over periods of 3 to 14 days, may obscure the real behaviour of the model, which operates with 1 minute time steps.

The canopy storage capacity S has a large uncertainty. Only the datapoints representing a situation with near zero evaporation should be included in the regression lines. In practise this difficult to achieve, especially with a small dataset such as this one. Bouten (1992) severely criticises this method to derive S . He optimizes S according to his dataset and uses it as a calibration parameter. Unfortunately the dataset presented in this chapter is not detailed enough to follow the same method. However, the sensitivity analysis shows that the size of S does not really influence the variation in the datapoints and a underestimation of the larger rainstorms is still expected.

Both models underestimate interception of high rainfall amounts. In the research area a high daily rainfall usually means several heavy rainstorms with intensities of up to 7 mm in 5 minutes. The mechanisms of water storage and drainage seem different during heavy rainstorms than during low intensity rainfall, among other things because the kinetic energy of the raindrops is higher (the leaves are "pushed" aside), and there is more turbulence. Jackson (1971, 1975) finds large standard errors in interception estimates for heavy rainstorms, which makes prediction and unreliable. Also he finds different regression equations for rainstorms with different intensities. Some analytical interception models are based on this fact, such as the one designed by Gash (1979), see also Gash et al. (1978, 1980), Bruijnzeel and Van Wiersum (1987), Lloyd et al. (1988) and Pook et al. (1991a,b). The difference of behaviour of the canopy for differences in rainfall intensity can be a result of drainage: Massman (1983) includes the rainfall rate in the equations that describe change of water storage and canopy drainage and obtains better results compared to Rutter drainage equations. Thus it seems that Rutter's empirical drainage equation needs revalidation for high intensity rainstorms or a different drainage model should be defined. Apart from the drainage the storage also differs with rainstorm intensity: Herwitz (1985) found much lower values for canopy storage capacity under turbulent air conditions ($S = 0.026-0.49$ mm) than under still air conditions ($S = 0.23-0.99$ mm), which also indicates that a model would need to include rainfall intensity.

With this in mind the following conclusions can be drawn. Measurements in two 1ha plots in Dry Evergreen forest and Mixed forest, show that the forest types are not significantly different in throughfall, stemflow and canopy cover fraction. The cumulative interception calculated by the Rutter model over a period of 14 months was underestimated: 13.4% as opposed to 17.3% measured for Dry Evergreen Forest and 16.0% measured for Mixed Forest. Comparing daily mean interception with rainfall shows that the underestimation is largest for days with a rainfall above

approximately 10 mm. Also the simulated values occur in a much narrower band than the measured values, indicating that the model may be too rigid and the processes involved may not be simulated accurately. However these conclusions are only tentative because there is a wide error margin in the measured interception.

The cumulative interception can be improved by increasing the canopy storage capacity (S) or the potential evaporation (PE) by 50% to 100%. However, a breakdown in mean daily values shows this is caused by an serious overestimation on the days with low rainfall amounts. Thus the results of the model not only depend on the stand parameters but also on the rainfall frequency distribution of the area, without which the Rutter model cannot be evaluated correctly.

The CASCADE model uses the drainage and evaporation principles of the Rutter model applied to a layered representation of the canopy. This results in a buffering effect which causes a large temporary storage of the rainfall, especially at the start of the rainstorm. The CASCADE model gives a good estimate of the total interception (16.4% over the measurement period), but performs markedly better in the range of 5 to 20 mm of daily rainfall. The scatter of simulated interception values resembles more that of the measured values.

7.1 Introduction

The permeability of the sandy and loamy soils in the research area is generally very high, causing most of the throughfall to infiltrate into the soil. On a catchment scale however, surface runoff does occur: analysis of the hydrograph of the experimental catchment showed that stormflow runoff amounts to a few percent of the annual rainfall (see chapter 11). For most rainstorms, the amount of stormflow can be attributed to direct rainfall on the channel and on the saturated or near saturated soils close to the creek. The largest rainstorms however, must have a larger contributing area to account for the amount of stormflow. Also, evidence of overland flow was seen in the field, such as bare patches of soil and accumulation of litter downslope against obstructions.

In general overland flow takes place when the infiltration rate of the soil is exceeded by the rainfall intensity. There are several situations in which this can occur (Ward and Robinson, 1990): Hortonian overland flow occurs when the rainfall intensity is larger than the infiltration capacity (depending on the soil characteristics and the antecedent soil moisture content), or saturation overland flow occurs when the groundwater rises to the surface so that the soil storage is filled up (which may occur at the bottom slopes and valley floors). A special case of the latter occurs when the topsoil becomes saturated so that overland flow occurs while a constant infiltration rate is maintained. Ward and Robinson (1990) mention a fourth type of overland flow that is not related to the soil moisture conditions: they note that overland flow occurs if the general alignment of the soil material is perpendicular to the slope, causing preferential flow paths that lead the water back to the surface (comparable to functioning of a thatched roof).

As an alternative to overland flow, much research has been done into the mechanism of fast throughflow. Germann and Beven (1981 a, b) describe a system whereby macro pores in the soil increase the conductivity considerably (up to a factor 75) if the other pores are saturated, in organic matter rich soil samples. Wilson et al. (1990) measured a subsurface stormflow in a forested catchment which amounted to 12.5% on a rainstorm basis and concluded that flow through macro and meso pores in the clayey soils were the predominant stormflow mechanism. Bonell et al. (1982) report large amounts of overland flow under rain forest in Queensland (Australia) but this is due to a low permeability of the clayey soils. However, they also note a "bypass mechanism" related to macro pores. It is not clear if lateral throughflow occurs in the experimental catchment. The bulk of the roots occur in the topsoil and for the subsoil often has only a very weak structure. Combined with the high permeability it seems that if subsurface throughflow occurs, it will be near the surface. Therefore this study concentrates processes near the soil surface.

Given the infiltration rates of the sandy and loamy soils given in table 5.2, Hortonian overland flow will seldom occur in the research area. On the other hand,

saturated topsoil conditions have been measured in the field. Also a sharp boundary frequently exists between the partly decomposed organic material of the litter layer and the mineral soil. Therefore the overland flow under rain forest can probably be described as saturation overland flow through preferential flow paths in the litter layer. The exact mechanism is unknown. To quantify this lateral flow, the processes can be regarded from two points of view: either it is seen as saturated overland flow with a very high surface resistance caused by the litter, or it is seen as saturated lateral throughflow through a very porous medium. As the litter varies considerably in composition and thickness both viewpoints may be true, or a change in type of flow may occur if the flow depth exceeds the litter depth.

In this chapter both viewpoints are used to analyze the lateral flow observed in the field and under experimental conditions. Two series of tests are done: in the Tropenbos Ecological Reserve, five small plots were established to measure the runoff under field conditions, and at the same time a series of flow tests were done on large soil samples under controlled circumstances.

7.2 Methodology

7.2.1 Throughflow theory

Assuming that the lateral flow through the litter layer behaves like flow through a rigid porous medium, the driving force is the difference in hydraulic head between two points. Lateral flow through the litter will only occur if the underlying mineral soil is nearly or fully saturated, and a water layer rises in the litter layer. To simplify calculations it is assumed that there is a sharp boundary between the saturated and non-saturated part of the litter, so that adhesive forces can be neglected and the difference in hydraulic head (dH) depends on the gravitational force only. Thus it equals the difference in height (dz) between the two points (with distance dx). The lateral flux can now be calculated as:

$$Q_r = K_{lat} * dH/dx = K_{lat} * dz/dx = K_{lat} * \sin(\alpha) \quad (7.1)$$

in which K_{lat} is the saturated lateral conductivity (m/s), and α is the slope gradient.

7.2.1 Overland flow theory

Overland flow can be described in the same terms as channel flow, when it is regarded as sheet flow with a given width and depth. An important factor in the overland flow is the flow rate which depends on the depth of the water layer, the slope gradient and the surface resistance. The relation between these factors is thought to change with the degree of turbulence within the flow. The turbulence can be expressed with the dimensionless Reynolds number (De Lima, 1989):

$$Re = 4 \frac{VR}{\nu} \quad (7.2)$$

where V is the flow velocity (m/s), R is the hydraulic radius (m) and ν is the kinematic viscosity (m^2/s). The hydraulic radius R equals the cross-sectional flow area divided by the wetted perimeter. According to De Lima (1989) the flow is laminar if $Re < 375$ and turbulent if $Re > 1500$. Chow (1984) uses a Re of 2000 as upper limit. In between a transitional stage exists. It should be noted that some researchers omit the factor 4 in equation 7.1 for arbitrary reasons (Abrahams et al., 1992). Note that all Reynolds numbers that are discussed in this chapter have been calculated using the factor 4.

The resistance to flow is usually expressed with the Darcy-Weisbach roughness coefficient f (De Lima, 1989, Gilley et al., 1992):

$$f = \frac{8gRs}{V^2} \quad (7.3)$$

in which g is the acceleration due to gravity and s is the average slope gradient. In overland flow, the depth of the water layer is usually much less than its width. Therefore the hydraulic radius is set equal to the flow depth D per unit width of a slope segment. However, in the flow tests described below, the soil samples have only a limited width and the actual hydraulic radius R is used to calculate both Re and f .

7.2.2 The experimental setup

The runoff research consisted of two experiments. First the amount of surface runoff generated under field conditions was measured at 5 plots on a hillslope in the Tropenbos Reserve. Second the behaviour of flow through the litter layer was studied with flow experiments on a number of large soil samples.

In the first experiment, 5 plots with a size of 150 x 200 cm were selected approximately 800 m south of the weather station (see chapter 2, figure 2.1). A detailed elevation map of a convex upper slope segment under Mixed forest was made by interpolating a series of level measurements using a WILT level. Plots were demarcated on slope segments which did not have any fallen trees or large branches. The plots had a uniform slope, with gradients varying between 25% and 60% (see table 7.1). Because of the litter layer it was impossible to judge which parts of the slope contributed to a plot. Therefore three sides of the plots were closed, using zinc strips that were pushed carefully into the ground. On the downward side a zinc tray was inserted just under the litter layer. The tray drained in a 25 litre container. This end of the plot was covered with a plastic roof to prevent runoff on the tray itself. Amounts of runoff were recorded every 1 or 2 days from 25 June to 21 September 1992.

Adjacent to each plot, 2 tensiometers were installed at 20 and 50 cm depth, with which pressure head of the top soil was monitored. The throughfall was recorded with a rain gauge next to each plot. The plots were all located on a Haplic Ferralsol (see chapter 2), which was relatively homogeneous to 2.5 m depth. The litter layer was very heterogenous in depth and composition, but there was usually a sharp boundary between the organic material and the mineral soil.

In the second experiment, 17 large soil samples of approximate dimensions (LxWxH) 40x20x15 cm were dug out of the soil surface. Care was taken to disturb the samples as little as possible. The samples were taken both from the runoff site and from other locations, but all on the same soil type and forest type. Because of the large short range variability in soil properties and litter thickness (see chapter 5), and the time it took to prepare each sample (see below), the number of samples was limited and it was impossible to differentiate between site characteristics (slope, tree species, litter type etc.) in the experiment. Therefore the 17 samples were taken at random locations. The thickness of the sample litter layer (d) varied from 0.5 to 7 cm.

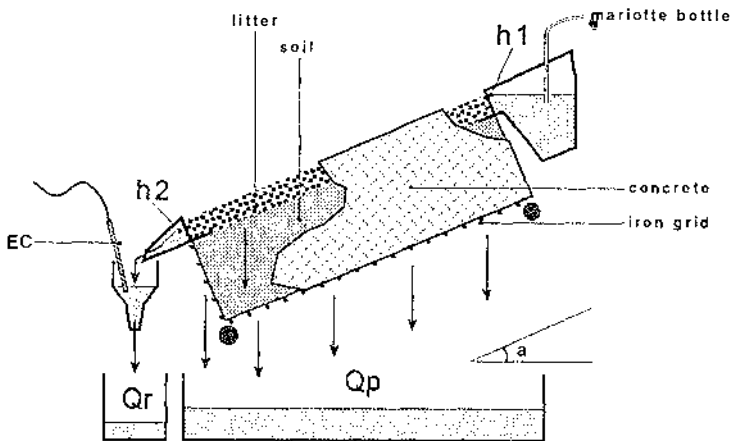


Figure 7.1 Experimental setup for flow tests on large soil samples (for the abbreviations see text).

The samples were prepared by covering the two long sides with a 3 cm thick cement layer directly to the soil, to prevent leakage along the sides. The bottom and the upper and lower sides were covered with a metal wire mesh to allow free drainage in the direction of flow (see figure 7.1). The soil and litter were kept moist while the cement dried. A zinc container with the same width as the sample was constructed and with a small lip inserted carefully just under the litter layer. The container was connected to a Mariotte bottle so that a constant head (h_1 in figure

7.1) could be maintained. On the lower side a small tray was inserted to collect the lateral flow through and over the litter (Q_r) while the total vertical flow (Q_p) was collected in a large container. A wooden frame allowed the whole construction to be set at various angles. Each measurement was continued until both fluxes Q_r and Q_p were constant, which meant that the sample was completely saturated. The following variables were calculated:

- 1 - The runoff percentage (RO%), i.e. the ratio between the lateral and total stationary discharge.
- 2 - The lateral hydraulic conductivity (K_{lat}) from equation 7.1. The thickness and porosity of the litter layer probably will have a large variation. Therefore the exact shape and size of the water layer in the litter cannot be reconstructed. In order to simplify the calculations, the assumption was made that the flow depth changed linearly between h_1 and h_2 .
- 3 - The equivalent throughfall intensity (T_e). To compare the flow tests and field experiment, it was assumed that runoff only occurs when the mineral soil is saturated. At the end of a test both discharges are stationary and the sample is saturated, creating the circumstances for ponded infiltration. It is assumed that the sum of vertical ponded infiltration rate and the lateral discharge, is the equivalent of the throughfall needed to produce a similar runoff behaviour under field conditions. The total stationary discharge Q is expressed in cm^3/min . Using the horizontal projection of the sample surface, Q is recalculated to mm/min .
- 4 - The flow velocity (V). When the flow was stationary, NaCl was added to the water at the upper end of the sample as a single "pulse". The time was measured for this "salt-pulse" to be registered at the lower end with an electrical conductivity (E) meter and thus V could be calculated, as well as the Reynolds number (Re) and surface resistance (f) with equations 7.2 and 7.3.

A number of flow tests were done with each sample: firstly the slope angles ranged from 10% to 60% with 10% intervals, and secondly two constant heads h_1 were applied to each series of slope angles. A low head at 0.5 to 0.75 of the litter layer thickness and a high head at 1.0 to 1.1 of the litter layer thickness were applied, representing measurements with respectively complete throughflow and partly overland flow (on top of the litter layer). After the 6 measurements at various angles, extra measurements with the conductivity meter were done at slope angles of 20%, 40% and 60%. Each of these EC measurements was done 3 times and the average was used in the calculations.

7.3 Results

7.3.1 The field experiment

The throughfall varied considerably between the five funnels: the minimum throughfall was 592 mm and the maximum 903 mm (mean throughfall 740 mm), recorded in 88 days. Table 7.1 gives the throughfall (corrected for plot slope angle) for which runoff was recorded, and the runoff amounts. Unfortunately on 4

occasions all containers overflowed and no reliable runoff values were obtained. The throughfall on these days was between 50 and 90 mm. Therefore the cumulative throughfall for which runoff was recorded amounted to 2/3 of the measured throughfall. The cumulative runoff percentage increased with slope gradient from 3.2% for a 25% slope to 13.3% for a 60% slope. Plot B had exceptionally low runoff amounts which could be a systematic error. Plot C was malfunctioning on 5 days with throughfall varying between 20 and 30 mm. Thus the runoff percentage in table 7.1 is very low. A better idea of the runoff is obtained from linear regressions

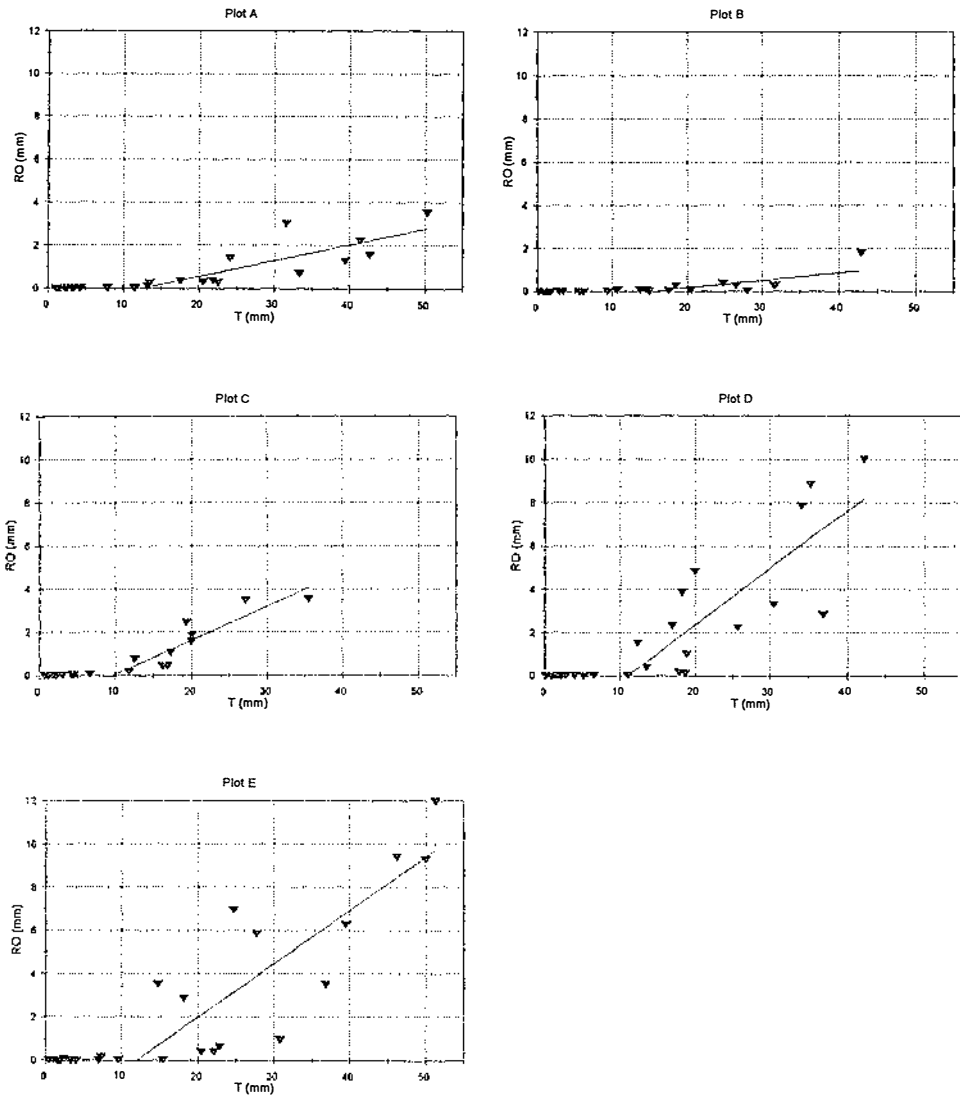


Figure 7.2 Runoff-throughfall relations at five small forest plots for throughfall amount less than 50 mm. The regression coefficients of the lines are given in table 7.1.

between runoff and daily throughfall amounts. All plots had very little runoff (on average 0.01 mm) when the daily throughfall was less than 10 mm. Figures 7.2 a to e show that above that value a linear relationship between throughfall and runoff exists. The regression coefficients are given in table 7.1. The values show that the runoff increases also with slope gradient and can be as much as 0.25 of the throughfall.

Table 7.1 Regression coefficients for runoff (mm) and throughfall (mm), for throughfall amounts larger than 10 mm.

Plot	<i>s</i> %	<i>T</i> mm	<i>RO</i> mm	%	<i>X-coeff</i>	<i>const</i>	<i>R</i> ²	<i>n</i>
A	25	500.3	15.6	3.22	0.074	-0.929	0.6654	14
B	35	414.2	4.0	1.01	0.036	-0.552	0.5199	14
C	40	373.6	16.0	4.62	0.158	-1.535	0.8002	10
D	50	429.8	49.4	12.86	0.263	-2.892	0.6401	15
E	60	547.6	62.4	13.29	0.247	-2.949	0.6886	15

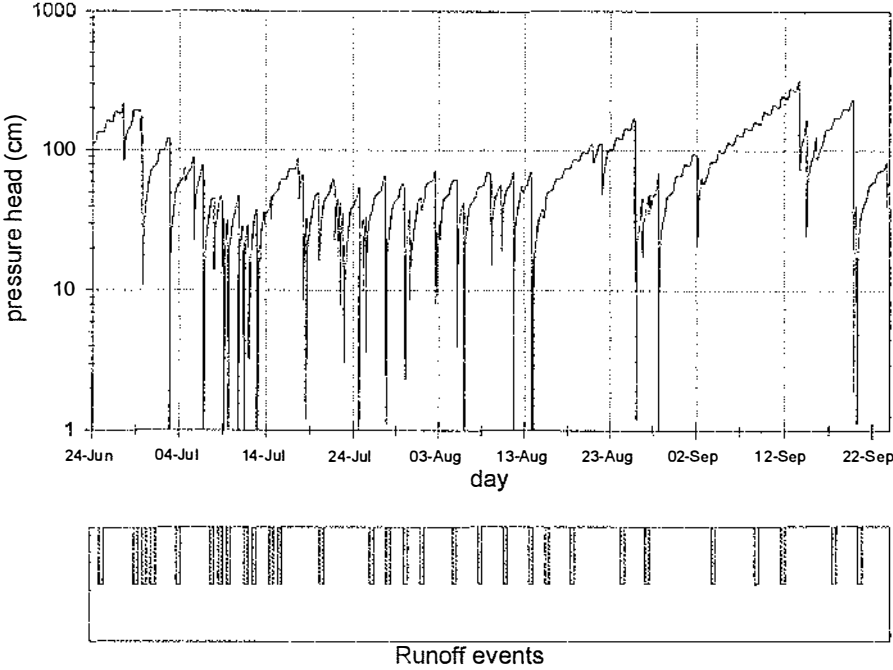


Figure 7.3 Simulated pressure head at the surface of plot A and the measured runoff events.

Runoff occurs probably only if the soil is nearly or fully saturated. To test this assumption the pressure head at the soil surface was simulated with the model SOAP. The model soil and plant characteristics that are used as input parameters are discussed in chapter 8, where the potentials measured adjacent to the plots are compared to the model results. In figure 7.3 the pressure head is shown together with the days that runoff was registered (the small fluctuations in the graph are caused by the daily course in evapotranspiration). The rainfall that is used in SOAP is measured at the weather station which was slightly different from the throughfall registered at the plots (particularly in September). Nevertheless most runoff coincides with a pressure head above -10 cm. This indicates that the soil does not need to be fully saturated for runoff to occur. This is noted by several researchers who use the so called "field saturation" in overland flow modelling which is often set at 95% of the pore volume and corresponds with the air entry potential (Slack and Larson, 1981; Moore 1979; Campbell, 1988).

7.3.2 The flow tests: surface runoff as litter throughflow

While the flow tests were done it appeared that for some slope angles between 10% and 30% no runoff was produced, even for constant heads larger than the litter layer thickness. These measurements were not included in the dataset since it is not known under what conditions these samples would produce runoff. A total of 94 tests remained for which the lateral conductivity (K_{lat}) was calculated with equation 7.1. The variable K_{lat} has a log-normal distribution, with a retransformed mean of $K_{lat} = 229$ m/day ($\sigma = 5$ m/day). It should be noted that all standard statistics given below are based on a log-transformation.

The influence of the litter thickness d , the constant head h_1 , and the ratio h_1/d , on the lateral conductivity is shown in figure 7.4. Graph a and b show that the dataset is split into two groups, a "thin" litter layer group with d below 2.5 cm and a "thick" litter layer group with d above 2.5 cm. The thin litter layer samples have an average K_{lat} of 278 m/day (std = 4.8 m/day) while the thick litter layer samples have an average K_{lat} of 159 m/day (std = 3.0 m/day). The low head and high head simulations were difficult to realise because the vertical and lateral fluxes were very high, so that there was no time to adjust the head before the Mariotte container was empty.

Figure 7.4c shows that the h_1/d ratio ranged from 0.2 to 2, with most tests between 0.5 and 1.0. It can be clearly seen that the variance in data points increases when the ratio h_1/d is smaller than 0.5 and larger than 1. Also, the highest conductivities were recorded for the thin litter layer samples and also for a h_1/d ratio larger than 1. Thus when runoff changes from flow below the litter surface to flow on top of the litter, the conductivity increases from roughly 200 m/day to values 10 times as high. A very shallow flow depth also results in high conductivities, possibly because only the largest macro pores and preferential flow paths are used so that there is no resistance from the smaller pores. Although the K_{lat} seems to decrease abruptly at a value of $d = 2.5$ cm, the actual relation between litter layer thickness and conductivity is probably more gradual, because there were no samples with a litter thickness between 2 and 3.2 cm.

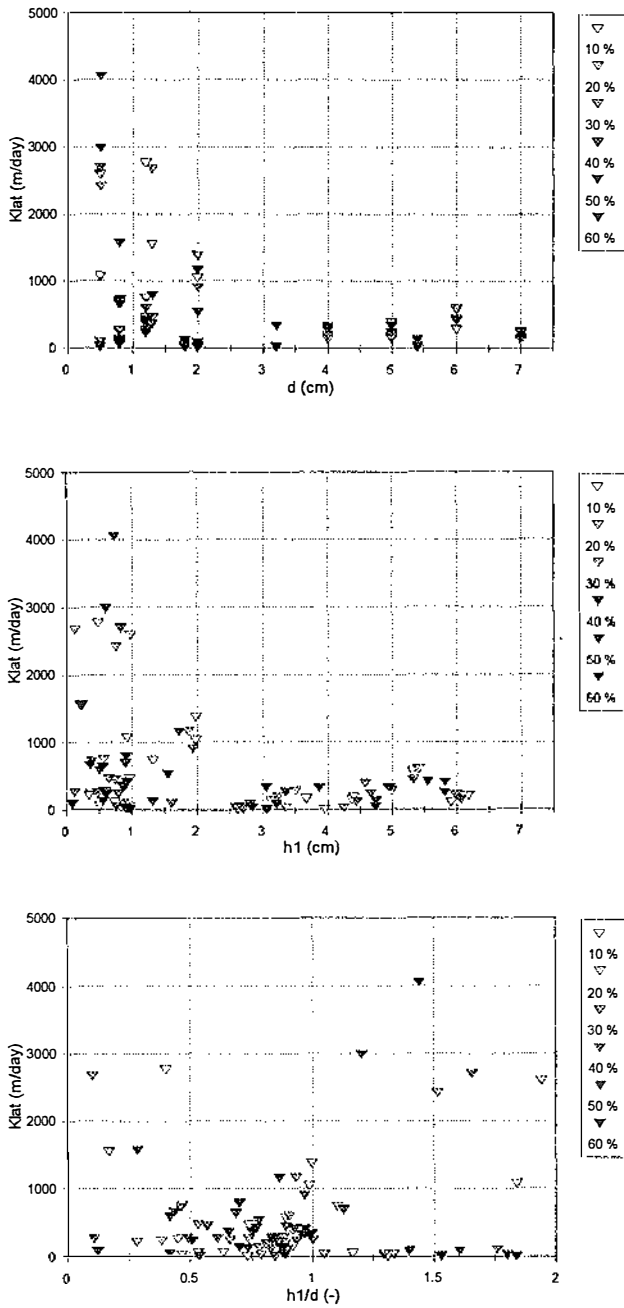


Figure 7.4 Lateral conductivity (K_{lat} in m/day) at 6 slope angles for all samples. a) with litter thickness d (cm), b) with constant head h_1 (cm) and c) with the ratio of h_1/d .

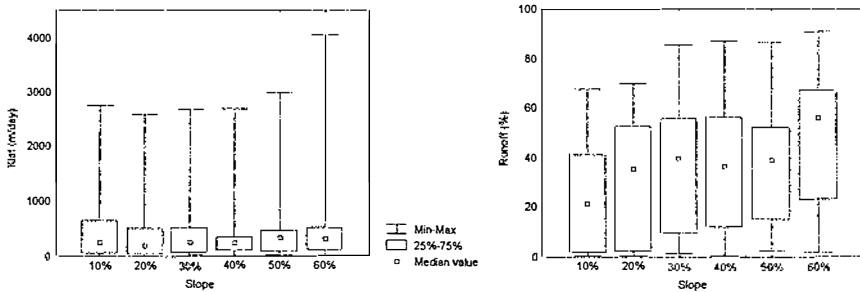


Figure 7.5 Box-whisker diagrams of lateral conductivity (K_{lat} in m/day) and Runoff % of all soil samples at 6 slope angles.

The size of K_{lat} was hardly influenced by the slope angle, with mean values between 171 m/day for a 20% gradient to 277 m/day at 60 , while for slopes of 10%, 30% and 50% about 240 m/day is calculated (see figure 7.5 a). The runoff % increased gradually with increasing angle, with median values ranging from 21% to 55% for slopes of 10 % to 60%(figure 7.5 b). However, above a 20% slope gradient, all series show a wide range of runoff values, from nearly 0 to 90%. This indicates that the resistance of the litter layer is the main factor controlling the conductivity, rather than the slope gradient.

Taking a closer look at the tests for each slope angle reveals a strong relationship between K_{lat} and runoff (figure 7.6). The runoff % increases more or less linearly with conductivity up to a given value of K_{lat} , beyond which no further increase in runoff is measured. Table 7.2 shows the regression parameters and maximum K_{lat} for which the regression equation holds. Explained variance ranges from 0.58 to 0.84 with maximum K_{lat} for which the regression equation holds decreasing from 1100 m/day for 10% slopes to 400 m/day for 60% slopes. The data points beyond these K_{lat} values are almost all related to flow at a h_1/d ratio larger than 1, i.e. flow on top of the litter layer. Thus as long as the flow depth remains smaller than the litter layer thickness, the amount of runoff is mainly determined by K_{lat} .

Table 7.2 Regression coefficients for runoff (%) and K_{lat} (m/day) in the range of K_{lat} from 0 to K_{max} .

Slope	<i>a</i>	<i>b</i>	R^2	<i>n</i>	K_{max}
10%	8.0117	0.0437	0.5692	12	1100
20%	9.2819	0.0953	0.6376	11	750
30%	0.8328	0.1367	0.7683	13	600
40%	2.3394	0.1494	0.5102	14	500
50%	6.5871	0.1430	0.6126	12	400
60%	8.0354	0.1764	0.6878	12	400

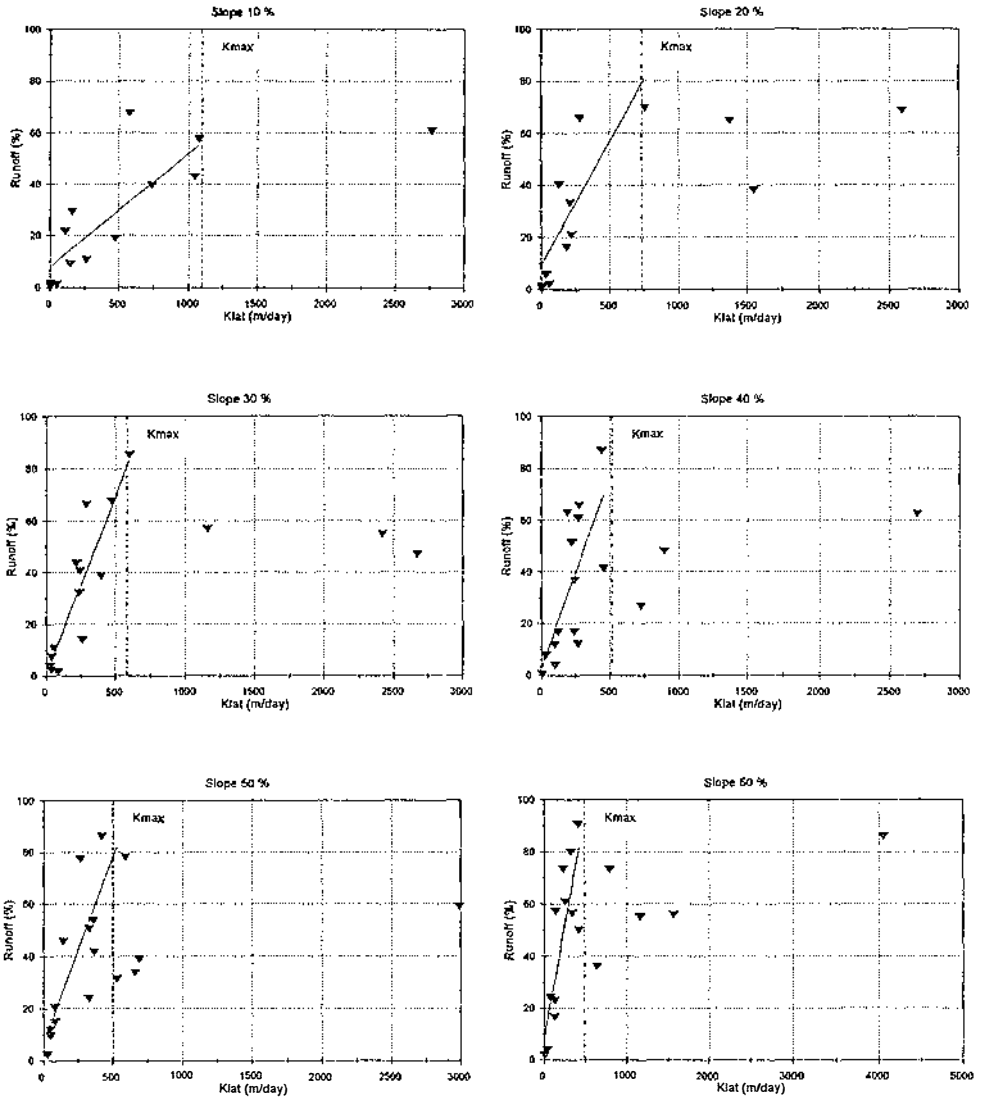


Figure 7.6 Relations between Runoff (%) and lateral conductivity (Klat in m/day) at 6 slope angles (graphs a to f). Regression coefficients for the first part, and the maximum K with which the regression analysis was done are given in table 7.2

It appears that there is a strong linear relation between the equivalent throughfall T_e , and the vertical infiltration flux ($r^2 = 0.9746$). This is a consequence of the experimental setup: the amount of discharge is determined by h_1 , the infiltration rate and the litter characteristics. Therefore T_e is not an independent variable. It varies between 1.2 and 116.6 mm/min, while actual throughfall intensities rarely exceed 2

mm/min. During the measurement period the maximum rainfall intensity recorded at the weather station was 1.52 mm/min. Analysis of T_e in relation to the ratio $h1/d$ gave a value of $T_e = 10$ mm/min above which overland flow on top of the litter ($h1/d > 1$) occurred. Thus, flow on top of the litter layer under field conditions would probably never occur as a result from throughfall alone. Only when combined with accumulated water from upslope will such a situation occur.

If the lateral flow is actually throughflow, K_{lat} should be a constant for each sample as it is a saturated conductivity, at least with a $h1/d$ ratio near 1.0. Although K_{lat} is independent of slope angle and the variance in data points is smaller in the range of $h1/d$ between 0.5 and 1.0, K_{lat} is not constant for each sample. The variation in depth of flow and composition and thickness of the litter layer is probably high, so that equation 7.1 does not describe the process adequately.

7.3.3 The flow tests: surface runoff as overland flow

The salt pulse added at the upper end of the sample produced a gradual increase and decrease of E at the lower end, because the water moves at different speeds through the macro pores. The moment with the highest E , i.e. the highest salt concentration, was taken as the average travel time of the salt, resulting in a velocity " v_{mean} ".

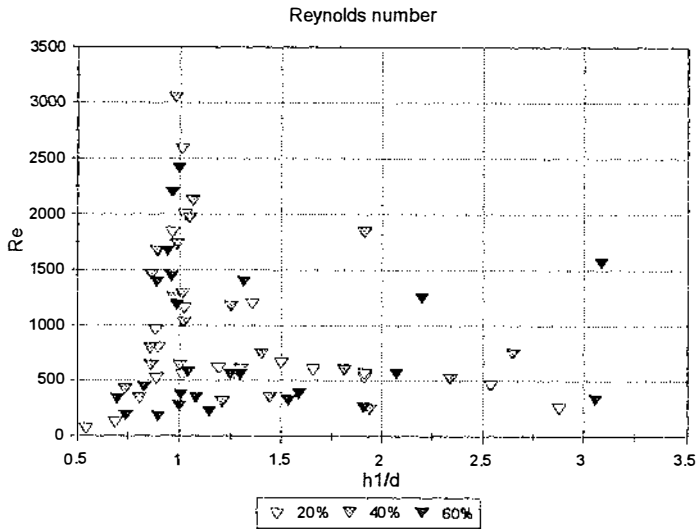


Figure 7.7 Reynolds number in relation to $h1/d$ ratio for the salt-flow tests of all samples at three slope angles. Grey shades indicate the slope angle.

Reynolds numbers vary roughly from 50 to 3000. The largest variation in Re is obtained when $h1/d$ is around 1: the flow becomes fully turbulent as the flow depth $h1$ crosses the surface of the litter layer, after which the Reynolds numbers decrease again and the flow is between laminar and turbulent (see figure 7.7). The flow

velocities range from 200 to 2200 m/day, which is about 10 times larger than the lateral conductivity (figure 7.8). It appeared that the slope angle did not have any clear relation with the mean velocity (figure 7.9). Figure 7.8 shows however, that there is a clear relation between litter layer thickness, velocity and Reynolds number. Most of the thick litter layer sample points (dark grey) have a $h/d < 1$ (not shown in the graph). Thus as long as the flow depth is smaller than d there is a well defined gradual linear increase of the velocity with the Reynolds number ($r^2=0.9592$). For thin litter layer samples the flow depth frequently exceeds the litter thickness and there is less gradual linear relationship between V and Re ($r^2=0.6869$). Flow in the thin litter layer samples never becomes fully turbulent if a boundary value of $Re = 1500$ is used (De Lima, 1989).

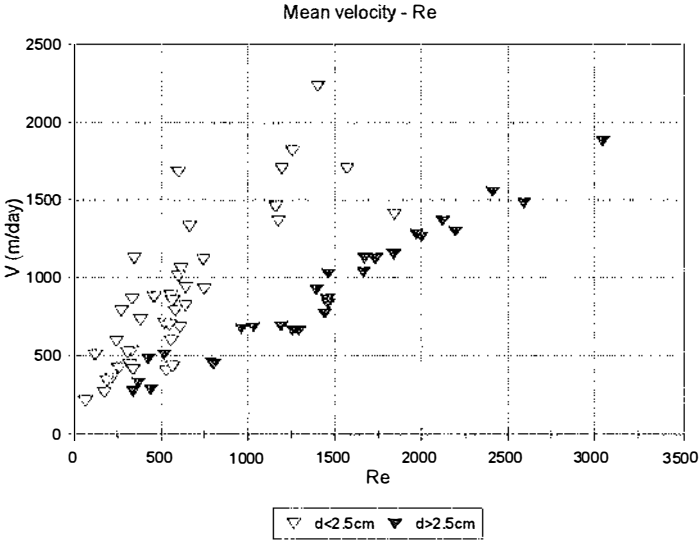


Figure 7.8 Mean velocity (V_{mean} in m/day) calculated with the EC tests and corresponding Reynolds numbers. The dataset is divided in thin ($d < 2.5$ cm) and thick ($d > 2.5$ cm) litter layer samples.

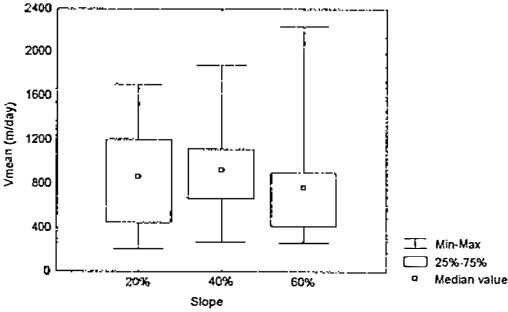


Figure 7.9 Box-whisker diagram of mean velocity calculated with the salt-flow tests for each slope angle.

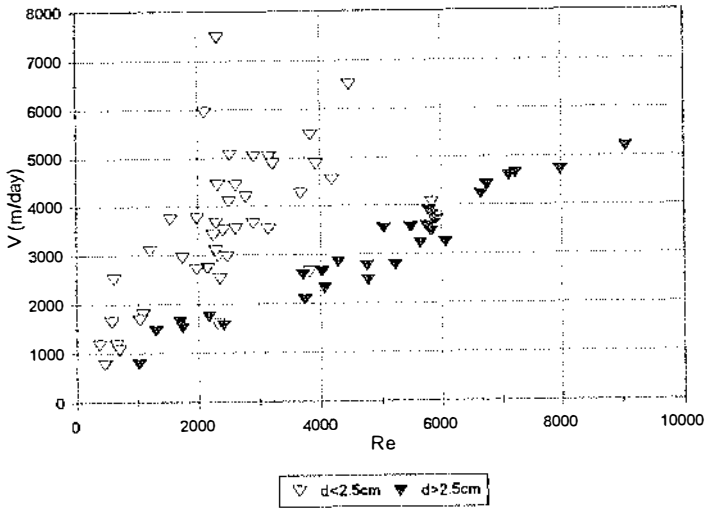


Figure 7.8 Fastest velocity (V in m/day) calculated with the EC tests and corresponding Reynolds numbers. The dataset is divided in thin ($d < 2.5$ cm) and thick ($d > 2.5$ cm) litter layer samples.

The water does not move at the same speed through the litter layer. There are preferential flow paths and macro pores where the water moves with a much higher velocity. Using the first increase in E after the salt pulse was added, a measure for the fastest flow was obtained (indicated with " V_{fast} "). Velocities range from 780 to 7500 m/day, about 3 times higher than the mean velocities, causing the Reynolds numbers to vary between 300 and 9000 (see figure 7.10). Thus water moving at velocity V_{fast} is fully turbulent for almost all tests. Again there was no relation between velocity and slope gradient (not shown) and a clear difference in V_{fast} between thin and thick litter layer samples (figure 7.10). This indicates that there is a difference in the amount of macro pores between the thin and thick litter samples. Therefore the litter thickness not only results in different velocities simply because of the difference in depth of flow, but probably also because the litter composition is markedly different above a given thickness.

Compared to other environments the surface resistance is extremely high. Emmett (1970) calculated surface resistance of bare rocky slopes and found values for the Darcy-Weisbach f varying from 1 to 0.05 for Re varying from 200 and 5000. For planar flow with flow resistance entirely due to grain resistance, the slope of the log-log regression of f and Re is -1.0 for laminar flow and -0.25 for turbulent flow, with a clear change in slope between $Re = 1500$ to 6000 (Emmett, 1970). However, on hillslopes planar conditions rarely exist as there are preferential flow paths, and the break in slope corresponding to transitional flow is seldom found (Roels, 1984; Abrahams et al., 1992). Also in this dataset there is no break in the slope of the graph, which is -1.53 for both thin and thick litter layer samples calculated for V_{mean} (see figure 7.11). For V_{fast} the slopes decrease to a value of -0.86 for thin

and -0.92 for thick litter layer samples, which is much more in the range of values found by Roels (1984) and Abrahams et al. (1992). However, the latter researchers found f values of up to 15 for bare slopes with a near 100 % gravel cover, while the f values corresponding with V_{fast} are still extremely high, ranging from 40 to 5200.

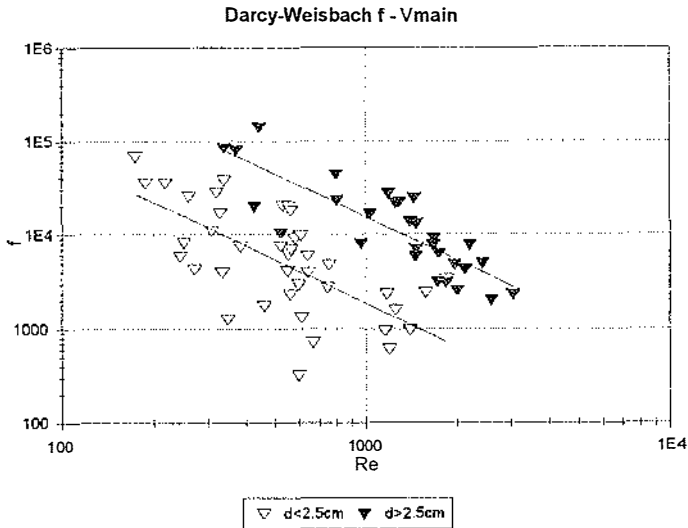


Figure 7.11 Darcy-Weisbach friction factor f corresponding with V_{main} . Grey shades indicate litter thickness d (cm).

Table 7.3 Darcy-Weisbach friction factors for various types of surface conditions.

<i>Residue type</i>	<i>Re 500</i>	<i>Re 5000</i>	<i>Reference</i>
Corn	15.6	9.1	Gilley et al. (1992)
Cotton	5.7	4.7	
Peanut	13.7	4.3	
Pine needles	22.9	5.1	
Sorghum	11.6	4.1	
Soybean	67.8	6.5	
Sunflower	10.6	4.7	
Wheat	17.6	4.2	
Gravelly slope	10.9	0.88	Abrahams et al. (1992)
Smooth channel	0.192	0.019	
litter < 2.5	5363.3	155.8	This study
litter > 2.5	44257.4	1313.1	

Gilley et al. (1992) found a strong relationship between the amount of plant residue after harvesting, the Reynolds number and f . The Reynolds numbers for his experiments varied from 2000 to 60000, indicating considerably higher flow velocities than occurred in the litter layer tests. Table 7.3 compares the f values calculated from his regression lines of various crops with the f values found in this study, using Reynolds numbers 500 and 5000 and a 95% surface cover of plant debris. For thick litter a log-log regression between Re and f was acceptable ($r^2=0.686$) and the friction coefficients for $Re=500$ and $Re=5000$ are calculated with it. For thin litter no relation existed ($r^2 = 0.443$) and only the average value is given in table 7.3. Depending on Re number and litter thickness, the f factors for litter are between 10 and 10^3 times larger than the values found by Gilley et al. (1992).

7.4 Discussion and conclusions

The average runoff percentages at the field plots are of the same order as the stormflow runoff at a catchment scale (see chapter 11). On a yearly basis the amount of stormflow discharge is approximately 3% of the total throughfall amount. However, the main process that determines the catchment geomorphology in the area is headward erosion (see chapters 2 and 11). The catchments usually consist of flat to convex watersheds and upper slopes, which become increasingly steep and change abruptly into a narrow floodplain. Thus the surface runoff that is generated on the slopes will infiltrate on the floodplain before it reaches the stream. The runoff registered as discharge is likely to be generated by rainfall falling on the channel itself for small storms, or it is generated by saturation overland flow due to the high groundwater table near the stream channel. In theory, the flow velocities are large enough for the water to travel a distance of several hundred meters, but only if near saturated conditions exist in the topsoil. SOAP simulated periods of up to 2.5 to 3.5 hours with a pressure head above -10 cm. Supposing that runoff is generated at this pressure head, the water could travel a maximum distance of approximately 80 to 110 m (with a range of 20 to 350 m), using an overall average velocity of 800 m/day. Therefore only the areas close to the stream will contribute to the stormflow.

The size of the field plots was determined by the fact that fallen logs and large branches and roots were avoided. It is not clear if the entire plot contributes to the runoff. Probably this happens only if the throughfall is larger than 10 mm, above which a linear relation between runoff and throughfall exists. For water at the top of the plot to travel 2 meters laterally, the soil has to be saturated for several minutes which is not unlikely.

When treating the surface runoff as throughflow in a porous layer, the following results are obtained:

- the lateral conductivity K_{lat} is determined by the litter layer characteristics and hardly by slope angle;
- K_{lat} is not constant for each sample, which indicates that there is a large variation in depth of flow, litter thickness and composition;

- K_{lat} varies considerably if the depth of flow exceeds the litter layer thickness, or if it is so small that only certain preferential flow paths and macro pores are used;
- the runoff percentage shows a linear relation with K_{lat} if the flow depth is less than the thickness of the litter;
- under field conditions the flow depth will rarely exceed the litter layer depth as the throughfall intensities are usually smaller than 12 mm/min.

If the lateral flow is seen as overland flow the following results are obtained:

- the bulk of the water moves at a speed where the flow is always laminar or transitional;
- turbulence increases (i.e. the Reynolds number) sharply when the flow depth passes the litter layer thickness, if the flow depth is smaller or larger than the thickness the Reynolds numbers are small and the flow is laminar or transitional;
- there is no relation between velocity and slope gradient;
- the surface resistance is extremely high compared to overland flow studies on bare slopes, but also compared to ploughed or harvested fields;
- there is a clear difference between flow velocities in thin and thick litter layers, both for mean and fastest flow velocities, which could be caused by a different composition related to thickness (e.g. the content of small partly decomposed particles could be higher in thick litter).

As long as the water layer stays below the litter layer, the lateral flow should probably be treated as saturated throughflow through a porous medium, i.e. with only gravity as the driving force. The lateral conductivity is independent of the slope angle, and the variation for each sample is relatively small if the water layer is thick enough but does not exceed the litter layer thickness (although K_{lat} is not constant). When the water flows on top of the litter the lateral flow resembles overland flow but still the surface resistance is very high. Both Abrahams et al. (1992) and Gilley et al. (1992) strongly emphasise the need to including the form and abundance of the "roughness elements" in the f - Re relationships, and argue that relations found in laboratory tests are seldom useful in the field. This is certainly true for the overland flow under rain forest, in which the litter composition and structure seems to play an important role.

8.1 Introduction

In the past many hydrological studies of tropical rainforest have concentrated on calculating the water budget over a given period of time, usually at a catchment scale. The discharge is seen as the variable integrating the water movement inside the catchment, from which assumptions can be made of groundwater flow, fast runoff, evapotranspiration and storage changes. Some examples of catchment studies are given in chapter 11. However, it has been recognised for several decades that also in the humid tropics there is a close link between the nutrient cycle and hydrological cycle (Bruijnzeel, 1989). In general, the nutrient cycle of the rainforest is exceptionally rapid and efficient with most nutrients concentrated in the above-ground biomass, although there are exceptions e.g. on fertile volcanic soils in South-east Asia (Proctor 1987). Because water is the transporting agent, solvent and catalyst, quantitative hydrological data are vital for the understanding of the forest nutrient cycle (Bruijnzeel, 1989). Thus, apart from research on a catchment scale, hydrological processes are studied in more and more detail, to understand and quantify all the water fluxes involved. Emphasis has been on micro-climate and transpiration (e.g. Shuttleworth et al., 1984; Roberts et al., 1990, 1993), interception (see chapter 6) while some studies involved soil water movement (e.g. Northcliff and Thornes, 1981). Examples of measuring and modelling of evapotranspiration and soil water status has been done by Parker (1985) in Costa Rica, Heuvelandop and Jordan (1981) in Venezuela and by Bonell et al. (1981, 1982) in Australia.

Apart from the quantification of the water balance for the sake of nutrient cycle research, this chapter aims to describe in detail the water balance of the undisturbed forest, in order to set the reference against which the impact of logging can be evaluated. The rainforest hydrology is not static, the fluxes differ in size and over time. Above ground fluxes have the intensity of rainfall (in the order of mm/min) or of evapotranspiration (in the order of mm/day), while in the soil water movement varies from mm/min to mm/week depending on the soil moisture status. Often considerable seasonal variation exists, while plant and soil characteristics, and their spatial variability, play an important role in modifying the seasonal response of the forest system (Northcliff and Thornes, 1981). If these dynamic aspects of the hydrological balance are quantified, the impact of disturbance can be evaluated properly.

These detailed water balance studies are mostly one dimensional: within an experimental catchment the vertical water movement from the top of a tree to the bottom of the root zone, or to the groundwater body, is calculated. Usually, the focal point is the root zone and the water fluxes that enter and leave it. The moisture content of the root zone, defined here as the top 120 cm of the soil, can be estimated from the hydraulic potential of the soil. As part of several experiments in the water and nutrient balance research (see below), the hydraulic potential was monitored in 1992 and 1993. The measurements cover dry and wet periods in two soil types: a very

permeable Ferralic Arenosol under Mixed Forest, and a typical Haplic Ferralsol under Mixed Forest. However the datasets do not cover a full year and do not include Dry Evergreen forest on the Albic Arenosols. Therefore they are used to calibrate and test the SOAP model (see chapter 4). With the calibrated model the vertical water balance over a full year is simulated.

Dry Evergreen Forest and Mixed Forest on Arenosols and Ferralsols constitute the largest part of the experimental catchment. In this catchment a logging experiment was done which started 1991, while the actual logging took place in October 1992 (see chapter 11). In order to use the simulation results of this chapter in the interpretation of the catchment water balance, atmospheric data of the year prior to the logging were used. Thus, the annual water balance was simulated for the following combinations:

- Dry Evergreen Forest on Albic Arenosols
- Mixed Forest on Ferralic Arenosols
- Mixed Forest on Haplic Ferralsols

The hydrological characteristics of these three "environments" are compared in terms of their variability in soil properties and the temporal variation in soil moisture content, evapotranspiration and percolation.

8.2 Methodology

8.2.1 Field data

Root zone moisture content in a Ferralic Arenosol under Mixed Forest was monitored for several months in 1992 and 1993. The measurements were part of the nutrient balance research (Brouwer, in prep., Van Brunschot and De Lange, 1992). In an experiment which started in January 1992, 2 gaps of different size were created about 1.5 km west of the Field Station (see figure 2.1). To assess the difference in leaching of nutrients between the two gaps and the forest adjacent to the gaps, the hydraulic potential was monitored in the gaps and in the forest. In this chapter the results of the 2 forest plots (called F1 and F2) are used to illustrate the seasonal differences in moisture content of the root zone. In each plot 3 tensiometers were installed on 30 cm, 70 cm and 120 cm depth. They were monitored every 3 days from 12 February to 21 April 1992, and every week from 11 March to 9 June 1993. These periods are representative for dry and wet season conditions respectively.

The tensiometers were placed at an angle to avoid disturbance of the soil above. The ceramic cups of the tensiometers can be connected to a DRUCK pressure transducer and filled with air-free water (obtained by applying a negative pressure of 1 bar to a container with boiled water). This system is capable of measuring up to 650 cm of hydraulic head, at higher pressure air moves through the cups into the system reducing the negative pressure, and the readings become unreliable.

The runoff experiment (see chapter 7) provided measurements of hydraulic potential in a Haplic Ferralsol under Mixed forest. Tensiometers were placed at depths of 20

and 50 cm below the surface on 5 plots on the top of a slope. Monitoring was done every 1 to 2 days in the wet season of 1992: from 1 June to 14 September. Three plots are used in this chapter, situated at the top of the slope, with slope angles varying from 25% to 40%.

Because monitoring was done with a minimum interval of one day, it is expected that the actual temporal variation in moisture content near the surface was not captured by the measurements. As a result percolation fluxes that are calculated directly from the tensiometer readings may not be accurate. Therefore the water balance was simulated during the same periods with SOAP. The water balance of the soil profile was calculated to a depth of 130 cm for the test datasets. As groundwater at the experimental sites was far below this depth, free drainage was assumed. The initial potentials at the nodes were set to the first measured values in the simulation of the measurement series. Input data for SOAP are: atmospheric variables, vertical leaf area distribution, vertical root distribution and soil physical properties. The vegetation structure is described in chapter 4. The soil properties and their spatial variability are discussed in chapters 5 and 9, but a summary of the soil input data is given below. Interception and throughfall were calculated with the CASCADE interception model (chapter 6).

8.2.2 Microclimate in the canopy

The atmospheric data were obtained from the weather station which is located about 3 km from the gap experiment and 1 km from the runoff experiment (see figure 2.1 for the exact locations). Incoming radiation, air pressure, temperature and relative humidity and wind speed were combined in the Penman-Monteith equation to calculate the potential evapotranspiration (see chapter 4). It was assumed that apart from the wind speed, the atmospheric circumstances at the clearing of the weather station were representative for those above the canopy. Therefore only the wind speed was extrapolated to a given level above the canopy, using the method described in chapter 4. Based on the canopy structure given by Roberts et al. (1993) for a Mixed forest in Manaus, SOAP uses a fairly straight forward vertical distribution of these variables. It should be noted that a vertical leaf distribution of Dry Evergreen Forest was not known and the same distribution as for Mixed Forest is used. To get an idea of the micro climate in the canopy, the relative humidity and temperature were measured every hour from 700 h to 1900 h on several days in March and April 1992. Measurements were done at 1.5 m above the surface with an Assmann 761 aspiration psychrometer, measuring wet and dry bulb temperature. From this dataset two days, a clear sunny day and a cloudy day with some rainfall, were selected.

8.2.3 Soil properties

Water retention and hydraulic conductivity were calculated with the Van Genuchten functions. Parameters for these functions and other soil properties and their variability, are discussed in chapters 5 and 9. It is assumed that the values are representative for the entire root zone.

Simulation of the measurement series was done with soil properties measured near the tensiometers. From table 8.1 it can be seen that the Ferralic Arenosol of the gap study is rather sandy, with a saturated hydraulic conductivity and parameters n and α higher than one standard deviation from the average. The Haplic Ferralsol has near average values.

The variability of the soil properties in the area is very large (chapter 5). To determine the influence of the variability, three sets of soil properties were defined: the average values and a range of plus and minus one standard deviation, i.e. the properties corresponding to a high and low permeability. In case of the Van Genuchten parameters it is assumed that a high porosity and conductivity result in a high value for n and a low value for α and vice versa. These datasets are indicated as avg, -std and +std as a subscript to the soil type (see table 8.1).

Table 8.1 Soil properties used in the simulations with SOAP, avg = average values, +std = average values + 1 standard deviation, -std = average values - 1 standard deviation.

Simulation of experiments:									
	ARo			FRh					
Pore	0.517			0.482					
Ks	720.0			114.7					
n	1.600			1.262					
alpha	0.060			0.059					

Simulation of annual water balance:									
	ARa			ARo			FRh		
	+std	avg	-std	+std	avg	-std	+std	avg	-std
Pore	0.597	0.545	0.493	0.517	0.479	0.441	0.435	0.482	0.527
Ks	5687.9	3369.6	1051.9	652.4	469.7	287.0	23.6	114.7	205.8
n	2.233	1.949	1.665	1.556	1.483	1.440	1.241	1.262	1.283
alpha	0.041	0.059	0.077	0.066	0.091	0.116	0.075	0.059	0.043

8.3 Results

8.3.1 Microclimate

The diurnal variation in temperature and relative humidity in the forest on ground level was measured on two days (Van Brunschot and De Lange, 1992). The first day is an example of a clear day without rain (27 March 1992), the second day is cloudy with rainfall around 1500 h (8 April 1992). The measurements are shown in figure 8.1, with the weather station readings of temperature, relative humidity and incoming radiation are added for reference.

Clearly there is a delay in warming up of the air in response to increasing radiation. The highest temperature at the weather station is recorded at 1500 h, under the canopy even later at 1630 h, after which both temperatures decline at the same rate. The difference between the maximum temperature at the weather station and below

the canopy is 3 °C. On 8 April 1992 the radiation is not so different but the afternoon shower cause an immediate decrease in temperature both at the weather station and in the forest. Compared to the weather station, relative humidity under the canopy has an even slower response to increased radiation. Whereas the lowest RH at the weather station is registered at the same time as the peak in radiation, the lowest RH under the canopy is measured at the end of the afternoon. Night time levels of both temperature and RH were not measured but the graphs suggest both to be higher under the canopy.

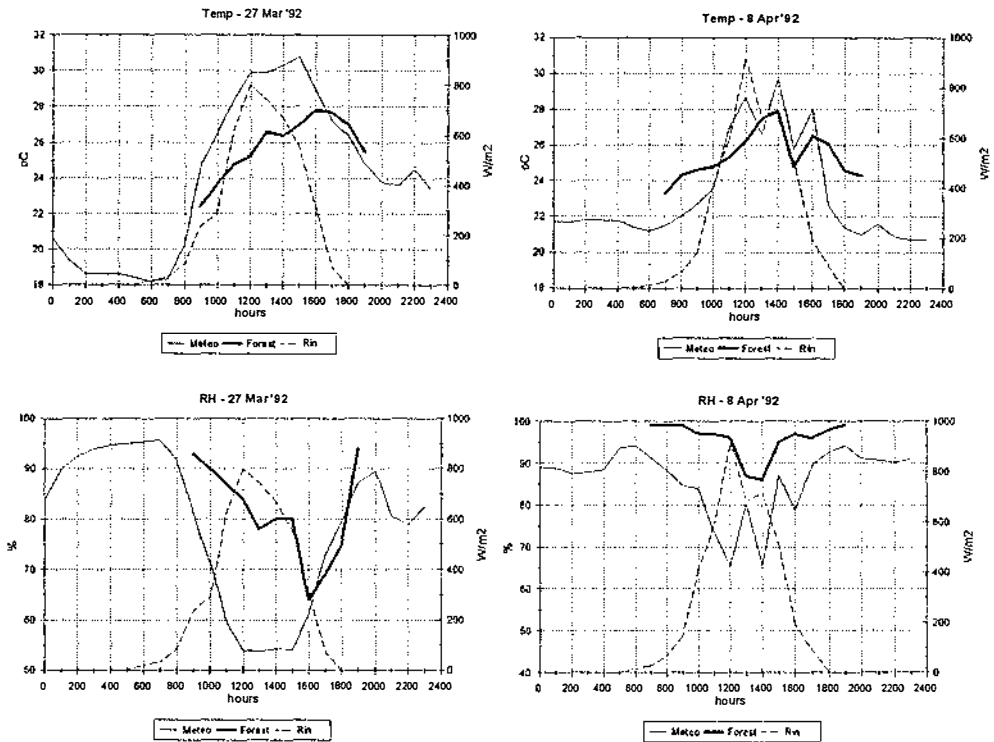


Figure 8.1 Temperature (°C) and relative humidity (%) measured on a clear sunny day (27 March 1992) and a cloudy rainy day (8 April 1992), beneath the forest canopy. Weather station readings of temperature, relative humidity and incoming radiation are added.

8.3.2 Mixed forest on Ferralic Arenosols (the gap experiments)

Measured matric potentials and model results are shown in figure 8.2, with the 1992 measurements at 3 depths on the left and the 1993 data on the right. The throughfall is added to the top graphs while the percolation is shown in the lower graphs, both in mm/day.

In the beginning of the 1992 series there was rainfall every few days and the topsoil stayed above field capacity. Subsequently it dried out in April after more than 10 days without rain. Nevertheless the profile did not become dry enough for water stress to occur and the transpiration was not reduced. The temporal variation in the measurements is simulated quite accurately, given the fact that the input values were measured at some distance from the plots. At 30 cm depth plot F2 dries out more than was estimated with the model. At 70 cm depth the first half of the series was estimated correctly but as the profile starts drying out, the estimated potentials remain too high. At the bottom of the profile the simulation is much better, particularly for plot F2. Because at 30 cm depth plot F2 dries out more and at 120 cm depth plot F1, the discrepancies between measurements and simulation could be a result of the difference between the actual root distribution at the plots and the average root distribution used in SOAP. If there are more roots lower in the profile of F1 the uptake there will cause higher potentials.

Comparing throughfall events with the percolation peaks, the latter follows the former only in a general sense and with a delay time of 3 to 5 days. The maximum percolation during the period is 7 mm/day and a significant flux is present only if the potential at 120 cm remains above -120 cm. The total percolation calculated by SOAP over the period of 75 days in 1992 was 191 mm, or 44% of the rainfall (which amounts to 437 mm). Evapotranspiration was estimated at 260 mm or 60% of the rainfall, leaving a moisture deficit of 4%.

To investigate infiltration and redistribution times in greater detail, the reaction of the profile to 7 rainstorms, recorded from 5 to 13 March 1992, are presented in figure 8.3. The top of the soil profile of course shows an immediate response to the throughfall influx, but at 30 cm depth the fluctuations are already strongly diminished. Below that depth only the general trend remains and small throughfall events are buffered out. This gives an idea of the response time of the soil at various depths. For instance the rainstorm registered on 8 March (with a size of 43.2 mm and a maximum intensity of 63 mm/h), gives a drop in potential at 30 cm depth after 5.5 hours and at 70 cm after 50 hours, whereas it takes about 103 hours before the potential at 120 cm reaches its minimum. Much of the water stays in the root zone and is subject to transpiration, or delayed drainage.

If the soil profile as a whole is wetter the response to rainfall is quicker and the percolation pattern follows the rainfall pattern more closely. This is illustrated by the 1993 measurement series of the same plots, from the beginning of March to the end of June. The right 3 graphs in figure 8.2 show the measured and simulated matric potentials. From April onward the soil is at field capacity or wetter. Taking the period of 1 April to 14 June as representative for the wet season, the percolation

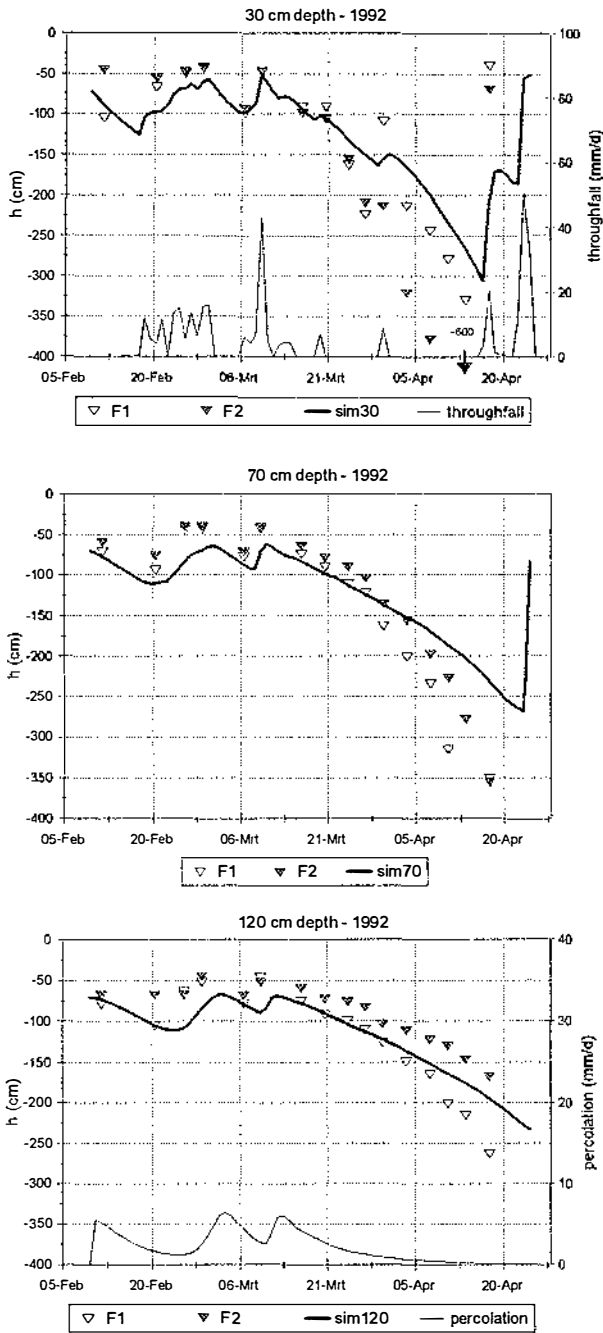


Figure 8.2 Measurements and simulation of the matric potential in a Ferralic Arenosol under Mixed Forest, at three depths (from top to bottom). This page shows the dry period in 1992, The next page shows the wet period in 1993. On the right y-axis the fluxes in mm/d are given.

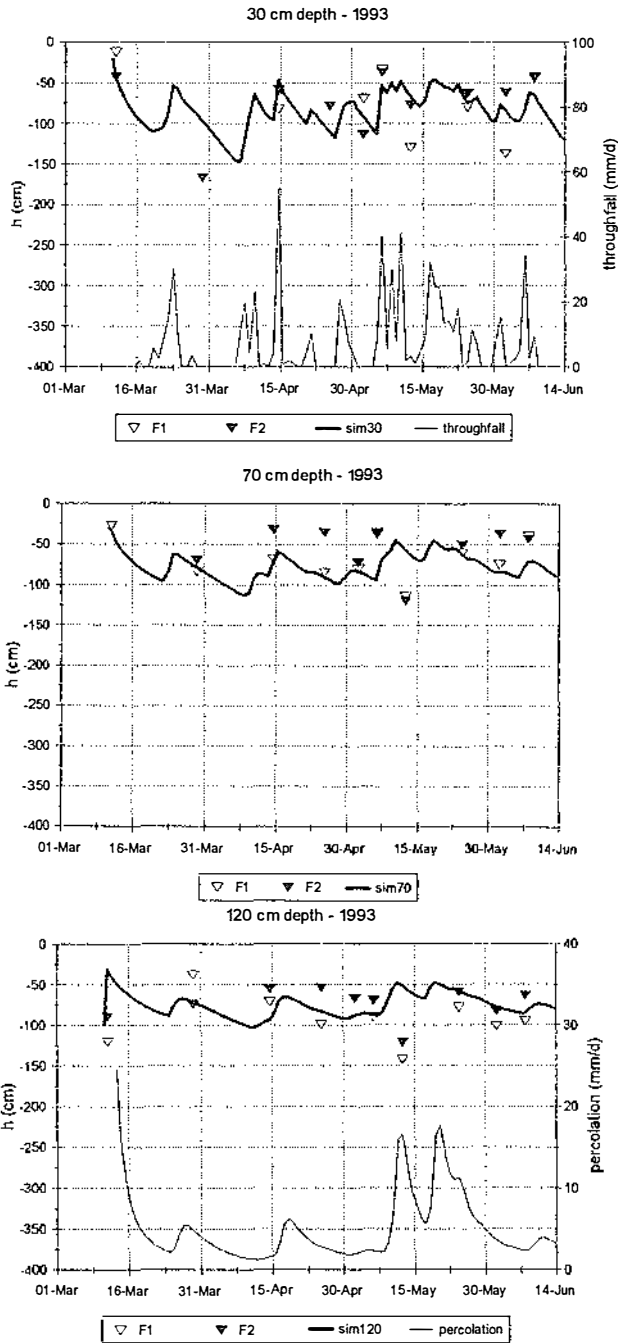


Figure 8.2 Continued.

amounted to 380 mm or 57% of the rainfall (669 mm) whereas the evapotranspiration was 335 mm (50%) leaving a negative soil moisture balance of 7%. Because the soil is wetter, the water moves faster and the reaction of the soil in terms of percolation is faster: the response times for an average sized rainstorm on 17 May 1993 were 4.6 hours, 31.4 hours and 55.6 hours for 30, 70 and 120 cm depth respectively. From analysis of several rainstorms larger than 20 mm, the reaction times in the wet period in 1993, appeared to be 50% to 60% of those in the dry period in 1992, while the amount of percolation increased with 10% to 15% of the rainfall.

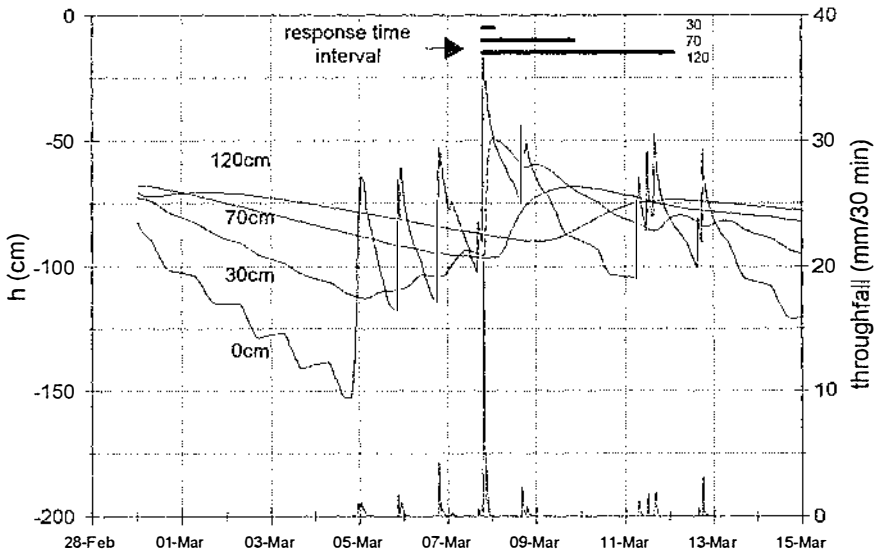


Figure 8.3 Response time of the soil for a 42 mm rainstorm on 8 March 1992. The horizontal bars at the top of the graph indicate the amount of time needed for the rainstorm to reach 30 cm, 70 cm and 120 cm.

8.3.3 Mixed forest on Haplic Ferralsols (the runoff experiments)

The third series was measured in a Haplic Ferralsol under Mixed Forest during the wet season in 1992. Figure 8.4 shows the measurements and simulated potentials at respectively 20 cm and 50 cm depth. The rainfall and percolation in mm/day have been added to the graphs. The soil stayed very wet at both depths with potentials frequently above -50 cm. Compared to the simulated potentials, the measured potentials fluctuated more in the beginning while at the end of the series the profile dried out more. This may be explained by a difference in rainfall between the weather station and the runoff experiment. While the soil is above -100 cm it reacts immediately to the influx of throughfall at the surface: on average it took 24 to 48 hours for the potential at 120 cm depth to react to a rainstorm. Towards the end of

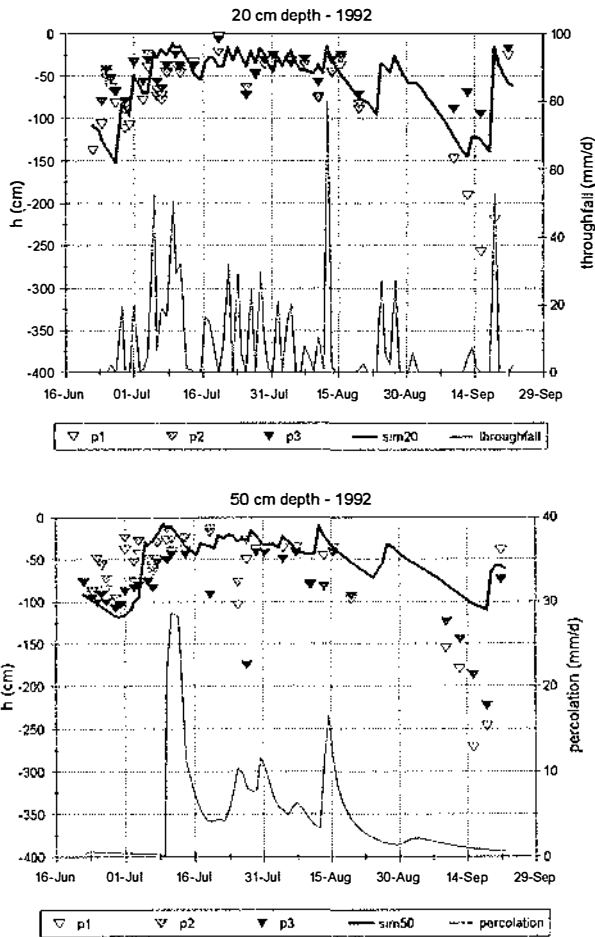


Figure 8.4 Measured and simulated matric potentials in a Haplic ferralsol under Mixed Forest in 1992 on a) 20 cm depth and b) 50 cm depth.

August the reaction time at 120 cm had increased to about 6 days. Thus the response times were similar to the Ferralic Arenosols. Taking the period until 15 August as representative for the wet season the total evapotranspiration was 40% of the rainfall, whereas the percolation was 55% leaving a moisture surplus of 5%. The evapotranspiration is low comparing to the Arenosols, but this could be a result of the specific circumstances or the length of the period. In the next section the annual variation is discussed for both soils, which gives a more complete picture. The ratios for the remaining part of the period are 75% evapotranspiration and 30% percolation with a moisture deficit of 5%. The latter period is only short and may not be representative for the dry seasons but it indicates that there are considerable seasonal variations in the fluxes.

8.4 Annual fluctuation of the water balance for three environments

To evaluate the seasonal differences in the various fluxes, the water balance for the year prior to the logging of the experimental catchment was simulated. Unfortunately the tipping bucket at the weather station was malfunctioning in the first 20 days of October 1992, so that the period covers 346 days. An estimated 2500 mm would have been measured on a yearly basis, which means that the period is relatively dry if compared to the mean annual precipitation of 2700 mm (see chapter 2). Due to lack of information about the canopy structure of Dry Evergreen Forest, the forest types in the simulations distinguish themselves only by a different root distribution. The interception and throughfall are nearly the same in all simulations. Note that differences of several mm/year occur in the cumulative interception, because the time step in the model varies with the number of iterations required. Therefore the iterations and time step vary per soil type and this affects the interception calculations. Simulation is done for a soil profile of 100 cm with a vertical resolution of 5 cm. Surface storage capacity is set at 5 mm with immediate runoff if this storage is exceeded. Also here it is assumed that the groundwater is far below the bottom of the root zone and that there is unimpeded drainage and no capillary rise.

The cumulative fluxes and percentages relative to the rainfall for all 9 combinations of soils and forest type (i.e. DEF on ARa, MF on ARo and MF on FRh, each with 3 levels of permeability) are given in tables 8.2 to 8.4. The daily fluxes between the combinations differed very little and only ARo-avg, which represents the average situation, is shown in figure 8.5. The soil hydraulic potential clearly reflected the variability in soil properties. Therefore the matric potential at 10 cm and 100 cm depth for the 3 combinations with average, minimum and maximum soil properties are shown in figure 8.6. The potentials simulated at 1200 h are given.

The rainfall graph in figure 8.5 shows that the beginning of the period was relatively dry with frequent periods of more than a week without rain (especially January was dry), while in the second half of the period there was rainfall every other day. In the following discussion, the "dry season" refers to the period from mid-October 1991 to mid-April 1992, the "wet season" refers to the remaining part of the year. This seasonal variation cannot be seen in the evapotranspiration graph. The uptake (solid line) is more or less the same throughout the year, fluctuating between 2 and 4 mm/day, although the daily variation in the wet season is higher. Interception evaporation reaches a maximum from May to July 1992 but also here the daily variation is much larger than the long term variation. The soil evaporation is very low and on a yearly basis it is less than 1% for all soils. Thus the total evapotranspiration (dotted line) fluctuates between 1 and 6 mm/day in the dry periods and between 1 and 9 mm/day between half of April and half of August. The potential evapotranspiration (PET) is calculated here as the total atmospheric demand as experienced by the forest canopy and amounted to almost 1450 mm or 61% of the annual rainfall. On a yearly basis the actual evapotranspiration (ET) is about 90% of the PET because the transpiration is assumed to be reduced if there is evaporation of interception water (see chapter 4). The deviation between interception evaporation and transpiration is roughly 30% and 70%.

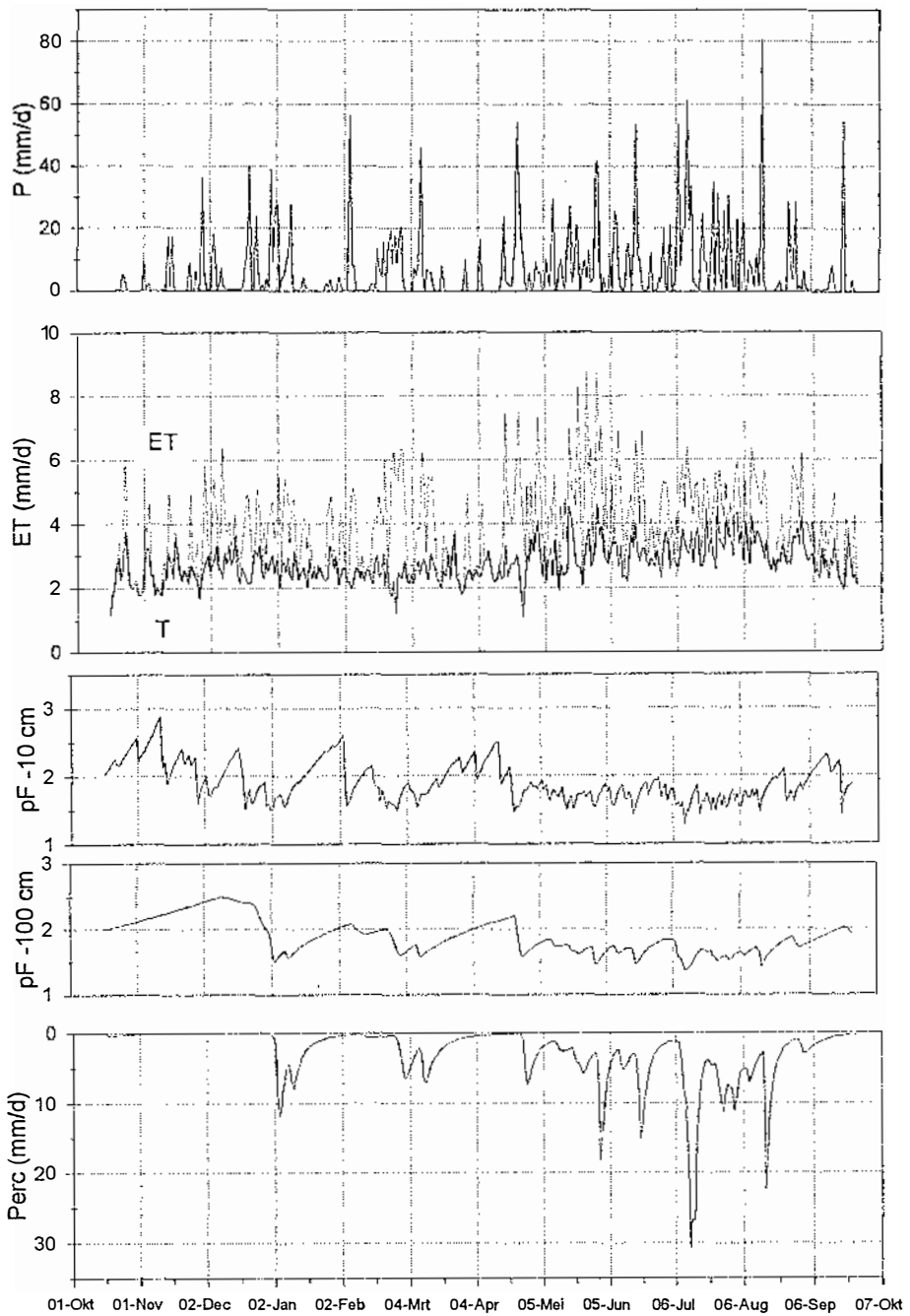


Figure 8.5 Model results for Ferralic Arenosols under Mixed Forest: (all fluxes are in mm/day): P = rainfall; ET = total evapotranspiration (dotted line) and transpiration (solid line); pF = average pF values at 10 cm and 100 cm depth; Perc = percolation.

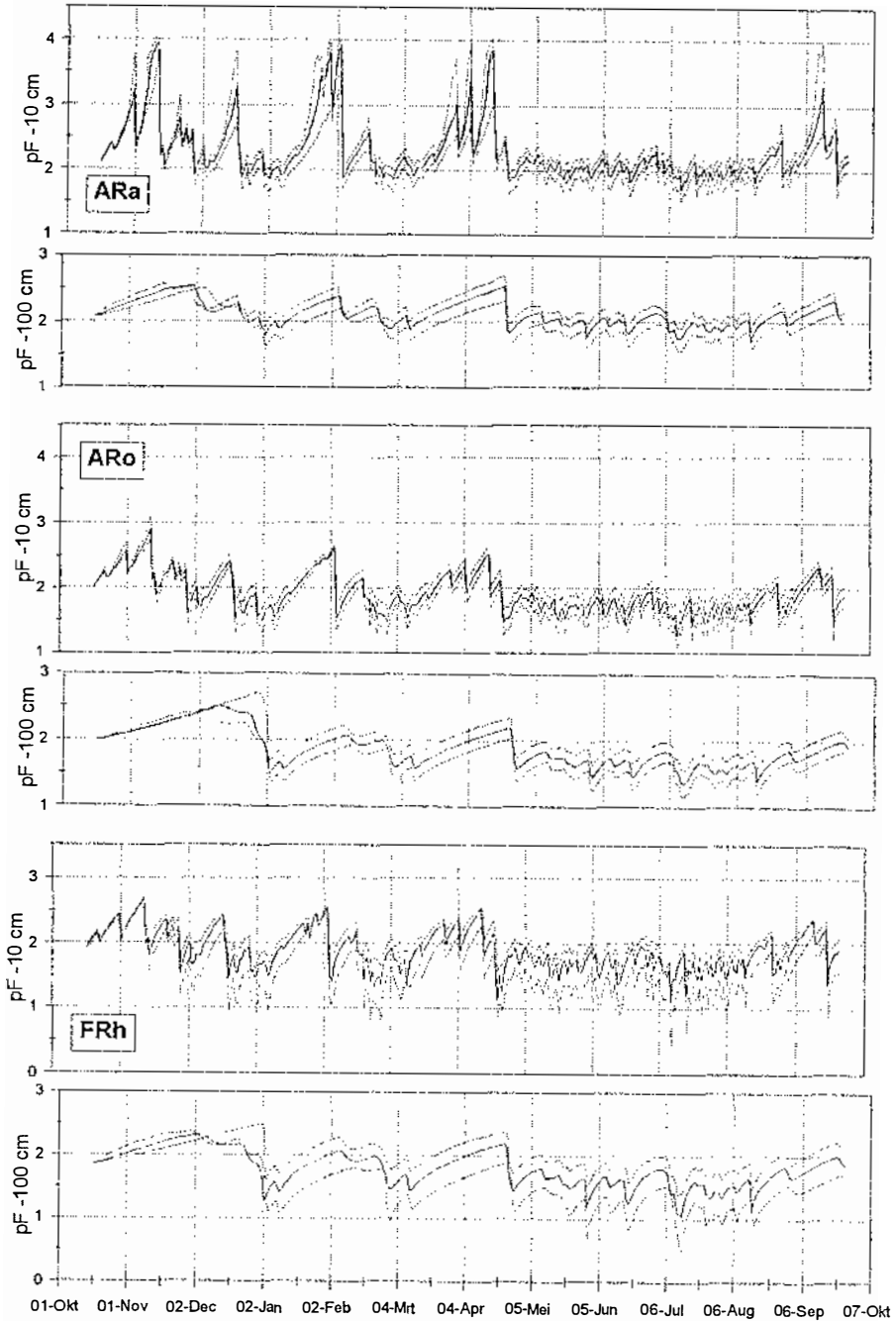


Figure 8.6 The simulated daily matric potentials (pF values at 1200h) at 10 cm depth and 100 cm depth, in the three soil types ARa, ARo and FRh. The solid line represents the avg soil properties, the dotted lines represent +std and -std..

Percolation shows a clear seasonal variation (lower graph in figure 8.5). For all soil types approximately 70% of the percolation takes place in the wet season, while in the dry season no significant percolation is estimated and most of the small rainstorms refill the soil storage above 100 cm and are subject to transpiration.

Comparing the cumulative values for Dry Evergreen Forest on Albic Arenosols in table 8.2, the difference in transpiration between ARa-std and ARa+std is 46 mm or 2% of the rainfall which was caused by water stress in the latter combination. The top graph in figure 8.6 shows that the potential at 10 cm depth reaches wilting point (pF 4.2) if there are periods of 7 to 10 days without rainfall. Assuming that transpiration is reduced if the soil dries out above pF 3 at 10 cm depth (where the bulk of the root mass is concentrated), water stress was simulated for 29 days in ARa-avg, and for 10 and 44 days in ARa-std and ARa+std respectively. The presence of large roots near the groundwater table (see above) indicates that dry season water stress may indeed occur.

In the wet season the soil fluctuates around field capacity. At 100 cm depth the potential was never lower than pF 2.7. Comparing the daily percolation with the potential at 100 cm depth, there is only a significant downward flux if the soil is above field capacity. Below field capacity the hydraulic conductivity decreases rapidly and percolation virtually stops. The exact value differs however per soil type: for ARa-avg it is pF 2.1 ($h = -125$ cm) and for ARa-std and ARa+std they are pF 2.0 ($h = -100$ cm) and pF 2.3 ($h = -200$ cm). Percolation is between 44 and 48% of the rainfall on a yearly basis and reaches maximum amounts of 30 to 35 mm/day.

There is hardly any variation in evapotranspiration in Mixed Forest on Ferralic Arenosols. Uptake proceeds at its maximum (40% of the rainfall), limited only by the evaporation of interception water and wetness fraction of the canopy. Indeed the matric potential in the top soil remains below pF 2.7 for all combinations and there is no water stress. The average wet season potential in the top soil in ARo-std was even very high (-40 cm) and some ponding occurred. Although the variance in soil properties is quite large this does not show in the simulated fluxes. Cumulative values for percolation are almost equal with a 60 mm difference between ARo-std and ARo+std (table 8.3). Because the soil is less permeable than ARa percolation from the root zone occurs at a higher potential: -80 cm for ARo-avg, and -60 cm and -125 cm for ARo-std and ARo+std.

The Haplic Ferralsols distinguish themselves because some surface runoff occurs. A surface storage capacity of 5 mm results in 147 mm of runoff or 6.2% of the rainfall (see table 8.4). All combinations of FRh are ponded during some time of the year, and near saturated conditions (Pf lower than 1) occur for about 15 days in FRh-std (see figure 8.6). This causes the uptake for this combination to be slightly lower, but as saturation usually occurs at the end of the afternoon, the transpiration on the next day is not affected because of redistribution of the infiltrated water. The runoff on FRh-std causes a difference in percolation as well. The potentials above which percolation is significant are -75 cm for FRh-avg, and -45 cm and -120 cm for FRh-std and FRh+std.

Table 8.2 Cumulative values of fluxes on ARa under DEF based on simulation of 346 days, fluxes are in mm and percentages are relative to rainfall. P = rainfall, Ei = interception, Th = throughfall, Ro = runoff, I = infiltration, U = uptake, Es = soil evaporation, Per = percolation, Moist = change of soil moisture storage, ET = actual evapotranspiration (sum of Ei, U and Es), PET = potential evapotranspiration, TimePond = ponding time (min), havg = average yearly pressure head (cm), hwet is the average wet season pressure head, hdry = average dry season pressure head.

DEF - ARa	avg	+std	-std			
	<i>mm</i>			<i>%</i>		
P	2361.2	2361.2	2361.2	100.00	100.00	100.00
Ei	380.6	376.5	376.5	16.12	15.95	15.95
Th	1980.6	1984.7	1984.7	83.88	84.05	84.05
Ro	0.0	0.0	0.0	0.00	0.00	0.00
I	1980.6	1984.7	1984.7	83.88	84.05	84.05
U	902.4	867.2	913.1	38.22	36.73	38.67
Es	18.3	17.3	19.7	0.78	0.73	0.83
Per	1069.3	1124.5	1036.1	45.29	47.62	43.88
Moist	-9.4	-24.3	15.8	-0.40	-1.03	0.67
ET	1301.3	1261.0	1309.2	55.11	53.40	55.45
PET	1448.0	1448.0	1448.0	61.32	61.32	61.32
TimePond	0.0	0.0	0.0			
	<i>cm</i>			<i>pF</i>		
havg	-493.8	-897.0	-211.0	2.694	2.953	2.324
hwet	-119.8	-159.2	-81.1	2.079	2.202	1.909
hdry	-783.7	-1390.4	-310.1	2.894	3.143	2.492

Table 8.3 Cumulative values of fluxes on ARo under MF based on simulation of 346 days, fluxes are in mm and percentages are relative to rainfall. The abbreviations are explained in table 8.2.

MF - ARo	avg	+std	-std			
	<i>mm</i>			<i>%</i>		
P	2361.2	2361.2	2361.2	100.00	100.00	100.00
Ei	380.9	376.5	389.4	16.13	15.95	16.49
Th	1980.3	1984.7	1971.8	83.87	84.05	83.51
Ro	0.0	0.0	0.0	0.00	0.00	0.00
I	1980.3	1984.7	1971.8	83.87	84.05	83.51
U	950.9	949.8	951.1	40.27	40.22	40.28
Es	20.9	21.1	20.6	0.89	0.89	0.87
Per	985.6	1017.3	956.8	41.74	43.08	40.52
Moist	22.8	-3.5	43.3	0.97	-0.15	1.83
ET	1352.8	1347.4	1361.1	57.29	57.06	57.64
PET	1448.0	1448.0	1448.0	61.32	61.32	61.32
TimePond	0.2	0.0	6.6			
	<i>cm</i>			<i>pF</i>		
havg	-106.2	-130.3	-92.7	2.026	2.115	1.967
hwet	-56.6	-80.9	-39.7	1.753	1.908	1.599
hdry	-141.7	-164.3	-132.4	2.151	2.216	2.122

Table 8.4

Cumulative values of fluxes on FRh under MF based on simulation of 346 days, fluxes are in mm and percentages are relative to rainfall. The abbreviations are explained in table 8.2.

MF - FRh	avg mm	+std	-std	%		
P	2361.2	2361.2	2361.2	100.00	100.00	100.00
Ei	388.3	388.0	383.4	16.44	16.43	16.24
Th	1975.5	1973.2	1977.8	83.67	83.57	83.76
Ro	2.2	0.0	147.4	0.09	0.00	6.24
I	1973.3	1973.2	1830.4	83.57	83.57	77.52
U	955.0	950.2	937.6	40.45	40.24	39.71
Es	21.1	21.1	20.8	0.89	0.89	0.88
Per	1022.1	1037.9	837.0	43.29	43.96	35.45
Moist	-24.9	-35.9	34.9	-1.06	-1.52	1.48
ET	1364.4	1359.2	1341.9	57.78	57.57	56.83
PET	1448.0	1448.0	1448.0	61.32	61.32	61.32
TimePond	307.1	31.4	2637.1			
	cm			pF		
havg	-98.4	-126.3	-61.5	1.993	2.101	1.789
hwet	-56.2	-80.7	-25.0	1.750	1.907	1.399
hdry	-126.8	-156.4	-87.7	2.103	2.194	1.943

With respect to response times the soil types are more or less the same in the wet season but differ considerably in the dry season. Taking the rainstorm of 7 March 1992 as an example (see above) it takes 5.4 days in ARa, 12.3 days in ARo and 11.7 days in FRh for the matric potential at 120 cm to reach its minimum value (corresponding to the maximum of the percolation peak).

8.5 Discussion

Comparison of simulated and measured potentials show that SOAP provides a good estimation of the soil moisture status. However, in all pressure head graphs in figures 8.5 and 8.7, the drying out of the soil in periods without rain seems to be too slow. The simulation of the wet season is probably more accurate than the dry season. It is not known if this is a systematic model error, or if it is related to the accuracy of the input variables. The rainfall input is taken from the weather station which is located at some distance from the plots, and also the difference between actual and average vertical root distribution, for which the model is very sensitive, will have large influence on the simulations. Assuming that the results of SOAP are adequate, the following remarks can be made.

The main reason for the similarity in results is the fact that the water stress and the resulting reduction in uptake hardly ever occurs in any of the combinations. Thus the transpiration is optimal at all times and the fraction of the rainfall which remains for percolation is more or less the same, regardless of soil properties. Only the response time of the soil to infiltrating water varies, but not so much the size of the fluxes. Permeability does play a role in the fact that there is a negative non-linear relation between hydraulic conductivity and hydraulic potential. From the description of the

soils in chapter 9 the unsaturated hydraulic conductivity appears to be almost the same for all three soil types (with average properties) around field capacity, while at a matric potential of -200 cm the conductivity of FRh is even higher than for ARo. Thus the less permeable soils stay wetter and have a relatively high percolation rate, while the more permeable soils dry out rapidly and stop percolating sooner. This mechanism brings the cumulative fluxes closer together than might be expected from the soil properties. It also shows that K_{sat} is not always a good estimator for the behaviour of the soils, while it is a property that is often measured in this respect (see chapter 9).

In chapter 5 it is shown that all soils are very different in the spatial variability of the hydrological properties and that the spatial structure can be accurately mapped with the right sample support. The Ferralsols require a dense sampling scheme as the scale of variation of most properties is somewhere in the order of 2 to 20 m. On the other hand, the presence of roots and macropores in the topsoil creates a high level of "noise" in the data. Thus, mapping the input parameters of SOAP (i.e. K_s , θ_s , n and α) for instance in the experimental catchment, requires an enormous amount of effort. This is certainly not justified in view of the fact that the evapotranspiration dominates the water balance, whereas the remaining water percolates regardless of the soil properties.

Because the transpiration proceeds at an optimal rate as soil conditions are not a limiting factor, the actual transpiration is determined completely by the interaction between microclimate and plant. Although the forest types do not differ significantly in interception and throughfall, both exhibit a large variation, with throughfall amounts ranging from 10 to 150% of the rainfall. The same could be the case with transpiration, of which the distribution is not known. Jordan and Kline (1977) measured uptake in Venezuela, and showed that transpiration was independent of species but highly correlated to sapwood area. Therefore the physiological and structural characteristics of the plants, in particular aerodynamic and stomatal conductance and root structure, are probably an important source of variation in the water balance, and the spatial variation of the various fluxes is probably much larger than shown here. A better estimation of the variability could be made if more data of plant structure were available, notably the vertical leaf area and the root distribution. Unfortunately most studies relate these factors to the biomass of the plant itself and not to the space it occupies.

An important source of error could be the simulated microclimate in the forest canopy. Measurements of temperature and relative humidity under the canopy suggest a daily course with an small but evident amplitude. In a review Kira and Yoda (1983) report that the vertical profile is related to the leaf mass, because the temperature rises with higher photosynthesis rates. At night the temperature profile in the canopy shows hardly any gradient. Relative humidity is also related to photosynthesis. However, simulation with SOAP is done by assuming the temperature and RH below the canopy to be at a constant level corresponding of the average for that day. This probably produces a systematic error in the calculation of daytime potential evapotranspiration, especially during clear days when the actual vertical gradient of the variables is larger than the simulated gradient.

In general the results are consistent with the results of other hydrological studies. In a detailed study of the lowland rain forest in Costa Rica, Parker (1985) measured the water balance for 686 days. The annual rainfall is much higher than in the Mabura area (4000 mm) and the soil is clayey with a Ksat comparable to FRh-std. Transpiration was measured with lysimeters and is somewhat higher than estimated for Mabura (41.7% of the rainfall), but there was hardly any seasonal variation, with daily fluxes ranging from 2.5 to 11 mm. Because the interception was lower (13% including stemflow and litter interception) the division of rainfall in evapotranspiration and percolation was 51.5% versus 49.5% with a small storage change. Maximum daily percolation was estimated at 28 and 39 mm, similar to the results obtained in this research. Heuveland and Jordan (1981) review the research done at San Carlos de Rio Negro in Venezuela. With an mean annual precipitation of 3565 mm, the interception is very low, 5% only with a throughfall of 87% leaf drip and 8% stemflow. The transpiration was 47% using the measurements of sapflow, while the soil evaporation measured with lysimeters was estimated at 20 -25 mm per year. The remaining 48% was attributed sub-surface runoff.

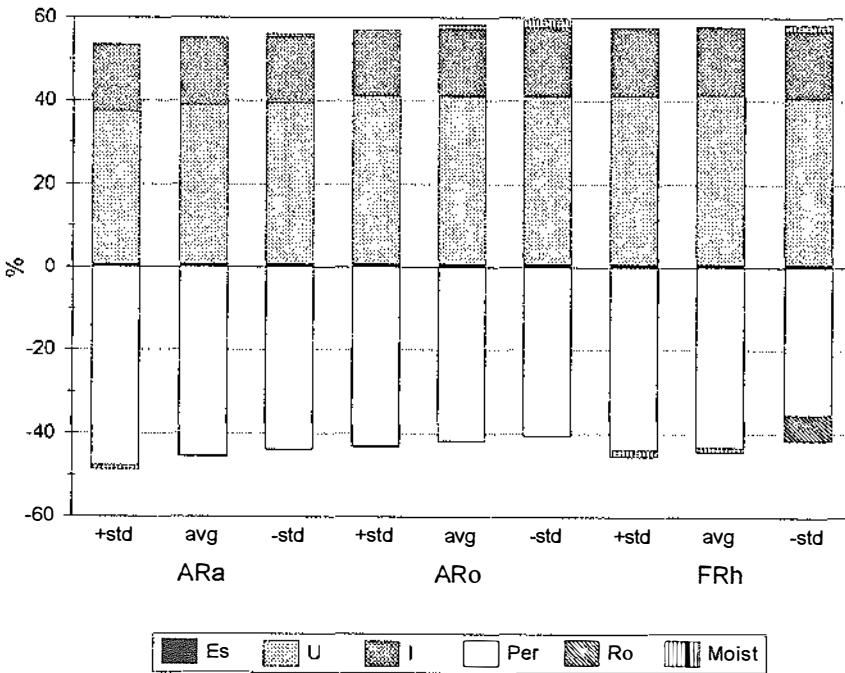


Figure 8.7 Summary of the water fluxes in percentage of rainfall over a 346 day period. The soils are arranged in order of a decreasing permeability from left (ARA+std) to right (FRh-std, see text for explanation of abbreviations). Ei = interception, U = uptake, Es = soil evaporation, Per = percolation, Ro = surface runoff, Moist = soil moisture change.

8.6 Conclusions

In spite of the wide variation in soil properties, with saturated hydraulic conductivities ranging from nearly 6000 cm/day to 25 cm/day, all combinations are very similar both in annual totals of the fluxes, and in temporal variation. This is caused by the fact that the evapotranspiration dominates the vertical water balance, while at the same time it is nearly identical, and fairly constant, for all combinations of soil properties. Seasonal variation is apparent in percolation fluxes, as 70% of the percolation occurred in the 4 wet months (mid-April to mid-August 1992). Differences between the soils are largest in the dry season, particularly in response time of the topsoil. However, true variation may be larger as only average plant structure and physiological properties are used. Figure 8.7 summarizes the results of the estimations of the 346 day period. Note that the interception is the same for all combinations because the same canopy structure is used. Dry Evergreen Forest on the most permeable Albic Arenosol experiences water stress and therefore the uptake is lowest. The Evapotranspiration for this combination is 53.4% of the rainfall, while for all other soil types it is about 56 to 57%. On the other end the least permeable Haplic Ferralsol produces runoff and therefore has the lowest amount of percolation (35.5%). The percentages for other combinations vary between these values.

9 THE IMPACT OF LOGGING ON SOIL HYDROLOGICAL PROPERTIES

9.1 Introduction

There is a large variation in the effects of logging on the hydrological behaviour of the soils. On the one hand the term logging encompasses a wide range of activities while on the other hand each soil type is affected differently. In terms of disturbed area one can generally distinguish between the areas that are cleared for infrastructure, areas that are partly cleared by skidders and bulldozers to reach the timber and haul out the logs and areas where the actual felling takes place. Although the construction of dirt roads often leads to severe erosion (Bruijnzeel, 1990) the actual area converted to infrastructural facilities is usually small compared to the logged areas and lies outside the scope of this study. The skidders however, make trails that are used only a few times which should revert to natural forest in time. The area cleared directly by skidding varies in size, depending on such factors as logging intensity, planning and skill of the driver. These areas are affected most (see below). The felling areas are larger in size but machine activity is less.

Important indications of the impact of logging on the water balance, are changes in water retention and hydraulic conductivity. These soil properties influence decomposition processes, leaching of nutrients and growth and development of seedlings. They are largely determined by the pore distribution and texture of the soil. Under undisturbed forest, pore distribution is related to root activity, macro and micro fauna, and macro and micro structural elements. In their turn these structural elements are related to texture and to such bonding agents as organic matter and sesquioxides. All these factors are influenced by the action of heavy machinery.

Assuming that dry bulk density, porosity, water retention and hydraulic conductivity characteristics (i.e. the Van Genuchten parameters) are appropriate properties that can be used to assess the damage done to the soil, these properties were measured before and after skidding on the 4 major soil types: Albic Arenosols (ARa), Ferralic Arenosols (ARo), Haplic Ferralsols (FRh) and Haplic Acrisols (ACh). A general description of these soils is given in chapter 2.

9.2 Impact of skidding on the topsoil

Access to the forest in Guyana is gained by wheeled skidders which have a small blade in front to push aside the trees and a winch to haul out the felled trees. The skidder has a pivot point in the middle enabling it to make very sharp turns. Here, the route which is cleared by the skidder is called a "skid trail" here, the actual places where the wheels have passed are called "skid tracks". The impact on the soil takes various forms. Firstly, there is the loss of structure as a result of compaction. The compaction is caused by the combined weight of the machine and its load, together with the shear stress of the rimpull (the turning force) of the wheels on the

surface. Secondly, the bulk of the root mass, which under natural forest is present in the upper 30 cm of the soil, is ripped apart by the wheels. Thirdly, there is the mixing of the litter and fresh organic debris from the logging with the topsoil by the revolving action of the skidder wheels.

Several researchers have monitored dry bulk density, porosity, hydraulic conductivity and infiltration characteristics after a controlled number of passes by a skidder. The state in which the soil remains after machine action depends on several factors, such as the type of soil, the number of skidder passes and degree of manoeuvring and the antecedent moisture content. According to Henrison (1990) who tested soils in Surinam which are similar to the soil types described in this research, the first 4 passes with a skidder created the largest change in bulk density (from 1.25 to 1.60 g.cm⁻³) after which only slight compaction took place. Similar results were obtained by Kamaruzaman (1991) on a clay loam soil in Malaysia. He measured the largest increase in bulk density of a clay loam soil in the first 2 passes of a rubber tyre log-loader (from 1.4 to 1.65 g.cm⁻³). Surprisingly it took more than 30 passes with a caterpillar bulldozer to achieve the same increase, which was also much more gradual. He also measured a decrease in porosity from 0.47 to 0.37, which was very sharp for the log loader as opposed to a more general decrease with the caterpillar.

The initial soil moisture content is important, a wetter soil resulting in more compaction. Henrison (1990) reported that a doubling of the gravimetric moisture content from 14% to 28% resulted in an increase in bulk density of 8% (1 skidder pass) to 14% (5 and more skidder passes). Dias and Nortcliff (1985) report for an Oxisol in Brazil an increase in dry bulk density of 0.85 to 1.1 g.cm⁻³ on a dry soil, to 1.2 g.cm⁻³ on a wet soil (above field capacity). The average surface level decreased with 5 cm on the dry soil and with 12 cm on the wet soil. Additional manoeuvring with the skidder resulted in further compaction.

Henrison further reports that saturated hydraulic conductivity decreased considerably in all skid trails and on all soils, sometimes up to 90%. Furthermore he found no significant difference between the skid tracks and the rest of the skid trail, apparently because the logs caused a disturbance identical to the skidder. In Malaysia, Malmer and Grip measured a 50 to 99% decrease in steady state infiltration rate between forest and tractor tracks for Orthic Acrisols (40% clay) and Gleyic Podzols (10% clay) respectively. Van der Plas and Bruijnzeel (1993) report an 85% decrease in steady state infiltration rate on clayey Ultisols between forest and 12 year old tractor tracks, but only a 10% decrease between undisturbed forest and recovering forest.

These are all direct consequences of machine compaction and disturbance. Indirect consequences depend on the development of the soil in time. Rapid decomposition of the organic matter on the open areas may cause an additional loss of structure. Surface sealing and subsequent erosion may take place (depending on texture, vegetation cover and location). Thus the effects of skidding are subject to temporal changes. Van der Plas and Bruijnzeel (1993) indicate the difficulty of recovery as a result of surface runoff and erosion.

9.3 Methodology

Three of the four major soil types, i.e. the Albic Arenosols, Ferralic Arenosols and Haplic Ferralsols were sampled approximately 3 months after logging took place in the experimental catchment (the logging experiment is described in chapter 11). All samples indicated as "disturbed" come from skid trails, the "undisturbed" samples were taken in under natural forest close to the trails. Unfortunately it is not clear how many times the skidder passed over each skid trail, but certainly more than once. The Haplic Acrisol samples were taken at a different location approximately one year after logging, in the Waraputa area (in the catchment described in chapter 3). Samples were taken under forest, on a gap and on a "market" on plots of 100 m². The market is the location where the logs are collected and is subjected to prolonged activity of heavy machinery. The gap samples were not taken on the skid trail itself but at locations where trees were felled. In addition many values for soil properties under undisturbed forest were available from measurements in the Tropenbos Reserve and other areas in the vicinity (see chapter 5). These values are added to the "undisturbed" dataset to increase the sample size.

The soil samples were all taken with 100 cm³ steel rings in the upper 20 cm of the soil. Dry bulk density (Bd) and porosity (θ_s) were determined by heating to a temperature of 105 °C for 24 hours. Saturated hydraulic conductivity (Ks) was measured by applying a hydraulic head of a few cm to the saturated samples and measuring the steady state outflow.

In order to compare the water retention and hydraulic conductivity characteristics a total of 64 pF-curves were measured in the Netherlands. Using a non-linear regression analysis the Van Genuchten parameters n and α were estimated (see section 5.4). With equations 5.8 to 5.10 the hydraulic conductivity was estimated from the Ks, the relative moisture content (Se) and n and α . Thus the unsaturated K(h) curves presented here are not actually measured.

The sample size of the dataset after logging is rather small and the statistical distribution is not known. Nevertheless, to test the significance of the differences before and after logging the data are assumed to be normally distributed and an ANOVA is used because the results are better interpretable than a non-parametric test such as Mann-Whitney.

9.4 Results

9.4.1 Texture and structure of undisturbed topsoil

The four soil types under investigation range in texture from pure sand to sandy clay loam. These are Albic Arenosols (Ara), Ferralic Arenosols (ARo), Haplic Ferralsols (FRh), and Haplic Acrisols (ACh) in order of increasing clay content (see table 9.1). These soil types are described in chapter 2. Under undisturbed forest, the textural and structural properties can be described as follows. The Arenosols are characterised by an absence of clay, a high sand content and a poorly sorted sand

fraction in the range of 150 to 400 μm . Both the Arenosols and Ferralsols have deeply weathered profiles with a texture that becomes slightly coarser with depth. In spite of the differences in texture there is hardly any macro structure present in any of these three soils. Both ARa and ARo have a granular structure and the sands are rather loosely packed. Also the Haplic Ferralsols have a granular structure, which is caused by the iron oxide content in the soil. As a result of chemical weathering processes these minerals are very stable (Driessen and Dudal, 1989). The iron oxides form very strong micro-aggregates which have a size comparable to silt. In table 9.1 two types of texture analysis are given, with and without destruction of micro-aggregates with peroxide and HCl (indicated with FRh and FRh-alt respectively). It shows that the fraction $<2 \mu\text{m}$ has dropped from 17.8 to 4.1%, whereas the fraction between 2 and 100 μm has increased by roughly the same amount. An alternative texture analysis on Ferralic Arenosols (ARo and ARo-alt in table 9.1) hardly results in a change of texture in spite of the brown colouring which indicates the presence of iron oxides. The Haplic Acrisols have an illuvation horizon with a clay percentage between 15 and 20%. Unfortunately, an alternative texture analysis of these soils is not available. The bright orange colour indicates that these soils are also rich in iron oxides, and stable micro aggregates will probably have formed as well. Moreover, these soils show a clear subangular blocky structure.

Table 9.1 Average texture of the top soil of the four main soil types (*alt* denotes the analysis without aggregate destruction, see text)

Soiltype	Sand%	Silt%	Clay%
Albic Arenosols (ARa)	90.37	9.69	0.01
Ferralic Arenosols (ARo)	92.01	5.94	1.98
ARo-alt	93.76	5.88	0.36
Haplic Ferralsols (FRh)	71.46	12.82	15.72
FRh-alt	82.44	13.46	4.10
Haplic Acrisols (ACh)	69.80	15.40	14.00

9.4.2 Saturated hydraulic conductivity, porosity and bulk density

The saturated hydraulic conductivity (cm/day), porosity ($\text{cm}^3.\text{cm}^{-3}$) and bulk density ($\text{g}.\text{cm}^{-3}$) of the undisturbed and disturbed topsoil of the four soil types are compared. Results of an ANOVA between the two situations for each property are shown as F-values in tables 9.2 to 9.5.

Albic Arenosols (ARa)

Although there is a high coefficient of variance, the differences are very clear for Ks which decreases from roughly 3400 cm/day to less than 10% of this value when disturbed (see table 9.2). However, this change in topsoil is not so clear from measurements of θ_s or Bd. The porosity for the disturbed soil is significantly higher, the bulk density is not significantly different at a $p = 0.05$ level. Also, two samples were taken from a depth of 30-40 cm which clearly show a decrease in θ_s and an increase Bd. This indicates that compaction did take place but that at the surface

other factors play an important role, such as mixing of fresh organic matter with the topsoil as mentioned above. Also, in Albic Arenosols the decomposed organic matter tends to be present in the form of fine particles or pellets, rather than as an amorphous dark colouring of the mineral particles. The particles are often sedimented in the skid tracks that channel the overland flow. At these places ponding has been observed, even on the coarse Arenosols. This relocation of organic matter could cause lower Ks values while θ_s and Bd remain more or less the same. For comparison one of the disturbed samples taken from a bare patch without organic matter gave a relatively high Ks of 785.3 cm/day.

Table 9.2. Soil properties of Albic Arenosols under forest (undisturbed) and on skid trails (disturbed), F values give the result of an ANOVA between the two situations.

ARa	mean	std	CV%	min	max	n	F
Ks (cm/day)							
<i>undisturbed</i>	3369.6	2318.3	68.8	576.0	7382.9	25	12.531 **
<i>disturbed</i>	372.8	201.4	54.1	166.2	785.3	8	
θ_s (cm ³ /cm ³)							
<i>undisturbed</i>	0.546	0.051	9.3	0.452	0.630	31	9.633 **
<i>disturbed</i>	0.594	0.030	5.0	0.548	0.657	12	
<i>dist.30-40cm</i>	0.434	0.001	0.2	0.433	0.435	2	
Bd (g/cm ³)							
<i>undisturbed</i>	1.144	0.123	10.8	0.912	1.405	30	2.961 n.s.
<i>disturbed</i>	1.213	0.091	7.5	1.038	1.374	12	
<i>dist.30-40cm</i>	1.379	0.062	4.5	1.317	1.442	2	

Ferralic Arenosols (ARo)

Skidding clearly affects Ks which decreases to about half of the value under undisturbed forest (see table 9.3). Pore volume and also bulk density significantly increase. All disturbed samples were taken from skid trails that were used more than once: the small coefficient of variance indicates these locations have reached a maximum compaction. The increase in pore volume could be a result of organic matter mixed with the topsoil.

Table 9.3. Soil properties of Ferralic Arenosols under forest (undisturbed) and on skid trails (disturbed), F values give the result of an ANOVA between the two situations.

ARo	Mean	std	CV%	min	max	n	F
Ks (cm/day)							
<i>undisturbed</i>	469.7	182.7	38.9	156.8	768.6	9	11.704 **
<i>disturbed</i>	211.4	87.8	41.5	12.4	330.3	8	
θ_s (cm ³ /cm ³)							
<i>undisturbed</i>	0.479	0.038	7.9	0.435	0.574	20	9.745 **
<i>disturbed</i>	0.524	0.019	3.6	0.488	0.550	8	
Bd (g/cm ³)							
<i>undisturbed</i>	1.235	0.119	9.6	1.012	1.403	13	4.422 *
<i>disturbed</i>	1.331	0.038	2.9	1.264	1.382	8	

Haplic Ferralsols (FRh)

In view of the high coefficient of variance of Ks for both undisturbed and disturbed Haplic Ferralsols it is difficult to give a clear view of the effects of skidding (see table 4). Nevertheless the conductivities are not significantly different. Porosity is significantly higher, as is bulk density although the latter only on a p = 0.1 level. It seems that the effects of skidding on the topsoil fall within the variability present in the soils.

Table 9.4. Soil properties of Haplic Ferralsols under forest (undisturbed) and on skid trails (disturbed), F values give the result of the ANOVA between the two situations.

FRh	Mean	std	CV%	min	max	n	F
Ks (cm/day)							
undisturbed	114.7	91.1	79.5	14.4	360.0	45	2.683 n.s.
disturbed	187.3	177.7	94.9	23.4	585.1	7	
θ_s (cm ³ /cm ³)							
undisturbed	0.482	0.045	9.3	0.346	0.580	45	5.230 *
disturbed	0.526	0.055	10.5	0.433	0.588	7	
Bd (g/cm ³)							
undisturbed	1.287	0.108	8.4	1.107	1.500	45	3.070 n.s.
disturbed	1.362	0.053	3.9	1.271	1.428	7	

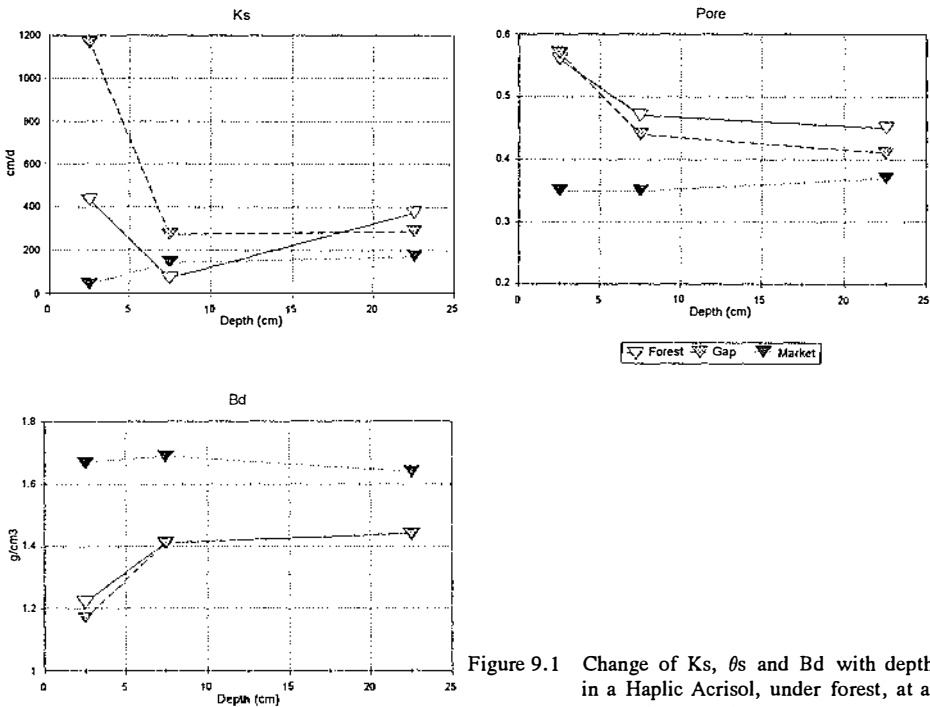


Figure 9.1 Change of Ks, θ_s and Bd with depth in a Haplic Acrisol, under forest, at a gap and at a market.

Haplic Acrisols (ACh)

As is mentioned above the three soil properties were sampled at three sites and at three different depths. Table 9.5 gives the values of the 0-5 cm depth for the three sites. All properties are significantly different ($p = 0.001$) on a depth of 0-5 cm, except for bulk density and porosity of forest and gap which are not significantly different (F values are not given). The change of these properties with depth on the three locations give a clear view of the degree of disturbance (see figure 9.1).

Clearly the topsoil of the market is most affected. The mean Ks is slightly more than 10% of the forest value (although the CV% is very high) and also porosity is very low and bulk density is very high. The changes with depth between either forest and market or gap and market remain significant on a $p = 0.001$ level. Between Forest and gap there is no significant difference for all properties deeper than 5 cm.

Table 9.5. Soil properties of Haplic Acrisols under forest, on a gap (not on skid trails) and on a market. Codes for ANOVA F-values: FG = forest vs. gap; FM = forest vs. market; GM = gap vs. market.

ACh	Mean	std	CV%	min	max	n	F
Ks							
Forest	428.1	444.9	103.9	nil	1599.8	30	FG 10.788 **
Gap	957.0	728.3	76.1	15.8	2937.6	27	FM 20.428 ***
Market	47.1	90.0	190.9	nil	391.7	30	GM 44.398 ***
θ_s (cm ³ /cm ³)							
Forest	0.557	0.032	5.8	0.480	0.630	30	FG 0.260 n.s.
Gap	0.562	0.093	8.0	0.480	0.610	27	FM 259.48 ***
Market	0.354	0.049	13.9	0.180	0.430	30	GM 327.59 ***
Bd (g/cm ³)							
Forest	1.217	0.097	8.0	1.030	1.390	30	FG 1.679 n.s.
Gap	1.184	0.093	7.8	1.010	1.360	27	FM 218.27 ***
Market	1.666	0.101	6.1	1.450	1.830	30	GM 337.53 ***

9.4.3 Water retention and hydraulic conductivity

The three basic soil properties Ks, θ_s and Bd do not give a complete picture of the effects of skidding. Particularly on the sandy soils, saturated conditions do not occur often, in spite of the high rainfall intensities that are common for the humid tropics. Therefore it is important to have an idea of water retention and hydraulic conductivity under unsaturated conditions. Table 9.6 gives the Van Genuchten parameters n and α for all soils and the results of ANOVA between datasets for disturbed and undisturbed situations. Available water is calculated as the difference between the moisture contents, calculated from equation 1, at field capacity (pF 2) and wilting point (assumed at pF 4.2).

The water retention curves of each soil are shown in figure 9.2 a to d. The points in the graphs represent the average from N measurements, which can be found in table 9.6. Figure 9.3 a to d shows the hydraulic conductivity curves (it is important to note that the points in these curves are also calculated with the relative water content (Se) from the pF curves and are not actual measured conductivities).

Albic Arenosols are affected most by skidding. The water retention curve of the disturbed soil increases more gradually than that of the undisturbed soil. Apparently the capillary suction has increased because of a shift in pore distribution towards the finer pores. The explanation for this may be compaction of the loosely packed sand or a mixing of fine organic matter with the mineral matrix of the soil. Especially between pF2 and pF4.2 the water retention has increased, resulting in a doubling of the water availability from approximately 0.08 to 0.18. Also Ferralic Arenosols are affected with a small but significant decrease of n . The curves have almost the same shape indicating that the change in water retention took place over the whole range from wet to dry. Nevertheless, the water availability increases only slightly from approximately 0.13 to 0.15. For Haplic Ferralsols, only α differs significantly but the curves have almost the same shape except between pF0 and pF1. Therefore there is only a very small decrease in water availability from approximately 0.19 to 0.18. Water retention of the disturbed Haplic Acrisol has decreased considerably. Again n and α are not significantly different for any of the locations, indicating a change in water retention over the whole range from wet to dry. Nevertheless, the actual moisture content between the locations is quite different and water availability changes from approximately 0.25 for gap and forest to 0.17 for the market.

Table 9.6 Van Genuchten parameters for all soils under forest (*und*) and on a skid trail (*dis*). Codes for ANOVA F-values of ACh: FG = forest vs. gap; FM = forest vs. market; GM = gap vs. market.

		Mean	std	CV%	min	max	n	F	
ARa									
	<i>und</i>	n	1.949	0.284	14.6	1.632	2.481	7	46.62 ***
		α	0.059	0.018	30.9	0.037	0.090		17.78 ***
<i>dis</i>	n	1.343	0.049	3.6	1.275	1.454	12		
	α	0.140	0.047	33.1	0.084	0.214			
ARo									
	<i>und</i>	n	1.483	0.043	2.9	1.411	1.554	7	29.11 ***
		α	0.091	0.025	27.0	0.053	0.132		3.76 n.s.
<i>dis</i>	n	1.333	0.053	4.0	1.276	1.415	7		
	α	0.173	0.101	58.5	0.086	0.406			
FRh									
	<i>und</i>	n	1.262	0.021	1.7	1.236	1.287	9	0.20 n.s.
		α	0.059	0.016	26.9	0.038	0.087		12.12 **
<i>dis</i>	n	1.256	0.029	2.3	1.208	1.293	7		
	α	0.116	0.043	36.8	0.062	0.208			
ACh									
	<i>forest</i>	n	1.253	0.023	1.9	1.213	1.279	5	FM 0.880 n.s.
		α	0.055	0.022	39.7	0.015	0.082		FM 0.001 n.s.
<i>gap</i>	n	1.238	0.021	1.7	1.205	1.270	5	GM 1.844 n.s.	
	α	0.054	0.020	36.2	0.035	0.091		GM 0.994 n.s.	
<i>market</i>	n	1.253	0.007	0.6	1.243	1.266	5	FG 0.996 n.s.	
	α	0.043	0.010	24.4	0.028	0.058		FG 0.004 n.s.	

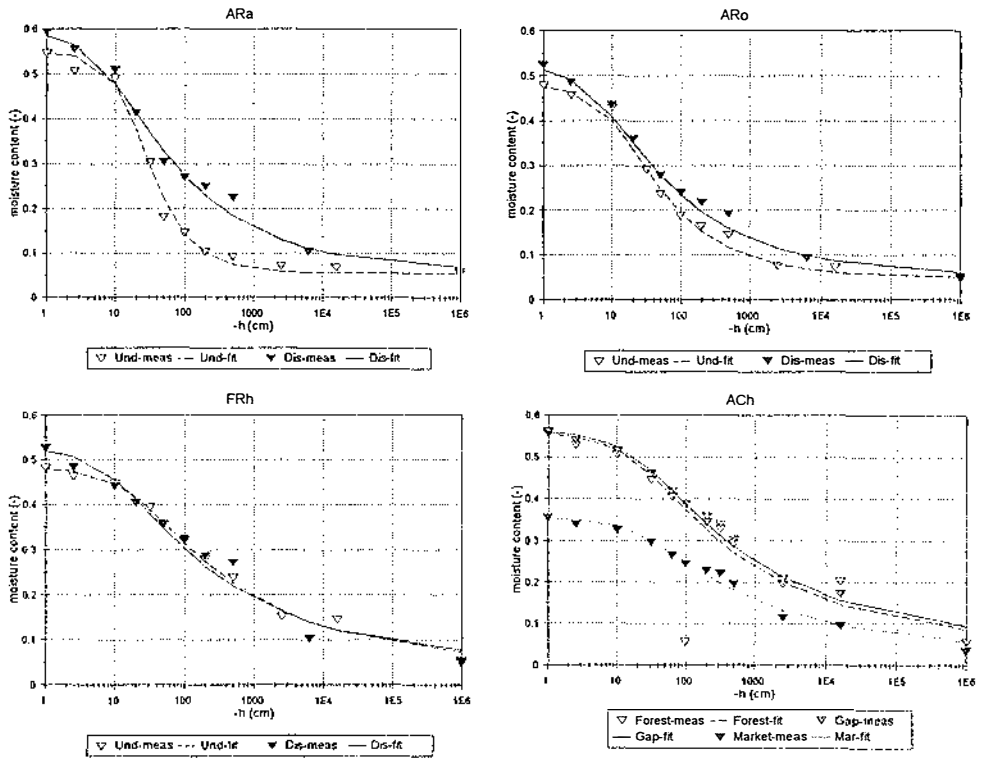


Figure 9.2 Moisture retention curves of the topsoil of the 4 soil types, in undisturbed and disturbed situations.

The hydraulic conductivity curves show similar results. Again the Albic Arenosols are affected most: not only is the K_s reduced to about 10%, in the wet range between pF 1 and pF 2 the conductivity on the skid trail decreases to less than 1% of the value under forest. The decrease in K is less for Ferralic Arenosols but still considerable: between pF1 and pF2 the conductivity decreases from 50% to 25% of the value under forest. Haplic Ferralsols do not show a significant decrease over the whole range of suction heads. However Haplic Acrisols show a significant decrease between forest and market ranging from 10% at saturation to 20% when dry, whereas between gap and market the differences are even larger, ranging from 7% at saturation to 10% when dry.

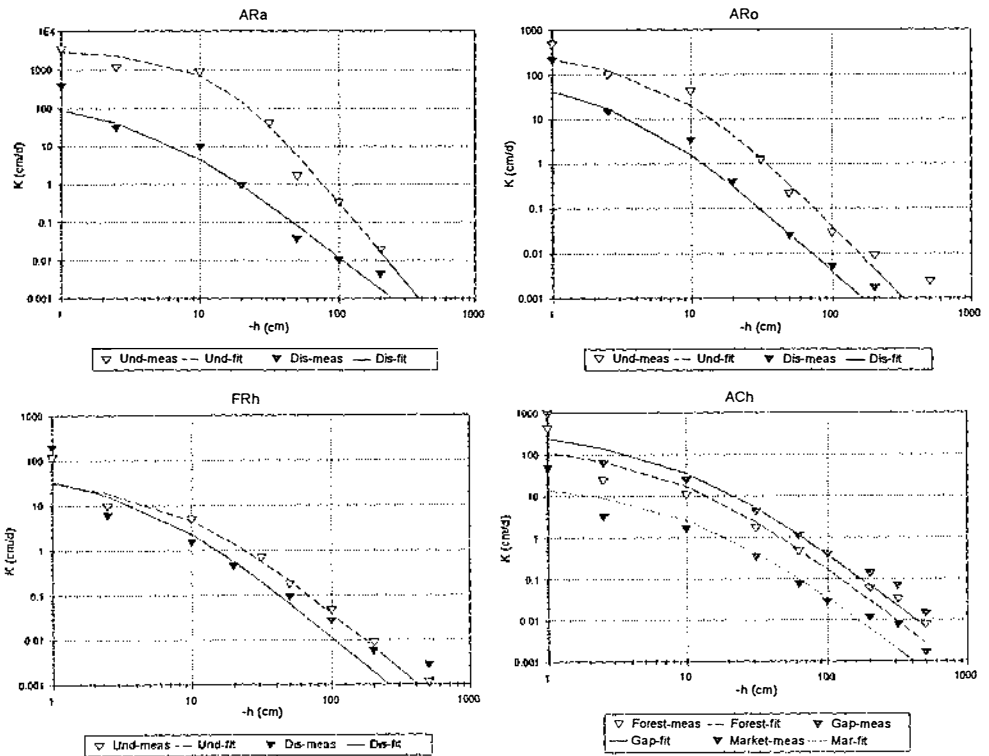


Figure 9.3 Hydraulic conductivity curves of the topsoil of the 4 soil types, in undisturbed and disturbed situations.

9.5 Discussion and conclusions

The impact of skidding on the four soil types is not very straight forward. There is a clear difference between the sandy Arenosols and the more clayey Ferralsols and Acrisols. Remarkable is the fact that there is a small but significant increase in porosity while at the same time the hydraulic conductivity strongly decreases over the whole range of matric potentials from wet to dry. The reason for this could be the method of analysis: because of the skidding there is often a mixing of fresh organic matter with the mineral part of the soil, resulting in a higher porosity when it is determined by heating to 105 °C (water evaporates from the organic matter which is then registered as pore space). At the same time compaction does take place: because there is no silt fraction the soil has a poorly sorted pore distribution, which changes drastically because of the disturbance. This causes a sharp reduction in hydraulic conductivity. Also in case of the Albic Arenosols it has been observed in the field that the organic matter is present in the topsoil in the form of small

discrete particles that tend to be sedimented in the skid tracks, and form black patches where ponding takes place. The water retention capacity of the Albic Arenosols strongly increases because of compaction, which may influence the establishment and growth of seedlings.

The Haplic Ferralsols are less affected than one would expect. The relatively high clay content and presence of a weak macro-structure seem likely to induce a decline in hydrological characteristics when compacted (disappearance of macro pores, surface sealing). Nonetheless, the data show that the water retention and conductivity remain at the same level before and after skidding. This is probably caused by the presence of stable micro-aggregates that are not destroyed by the skidder. Thus the clay remains bound in particles with a size of silt to fine sand (50-210 μm), so that structure decline, and surface sealing or crusting do not take place. Apparently the undisturbed soil is already rather compact and the pore distribution seems not to be affected much by skidding. However, the undisturbed Ferralsols have a high variability of hydrological properties (chapter 5) which may obscure the impact of skidding.

The mixing of fresh organic debris with the soil also may obscure the effects of compaction. The Haplic Acrisols samples were taken a year after logging while the other samples were taken only three months after logging took place. The results of ACh clearly show that there is a strong decline in structure which is probably a temporal effect. When the skid trails and markets remain bare there will be a rapid decomposition of organic matter causing a decrease of soil fauna. Both are factors that provide the soil with a loose structure. Thus in time one can expect a further change of the water retention and decline of hydraulic conductivity.

10.1 Introduction

Disturbance of the rain forest varies in scale and intensity, from low intensity logging and shifting cultivation, to complete clearing of larger drainage basins followed by a change in land use. In case of selective logging a series of gaps and skid trails are created which are surrounded by relatively undisturbed forest. On a catchment scale, the effects of logging on the size and frequency of the various water fluxes may be buffered by the surrounding forest. If no changes in the discharge are detected, either in the baseflow which represents the groundwater fluctuations, or in stormflow which represents the surface runoff, the impact of the disturbance is seen as minor.

However, at the location where the actual logging takes place the forest has to regenerate, if a sustained yield over a longer period in time is envisaged. In the research area, the forest itself plays a large role in the water balance, since the evapotranspiration determines much of the size of the other water fluxes, whereas the variation in fluxes is determined by the variation in throughfall. Consequently removal of the forest cover must have a tremendous impact on the water balance. Much depends on the intensity and method of felling and the method of clearing, but regardless of the method, the greatest changes occur because interception and transpiration decrease or disappear and are replaced by soil evaporation. This usually results in a sharp increase in percolation (Parker, 1985; Bruijnzeel, 1990). On top of that, heavy machinery changes the soil structure and causes strongly decreased permeability on most soil types (see chapter 9).

The impact of the change from forest to gap on the nutrient balance may be even bigger. A large amount of nutrients is removed with the logs, while the debris that is left behind starts decomposing. As the percolation increases, so does the leaching of nutrients. Moreover the direct irradiation on the gap causes higher surface temperatures which influences the speed of the chemical reactions. Also chemical reactions and litter decomposition are related to the moisture content of the top soil.

The determination of average values for the change in water and nutrient balance is made difficult by the fact that the size and shape of the gap are likely to influence both (Bruijnzeel, 1990). The smaller the gap the more the microclimate is influenced by the surrounding forest. The opening in the canopy is smaller and therefore the amount of direct irradiation is less. Surface resistance is larger and the vertical reduction of wind speed towards the surface will be larger. Also the influence of the root system of the surrounding forest is larger and with it the uptake of water from the soil in the gap. In the gap itself there is a large spatial variation as some areas will be highly disturbed by the skidder, whereas other areas will have experienced only the impact of the falling log or hardly any disturbance at all. The felled tree is stripped from branches and crown which leaves an extra amount of organic matter on the gap. Theoretically, at places where the debris is left after logging nutrient concentration levels in the topsoil will increase. If there is more leaching from these

areas depends, among other things, on the percolation. Thus, in a general sense, there is a large variability between gaps and in the gap itself.

The water balance will probably be back to its original equilibrium fairly quickly, at least in comparison with the restoration of the forest itself. Invasion of the gap by pioneer species and the development of a plant cover usually occurs within a year. From a hydrological point of view an increase in leaf area and development of a root system will result in a evapotranspiration/percolation ratio which resembles the forest level.

In this chapter the development of the water balance of a gap environment is described. The differences between skid trails, crown zones (zones with an accumulation of logging debris) and relatively undisturbed areas are estimated and a comparison with the water balance of an intact forest is made. Not all combinations of forest and soil types were actually measured. As part of the nutrient research of the Tropenbos Programme (Brouwer, in prep.; De Lange and Van Brunshot, 1992) two gaps of different size were created in Mixed Forest on a Ferralic Arenosol. To estimate the amount of leaching, soil moisture conditions were monitored with tensiometers on the gaps for several months: directly after logging in January 1992 and one year later. During the same periods the hydraulic potential under the undisturbed forest was measured (see chapter 8).

However the measurements do not cover a full year and do not include gaps on Albic Arenosols (ARa) and Haplic Ferralsols (FRh). Therefore, after calibration for gap conditions, the vertical water balance over a full year was simulated with SOAP for a gap on the 3 main soil types: ARa, ARo and FRh. In order to use these simulation results in the interpretation of the catchment experiment (see chapter 11), atmospheric data are used for the year after logging: October 1992 to October 1993.

10.2 Methodology

10.2.1 The gap experiment

Two gaps were created in January 1992 in the vicinity of the field station (see figure 2.1). The large and small gap indicated here with LG and SG were 3440 m² and 730 m² in size and had a more or less circular shape. On the gaps, zones were demarcated with different degrees of disturbance: the skid trails, the crown zones and the undisturbed areas. The latter areas were only damaged to a small extent during felling and removal of the logs, and a cover of seedlings and trees with a DBH smaller than 15 cm was present after logging. Each of the zones covered approximately 1/3 of the gap area, in both gaps. In all three zones on both gaps, sets of 3 tensiometers were placed at depths of 30, 70 and 120 cm (see also chapter 8). In the large gaps 2 tensiometer sets were placed on the skid trails (plots indicated with LGS1 and LGS2), 2 sets in the crown zone (plots LGC1 and LGC2) and 1 set in the undisturbed zone (plot LGU). Of these plots LGS2 and LGU1 were located in the centre of the gap, LGS1 and LGC2 were placed approximately 10 m from the edge of the gap and LGC1 5 m from the edge. On the small gap each of the zones

had 1 set of tensiometers (indicated with SGS, SGC and SGU) which were all located between 5 and 10 m from the gap edge. The plots were monitored every 3 days from 12 February to 21 April 1992, and every week from 11 March to 9 June 1993.

These datasets were simulated with SOAP. Because SOAP is a one dimensional model it is not possible to include the influence of the surrounding forest. Therefore simulations represent the water balance at the centre of the gap, where extraction of water by the root system of the surrounding forest is assumed to be close to nil. To estimate the atmospheric circumstances on the gap and evapotranspiration by the soil and plant cover, some assumptions have to be made which are discussed below.

10.2.2 Microclimate on the gaps

The relative humidity and temperature were measured every hour from 700 h to 1900 h on several days in March and April 1992, on both gaps. Measurements were done at 1.5m above the surface with an Assmann 761 aspiration psychrometer, measuring wet and dry bulb temperature. Of this dataset two days, a clear sunny day and a cloudy day with some rainfall, were selected as an example of the microclimate.

The meteorological data of the weather station were used directly to calculate the atmospheric circumstances on the gaps. However, the gaps are small in size and this will affect both wind speed and radiation. The evapotranspiration in the gap consists entirely of soil evaporation if the soil is bare or of combined soil evaporation and transpiration in the case of a cover with seedlings. The size and structure of the plants is discussed below. Because the seedlings are not very tall and the leaf area increases from almost 0 to between 1 and 2 m².m⁻², the vertical temperature and relative humidity distribution are assumed constant: in other words, the microclimate below the seedlings is the same as above. The wind profile was extrapolated downward using the wind speed of the weather station (measured at 10 m height) and the logarithmic equations relating wind speed to surface resistance (equations 4.13 and 4.14). Radiation extinction depends on the vertical leaf area distribution.

However, because of the size of the opening in the canopy the cumulative daily irradiation is smaller than at the weather station. This can be assessed with the program HEMIPHOT (Ter Steege, 1994) which analyzes vegetation indices and light climate from hemispherical photographs. Hemiphot calculated a total of 13.2 MJ.m⁻².day⁻¹ above the canopy and 10.9 and 7.8 MJ.m⁻².day⁻¹ for the centre of the large and small gap, which gives a ratio of 0.825 and 0.598 respectively. This is simulated in SOAP by assuming that direct radiation takes place only if the sun is above the gap horizon. In the hours between the actual sunrise and "sunrise" at the gap only indirect (diffuse) radiation is assumed, which can be calculated as 15% of the direct radiation (Goudriaan, 1977). The same was done between sunset at the gap and the actual sunset. The "horizon" of the large gap is at an azimuth of approximately 60 degrees, of the small gap at an azimuth of 50 degrees. Translating this to hours of sunrise and sunset, the length of direct irradiation was decreased by 2.5 hours for the large gap and by 3.5 hours for the small gap.

In addition the albedo of the gap changes gradually as the plant cover increases. For most soils the albedo is between 0.4 and 0.5 (Pearcy et al. ,1989) and for a closed leaf surface the same albedo as for the forest is used. In the model simulations the albedo is set to the albedo of vegetation if the LAI if it is more than 1 m².m⁻². If the LAI is less the albedo is calculated as 0.12*(LAI)+0.45*(1-LAI).

10.2.3 Seedling cover

Immediately after logging, and in the measurement period of 11 February to 21 April, plant cover was assumed to be absent on the skid trails and in the crown zone. Thus for the simulations of LGS1-2, LGC1-2, SGS and SGC the only water fluxes across the soil boundary are rainfall and soil evaporation. By the time of the second measurement period in 1993 a seedling cover had been established and interception and transpiration returned, in favour of soil evaporation.

Parker (1985) measured the increase in average LAI on two gaps of different size in a rain forest in Costa Rica. Figure 10.1 shows his results for a period of 400 days after logging. He reports that the sharp increase in LAI after 200 days was related to an exceptional increase in lianas. For comparison the development of seedlings of 2 very common pioneer species and 2 common climax species (figure 10.2), measured at a 1 year old gap south of the Tropenbos Reserve (unpublished data Raaymakers). The increase in leaf surface with plant height is logarithmic in case of the pioneer species *Goupia glabra* ($r^2 = 0.77$), whereas *Cecropia obtusa* does not show any linear or logarithmic relation. The climax species *Dycimbe altsonii* and *Chlorocardium rodiei* both have a linear relation of leaf surface with height ($r^2 > 0.75$ in both cases).

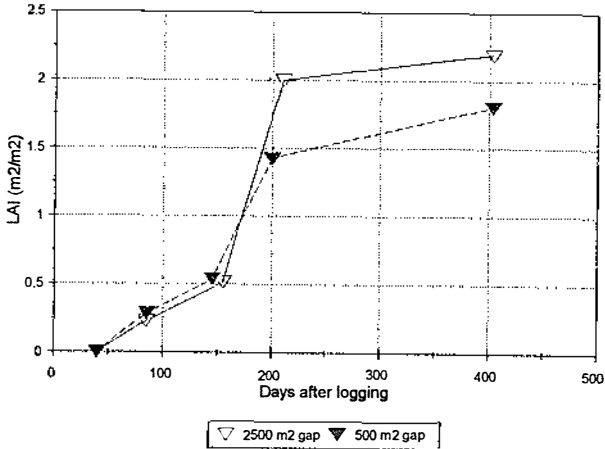


Figure 10.1 Increase in Leaf Area Index on two gaps in the La Selva Reserve in Costa Rica (Parker, 1985).

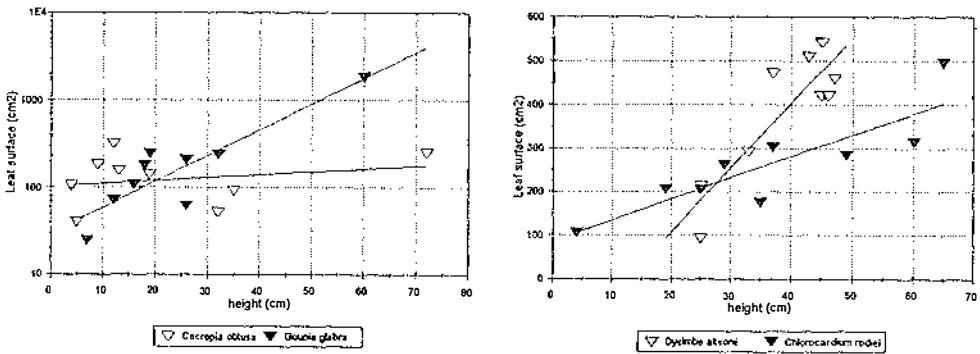


Figure 10.2 Increase in leaf surface with seedling height for two pioneer species (left) and two climax species (right) (Raaymakers, unpublished data).

The relation of root weight with height is less clear (figure 10.3), in case of the pioneer species the increase is linear ($r^2 > 0.6$) but the climax species do show not significant linear or logarithmic relation. In fact the increase of total plant weight with height is linear for all species except *D. altsonii*, but the individual plants invest in different parts depending on the local circumstances.

Given these results a linear increase in both leaf area and root system was assumed in the simulations. The average LAI on the gaps after 1 year will be approximately $1.2 \text{ m}^2 \cdot \text{m}^{-2}$ (simulated as 2 layers with an LAI of 0.6 each), the root system will have developed to a depth of 40 to 50 cm with a maximum between 5 and 20 cm.

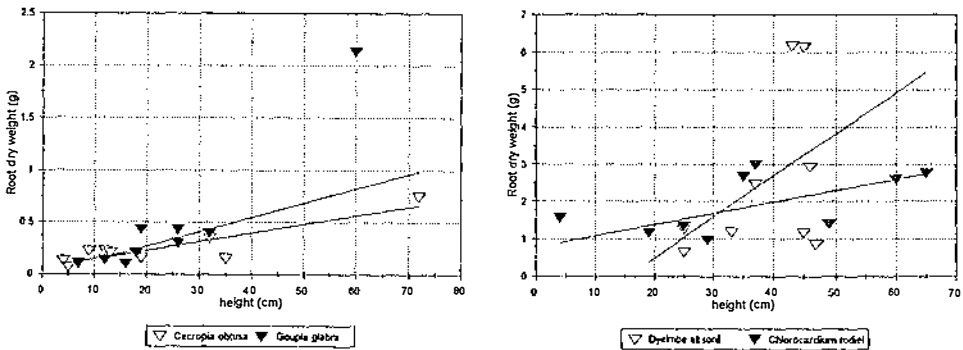


Figure 10.3 Increase in root mass with seedling height for two pioneer species (left) and two climax species (right) (Raaymakers, unpublished data).

10.2.4 Simulations with SOAP

To evaluate the seasonal variation of the gap water balance under conditions of restoring vegetation, the year after the logging of the experimental catchment was simulated. Calculations were done for a soil profile of 100 cm depth with a vertical resolution of 5 cm. Surface storage capacity was set at 5 mm with immediate runoff if this storage is exceeded. It is assumed that the groundwater is far below the bottom of the root zone and that there is unimpeded drainage and no capillary rise. As most gaps are situated on the flat watershed, these conditions represent the normal gap situation in the area (see also chapter 11).

A combination of the soil properties discussed in chapters 8 and 9 were used in the simulations. The crown zone and undisturbed zone are hardly compacted and the porosity, saturated hydraulic conductivity and Van Genuchten parameters shown in table 8.1 were used. The skid trails are compacted to a depth of approximately 20 cm and the soil properties of disturbed Ferralic Arenosols, given in tables 9.3 and 9.5 were used. Below 20 cm depth the soil was assumed identical to the other plots. Using the same reasoning the soil properties of the other soil types were compiled from chapters 8 and 9 with the simulation of the annual water balance.

10.3 Results of the gap experiments

10.3.1 Microclimate

Air temperature and relative humidity were measured every hour from 7 am to 7 pm on 27 March 1992 and 8 April 1992 on both gaps (figure 10.4). The first day was dry and sunny with a few clouds, the second day was cloudy in the morning and late afternoon with rainfall in the afternoon. For comparison the weather station readings of relative humidity temperature and incoming short wave radiation have been added. On both gaps the relative humidity started to drop and the temperature started to rise about an hour later than at the weather station. This supports the fact that sunrise on the gap will be later. On the clear day the humidity in the small gap dropped even 2 to 3 hours after that on the weather station. On the cloudy day the differences are less evident. Also the humidity increase and the temperature decrease in the second half of the day was slower than at the weather station, because the warm air is contained more on the gaps. The differences between the gaps are clear once the direct radiation increases: on the small gap the humidity was higher and the temperature lower. Especially during the cloudy afternoon on 8 April the humidity on the small gap increased sharply. Before sunrise the microclimate in the gaps was more or less the same.

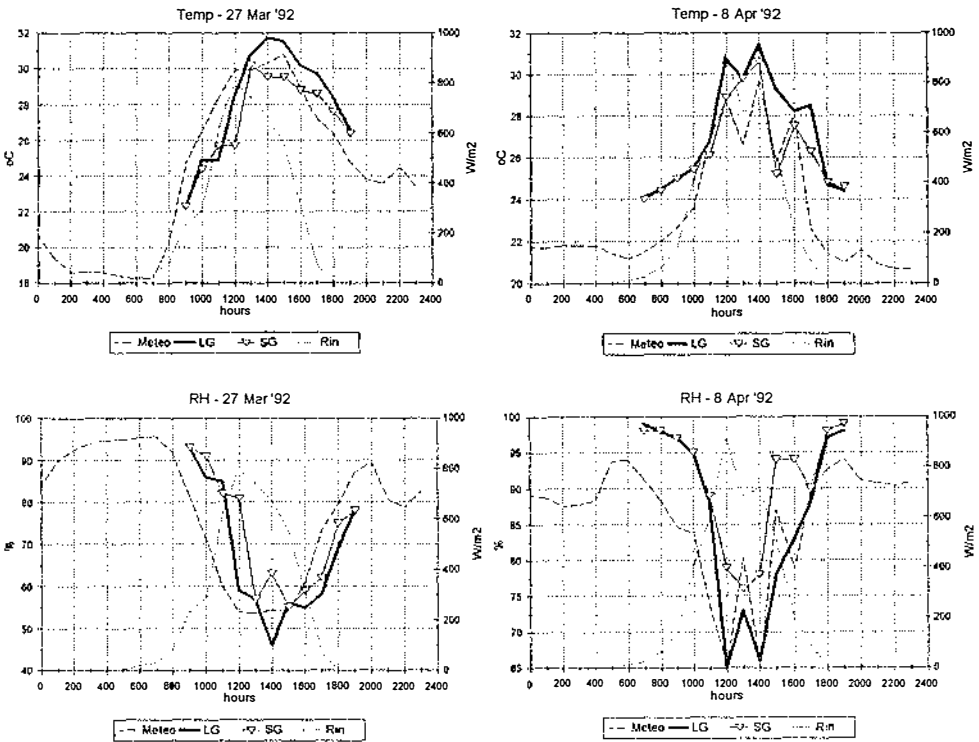


Figure 10.4 Temperature (Temp) and relative humidity (RH) on two days on the large gap (LG) and small gap (SG). Weather station data (Meteo) of temperature, relative humidity and radiation (Rin) have been added.

10.3.2 Skid trails

Measurements of the dry season hydraulic potential under the bare skidtrails show that the soil remains very wet (figure 10.5, graphs on left hand side). There is some variation between the plots especially near the surface, where the influence of skidder disturbance is highest. Plot LGS1 was located near the edge of the gap but this does not seem to have caused a systematic difference with LGS2 at the centre of the gap. If there would be additional water extraction by the forest root system LGS1 would be drier, especially deeper in the profile, but this was not the case. The plot on the small gap however, was generally wetter than both plots on the large

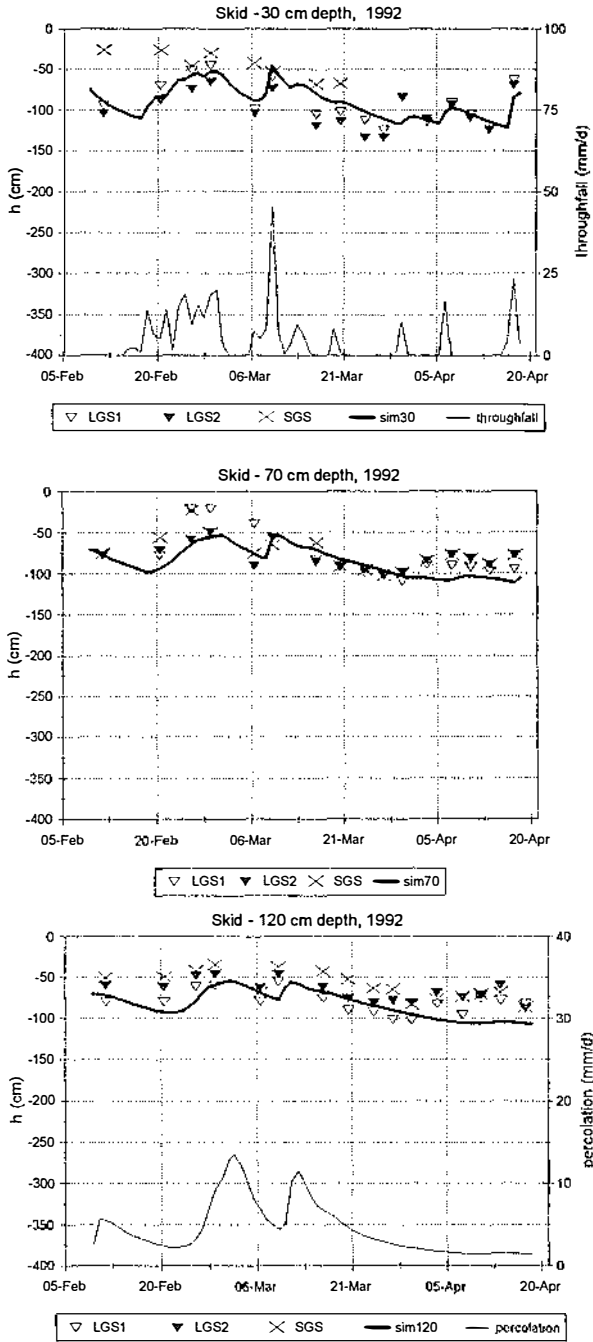


Figure 10.5 Skid trail: measured and simulated matric potentials at 3 depths (top to bottom) in the dry season of 1992 (this page) and the wet season of 1993 (next page).

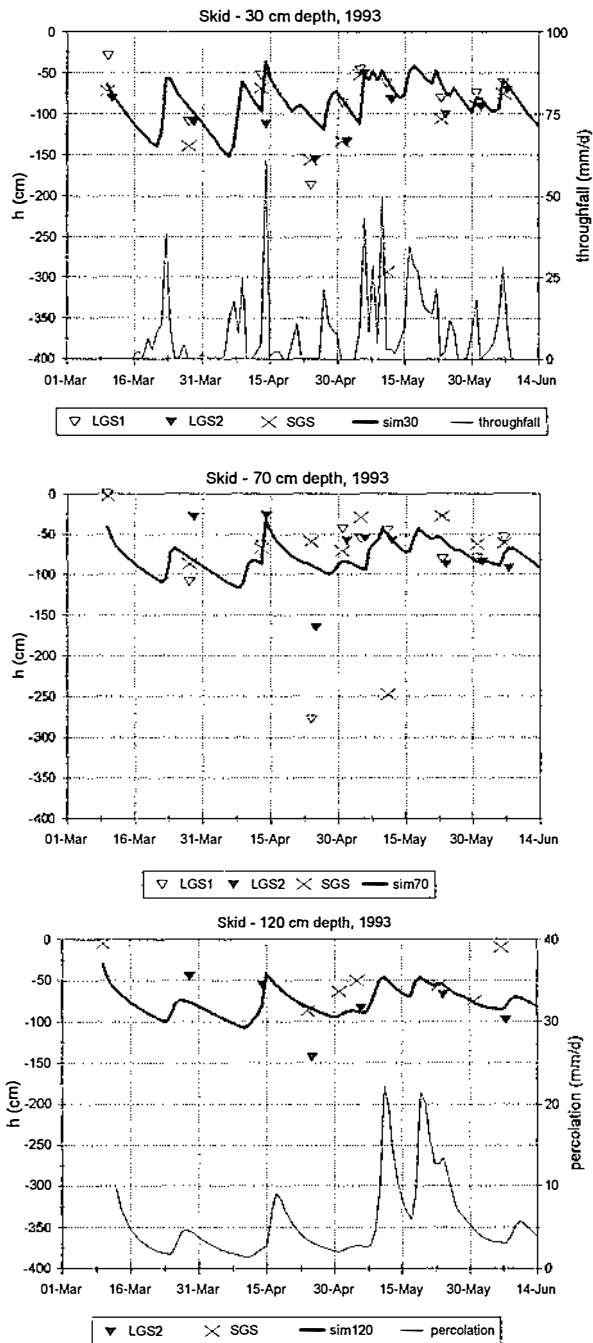


Figure 10.5 Continued.

gap, especially in the first half of the measurement period when it rained every day and the soils were wetter. This could be caused by a difference in microclimate between the gaps, if the air humidity is generally higher and temperature lower. However, variability in soil properties will be of influence too.

The simulations with SOAP gave good results at all depths. A change in radiation regime to simulate differences between the large and small gap gave a small difference in cumulative fluxes but hardly any change in matric potential. Therefore only the large gap simulations are shown in figure 10.5. Near the surface the matric potential can fall below -125 cm but at 70 and 120 cm depth it remains above -100 cm. Thus even during several weeks without rain there was a small but steady percolation. The cumulative percolation is 316 mm which is 91% of the rainfall (347 mm), whereas the soil evaporation is 46 mm or 13% of the rainfall. This leaves the soil at a moisture deficit of 4%.

Measurements at start of the wet season of 1993 give a similar picture (figure 10.5, graphs right hand side). Soil hydraulic potential remained above -125 cm during the whole period. Sharp fluctuation can be seen at all depths. At 30 cm depth the concurrence between the plots is large, indicating that extraction of water by seedlings did not cause much variation. Thus the bulk of the root system is probably above 20 cm. Deeper in the profile the variation between the plots seems much larger, with the SGS generally wetter than LGS1 and LGS2. However the saturated conditions measured at 120 cm depth could be caused by malfunctioning of the system. Cumulative values are 484 mm percolation which amounts to 64% of the rainfall (762 mm), and 281 mm total evapotranspiration which is 37% of the rainfall, leaving a soil water shortage of 1% since the start of the measurement period. Thus a even a sparse seedling cover greatly reduces the percolation and increases evapotranspiration.

From field observations it appeared that seedlings were well established on the skid trails after one year. Apparently the compaction and topsoil disturbance did not restrict establishment and growth. This may be a result from an increase in the water holding capacity (see chapter 9).

10.3.2 Crown zone

All 3 crown zone plots are near the edge of the gaps. This can be clearly seen from the potentials registered in plots LGC1 and SGC which decrease considerably towards the end of the first measurement period (figure 10.6, graphs left hand side). The course of the hydraulic potential resembles that of undisturbed forest (chapter 8). Plot LGC2 is located about 10 m from the edge of the gap and no influence of the surrounding forest can be detected. Using the results of the simulation by SOAP, the cumulative evaporation and percolation of this plot were respectively 25% (86 mm) and 80% (277 mm) leaving a soil moisture shortage of 5% compared to the start of the measurements. These values are quite different from those estimated for the skid trail, which is a result of the compaction of the latter. The decrease in hydraulic conductivity caused by compaction reduces the flow of water towards the soil surface and thus reduces the evaporation flux.

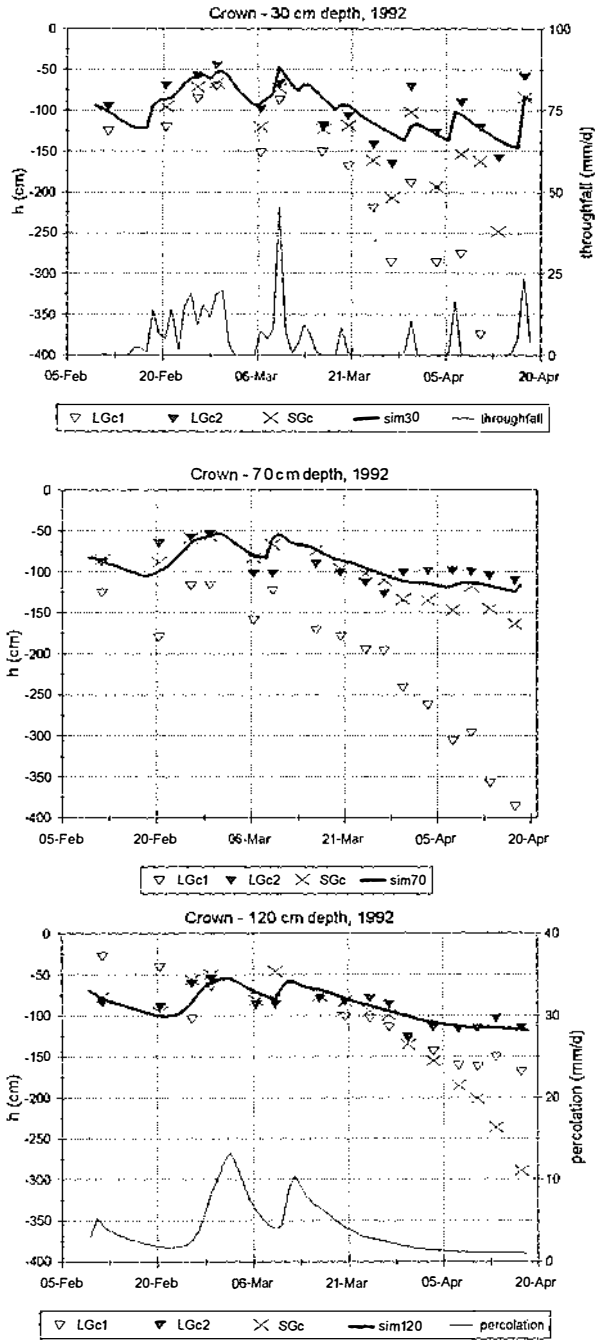


Figure 10.6 Crown zone: measured and simulated matric potentials at 3 depths (top to bottom) in the dry season of 1992 (this page) and the wet season of 1993 (next page).

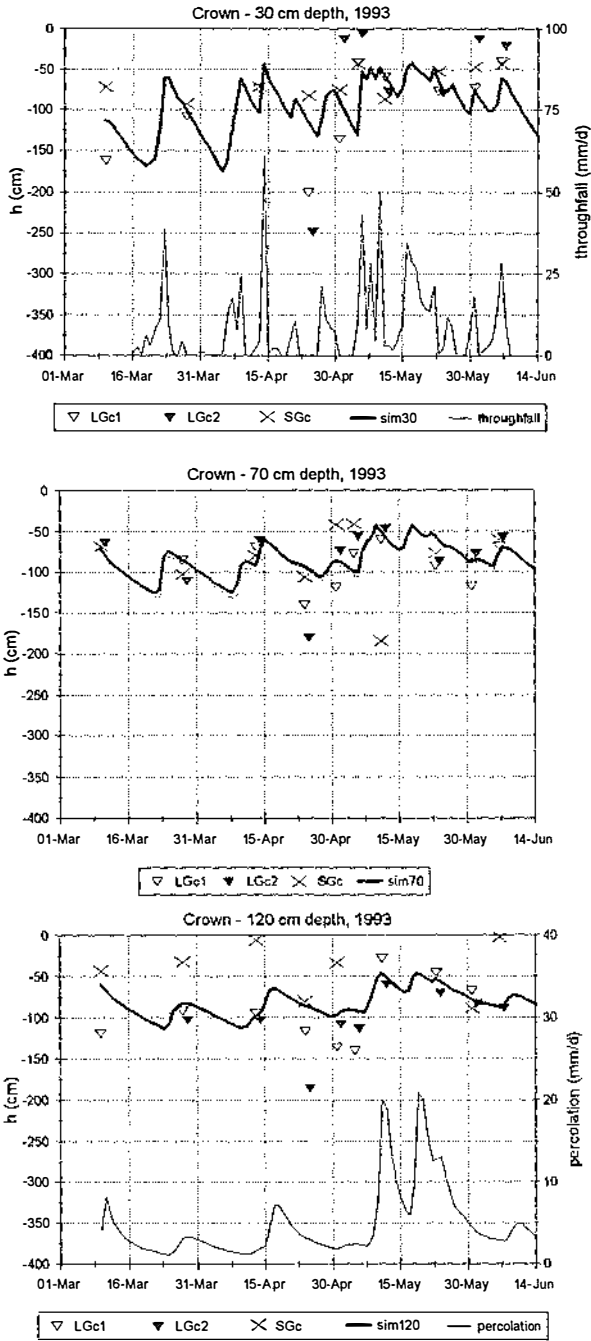


Figure 10.6 Continued.

Theoretically a large loss of nutrients from the soil and litter is expected in the crown zone because of the accumulated organic matter. Thus the amount of percolation is very important. Unless the gap is very large, the crown zone will usually be at the edge. This means that, fortunately, the influence of the surrounding forest in terms of evapotranspiration is high and percolation is low.

In the wet season of 1993 the soil moisture status was similar to that of the dry season with potential fluctuations around -100 cm, although the fluctuations were much larger than in the dry season (see figure 10.6, graphs right hand side). Generally, the soil in the crown zone of the small gap was wetter than in the large gap. The soil reaches near saturation on several occasions. There are no clear differences between potentials at 30 cm, 70 cm and 120 cm depth, indicating that probably the bulk of the roots are present above 30 cm. Simulations with SOAP, using a seedling cover with a LAI of $1.2 \text{ m}^2.\text{m}^{-2}$ and roots to a depth of 35 cm, follow the trend in measurements but do not capture the fluctuations of all the plots. Again concurrence with LGC2 was best, although unfortunately there were no measurements at 30 cm for the first half of the period. SOAP estimates a cumulative evapotranspiration of 315 mm (41% of a rainfall of 762 mm), which is much larger than in the dry season, whereas the percolation has reduced to 453 mm (60% of the rainfall). Thus it seems that a relatively low and thin plant cover greatly reduces percolation in the crown zone.

The large variation in potentials and difference between the crown zone plots, could also be related to the thickness of the litter layer. At some places a very thick layer of logging debris was left, which decreased only slowly. This means that considerable interception may take place. Moreover, the seedling cover was erratic because the establishment and growth was hampered by the thick layer of debris.

10.3.3 Undisturbed zone

Apart from seedlings, small trees are present in the undisturbed zone. At the small gap plot SGU was located close to a tree of 9 cm dbh, at the large gap plot LGU was located about 1 m from a tree with 17 cm dbh. These trees have some influence on the hydraulic potentials, as all SG measurements showed lower potentials than was simulated (see figure 10.7 graphs left hand side). Both plots were placed far enough from the edge of the gap so that the root system of the surrounding forest did not have much influence. Because LGU is wetter at all depths throughout the measurement period, the large tree next to the plot could have been damaged or at least it showed no "normal" evapotranspiration.

Simulations with SOAP were done assuming the presence of a seedling cover immediately after logging, from the start of the measurements. The estimated potentials concur most with the SGU readings at 30 cm depth and with the LGU readings at 70 cm depth. At 120 cm depth any roots of significance are absent and both plots have more or less the same moisture content. SOAP estimated the evapotranspiration at 169 mm (49% of the rainfall) and the percolation at 176 mm (51% of the rainfall). These values are not so different in the wet season of 1993 (see figure 10.7, graphs right hand side). Also here fluctuations are larger than in

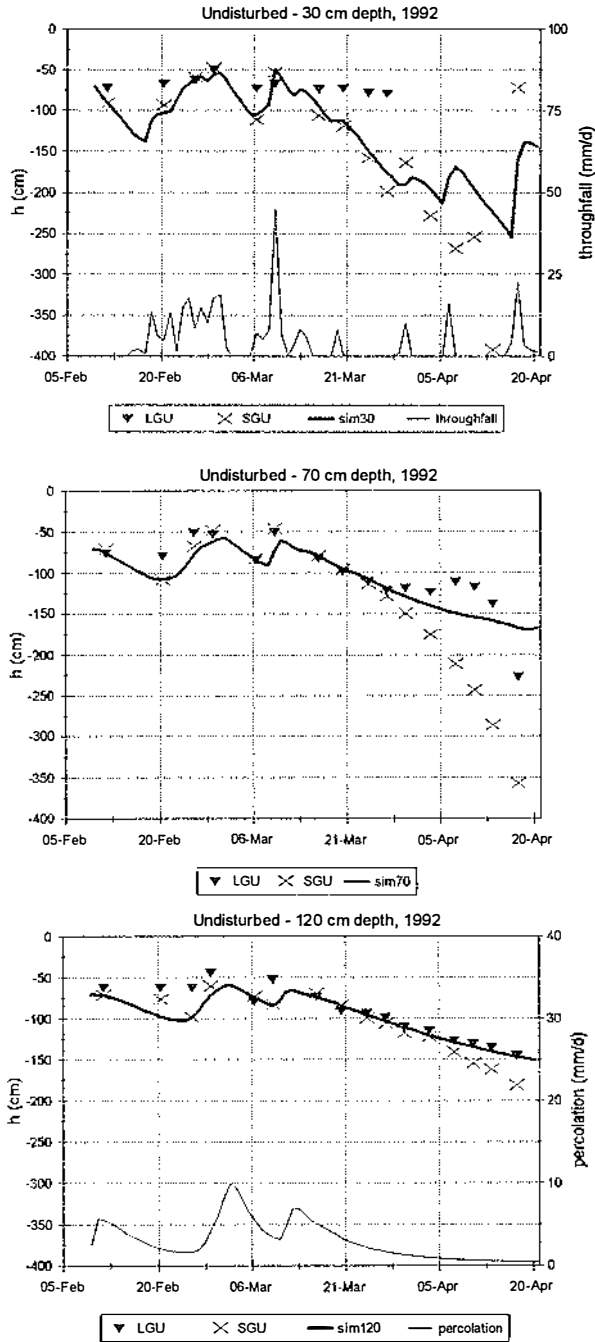


Figure 10.7 Undisturbed zone: measured and simulated matric potentials at 3 depths (top to bottom) in the dry season of 1992 (this page) and the wet season of 1993 (next page).

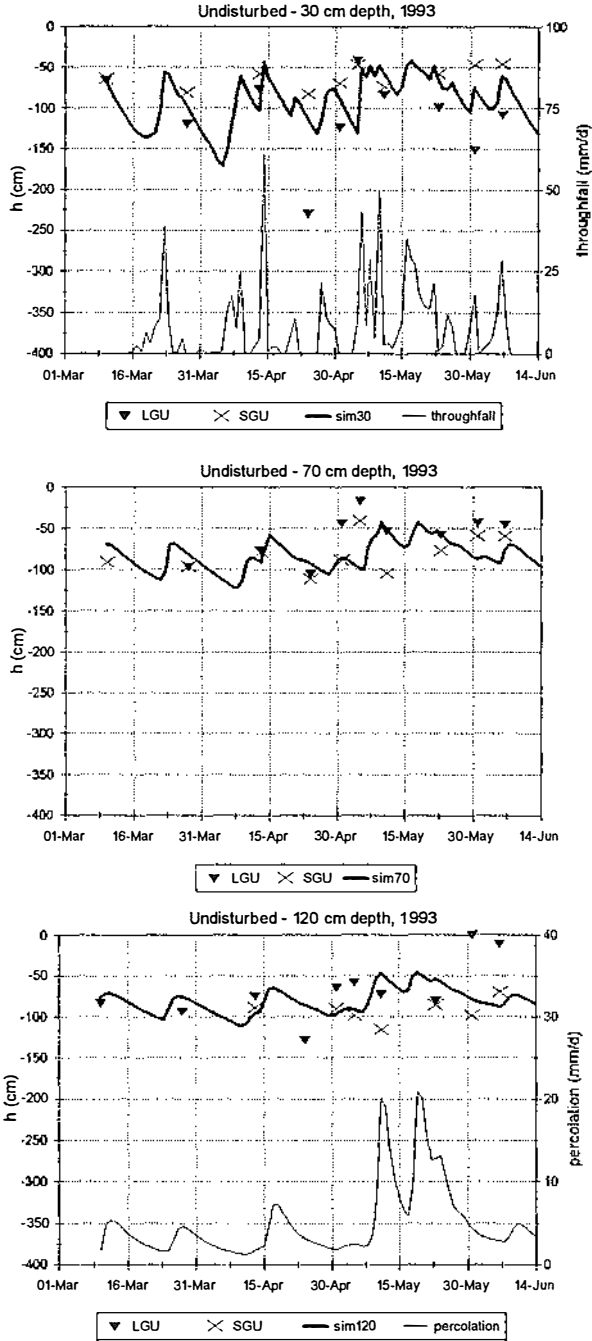


Figure 10.7 Continued.

the dry season of 1992 but the soil remains above field capacity throughout the period. Total evapotranspiration is estimated at 312 mm (46% of the rainfall) and percolation at 456 mm (54% of the rainfall) leaving a small moisture deficit.

10.3.4 Differences between gaps and zones

The measurements show that in general the topsoil in the small gap is wetter, probably due to reduced evapotranspiration levels caused by the difference in microclimate. However measurement of the microclimate was not sufficient to calibrate SOAP for both the large and the small gap and the estimated fluxes represent the average of the two.

The water balance of the skid trail, crown zone and undisturbed area differ more in the dry season of 1992 than during the wet season of 1993. This is caused by the increase in plant cover which brings the ratio of evapotranspiration and percolation closer to that of forest. On the other hand there is also the seasonal variation of rainfall to consider. To distinguish between the two effects, the second measurement period was simulated without plant cover. These estimations, as well as the results described above and the percentages found under forest (see chapter 8) are summarized in table 10.1. The gap average was calculated by assuming that each zone accounts for 1/3 of the gap area. If the surface remained unchanged after logging (i.e. bare for skid trail and crown zone and with some plant cover in the undisturbed zone), the percolation in 1993 would be even higher than during the dry period in 1992. Thus it seems that even a relatively open and low plant cover brings the evapotranspiration and percolation to a level close to that of the undisturbed forest.

Table 10.1 Partitioning of rainfall on the large gap and in the adjacent forest in 2 seasons. Simulation of the 1993 gap data with restoring plant cover or without plants.

	1992		1993 (plants)		1993 (no plants)	
	ET	Per	ET	Per	ET	Per
Skid trail	13	91	37	64	9	92
Crown zone	25	80	41	60	17	83
Undisturbed	49	51	46	54	41	60
Gap (average)	29	74	41	59	22	78
Forest	60	44	50	57		

However, it should be emphasized that these are model simulations, based on a number of assumptions especially where transpiration is concerned. For instance it is implied that all seedlings on the gap are "gap specialists" and well adapted to the light conditions, and that they have a symmetrical above and below ground structure. Also the aerodynamic and stomatal resistance to transpiration are assumed to be identical to that of the climax forest.

10.4 Annual fluctuations in the water balance for gaps in three environments

The period used to simulate the annual water balance is much wetter than that before the logging of the experimental catchment took place (see chapter 8). Especially the second half of January and March are wetter in 1993 than in 1992, and the total rainfall was 2734 mm.

The number of combinations of soil properties is very large if the three zones in the gap as well as the variance in soil properties of both compacted and undisturbed soils are taken into account. To restrict the number of model simulations the following assumptions were made:

- undisturbed zones are disregarded and the gap is assumed bare after logging, with compacted and non-compacted areas (i.e. skid trails and crown zones only);
- the skid trail variance in soil properties is used for the topsoil only, below that soil properties are assumed to have the average value used in chapter 8;
- skid trails account for 1/3 of the gap water balance and the average values discussed below are calculated accordingly;
- the gaps are large and the influence of the surrounding forest negligible;

Thus for each gap 6 simulations were done: a compacted and non-compacted zone, both with average soil property values, and with the values of the mean plus and minus one standard deviation.

The cumulative fluxes and percentages relative to the rainfall for all combinations are given in tables 10.2 to 10.4. The daily fluxes between the combinations differed very little and only ARO-avg, which represents the average situation, is shown in figure 10.8. The variability in soil properties was more evident in the fluctuation in matric potential. The daily values for 1200 h on 10 cm and 100 cm depth are shown in figure 10.9 for all three soil types.

All cumulative fluxes have changed considerably compared to undisturbed forest. At the soil surface the runoff on FRh has increased to 18% and 15% of the rainfall for skid trail and crown zone respectively (the latter is not shown in table 10.4). Pondered conditions occur on the least permeable ARA skid trails, and all skid trails on ARO and FRh that have average permeability or less. Crown zone ponding and runoff occurred in FRh. In other words the decrease in surface hydraulic conductivity may produce surface runoff (especially in sloping terrain) on all severely compacted soil types, even on ARA.

In 365 days the LAI increased from 0 to 1.20 m².m⁻². Interception reaches only 74 mm or 2.7% of the rainfall. The uptake was also the same for all combinations, except where surface runoff occurred, and reached a value of 550 mm to 560 mm or 20% of the rainfall. Figure 10.8 shows that the daily uptake fluctuates between 0 and 3 mm. Soil evaporation varies more because it is related to the hydraulic conductivity of the top layer. Therefore the soil evaporation is lowest on the skid trails, especially of the Arenosols, because the hydraulic conductivity is only 1 to 10% of that of the non-compacted areas (see chapter 8). Not considering the soils

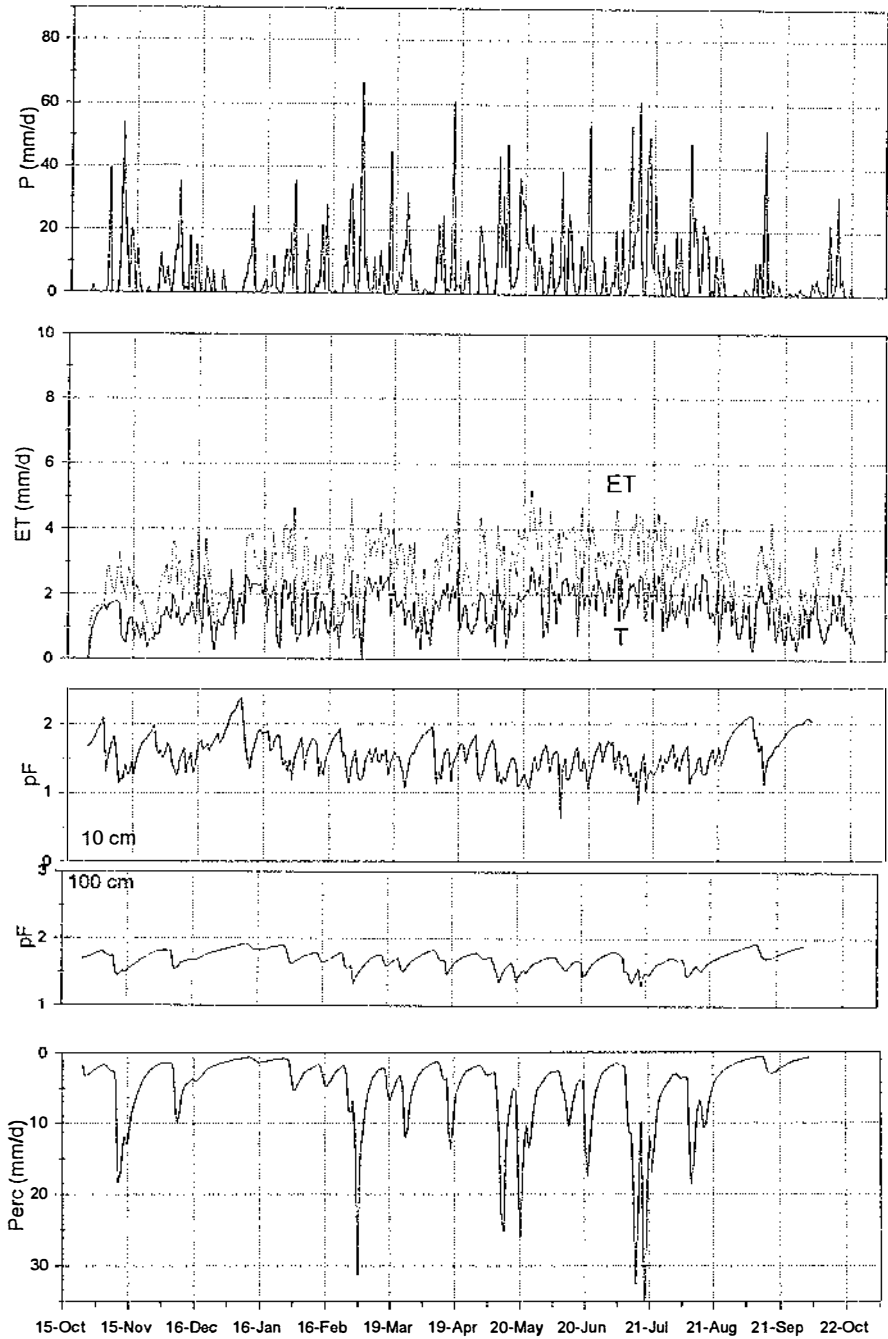


Figure 10.8 Annual variation in daily fluxes (in mm/day) on a gap on a Ferralic Arenosol. P = rainfall, ET = evapotranspiration (dotted line, solid line is transpiration), pF = pF values at 10 cm and 100 cm depth, Per = percolation.

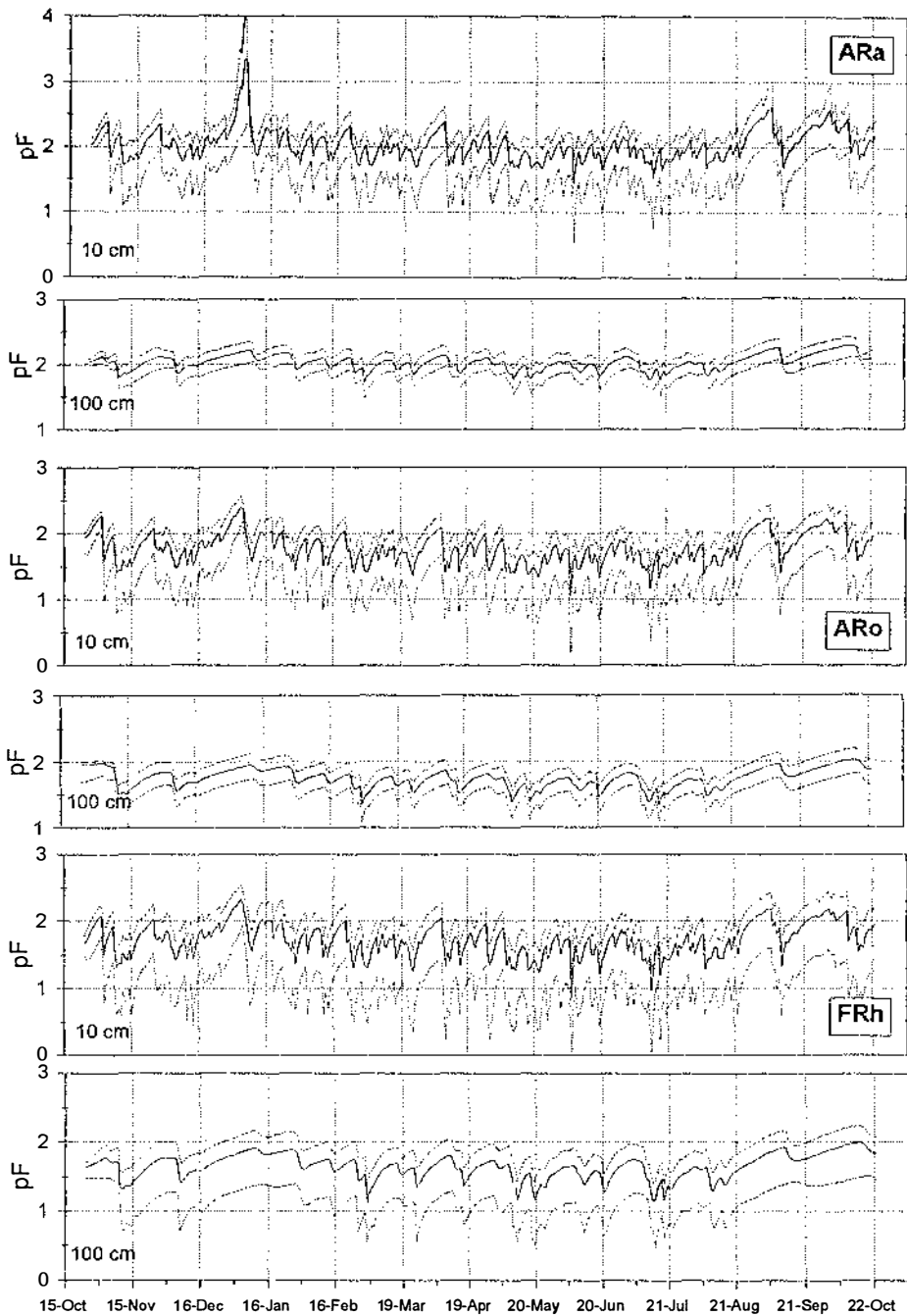


Figure 10.9 Daily values of matric potential at 1200 h for three soils at 10 cm depth and 100 cm depth). The solid line is the gap average (1/3 compacted, 2/3 uncompacted top soil), the upper and lower dotted lines are the minimum and maximum midday potentials.

Table 10.2 Cumulative values of fluxes on ARa in a gap, based on simulation of 365 days. Fluxes are in mm and percentages are relative to rainfall. P = rainfall, Ei = interception evaporation, Th = throughfall, Ro = runoff, I = infiltration, U = uptake, Es = soil evaporation, Per = percolation, Moist = change of soil moisture storage, ET = actual evapotranspiration (sum of Ei, U and Es), PET = potential evapotranspiration, TimePond = ponding time (min), havg = average yearly pressure head (cm), hwet is the average wet season pressure head, hdry = average dry season pressure head.

ARa	avg	max	min			
	<i>mm</i>			<i>%</i>		
P	2734.0	2734.0	2734.0	100.00	100.00	100.00
Ei	73.7	74.1	73.7	2.70	2.71	2.70
T	2660.3	2659.9	2660.3	97.30	97.29	97.30
Ro	0.0	0.0	0.0	0.00	0.00	0.00
I	2660.3	2659.9	2660.3	97.30	97.29	97.30
U	558.3	562.2	560.8	20.42	20.56	20.51
Es	426.0	333.2	459.3	15.58	12.19	16.80
Per	1700.7	1751.8	1646.3	62.21	64.08	60.22
Moist	-24.8	12.7	-6.1	-0.91	0.47	-0.22
ET	1058.0	969.5	1093.8	38.70	35.46	40.01
PET	1285.9	1289.1	1286.8	47.03	47.15	47.07
TimePond	0.0	161.5	0.0			
	<i>cm</i>			<i>pF</i>		
havg	-139.6	-270.9	-44.8	2.145	2.433	1.652
hwet	-99.2	-159.1	-30.0	1.997	2.202	1.477
hdry	-164.6	-339.8	-54.1	2.216	2.531	1.733

Table 10.3 Cumulative values of fluxes on ARo in a gap, based on simulation of 365 days, fluxes are in mm and percentages are relative to rainfall. The abbreviations are explained in table 10.2.

ARo	avg	max	min			
	<i>mm</i>			<i>%</i>		
P	2734.0	2734.0	2734.0	100.00	100.00	100.00
Ei	73.9	74.3	73.7	2.70	2.7	2.70
T	2660.1	2659.7	2660.3	97.30	97.3	97.30
Ro	0.0	0.5	0.0	0.00	0.0	0.00
I	2660.1	2659.2	2660.3	97.30	97.3	97.30
U	562.3	549.0	560.5	20.57	20.1	20.50
Es	418.0	312.6	475.1	15.29	11.4	17.38
Per	1679.3	1744.2	1641.8	61.42	63.8	60.05
Moist	0.5	53.3	-17.1	0.02	2.0	-0.62
ET	1054.2	936.0	1109.3	38.56	34.2	40.57
PET	1287.5	1289.3	1286.3	47.09	47.2	47.05
TimePond	15.2	608.1	0.0			
	<i>cm</i>			<i>pF</i>		
havg	-67.6	-109.8	-24.0	1.830	2.041	1.379
hwet	-49.3	-83.0	-15.4	1.693	1.919	1.187
hdry	-79.0	-126.5	-29.3	1.898	2.102	1.466

Table 10.4 Cumulative values of fluxes on FRh in a gap based on simulation of 365 days, fluxes are in mm and percentages are relative to rainfall. The abbreviations are explained in table 10.2.

ARo	<i>avg</i>	<i>max</i>	<i>min</i>			
	<i>mm</i>			<i>%</i>		
P	2734.0	2734.0	2734.0	100.00	100.00	100.00
Ei	73.9	74.6	75.1	2.70	2.7	2.75
T	2660.1	2659.4	2658.9	97.30	97.3	97.25
Ro	0.7	494.7	0.0	0.02	18.1	0.00
I	2659.4	2164.7	2658.9	97.27	79.2	97.25
U	562.2	488.8	560.9	20.56	17.9	20.52
Es	405.0	182.6	489.8	14.81	6.7	17.91
Per	1714.6	1480.5	1683.5	62.71	54.2	61.58
Moist	-22.3	12.8	-75.3	-0.82	0.5	-2.75
ET	1041.1	745.9	1125.8	38.08	27.3	41.18
PET	1287.6	1289.6	1286.8	47.09	47.2	47.07
TimePond	411.0	8717.6	26.4			
	<i>cm</i>			<i>pF</i>		
havg	-62.0	-109.2	-14.4	1.793	2.038	1.159
hwet	-45.3	-80.7	-9.6	1.656	1.907	0.981
hdry	-72.4	-126.9	-17.5	1.860	2.104	1.242

with surface runoff, the lowest soil evaporation is 312 mm (11.4%), while the highest is 475 mm (17.4%). The daily evaporation decreases to less than 0.5 mm/day if the soil potential drops below field capacity. The highest flux is about 2.5 mm/day. Thus the second graph in figure 10.8 shows that the total evapotranspiration varies between 1 and 5 mm/day.

The cumulative percolation varies between 1640 and 1770 mm (60 to 65%), except for if surface runoff takes place (such as on the Haplic Ferralsols) in which case the percolation is less: 1480 mm (54%). The skidtrails all have a higher percolation than the crown zones, because the evaporation is lower and more water is able to percolate despite the decrease in conductivity caused by compaction.

10.5 Comparing gap and forest

Converting forest to gap causes an increase in percolation of approximately 15% of the rainfall, assuming a linear growth rate of a seedling cover to an LAI of 1.2 m².m⁻² in one year (compare figures 8.7 and 10.10). Daily fluxes have the same rate as under forest with a maximum of 30 to 35 mm/day. However, the matric potential in the root zone remains above -100 cm almost permanently, resulting in percolation throughout the year, whereas under forest it is strongly reduced in the dry months.

The evapotranspiration decreased to about 40% of the rainfall of which half is soil evaporation. The maximum daily evapotranspiration has dropped from 9 to 5 mm/day, which is caused by the change in microclimate on conversion from gap to forest and by the soil moisture content. Low wind activity and less direct radiation

cause the potential evapotranspiration to decrease: under forest it is approximately 1400 mm per year while in the gap it is 1290 mm. Also the size of the soil evaporation flux depends on the hydraulic conductivity of the soil and therefore the evapotranspiration is much more determined by the soil moisture content on the gap than under forest.

Surface runoff almost tripled on the Haplic Ferralsols when the top soil was severely compacted, whereas in general ponding occurred on all the skid trail combinations (even the Albic Arenosols) except for the most permeable profiles.

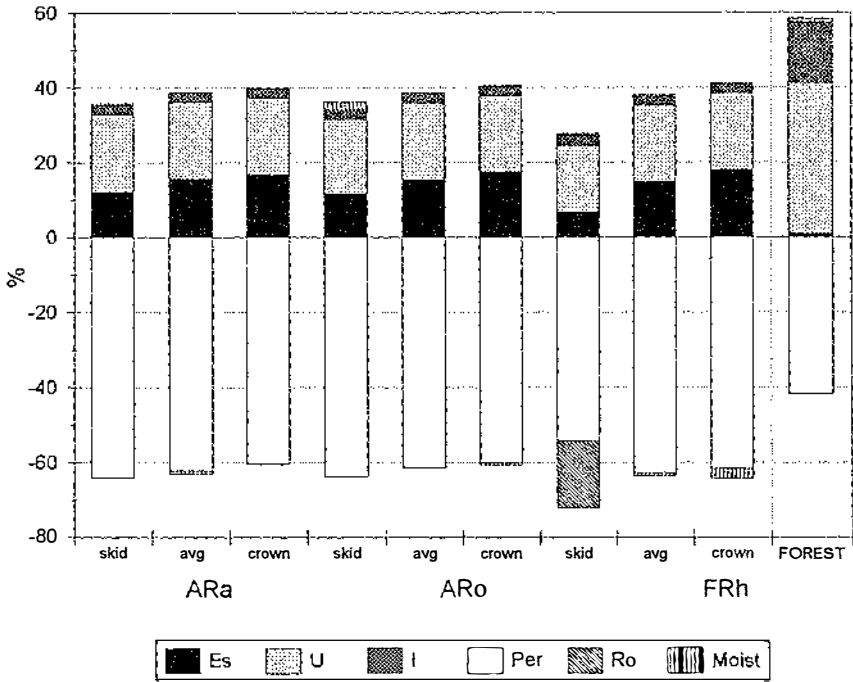


Figure 10.10 Summary of annual simulation in percentage of rainfall. Avg = average calculated from 1/3 compacted and 2/3 non-compacted topsoil, min = least permeable compacted topsoil (skid trail), max = most permeable undisturbed soil (crown zone). Es = soil evaporation, U = uptake, Ei = interception evaporation, Per = percolation, Ro = surface runoff and Moist = soil moisture change.

Given that the assumptions about LAI and root development are correct, 2 years on a gap on an Albic Arenosol have been simulated with SOAP (October 1991 to October 1993). The total LAI was 2.7 m².m⁻² at the end of that period. Figure 10.13 shows the development of relative cumulative fluxes (i.e. as percentage of the combined rainfall and soil moisture storage) of percolation, interception, soil evaporation and uptake. The last part of the graph shows the percentages of undisturbed forest with an LAI of 6.3. Because the soil evaporation flux is

determined by the hydraulic conductivity, and the beginning of the simulation period is the 1992 dry season, the graph shows a large variation. After a plant cover has developed the increase in transpiration stabilises the fluxes, and the gradually a level is obtained where the gap-ET is 76% of the forest ET and percolation is 130% of the forest value. Soil evaporation is still much higher and transpiration lower and therefore the ET on the gap will react more to the soil moisture status than under forest. Since the development of a plant cover may not be linearly proportional to time, it is not known how long it takes for the water balance to be restored, but the simulation indicates that a small plant cover already has a large stabilizing influence.

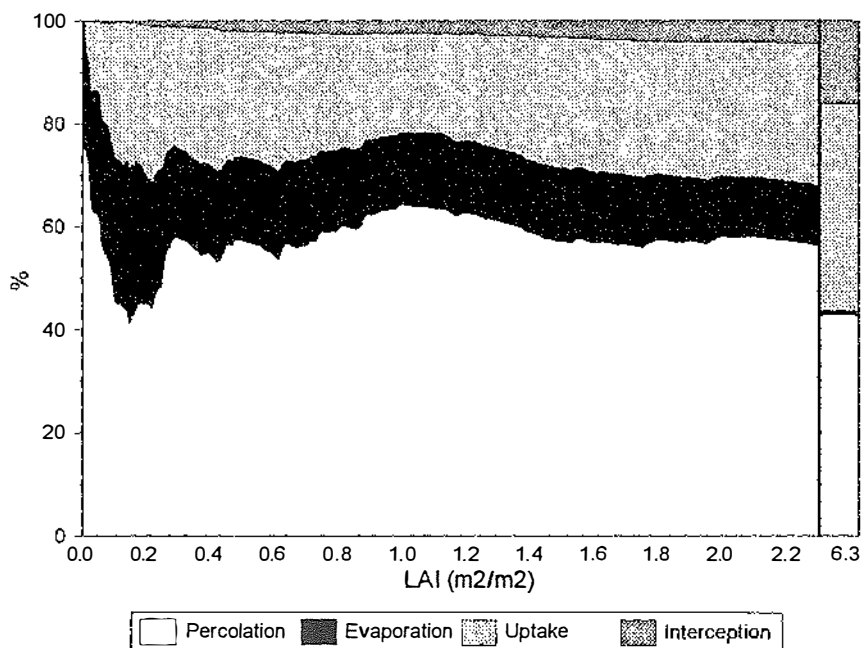


Figure 10.11 Simulation of fluxes as percentage of rainfall, related to a linear increase in LAI. The period covers 2 years, LAI = 0 in October 1991 and LAI = 2.3 in October 1993. Left end bar is undisturbed forest situation (LAI = 6.3).

These results are confirmed by a detailed study in the La Selva Reserve in Costa Rica, where Parker (1985) measured water and nutrient balance of a forested slope before and after logging. He created two gaps of 500 m² and 2500 m² on which rainfall, transpiration, soil evaporation and soil moisture content were assessed. Percentages of evapotranspiration (ET) and percolation (Per) were similar to those found in this study. After 404 days the ET reached a level of 70% of the forest value while Per was 1.5 times that of the forest. These levels were reached very quickly, between 65 and 100 days after felling. The LAI increased from 0 (35 days after logging) to 0.5 during that first period. This compares well with the

simulations in figure 10.13 where the percentages of ET and Per stabilise after a LAI of 0.4 to 0.6 has formed, although the LAI increased faster than was assumed here due to the growth of lianas. Parker also reported that the soil in the large gap stay much wetter than under forest, especially in the dry season immediately after logging. The soil in the small gap was drier than the large gap in both periods, but since it had an elongated shape (10 x 50 m) the influence of the forest was much higher. Because the gaps in this research were not so different in behaviour of soil moisture variation, it shows that the shape of the gap in relation to the size is very important.

10.6 Conclusions

Creation of a gap alters the water balance completely. Expressed in percentage of annual rainfall, percolation increases from an average of 43% under forest to 75% of the rainfall immediately after logging. A transpiration of 40% is replaced by soil evaporation of 25%, while the interception evaporation disappears completely. With an increase in LAI to only 0.4-0.6 $m^2.m^{-2}$ and a matching development in root structure, the evapotranspiration rapidly stabilizes at a level of 0.76 of the forest value. Still a large part consists of soil evaporation which makes the evapotranspiration much more susceptible to changes in soil moisture.

The difference in percolation between forest and gap is especially apparent during dry periods. While the forest dries out the soil in the gap is above field capacity for most of the year, and consequently percolation continues in the dry season under the gap while it stops under the forest. The magnitude of the fluxes however is the same: a maximum of 30 to 35 mm/day is estimated for all soil types.

Runoff increases on the least permeable Ferralsols with 100 to 200% if the soil is compacted. For the other compacted soils some runoff is predicted by the water balance model. However, the surface storage was assumed to be large and ponding occurred on all but the most permeable soils. Thus if the gaps are created on slopes runoff may be produced by all soils including the Arenosols.

It is important to realise that these results represent the centre of the gap. The gap however shows a large spatial variation in water dynamics related to several factors:

- the variability of soil properties caused by compaction during logging,
- the influence of the surrounding forest (related to gap shape and size),
- the amount of debris left in certain areas causing possible interception, and
- the development and abundance of seedlings, which can show a large spatial variability (e.g. seedlings were more abundant on the skid trails than in the crown zone where the thick litter layer seems to hamper growth).

11 THE IMPACT OF LOW INTENSITY LOGGING ON THE WATER BALANCE OF A SMALL CATCHMENT

11.1 Introduction

In previous chapters it was shown that the impact of logging on the water balance is very large at the location where the logging takes place. The size of the disturbed area depends of course on the logging intensity and the method of clearing. In a partially logged catchment both disturbed and undisturbed areas are present, which interact in a complex way in terms of microclimate and lateral movement of water both on the surface and in the soil. The affect of logging on the microclimate in a spatial sense is beyond the scope of this study. In fact it is hardly researched at all, most studies involve only isolated gaps and use a one dimensional approach. Nevertheless the question when the logged forest stops to behave like a forest in a climatological sense is highly relevant although extremely difficult to answer. Macro-climatological modelling, for instance of conversion of parts of the Amazon basin from forest to rangeland, indicate a considerable decrease in rainfall (Bruijnzeel, 1990). Such scenarios can hardly be validated but are supported by the fact that about half of the rainfall is generated by transpiration from the forest itself (Heuveldop and Jordan, 1981).

Catchment scale research of the water balance therefore concentrates usually on what happens on the surface, with the discharge taken as a representative parameter to describe changes in the catchment water balance. This assumption is valid only if the other components are calculated as well. However, catchment leakage is often not assessed while changes in soil and groundwater storage are assumed to be negligible over a given period of time. Bruijnzeel (1990) shows that these assumptions frequently lead to widely varying estimations of evapotranspiration. Thus it is imperative that the processes that occur inside the catchment are quantified as much as possible. Examples of studies in undisturbed tropical rainforest first or second order catchments (see also table 11.4) are Lesack (1993) in Brazil, Heuveldop and Jordan (1981) in Venezuela, Bruijnzeel (1983) in Indonesia, Bonell et al. (1981, 1982) in Australia, Leopoldo et al. (1982) in Brazil and Poels (1987) in Surinam. Paired catchment studies involving partial or complete logging are documented by Fritsch (1990) in French Guyana, Malmer (1993) in Malaysia, Gilmour (1977, in Bruijnzeel, 1990) in Australia and Abdul Rehem (1989, in Bruijnzeel, 1990) in Malaysia. These studies used the paired catchment technique to separate changes resulting from disturbance, to annual climatological fluctuations. Originally, this study was intended as a paired catchment study as well, but problems with data collection in the reference catchment could not be overcome and the dataset proved too erratic to be used.

However, the lack of a second reference catchment may not be a problem, or to put it differently, a second catchment may not be helpful in the assessment of the impact of the disturbance. The paired catchment approach is a black box technique based on correlation between catchments. It is done to distinguish between temporal climatological fluctuations and the impact of disturbance on the water balance. When the discharges between the two catchments are correlated, the explained variance is

usually in the order of 89-97% (Malmer, 1993; Fritsch, 1990), changes in the water balance have to be in the order of 10% or more, otherwise this research method would give no extra certainty. Most studies mentioned above concentrate on large disturbances, varying from heavy timber extraction to clear felling, with conversion to plantations or agricultural types of land use. In that case, catchment water yield usually increases by several 100% in the first year (see section 11.4) while it may take about 5 to 8 years for the discharge to return to its original level. The paired catchment technique is well suited to investigate this type of disturbance.

However, Bruijnzeel (1990) concludes from a literature review that "carefully executed light selective harvesting will have little (if any) affect on the streamflow, whilst the effect increases with the amount of timber removed". He mentions two studies that involve low intensity logging (selective logging in Babinda, Queensland studied by Gilmour, 1977; and 20% thinning in Rajpur, India, studied by Subba Rao et al. 1985). Both catchments had no significant changes in water yield after logging. Thus, it seems that correlation with a second catchment does not increase the accuracy of the results, or the certainty of the conclusions. Working with a single catchment should not be a serious shortcoming in this research.

In this chapter, the impact of low intensity timber extraction on the water balance of a small catchment is described. In accordance with the Tropenbos goal to search for sustainable levels of forest use, the aim was to define a boundary level of extraction at which the changes on the water balance are acceptable.

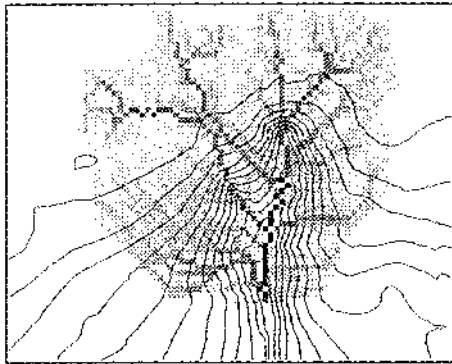
11.2 Methodology

11.2.1 The experimental catchment, topography and soils

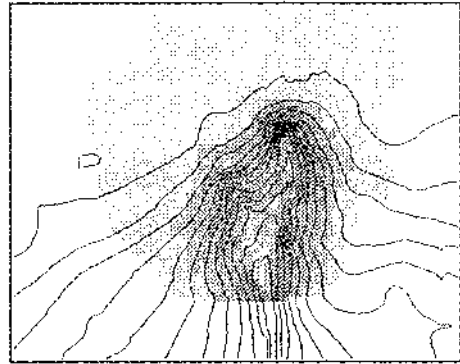
A first order catchment was located south of the weather station. At the outlet a concrete dam was constructed (see below and figure 11.2). The distance between the outlet and the weather station, where the rainfall was measured, is approximately 2.5 km in a straight line. Adjacent to the stream and higher on the slopes, 24 piezometers were placed (see below). A topographical map at a scale relevant to the research was not available. Therefore the height of the stream bed and the piezometers were measured relative to the concrete dam, with a Wilt level. In addition the surface was measured along a number of lines perpendicular to the creek. The remaining area was measured relative to these lines using a simple clinometer. After conversion to X,Y,Z coordinates the 600 data points were interpolated using Block Kriging to a digital elevation model (DEM) with 5x5 metre grid cells. Note that in all maps displayed in this chapter the top of the map is the south of the catchment (the weir is located at the north end). In the description and discussion of the results below the compass directions are used.

From the DEM a drainage network and the catchment size were calculated. To achieve this the module WATERSHED from the PCRASTER geographical information system (Wesseling et al., 1993) was used. Based on slope gradient and aspect, this program searches all the grid cells that drain towards a given outlet and

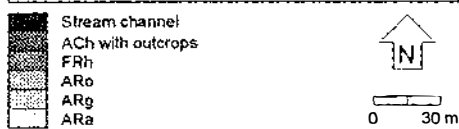
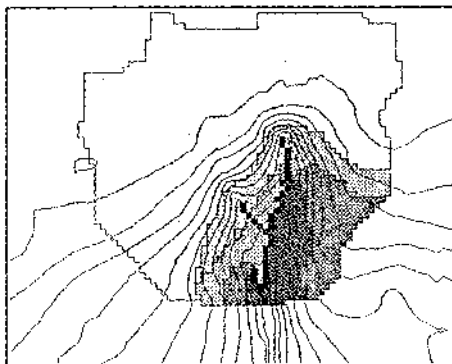
Upstream elements (ha)



Slopes (%)



Soil types



Skid trails

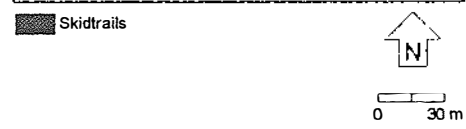
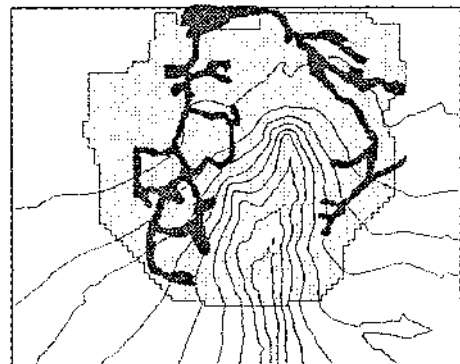


Figure 11.1 Derivatives of the digital elevation model of the experimental catchment and the main soil types (note that north is downward): a) Upstream Elements, b) Slope map (%), c) Soil types, and d) Skid trails.

gives each grid cell a value that represents the number of cells upstream of that cell (so called upstream elements). The upstream element map and the slope map are shown in figure 11.1a and 11.1b. The exact size of the catchment was difficult to determine because of the poorly defined watershed in the east and particularly in the south. The elevation with clinometer and level were continued over the top of the catchment until the elevation decreased again with 50 cm. However this is in the same order as the large scale surface roughness and the watershed is therefore somewhat arbitrary. WATERSHED found 2427 cells draining toward the weir, resulting in a catchment size of approximately 6.18 ha.

The experimental catchment included the most important sandy and loamy soil types of the research area. Its form is typical for the area. In general the water divides of the White Sand Plateau are flat and have an altitude of approximately 150 m. Because the soils are so permeable there is little surface runoff and erosion (see chapter 7). In chapter 2 a brief explanation of the genesis of the landscape is given. The valleys usually have steep slopes with wide valley floors. The steep slopes are caused by headward erosion from the sources of the creeks (see chapter 2).

The groundwater body in the catchment is located on top of a virtually impermeable kaolinite clay layer. From field observations it seems that large parts of the White Sands in the area are underlain by this kaolinitic layer, probably formed by clay illuvation on top of the bedrock and weathering of the dolerite. The extent of the layer is not known but its presence seems more rule than exception. In general the gradient along the channels of the creeks is small but nevertheless they all start with a steep, deeply incised gully head. The valley floor is flat and almost all first order catchments start as swamps with accumulation of organic matter in the top soil. The organic acids in the water cause the water to have a dark red-brown colour. This description fits this catchment which has a typical geomorphology, with the exception that the creek has cut through the clay layer into the bedrock. Dolerite outcrops occur in the larger part of the stream channel which is well defined and therefore the discharge is relatively easy to measure compared to a swamp. Because the creek has cut through the kaolinite layer, it emerges somewhat higher on the slope and a very small swamp occurs only at the top of the catchment.

A soil map was made based on 71' augerings to 120 cm depth, 12 deep augerings and two soil pits (see figure 11.1 c). Roughly 3/4 of the area consist of Albic Arenosols, with the southern part taken up by Haplic Ferralsol. In between lies a narrow band of Ferralic Arenosols. The soil types have a typical appearance and the description given in chapter 2 is appropriate. The hydrological properties of the soil types are described in chapters 5 and 9. However, the classification is based on the upper 120 cm of the soil only. Below that sharp changes in material and texture were observed at several locations. In particular near the outlet of the catchment (soil type ACh) both heavy clay and weathered bedrock layers were encountered while placing the deep piezometers, with colours changing from bright orange yellow to reddish purple. The ARa was relatively homogeneous usually with a change from medium to coarse sand below 300 cm depth. While placing the piezometers it appeared the contact zone with the bedrock on the west side and the kaolinite on the east side is very sharp.

11.2.2 Hydrological measurements

A concrete dam with a sharp crested V-notch weir cut from a zinc plate was constructed in 1991 (see figure 11.1 d). Measurements of the water level started 8 August 1991 and continued until 12 December 1993. The water level was measured with a DRUCK 830 pressure sensor connected to a Campbell CR10 datalogger. The pressure sensor was placed in a perforated PVC pipe which functioned as a stilling well. A measuring rod enabled hand readings of the level. The V-notch weir was calibrated by closing it and allowing the water level to rise, after which the discharge was measured with buckets. A $Q(h)$ relation was defined by log-log interpolation. The maximum thickness of the water jet through the weir that could be calibrated was about 15 cm. However, some rainstorms produced higher levels and the discharge was calculated by extrapolation of the $Q(h)$ function. The accuracy of the whole system is probably in the order of ± 5 mm. On various occasions the system was damaged and the weir had to be renewed and recalibrated (see below).

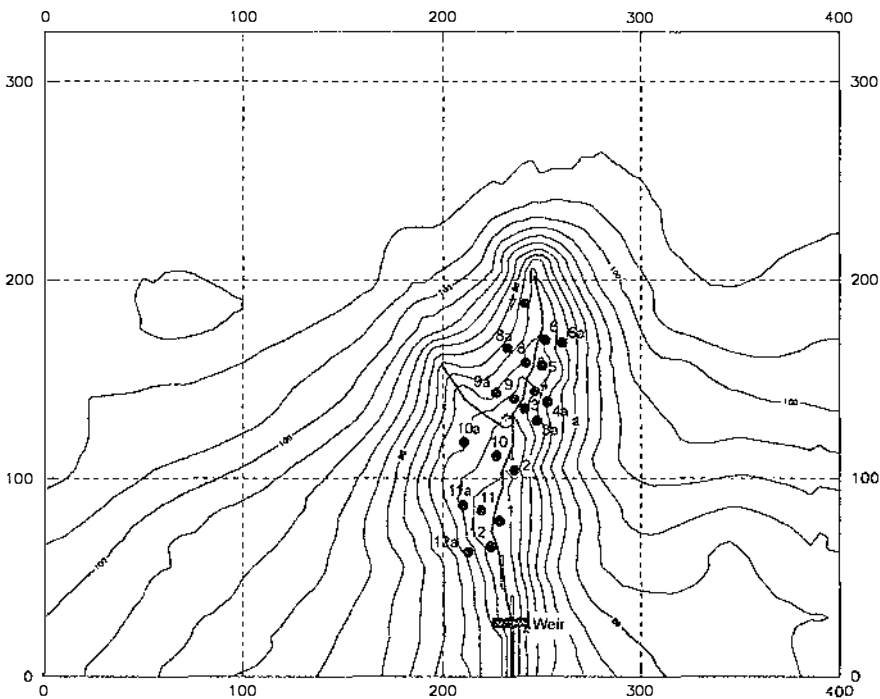


Figure 11.2 Topographic map with the locations of the weir and piezometers.

There are several techniques to separate the baseflow (Q_b) from stormflow runoff (Q_p) in the hydrograph of a storm (Dunne and Leopold, 1972). Lesack (1993) in a

study of the water balance of a first order catchment in the Amazon, obtained good results with a simple linear separation technique, which has the advantage that a computer program could be written to do the separation automatically. The results could then be verified graphically. The technique assumes that from the start of the rainstorm the baseflow rises gradually until the overland flow and channel precipitation stop. The increase in baseflow with time (dQ_b/dt) is represented by the slope of the separation line. This was determined by analysis of a number of well documented hydrographs. Following the method of Lesack (1993), the log-transformed discharge of each hydrograph was plotted against time and a line was drawn from the start of the storm to the inflection point, that marks where recession curve starts to decline with approximate linearity. A slope of $dQ_b/dt = 0.0018$ litres. s^{-1} .min $^{-1}$ seemed to provide a reasonable separation. The slope is also used as the threshold value that marks the start of the storm.

Apart from the weir, 22 piezometers of 1.5" PVC tubes were installed on both sides of the creek (see figure 11.2). Because of the steepness of the slopes the lateral distance between the lower and the higher piezometers was only between 10 and 30 m although most of the latter were 4 to 6 m deep. Groundwater depth was measured with intervals of 1 to 2 weeks, the piezometers adjacent to the creek from 22 August 1991 to 10 July 1993, while the piezometers higher up the slope were installed later and measurements began in April 1992. Conductivity measurements with the reversed auger hole method were done by the Hydrometeorological Department of Guyana but unfortunately the results are not available yet.

11.2.3 The logging experiment

The experiment was set up to assess low intensity logging. In the policy charter of Demerara Timbers Ltd. low intensity logging was defined as an average extraction of 20m³ of timber volume per hectare, including inaccessible areas. Thus in some areas the extraction may be higher. This volume was used as a guideline in this experiment. The logging took place within a week and the period after logging was assumed to start at day 290. In total 70 trees were felled with a total stem volume of 129.6 m³. With a catchment size of 6.18 ha the logging intensity is estimated at 21 m³/ha. In term of the area available to logging, the operations are confined to the flat watershed area with a size of 4.75 ha (see section 11.3.4), which leads to a intensity of 27 m³/ha.

As most of the area is covered with Dry Evergreen forest, 67 of the logs belonged to Wallaba species (*Eperua falcata* and *Eperua grandiflora*) and 3 logs to Greenheart (*Chlorocardium rodiei*). Because the trees that were marked for felling were evenly distributed over the catchment, and the basal area in Dry Evergreen Forest is lower than in most other forest types (Ter Steege, 1993), the number of skid trails and gaps is quite large (figure 11.2). Most trees on top of a steep slope fell downward headfirst so that the log could be removed easily with the skidder after the crown was cut. On the north east boundary however, the slope was too steep for the skidder and the Greenhearts were removed with a winch. Although the spot where the winch was anchored was severely damaged, the extraction method was by far the least disturbing in terms of soil compaction and damage to forest.

11.3 Results

11.3.1 Discharge

The dataset was divided into a period before and a period after logging. In the period before logging the datalogger operated 240 out of 432 days. In August 1992 the weir was damaged by a falling tree. After logging the datalogger functioned for 260 out of 410 days. The equipment was stolen at the end of June 1993 and replaced in the beginning of August 1993. So in both periods there was a gap in the data of the wet season and the dataset as a whole is very erratic. However, hand level readings were continued throughout the period as frequently as possible. These readings represent mostly baseflow levels and were used to supplement the automatic recordings. A relation between rainfall and stormflow runoff provided an estimation of the peakflow during those periods.

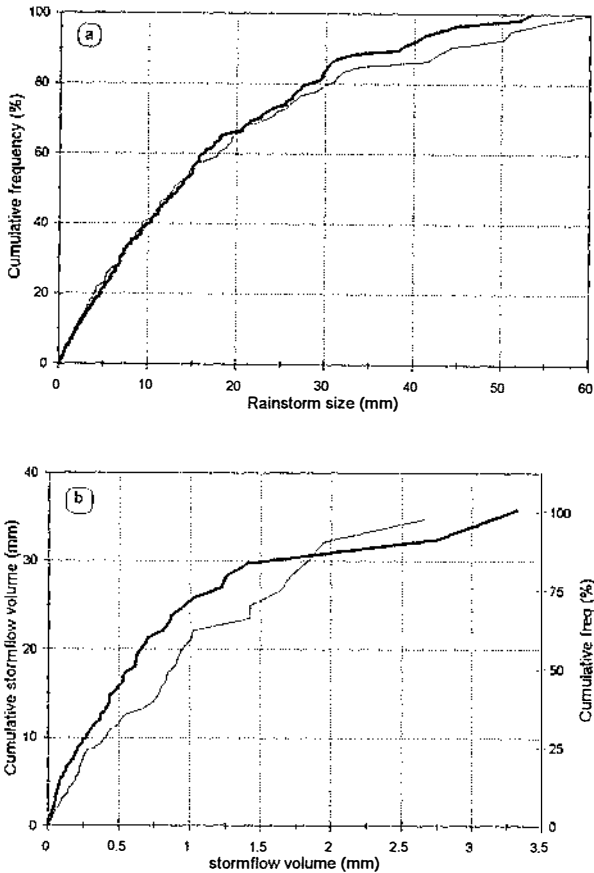


Figure 11.3 Cumulative frequency of a) rainstorm volumes (P in mm) relative to the total amount of rainfall, b) stormflow volumes (Q_p in mm) relative to the total amount of stormflow.

Based on the linear hydrograph separation method, 274 peakflow events were recorded before logging, and 156 events after logging. They were converted from m^3 to mm using the catchment size of 61800 m^2 . Figures 11.3 a and b show the frequency curves of the rainstorms and peakflow events. Comparing the X-axis scales, the stormflow volumes are about 6% of the rainstorm volumes. At half the maximum size recorded (1.75 mm), about 80% of the total stormflow volume is covered. This is also the case for the rainstorm frequency. The shape of the first part of both curves is roughly the same, indicating that there is a similar runoff mechanism for rainstorms with a size between 0 and 30 mm. Analysis of the peakflow size shows that 95% of the peaks are less than 0.5 mm in size. Yet they account for 40% of the stormflow volume only, which indicates the relative importance of the large storms. There is a small difference in the division of peakflow events before and after logging. The cumulative frequency of the rainstorm size is virtually the same before and after logging (figure 11.3 a). Nevertheless, there were more small peakflow events before than after logging, as the beginning of the frequency curve is steeper (figure 11.3 b). Thus it seems that an identical rainfall distribution produced larger peakflow events.

In order to supplement the dataset for the intervals when only baseflow hand readings were available, the automatic recordings were used to determine a relation between the size of a rainstorm and the corresponding volume of stormflow runoff, both before and after logging. Selecting all runoff events with an adequately recorded rainstorm, 90 events before logging gave the following relation:

$$\log(Q_s) = 0.8820 * \log(P) - 1.7200 \quad n=90, r^2 = 0.7112 \quad (11.1)$$

in which Q_p is peakflow (in mm) and P is the size of the rainstorm (in mm). Because of the distance between the weather station and the weir the data points have some scattering (see figure 11.4 a). Nevertheless the complete range of rainstorm and peakflow size is covered, up to the maxima of respectively 60 mm and 3.45 mm (or 213.5 m^3). The fraction of runoff is 1.64%, calculated from the mean of the $\log(P)$ and $\log(Q_p)$. If this fraction is interpreted as the fraction of the catchment contributing directly to runoff, the size of the contributing area is on average 1012 m^2 . Comparing this to the DEM where 1150 m^2 (or 46 grid cells) are allocated as creek channel and flooded areas, it seems that precipitation on the channel and adjacent areas, is the main source of stormflow runoff.

After logging 60 rainstorm/peakflow events were adequately documented with an identical range in events: maxima for P and Q_p were 60.6 mm and 2.67 mm (164.8 m^3). This yielded almost the same relation between P and Q_p (see figure 11.4 b):

$$\log(Q_p) = 0.9189 * \log(P) - 1.7442 \quad n=60, r^2 = 0.7234 \quad (11.2)$$

The runoff percentage was also nearly the same, namely 1.67%, based on the mean of $\log(P)$ and $\log(Q_p)$.

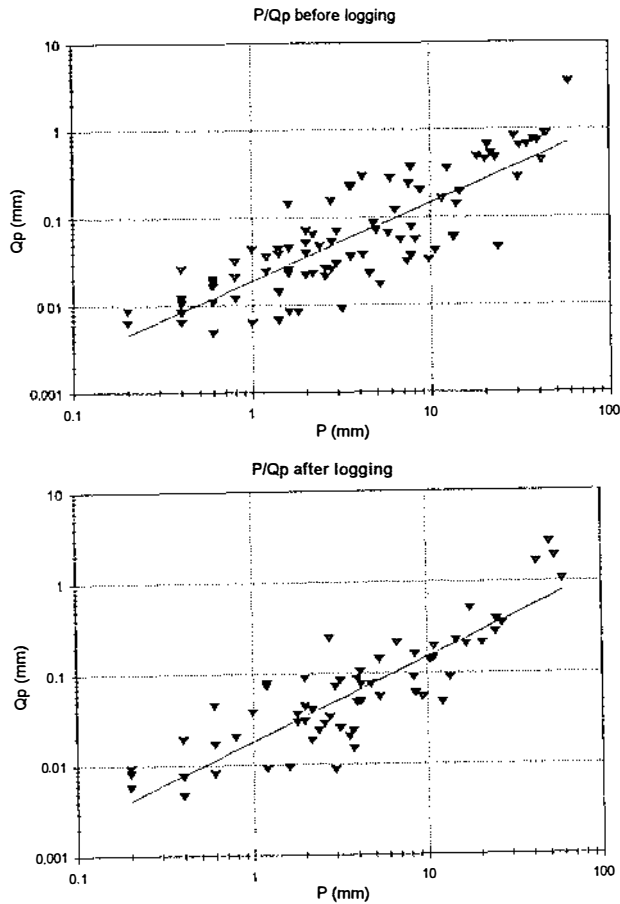


Figure 11.4 Double logarithmic regression of rainfall (P in mm) and stormflow event (Q_p in mm): a) before logging, $n = 90$ and $R^2 = 0.7112$, and b) after logging, $n = 60$ and $R^2 = 0.7234$.

Using equations 11.1 and 11.2 for peakflow estimations and hand level readings for baseflow, to supplement the automatic recordings, a complete series of daily discharge records were generated, spanning the whole period from 6 August 1991 to 10 December 1993. The total discharge for the 809 days was 152360 m^3 , which gives an average daily discharge of $188 \text{ m}^3/\text{day}$ or 2.18 l/s . Baseflow varied from 50 to 550 m^3 with an average dry season value of about $103 \text{ m}^3/\text{day}$ and a wet season value of $215 \text{ m}^3 \text{ day}$ (respectively 1.1 and 2.5 l/s). The 30-day discharge

(recalculated to mm with the catchment size) and rainfall for this period are shown in figure 11.5. Lowest discharge occurs in March 1992, while this is not the period with the lowest rainfall. It seems that there is a delay time of several months as the July and August rainfall is still notable in the baseflow of October.

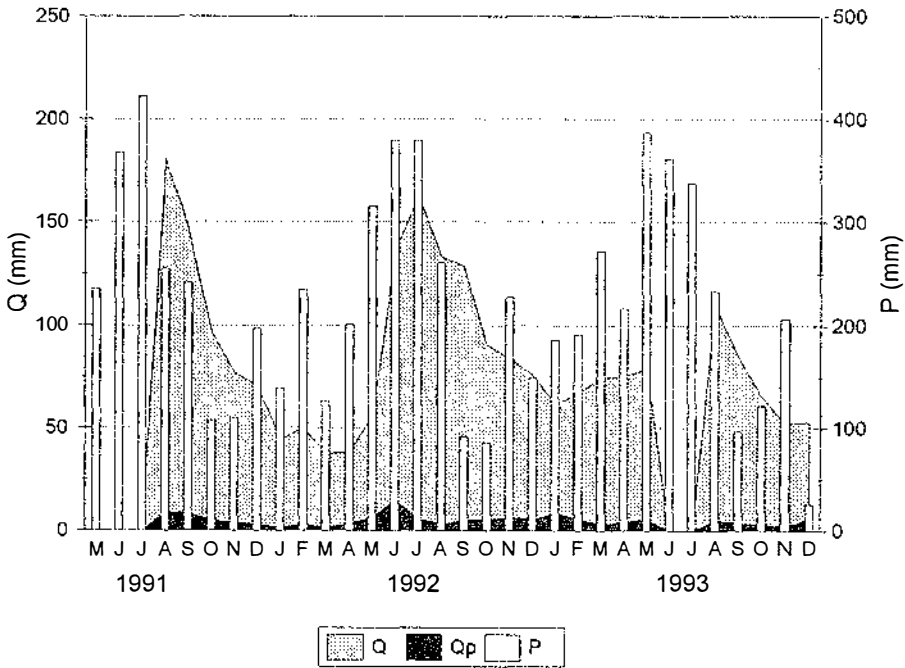


Figure 11.5 30-day total discharge (Q), peakflow (Qp) and rainfall (P) (both in mm) during the entire measurement period.

A better estimate of the response time is obtained by looking at the 5-day discharge (figure 11.6). To emphasize the relation between rainfall and discharge a moving average of the 5-day rainfall totals has been added to the graph. From the rise in discharge in the beginning of June 1992, as a reaction to the increase in rainfall during the second week of April 1992, the catchment appears to have a response time of approximately 60 days. It seems that the discharge is somewhat higher and more variable immediately after logging than at the end of 1991, but unfortunately the datalogger was malfunctioning at the end of 1991 (indicated with the thick line at the top of figure 11.6) and only weekly hand readings were available. Therefore it cannot be said with certainty that the increase in discharge or the larger temporal variability is caused by the increased percolation from the logged sites.

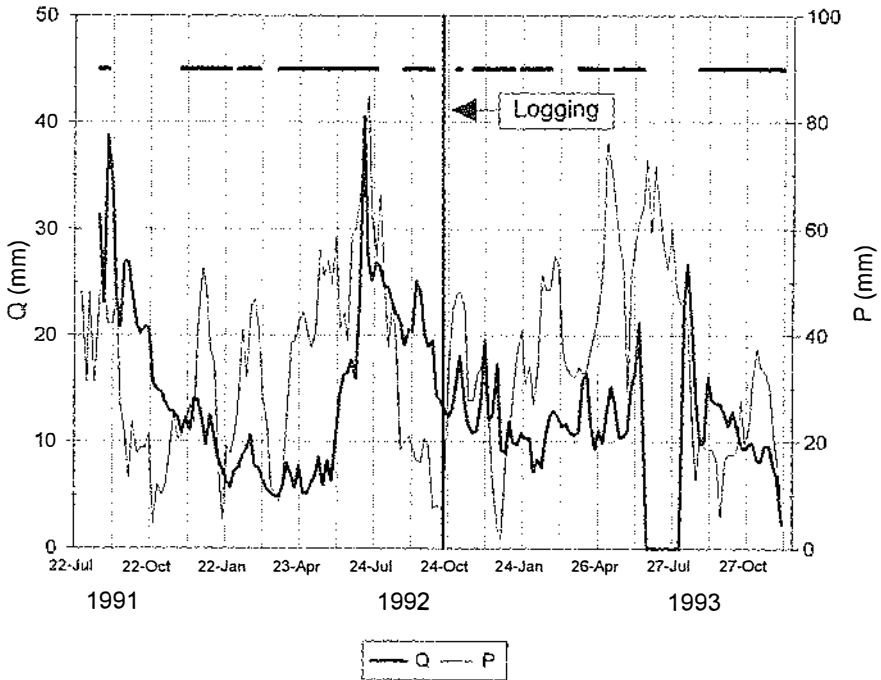


Figure 11.6 Total discharge in 5 day totals and running average of the 5-day totals of rainfall (both in mm). The thick line at the top of the graph shows the periods in which the datalogger was operative.

11.3.2 Groundwater fluctuations

To interpret the temporal variation in groundwater levels the piezometers were grouped according to soiltype. Most piezometers were placed in pairs whereby if the piezometer close to the creek was e.g. numbered 9, the piezometer upslope was numbered 9a. The piezometers on the sandy soil types ARa and ARo (indicated with SSGW), included numbers 10 and 10a, 9 and 9a, 8 and 8a, 7, 6 and 6a, and 5. The piezometers on loamy soil types FRh and ACh (indicated with LSGW), included numbers 1, 2, 3 and 3a, 4 and 4a, 11 and 11a and 12 and 12a. Figure 11.7 a and b show the fluctuations in groundwater level for the whole measurement period, relative to the elevation of the stream channel.

Seasonal fluctuation is evident from all graphs, with maximum levels reached at the end of July 1992 and minimum values in March and April 1992. This is in spite of

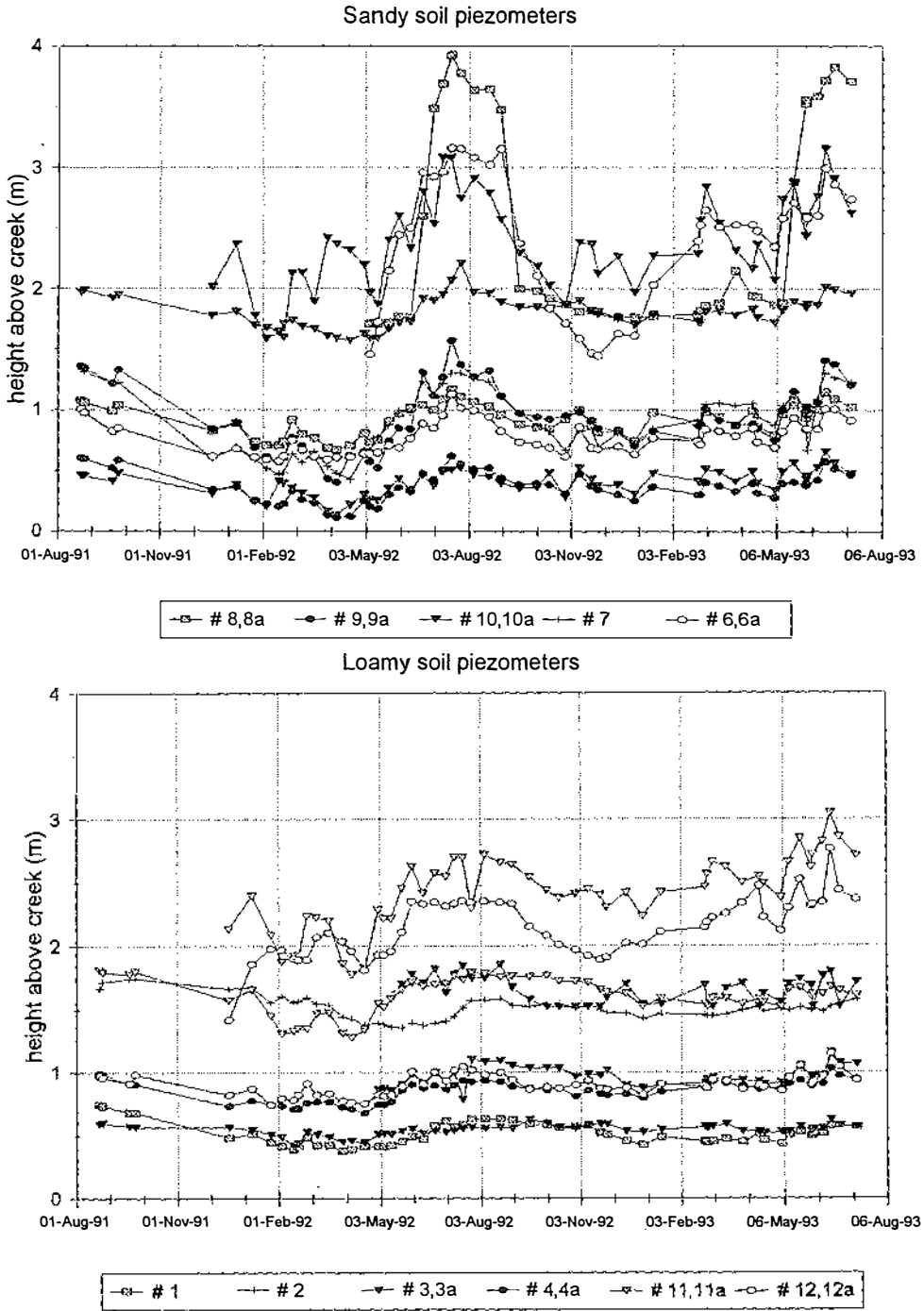


Figure 11.7 Groundwater fluctuations (in m) relative to the streambed for the entire measurement period: a) piezometers in sandy soil types (ARa and ARo), and b) piezometers in loamy soil types (FRh and ACh).

the fact that rainfall was least in October and November 1991. Apparently the influence of the preceding wet May to August season was very great and levels continued to drop until March 1992. The amplitude and variation of the fluctuations depends on the soil type and position on the slope. The lowest graphs show the fluctuations in the piezometers on the valley floor, directly above the stream. The difference between minimum and maximum levels was about 50 cm for the SSGW and about 25 cm for the LSGW. Also, the former show more variation in the fluctuations than the latter, The variation in levels increases upslope. Whereas seasonal fluctuations at the bottom of the slope for SSGW (second level graphs) span about 100 cm, the LSGW fluctuations span only 50 cm. The highest piezometers have seasonal fluctuations in the order of 200 cm for SSGW and 100 cm for LSGW. Thus the amplitude of the seasonal fluctuations in the sandy soils is about twice as large as in the loamy soils. The variation increases with the height above the creek, because the distance between the groundwater and the surface increases even more. Thus it takes longer in the dry months for the percolation water to reach the groundwater, and the level continues to drop until the start of the wet season when a sharp rise occurs.

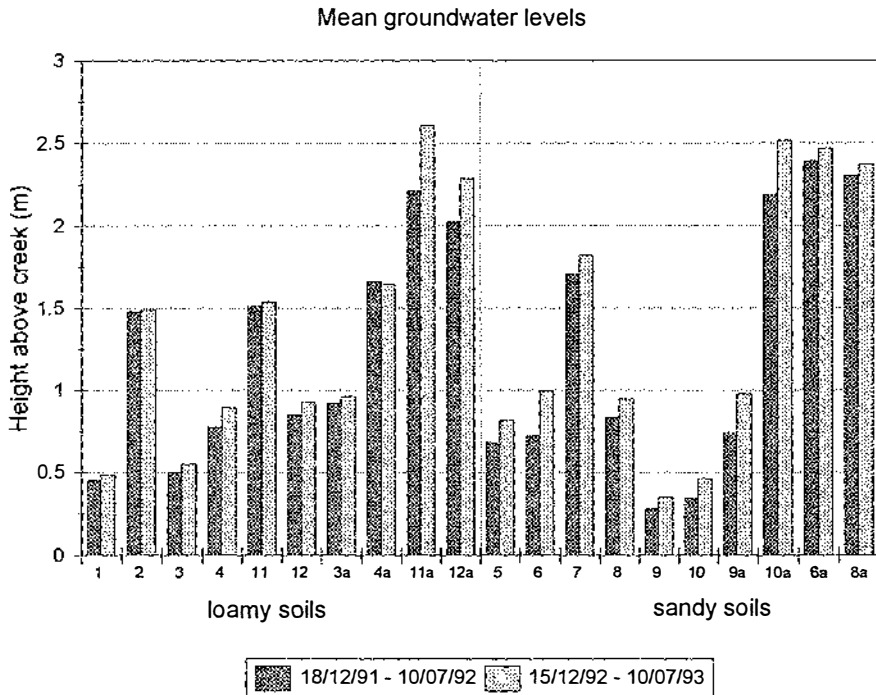


Figure 11.8 Mean groundwater levels relative to the streambed for two periods of more or less equal length, before and after logging.

This seasonal delay obscures a change in groundwater levels as a result of logging. Disturbance was greatest above piezometers 6a, 11a and 12a. The level of piezometer 6 (top graph with open circles in figure 11.7a) did not seem to change after logging, while the levels in 11a and 12a (the two top graphs in figure 11.7 b) seemed to rise gradually. Other piezometers also have a small rise in level. Comparing the levels from 15 September to 10 July in 1991-1992 with the same period in 1992-1993 (the longest possible period that could be compared), an analysis of variance shows that all piezometers except numbers 1, 2, 9 and 11 are significantly higher ($p = 0.05$). This is illustrated by figure 11.8, showing the mean levels of the 2 periods. The average difference is 12.6 cm, which represents a change in storage of approximately 63 mm (using a pore volume of 50%). Also it appeared that SSGW had a larger mean rise of the groundwater level (about 15 cm), while the rise in level of the LSGW was about 5 cm. Because the logging took place mainly on the Arenosols, the rise in groundwater level could be related to the disturbance. In chapter 10 it was shown that there is an increase in percolation from 45% to 55% of the rainfall on the disturbed areas. However, this conclusion is tentative because the dataset is too small to distinguish between annual climatic variations and a trend as a result of logging. In any case the rise in groundwater is very small.

11.3.3 Surface runoff

The logging took place on the flat water divide only, with skid trails occurring on slopes with maximum angles of 20 to 30%. Thus the process of overland flow, described in chapter 7, remains unaltered and concentrates on the steep slopes of the valley sides (see figure 11.1 b). Only in the northeast there was probably an increase in runoff, generated on the skid trails on the loamy FRh soils. However, the extra runoff infiltrates on the lower parts of slope and is added to the normal process of fast lateral flow. Surface erosion was not observed on any of the skidtrails.

11.3.4 Annual water balance before and after logging

In the year before logging the total discharge was 60979 m³ divided into 5.6% peakflow (3404 m³) and 94.4% baseflow (57575 m³). The amount of rain that fell in the same period, used to calculate the evapotranspiration (ET) and fast runoff (Qp), was 2405 mm. For the percolation and baseflow (Qb) a reference period was taken that started 60 days earlier, the response time of the catchment, which resulted in a total of 2577 mm. It is assumed that the bulk ET of the catchment is the average of the ET calculated with the vertical water balance of each soil type (see chapters 8 and 10), weighted by the percentage of catchment area that the soil type occupies. This leads to an overall ET of 55% of the rainfall. Depending on the slope gradient and the prevailing soil moisture content a certain amount of overland flow is produced. The remaining water percolates. Analysis of the drainage pattern and slopes derived from the DEM lead to a division of the catchment into 3 zones:

- the watershed (76.9% of the area) which produces no surface runoff and has 45% of percolation to the groundwater;
- the slopes steeper than 20% (21.2% of the area), which are assumed to produce 5% runoff and 45% percolation of the remaining infiltrating water;

- the stream channel and adjacent wet areas (1.9% of the area) which have 100% surface runoff.

Table 11.1 Annual catchment water balance before logging. "Estimated" is the discharge calculated from the rainfall with the method explained in the text, "Measured" is the discharge at the weir. P = rainfall, ET = evapotranspiration, Q = total discharge, Qp = peakflow, Qb = baseflow (all in 1000 m³).

Estimated	<i>Size (ha)</i>	<i>P</i>	<i>ET</i>	<i>Qb</i>	<i>Qp</i>	<i>Q</i>
watershed	4.750	117.9	62.8	55.1	0.0	55.1
slopes	1.315	32.6	16.5	14.5	1.58	16.0
valley floor	0.115	2.8	0.0	0.0	2.77	2.8
Total	6.180	153.3	79.3	69.6	4.35	73.9
Measured				60.5	3.58	64.0
<i>Difference</i>				-9.1	-0.77	-9.9
Summary	<i>P</i>	<i>ET</i>	<i>Q</i>	<i>Qp</i>	<i>diff.</i>	
mm	2480.4	1284.1	1036.1	57.8	-160.2	
%	100.0	51.8	41.8	2.3	-6.5	

With the size of these zones, the annual rainfall corresponding to ET and percolation, the annual water budget can be calculated and the theoretical baseflow and peakflow can be compared to the measured values (see table 11.1). Using a catchment size of 6.18 ha there is a discrepancy between the estimated and the measured discharge. Since the fast runoff component is somewhat arbitrary (using a fixed runoff percentage on the slopes as well as a fixed contributing area), the difference can best be seen by comparing the baseflow components. The difference is 9131 m³ or 147 mm which amounts to 5.7% of the "baseflow" rainfall. Reasons for this discrepancy are discussed below.

The same calculations were done for the year after logging (see table 11.2), with the exception that a different ET/percolation ratio was used for the watershed area because of the logging. On average the disturbed areas proper will have an ET of 45% and a percolation of 55% of the rainfall (see chapter 10). Since the logging all occurred in the watershed zone, the water balance for this area is calculated with an alternative percolation/ET ratio. Approximately 1.4 ha out of 4.75 ha were disturbed, which leads to an alternative ET and percolation of 51.8% and 48.2%, instead of the normal 45% and 55%. Unfortunately, days 175 to 223 have to be excluded because of the stolen equipment, while hand readings were not available. Therefore, while the total rainfall was 2734 mm, the amount of rain corresponding to the ET and runoff is 2225 mm, whereas the total rainfall corresponding to the baseflow/percolation is 2148 mm (again using a 60 day response time). The difference between measured and estimated baseflow is slightly higher: 10633 m³ or 172 mm, which is 8% of the "baseflow" rainfall.

Table 11.2 Annual water balance after logging. "Estimated" is the discharge calculated from the rainfall with the method explained in the text, "Measured" is the discharge at the weir. P = rainfall, ET = evapotranspiration, Q = total discharge, Qp = peakflow, Qb = baseflow (all in 1000 m³). Days 174-223 of 1993 are excluded from the calculations, see text.

	Size <i>ha</i>	P <i>10³ m³</i>	ET	Qb	Qp	Q
Estimated						
watershed	4.750	103.9	54.7	49.2	0.0	49.2
slopes	1.315	28.8	15.3	12.1	1.46	13.5
valley floor	0.115	2.6	0.0	0.0	2.56	2.6
Total	6.180	135.3	70.0	61.3	4.02	65.3
Measured				50.7	3.38	54.1
<i>Difference</i>				-10.6	-0.64	-11.2
Summary						
mm	P	ET	Q	Qp	Diff.	
	2189.8	1132.6	874.7	54.7	-182.5	
%	100.0	51.7	39.9	2.5	-8.3	

The difference between measured and estimated baseflow could simply be the result of errors, because the annual discharge is calculated from automatic readings supplemented with less frequent hand readings (errors related to the P/Qp relations will be very small because of the small amount of peakflow). Also, the exact catchment size, both for the surface drainage pattern and for the groundwater body, is not known which adds to the uncertainty. However to account for a difference of 9000 to 10000 m³ the catchment size would have to be 5.5 ha which seems too small. If anything the catchment size may be bigger because of the poorly defined southern boundary. Other changes are a small increase in Qp/Q ratio from 5.6% to 6.2%, which would correspond to the change in the peakflow frequency towards higher peakflow volumes described above. However, because of the laps in data in the wet season in 1993, this conclusion is only tentative.

Physical explanations of the difference between measured and estimated baseflow include groundwater flow out of the catchment that does not go via the weir, or a change in storage. Because of the kaolinite layer below the Arenosols and the bedrock below the other soils, percolation to deeper layers is not likely, at least not in such a quantity. Groundwater flow out of the catchment parallel to the creek could occur for instance if the kaolinite layer is not level, but slopes downward towards the outlet. However, annual differences in groundwater level and related storage of water in the soil could well explain a 150 mm difference. Figure 11.9 shows the annual difference in storage (a pore volume of 50% is assumed) at 4 moments in time spread evenly over the year. The difference between December 1991 and December 1992 is negative for most of piezometers, especially for the higher ones. A depletion of storage between 150 and 300 mm was measured for piezometers 10a, 11a and 12a. Considering the other values the annual change in storage varies between over 200 mm surplus to more than 500 mm shortage for some of the piezometers. This indicates that a difference of 150 mm in the measured and estimated water balance is of the same order as the storage change. Moreover it

is apparent that the start and end of the period for which the annual water balance is calculated are very important and change in catchment storage cannot be assumed insignificant over a year. In addition there is a change in soil water storage above the groundwater. In the upper 100 cm annual differences can be in the order of 20 mm/m depending on the period considered (see chapters 8 and 10).

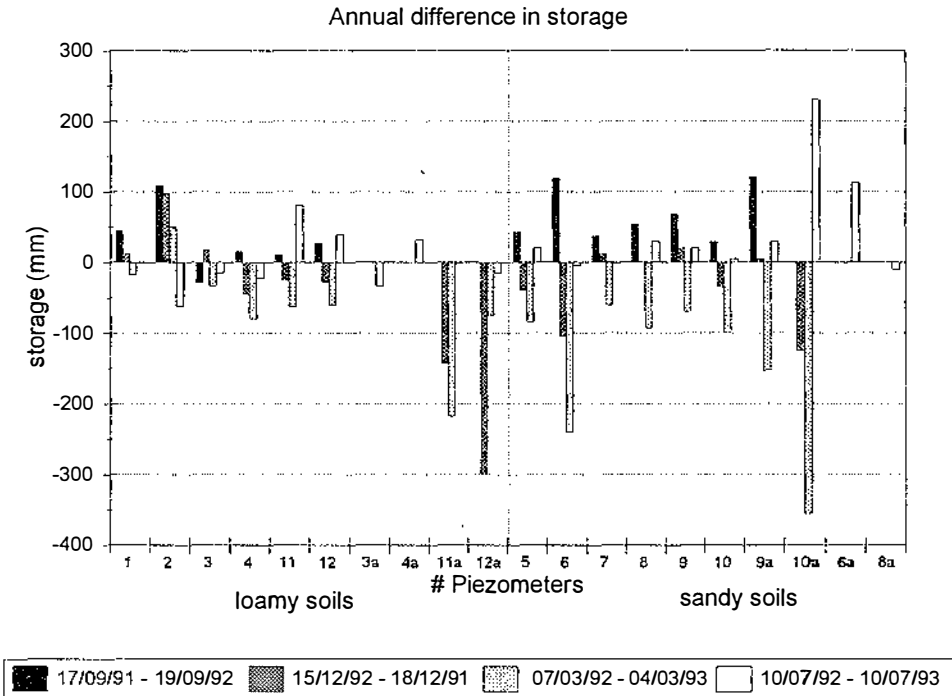


Figure 11.9 Difference in storage (in mm) between two moments in time 1 year apart, for 4 dates spread evenly throughout the period.

After logging the difference has increased by 1500 m³ (24.3 mm). This could be a result of the small rise of the groundwater level that was mentioned above. However, a rise in groundwater level should be directly related to a rise in the water level of the creek (even if a delay time is taken into account), and an increase in baseflow. This is not the case, although 49 days were not recorded in the wet season of 1993. Therefore it must be concluded that the impact of the low intensity logging on the catchment water balance was too small to be detected within the levels of accuracy of the measurements.

11.4 Comparison of low intensity logging with heavy disturbance in French Guyana

From the results described above the impact of logging is undetectable within the accuracy of the measurements. For comparison, the research of Fritsch (1990) in the ECEREX project in French Guyana provides a good example of the impact of a variety of high level disturbances in a similar area. Using the paired catchment technique, he studied the effects of clearfelling with different treatments on the water balance of small catchments. In the 2nd order basin (4.2 km²) of the Crique Délises, he selected 10 catchments between 1 and 2 ha each. The annual water budget is very similar to the Tropenbos area (see table 11.3). Although the area was located on schists and migmatites, the soils in 5 of the catchments were very permeable due to a microaggregate structure (Ksat comparable to the Arenosols). The other 5 catchments had more rapid surface runoff (Ksat comparable to the Ferralsols). All soils were shallow and lateral surface runoff was the contributor to discharge. He selected 2 control basins, while 1 basin was subjected to heavy timber extraction (192 m³.ha⁻¹), 6 basins were cleared completely with tyre or caterpillar machines and 1 basin was cleared by hand with the traditional slash and burn method (see table 11.4). Land use after clearing varied from pasture to Caribbean pine, Eucalyptus and grapefruit plantations. In two catchments natural regrowth of the rain forest was permitted. A fallow period with bare soils of 6 months to 1 year followed the clearing (except for basins I and E which were left untouched).

Table 11.3 Percentage increase in discharge as a result of a change in land use (Fritsch, 1990), for 8 catchments of 1 - 2 ha in size. All catchments are situated in the Crique Délice catchment in French Guyana, listed in table 11.4. The "fallow" period in which the soils were bare lasted 6 months to 1 year, the "growth" period is given in years. Clearing method: T = Tyre, C = Caterpillar, Man = Manual clearing.

<i>Treatment</i>	<i>Fallow</i>		<i>Growth period (yrs)</i>					<i>Clearing Method</i>
	<i>start</i>	<i>stable</i>	<i>1</i>	<i>2</i>	<i>3</i>	<i>4</i>	<i>6</i>	
Grapefruit plant. + pasture	75	146	73	17	63	46	-	T+C
Slash and burn	-	-	23	30	-	-	-	Man
Intensive logging + regrowth	-	-	4	26	2	-6	-	T
Clearfelling + regrowth	104	96	40	32	16	-	-	C
Pasture	90	112	59	63	47	27	-	T+C
Fodder	59	61	-	-	-	-	-	C
Caribbean Pine plantation	81	92	62	33	-	-	-12	+C
Eucalyptus plantation	63	66	47	12	-	-	-8	T+C

Table 11.3 shows the increase in discharge. During the fallow period the total runoff was 44% to 146% more than under forest, although in the rainy season the increase could be as much as 200% and more. Most treatments took a few months to reach a higher equilibrium. This increase was almost entirely caused by surface runoff, the vertical percolation increased only with 20% to 35%. The surface runoff was related to the change in hydrological characteristics of the soils caused by the heavy machinery. Initially in the growth period the discharge dropped rapidly but it took 4 to 6 years for almost all treatments to reach the discharge levels of undisturbed

forest, except for the natural regrowth basins which took only 2 to 3 years to recover. The traditional slash and burn method proved very disturbing, comparable to heavy mechanised logging. Other than that the method of clearing (tyre or caterpillar) and the season in which clearing was done (wet or dry) did not seem to have a differentiating effect. The increase in runoff caused an increase in sediment between 25 and 500%, which happened especially in the fallow period. However in absolute weight this represented an erosion of 3 to 17 ton.ha⁻¹.yr⁻¹ a relatively small amount. A study of Wischmeyer type erosion plots indicated that the erosion under forest was only 50 to 70 kg.ha⁻¹.yr⁻¹ while the pastures yielded about 10 times that amount.

11.5 Conclusions

Brinkman (1989) reviewed several basin studies and attempts to bring them together on a global scale, in terms of a division of rainfall in runoff and the sum of ET and retention. In general he concludes that in order of decreasing runoff, the Asian studies show a runoff of 80% to 60%, followed by Amazon and Malaysian studies which have a runoff between 55% and 45%, while the African catchments have up to 80% evapotranspiration (especially the Zaire basin). He also shows that the combined ET and retention increases from steep mountainous areas to homogeneous lowland areas. In view of this the catchment of this study has a division between ET and percolation that is typical for the Amazon basin.

An overview of catchment studies and remarks on the quality of the results, are given by Bruijnzeel (1990). However the size of the catchment varies from 1-2 ha (e.g. Fritsch, 1990) to over 1 million km² (e.g. Walker et al., 1993). A selection of research in first and second order catchments is given here. Table 11.4 shows the main components of the water balance, before and after disturbance if appropriate. With respect to the errors involved in the measurements, Lesack (1993) calculates an uncertainty of 16-21% in his annual water balance of a small Amazon basin. Related to this is the fact that a paired catchment technique is useful to correct for seasonal trends. However, the comparison is done with regression techniques and Malmer (1993) finds R² levels between 0.90 and 0.93 for 5 catchments in Malaysia, while Fritsch (1990) finds maximum R² levels of 0.9 to 0.98 and Hsia & Koh (1983) give and R² of 0.98. There is still 2 - 10% unexplained variance which adds to the uncertainty in the results, which is in the same order of the effects of low intensity logging. Therefore it seems that a paired catchment approach is only useful if the disturbance is extreme.

Compared to the clearfelling or heavy logging (extraction of 192 m³.ha⁻¹) in the ECEREX research, the results presented in this study provide a sort of "best case" scenario. The low logging intensity (21 m³.ha⁻¹), combined with a concentration of the disturbance on the flat watersheds, has an effect on the catchment hydrology which is barely noticeable. Theoretically, the logging should cause an overall increase in percolation in the first months after logging, causing an increase in groundwater level and baseflow in the creek. Differences in groundwater level and discharge before and after logging were observed but they were well within the

accuracy of the measurements and could not be related to the logging event. It seems that the effects of logging were completely neutralised. It takes on average about 60 days for the rainfall on the water divides to reach the stream channel (the distance from the soil surface to the groundwater is between 5 and 10 m). Because 77% of the catchment is still undisturbed the effects of the logging are absorbed by the surrounding forest. Also the logging was done in the dry season (end of October 1992) while the groundwater is still under the influence of the previous wet months.

In other words in a spatial sense the effects are buffered by the remaining forest, in a temporal sense the effects are buffered by the seasonal fluctuations. Because the logging took place mainly on areas with a slope angle less than 20%, while the steep slopes remained undisturbed, overland flow did not increase. Analysis of the discharge showed that there was no difference in stormflow runoff of the creek before and after logging. Also, erosion was not observed. Thus, from a hydrological point of view, a logging intensity of $21 \text{ m}^3 \cdot \text{ha}^{-1}$ which is evenly applied has no detectable influence on the catchment water balance. It should be noted that the buffering effect is primarily caused by the high permeability of the Arenosols and Ferralsols and the fact that the groundwater body is far below the surface. Thus these results cannot be extrapolated to other types of environment.

Table 11.4 A selection water balance studies of small and medium sized catchments under tropical rainforest. P = annual rainfall; Q = total discharge; Qp = stormflow; Perc = deep percolation; ET = total evapotranspiration; Store = catchment storage

Location	Forest type	Disturbance	Size ha	P mm	Q %	Qp %	Perc %	ET %	Store %	Year	Reference [remarks]
Lake Calado, Central Amazon, Brazil	Terra Firme	none	23.4	2870	57.5	3.0	1.5	39.0	2.0	'84-'85	Lesack (1993) [wet year]
Barro Branco, Central Amazon, Brazil	none	none	130	2076	19.3			80.7		'76-'77	Franken and Leopoldo (1984)
id. 2nd period of obs.	none	none	130	2510	34.6			65.4		'81-'82	id.
Bacia Modelo, Central Amazon, Brazil	none	none	2350	2089	25.9			74.1		'80-81	id.
Gregoire I, II & III, French Guyana	Mixed	none	320 - 1240	3695	60.2			39.8		8 yrs	Rocher (1982)
Mondo, Java, Indonesia	Agathis plant	none	190	3578	74.0	6.4		26.2	-0.2	'76-'78	Bruijnzeel (1982)
Tonka, Surinam	Mixed	none	295	2143	23.9			76.1		'78-'83	Poels (1987) [high annual var]
Mendolong, Sabah, Malaysia	Dipterocarp	none	3.4 - 18.2	3350	61.0	33.0		39.0		'85-'90	Malmer (1991)
5 basins: 2 control, 3 treatments	slash/burn	slash/burn		3804	69.8			30.2		'87-'90	[high rainfall variation]
	clearf./manual	clearf./manual		3804	64.9			35.1			
	clearf./tractor/burn	clearf./tractor/burn		3804	71.4			28.6			
Sun Moon Lake, Central Taiwan	Mixed	none	5.68	2100	52.4			47.6		'78-'79	Hsia and Koh (1983)
2 basins: 1 control, 1 treatment	clearfelling	1st yr	8.39	2074	74.6			25.4		'79-'80	[high rainfall variation and
		2nd yr	8.39	1498	72.7			27.3		'80-'81	2nd yr only 11 months]
ECEREX, French Guyana	Mixed	none	420	2979	42.7	23.0	8.0	49.3		'77-'83	Fritsch (1990)
TROPENBOS, Guyana	DEF+Mixed	none+sel logging	6.18	2449	41.8	2.3		51.8	6.6	'91-'93	This study [dry and avg year]

SUMMARY AND CONCLUSIONS

Modelling the effects of logging on the water balance of a tropical rain forest, a study in Guyana

Tropical rain forest has an important ecological and economic function. Often it is the most suitable form of land use for the area it occupies. Nevertheless, forests are almost always mined. The Tropenbos Foundation was established to generate tools for policy makers and managers, for the conservation and wise use of the tropical rain forest (Tropenbos, 1990). Under its supervision, the governments of Guyana and the Netherlands have been cooperating in a research programme that started in 1989.

The interior of Guyana is scarcely populated. The main pressure on the rain forest ecosystem is selective commercial logging. Therefore, the Tropenbos research programme focuses in Guyana on the functioning of the undisturbed forest ecosystem and the changes that take place as a result of low intensity logging. The research described in this thesis forms one of the main projects in the programme: the effects of logging on the water balance.

The water balance research was located in the Tropenbos Ecological Reserve and its surroundings, which is situated in north central Guyana (some 250 km south of the capital Georgetown). The water balance is determined by the climate, and the hydrological characteristics of vegetation and soils. Not all forest and soil types could be investigated, the research focused on three main combinations of forest types and soil types that are widespread and in which logging takes place. These are: Dry Evergreen Forest on white very sandy Albic Arenosols (indicated as DEF-ARa), Mixed Forest on brown sandy-loamy Ferralic Arenosols (MF-ARo) and Mixed Forest on brown loamy Haplic Ferralsols (MF-FRh).

The impact of logging on the water balance was studied on two scales: on a "tree" level, where only the vertical (one-dimensional) water balance was investigated, and on a "catchment" level, where lateral water flows were considered as well. This resulted in a research in 4 parts. First, the spatial relations between forest type patterns and soil type patterns were studied, and the spatial variability of soil hydrological properties was quantified. Second, the vertical water balance of the undisturbed forest was modelled. Third, the effects of logging on the vertical water balance were assessed and the hydrological processes in a gap were compared to the forest. Finally the impact of logging on a small catchment was assessed. This approach led to the following research questions:

- To what extent are patterns in forest types related to patterns in hydrological characteristics of the soils?
- What is the spatial variability of the hydrological properties of soils and vegetation and is it feasible to map them?
- Can a water balance model be used in the assessment and comparison of all the water fluxes in the various environments?
- How does the variation in soil and plant properties affect the vertical water balance?

- What is the nature of the processes that lead to surface runoff, how much is it and where does it occur?
- What is the effect of skidding on the soil hydrological properties?
- What are the changes in water fluxes on a gap compared to the forest and how do they develop in time?
- How does low intensity logging effect the water balance of a small catchment?

It is important to know the spatial distribution of the combinations of forest and soil type for which the water balance was modelled. The forest types were classified according to their tree species composition (Ter Steege et al., 1993). Analysis of the tree species composition of a 480 ha area suggested that the species abundance should be seen as a spatial variable. This yielded three broadly defined forest types only: Dry Evergreen Forest, Mixed Forest and forest on flood plains and swamps, which is termed Wet Forest in this study. A further division of these forest types was not feasible because it could not be mapped. Even with this broad classification, it appears that half of the study area does not belong to any of these three forest types for more than 60%. There are several contiguous areas where the forest has a species composition typical for one of the forest types, but in between there are gradual changes. There appears to be a strong association between spatial patterns of species composition, the texture of the topsoil, the surface drainage network, and a hydrological gradient from the water divide to the valley floor. Thus it seems that on a large scale hydrology has an important influence on the spatial distribution of tree species.

Almost all soil hydrological properties of the Arenosols and Ferralsols exhibit a large short range spatial variability. In Albic Arenosols, properties such as bulk density, porosity, saturated hydraulic conductivity and rooting characteristics have a distance of variation around 200 m. Ferralic Arenosols and Haplic Ferralsols have spatial patterns which vary at distances of less than 20 m for almost all properties. In view of this it is not feasible to map any of the hydrological properties. The number of sample points required to represent the spatial structure adequately is prohibitive. Therefore, the best strategy is random sampling, to ensure that the values of the soil properties are good representatives of the areal mean and variance (see e.g. Brus, 1993).

Hydrological characteristics of the forest types also show a large spatial variability, which was investigated in this research only in an indirect way. Measurements show that the throughfall in both Dry Evergreen Forest (DEF) and Mixed Forest (MF) has a large spatial variability with throughfall/rainfall ratios that vary from 0.5 to 2.0. Nevertheless, the interception of both DEF and MF is not significantly different. It is between 15% and 17% annually. Also stemflow and canopy cover fraction are not significantly different. Modelling the interception and throughfall processes with the canopy seen as a single storage container, resulted in a poor estimate of the interception on a daily basis. Incorporating the vertical leaf area distribution in the model, improved the estimates, in part because this enabled the simulation of the micro climate inside the canopy. However, the vertical leaf area distribution was not measured in the study area and the average canopy structure of a Mixed forest near Manaus (Brazil) was used. Although this gives adequate results, there is a strong

need to quantify the large variation of the canopy structure in the research area, in order to be able to differentiate between the micro climate of the various forest types. The micro climate determines both the interception evaporation and the transpiration and is therefore of paramount importance to the forest water balance.

Measurements of the vertical root distribution showed that on average the percentage of fine roots decreases sharply with depth and more than 95% of the roots are found in the top 100 cm of the soil. Dry Evergreen Forest tended to have more roots in the upper 20 cm than Mixed Forest. Eernisse (1993) found that both forest types had a few roots several meters below the surface which are probably related to the presence of groundwater (in the case of the Arenosols) or to the availability of nutrients in the weathering zone (in the case of the Ferralsols).

Using these properties as input for the SOAP water balance model, the soil moisture content could be simulated adequately for dry and wet periods in Ferralic Arenosols and Haplic Ferralsols (measurements of soil moisture in Albic Arenosols were not available). After calibration SOAP was used to simulate the annual water balance of the three combinations of forest type and soil type, whereby a range of input values was used for each combination. In spite of the wide variation in soil properties, with for instance saturated hydraulic conductivities ranging from nearly 6000 cm/day to 25 cm/day, all combinations yielded a very similar annual water balance. Also the temporal variation was identical. This was caused by the fact that the evapotranspiration dominates the vertical water balance, while at the same time it is nearly identical for all combinations of forest and soil type. The daily evapotranspiration flux varied between 1 and 8 mm/day without a clear seasonal variation. Because of the sandy nature the hydraulic conductivity decreases strongly with decreasing moisture content. Therefore it takes about 5 days in the dry season before the wetting front of a large rainstorm arrives at a depth of 100 cm, while the response time in the wet season is only 2 days. Percolation from the bottom of the root zone occurs mainly when the soil is above field capacity at that depth. Thus 70% of the percolation takes place in the wet season. On an annual basis the evapotranspiration is 55% of the rainfall, percolation and overland flow constitute 45% (see figure 12.1). This is the same for almost all combinations, except for the most permeable Arenosols in which moisture stress and reduced transpiration may occur, and for the least permeable Ferralsols where overland flow may take place.

Overland flow only occurs on the less permeable Ferralsols on steep slopes. The average amount in the wet season of 1992 varied from 3% to 15% of the rainfall, for slope angles varying from 25% to 60% respectively. The overland flow occurred each time the soil was nearly or completely saturated. Compared to agricultural areas the resistance to flow under forest is extremely high. The water flows through and over the litter layer on top of the soil. A series of flow tests on large soil samples showed that the amount of overland flow was not determined by the slope angle but by the thickness and characteristics of the litter. The flow should be seen as throughflow in a porous medium, instead of overland flow with a high surface resistance. Variation in the lateral conductivity was smallest when the flow depth was the same as the litter depth. When the flow depth was very shallow only preferential flow paths were used and the flow velocity increased sharply. Also when

the water layer was thicker than the litter layer the velocity increased considerably as the water flowed on top of the litter. By relating the flow velocity with the duration of saturated condition of the topsoil, a lateral distance of flow may be estimated, which varied between 20 and 350 m (with an average of 80 m).

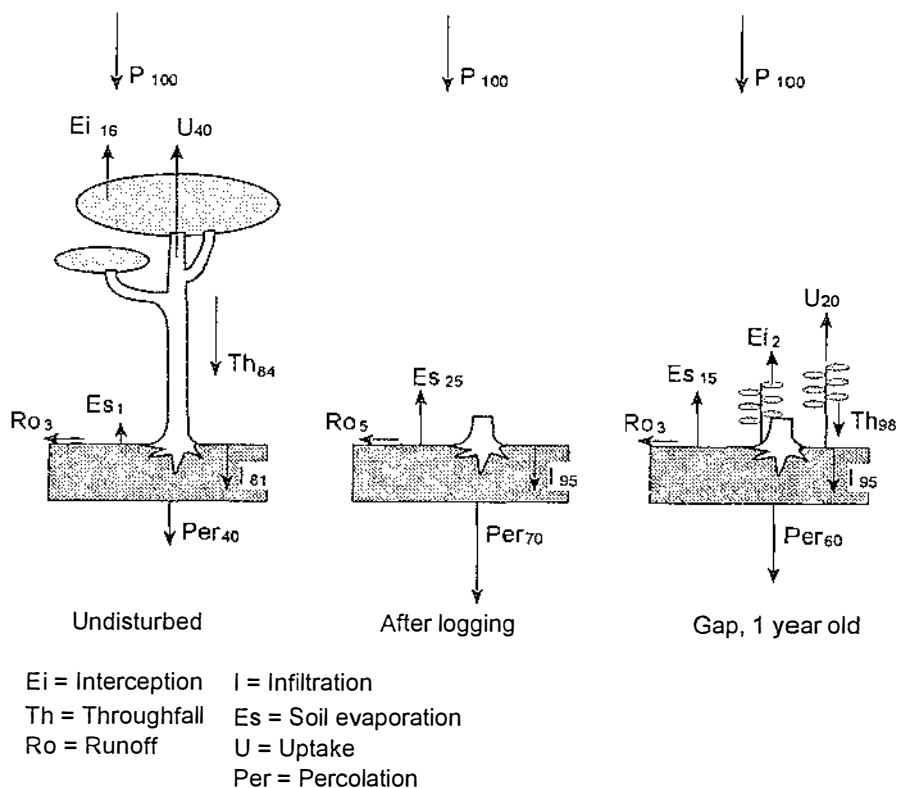


Figure 12.1 Comparison of the vertical water balance of undisturbed forest, a gap immediately after logging, and a gap one year after logging. All water fluxes are given as a percentage of the annual rainfall (approximately 2700 mm).

Selective logging creates artificial gaps in the forest. On these gaps the water balance changes considerably because of the disturbance to vegetation and because the topsoil is compacted by the heavy machines. The compaction of the topsoil by skidders causes a sharp decrease in hydraulic conductivity for all soil types. The changes are greatest for the Albic Arenosols because there is no silt fraction and the soil has a poorly sorted pore distribution, which changes drastically because of the disturbance. This causes a sharp reduction in hydraulic conductivity to about 10% of

its original value at saturation, to about 1% at field capacity. At the same time the compaction causes the water retention capacity to increase considerably, so that the overall effect on for instance the establishment and growth of seedlings is not clear. The other soil types are affected to a lesser degree, in particular the Haplic Ferralsols. In spite of its loamy texture, the hydrological properties are not significantly different before and after logging. This soil type has very strong micro aggregates caused by iron oxides which have the size of fine sand. These micro aggregates are not destroyed by skidding and, in the absence of macro structure in the undisturbed soil, the hydrological characteristics of the soil do not change much. This is also the reason that surface sealing does not take place on these soils. The mixing of fresh organic debris with the soil may partly obscure the effects of compaction. However, a study of Haplic Acrisols about one year after logging, showed that there was a strong decline in structure which is probably related to the decomposition of the organic matter and a decrease in soil fauna. Thus the effect of compaction in the Ferralsols may change with time.

Using the soil properties of disturbed soils and making assumptions about the establishment and growth of seedlings, SOAP was used to simulate the water balance of a gap. measurements of soil moisture in two gaps created in Mixed Forest on Ferralic Arenosols were used to validate SOAP. Three different levels of disturbance were recognised on the gap. Simulations for each of these zones were accurate as long as the monitoring of the soil moisture was not done close to the forest edge. The influence of the forest, in particular the evapotranspiration, was noted up to 10 to 15 m from the edge of the gap.

Figure 12.1 shows the annual water balance of the gap centre, immediately after logging and one year after logging. Assuming a linear increase in seedling leaf area from 0 to $1.2 \text{ m}^2 \cdot \text{m}^{-2}$, the evapotranspiration decreased from 55% on an annual basis in forest, to 25% directly after logging (consisting mainly soil evaporation), to 37% after one year (both soil evaporation and transpiration). The evapotranspiration flux on the gap is determined to a large degree by the soil moisture content and varies between 0 and 5 mm/day. Percolation increases from 40% on an annual basis under forest, to 70% immediately after logging, to 60% after one year. This increase in percolation is not related to an increase in the size of the flux but to a seasonal effect. Because the soil on a gap remains around field capacity throughout the year, the percolation in the dry months continues while in the forest the percolation stops. The difference between forest and gap is therefore greatest in the dry season. Simulations over a two year period with an increase in LAI to $2.7 \text{ m}^2/\text{m}^{-2}$ (based on a study in Costa Rica by Parker, 1985) shows that the water balance partly restores itself. After only a small increase in LAI to approximately $1.0 \text{ m}^2/\text{m}^{-2}$ the evapotranspiration is at a level of 75% of the forest, after which it increases only very slowly. This indicates that a thin cover of plants already has a stabilizing effect.

A 6.18 ha catchment, consisting of Dry Evergreen Forest on Albic Arenosols (80% of the area) and of Mixed Forest on Ferralsols (20% of the area), was logged with an intensity of $21 \text{ m}^3 \cdot \text{ha}^{-1}$. The disturbance took place in the part of the catchment that was accessible to the skidders: on the water divide and top slopes, approximately 23% of the area was converted to gaps and skid trails. The steeper

parts of the slopes and the valley floor remained untouched. Theoretically, the logging should cause an overall increase in percolation in the first months after logging, causing an increase in groundwater level and baseflow in the creek. The observed differences in groundwater level and discharge before and after logging were well within the accuracy of the measurements and could not be related to the logging event. It takes on average about 60 days for the rainfall on the water-divides to reach the stream channel. Therefore the effects of logging were masked by the delayed seasonal fluctuations. Also, 77% of the catchment is still undisturbed causing the effects of the logging to be absorbed by the surrounding forest. Because the logging took place mainly on areas with a slope angle less than 20%, while the steep slopes remained undisturbed, overland flow did not increase. Analysis of the discharge showed that there was no difference in peakflow of the creek before and after logging. Therefore it can be concluded that a logging intensity of $21 \text{ m}^3 \cdot \text{ha}^{-1}$ has no detectable influence on the catchment water balance. It should be noted that the buffering effect is primarily caused by the high permeability of the Arenosols and Ferralsols and the fact that the groundwater body is far below the surface. Thus these results cannot be extrapolated to a different type of area.

SAMENVATTING

Modellering van de effecten van houtkap op de waterbalans van een tropisch regenwoud, een studie in Guyana

Tropisch regenwouden staan in de belangstelling vanwege de belangrijke economische en ecologische functies die zij vervullen. Het bos is vaak de meest geschikte vorm van landgebruik op de plekken waar het voorkomt. Niettemin is het gebruik van bossen tot nu toe vrijwel altijd roofofbouw. De Stichting Tropenbos richt zich op het definiëren van manieren van bosgebruik die economisch rendabel zijn maar ook ecologisch verantwoord, en laat daartoe onderzoek uitvoeren in verschillende landen. Sinds 1989 wordt in Guyana onderzoek gedaan door de Faculteiten Biologie en Ruimtelijke Wetenschappen van de Universiteit Utrecht.

In Guyana is de bevolkingsdruk op het bos erg laag. Het bos wordt alleen gebruikt voor commerciële selectieve houtkap. Het Tropenbos onderzoekprogramma richt zich dan ook op het functioneren van het ongestoorde ecosysteem zoekt verbanden tussen de mate van verandering en de intensiteit waarmee gekapt wordt. Het onderzoek dat beschreven wordt in dit proefschrift vormt een van de aandachtsvelden binnen het onderzoekprogramma: het richt zich op de gevolgen van een lage intensiteit houtkap op de waterbalans.

Het waterbalans onderzoek vond plaats in en om het "Tropenbos Ecological Reserve" een klein reservaat in noord Guyana. De waterbalans wordt bepaald door het klimaat, en de hydrologische eigenschappen van planten en bodems. Niet alle bos- en bodemtypen konden onderzocht worden. Het onderzoek concentreerde zich op drie wijd verspreide combinaties van bos- en bodemtypen waarin commerciële houtkap uitgevoerd wordt: "Dry Evergreen Forest" op de witte zeer zandige Albic Arenosols (aangeduid met DEF-ARa), "Mixed Forest" op bruine zandig-lemige Ferralic Arenosols (MF-ARo) en "Mixed Forest" op de bruine lemige Haplic Ferralsols (MF-FRh).

De gevolgen van het kappen op de waterbalans werden op twee schaal niveaus onderzocht: op "boom" niveau waarbij alleen naar de verticale (een-dimensionale) waterbalans gekeken werd, en op stroomgebied niveau waarbij ook laterale water stromen onderzocht werden. Hierdoor is deze studie uit vier delen opgebouwd. Als eerste werden de verbanden tussen de ruimtelijke patronen van enerzijds bostypen en anderzijds bodemtypen onderzocht, en tevens werd de ruimtelijke variabiliteit van hydrologische bodemeigenschappen beschreven. Ten tweede werd de verticale waterbalans van het ongestoorde bos gemodelleerd. Ten derde werden de veranderingen in de waterbalans onderzocht op de open plekken in het bos die ontstaan zijn door het kappen. Als laatste werden de gevolgen onderzocht van een lage intensiteit kap op de waterbalans van een klein stroomgebied.

Deze indeling leidde tot de volgende onderzoeksvragen:

- In welke mate worden de ruimtelijke patronen van de bostypen bepaald door de hydrologische eigenschappen van bodems en reliëf?
- Wat is de ruimtelijk variabiliteit van de hydrologische bodemeigenschappen en is het mogelijk deze eigenschappen in kaart te brengen?
- Kunnen met behulp van een waterbalans model de verschillen in waterstromen tussen de bos-bodem combinaties beschreven worden?
- Wat is de invloed van de ruimtelijke variabiliteit van bodem- en plant-eigenschappen op de verticale waterbalans van het bos?
- Hoe groot zijn de laterale waterstromen over het oppervlak en welke processen spelen hierin een rol?
- Wat voor effect heeft het berijden met zware machines op de waterhuishouding in de bodem?
- Hoe verandert de waterbalans op een gekapte open plek ten opzichte van de situatie in ongestoord bos, en hoe ontwikkelt de waterbalans zich in de tijd?
- Wat zijn de gevolgen van het kappen met een lage intensiteit op de waterbalans van een stroomgebied?

Het is belangrijk te weten wat de ruimtelijke verspreiding is van de bos-bodem combinatie waarvoor de waterbalans gemodelleerd werd. De bostypen worden geïnclassificeerd aan de hand van hun soortenamenstelling. Een ruimtelijke analyse van de verspreiding van boomsoorten in een gebied van 480 hectare laat zien dat weliswaar drie belangrijke bostypen onderscheiden kunnen worden, maar dat een verdere verdeling in sub-bostypen ruimtelijk slecht gedefinieerd is. Dat wil zeggen dat blijkt dat, zelfs als een brede classificatie gehanteerd wordt met alleen Dry Evergreen Forest (DEF), Mixed Forest (MF) en "Wet Forest" (WF, bossen langs rivieren en in moerassen), slechts 40% van het gebied tot een van deze typen behoort. De rest van het gebied heeft een soorten samenstelling die een continue overgang vormt tussen de plekken met een "typische" samenstelling. Voorts bleek dat deze continue overgangen sterk gerelateerd zijn aan de textuur van de bodem, en aan een hydrologische gradient van waterscheiding tot dalbodem. Hieruit kan geconcludeerd worden dat in ieder geval op grote schaal de hydrologie een duidelijke rol speelt in de ruimtelijke verspreiding van boomsoorten.

Vrijwel alle hydrologische bodemeigenschappen laten een grote variabiliteit over korte afstand zien. In de Albic Arenosols variëren bulkdichtheid, porositeit en waterdoorlatendheid over een afstand van 200 m. In Ferralic Arenosols en Haplic Ferralsols variëren bijna alle eigenschappen binnen een afstand van 20 m. Hierdoor is het nauwelijks mogelijk deze eigenschappen in kaart te brengen. De beste strategie is om een voldoende grote steekproef te nemen op willekeurige lokaties in alle bodemtypen (zie Brus et al., 1993).

Binnen de bostypen vertonen de hydrologische kenmerken eveneens een grote ruimtelijke variabiliteit. In dit onderzoek werd alleen de variabiliteit van de plantenstructuur in indirecte zin bekeken: met behulp van het meten van de doorval. De interceptie van de beide bostypen (DEF en MF) is niet significant verschillend en ligt tussen de 15% en de 17% op jaarbasis. Niettemin is de spreiding in interceptie

in beide bostypen groot: de doorval varieerde van 0.5 tot 2 keer de neerslag. Een gangbaar model voor het voorspellen van interceptie en doorval, dat de boomkruin beschouwd als een enkele container, werd verbeterd door de kruin te verdelen in een aantal lagen met een opslagcapaciteit die afhangt van de verticale bladverdeling. Hierdoor werd het tevens mogelijk de evapotranspiratie beter te modelleren. Omdat echter de verticale kruinstructuur van de bostypen DEF en MF niet bekend is, werden gegevens van Mixed Forest bij Manaus gebruikt. Ook al waren de model resultaten met deze gegevens acceptabel, er is duidelijk grote behoefte aan het kwantificeren van de kruinstructuur van de verschillende bostypen in het gebied, gezien het belang van de evapotranspiratie voor de waterbalans.

De gemiddelde verticale wortelverdeling van beide bostypen was verschillend. Meer dan 95% van de fijne wortels werd in de bovenste 100 cm van de bodem aangetroffen, maar in DEF bevonden zich meer wortels in de bovenste 20 cm dan in MF. Niettemin werden in profielkuilen op enkele meters diepte nog wortels aangetroffen (Eernisse, 1993). Dit is waarschijnlijk in het geval van Arenosols gerelateerd aan voorkomen van grondwater, en in het geval van Ferralsols aan het voorkomen van een hoger gehalte aan mineralen in de verweringszone.

Teneinde de verticale waterbalans van het ongestoorde bos te modelleren, werden de bovengrondse en ondergrondse plantstructuur, en de hydrologische bodemeigenschappen, gebruikt in het SOil Atmosphere Plant waterbalans model (SOAP). Het model werd getest met behulp van bodemvocht metingen voor twee combinaties: MF-ARo en MF-FRh. Uit de simulaties blijkt dat ondanks de grote variatie in bodemeigenschappen (met verzadigde waterdoorlatendheden van 25 cm/dag tot 6000 cm/dag), de jaarlijkse waterbalans vrijwel gelijk is voor alle bos-bodem combinaties. Ook de temporele variatie is identiek. Deze gelijkensis komt omdat bij alle combinaties de evapotranspiratie de waterbalans in hoge mate bepaald en de bodemeigenschappen hierop nauwelijks invloed uitoefenen. De dagelijkse evapotranspiratie varieert van 1 tot 8 mm terwijl geen duidelijke seizoensvariatie aanwezig is. Door het zandige karakter van de bodems neemt de hydraulische geleidbaarheid sterk af als de bodem uitdroogt. Daardoor duurt het in het droge seizoen ongeveer 5 dagen voordat het vochtfront van een grote regenbui een diepte van 1 meter bereikt, terwijl de respons tijd in het natte seizoen de helft bedraagt. Percolatie onder de wortelzone treed pas op als het de bodem voldoende nat is (veldcapaciteit of hoger). Daardoor vindt 70% van de percolatie in het natte seizoen plaats. Op jaarbasis is de evapotranspiratie 55% en de totale drainage (over het oppervlak en via het grondwater) ongeveer 45% (zie figuur 12.1) voor vrijwel alle bos-bodem combinaties. Uitzonderingen daarop zijn de meest doorlatende Arenosol waar een vochttekort kan optreden met als gevolg een vermindering in verdamping, en de minst doorlatende Ferralsol waar oppervlakkige afstroming plaatsvindt.

Oppervlakkige afstroming treedt alleen op steile hellingen op de minder doorlatende Ferralsols. In het natte seizoen in 1992 werd een percentage oppervlakkige afstroming gemeten dat varieerde van 3% tot 15% voor hellingen van respectievelijk 25% tot 60%. Afstroming trad alleen op wanneer de bodem bijna of geheel verzadigd was (matrix potentiaal hoger dan -10 cm). Vergeleken met afstroming in landbouwgebieden is de oppervlakte weerstand onder bos extreem hoog. Het water

stroomt onder en door de strooisellaag op de bodem. Uit stromingsproeven bleek dat de hoeveelheid afstromend water niet gerelateerd is aan de hellingshoek maar aan de structuur van de strooisellaag. De stroming kan het beste gezien worden als stroming door een poreus medium in plaats van oppervlakkige afstroming met een hoge weerstand. Laterale stroomsnelheden waren het grootst bij een dunne waterlaag waarbij waarschijnlijk alleen de macroporiën in het strooisel gebruikt worden, of bij een dikke waterlaag waarbij het water over het strooisel stroomde. Door de snelheid te relateren aan de duur van de verzadigde omstandigheden in de bovenlaag van de bodem, bleek dat het water over een afstand van 20 m tot 350 m (gemiddeld 80 m) over de helling zou kunnen stromen.

Door selectieve kap ontstaan open plekken in het bos die ernstig verstoord zijn. Door het verwijderen en beschadigen van bomen verandert de waterbalans. Bovendien wordt de bodem gecompacteerd door de zware machines. Dit leidt bij alle bodems tot een vermindering in doorlatendheid. De veranderingen zijn het grootst bij de Albic Arenosols waar de hydraulische geleidbaarheid afneemt tot 10% van de oorspronkelijke waarde bij verzadiging tot 1% bij veldcapaciteit. Tegelijkertijd neemt het vochtvasthoudend vermogen sterk toe, waardoor de gevolgen van compactie voor de groei en ontwikkeling van jonge planten niet duidelijk zijn. De andere bodemtypen veranderen minder sterk. Met name de Ferralsols laten geen significante verschillen zien in bodemeigenschappen voor en na de compactie, ondanks dat men dit wel zou verwachten bij deze lemige bodems. Dit komt waarschijnlijk door de aanwezigheid van zeer sterke microaggregaten als gevolg van ijzeroxides, terwijl er nauwelijks een macro-structuur aanwezig is, en de compactie in eerste instantie nauwelijks invloed heeft. Na verloop van tijd blijken wel veranderingen op te treden: structuurverval en afname in doorlatendheid werden gemeten op lemige Acrisols een jaar na het kappen. Dit is waarschijnlijk het gevolg van een afname van organische stof en bodemfauna.

Het waterbalansmodel werd gevalideerd voor een open plek gemaakt tijdens het kappen, waarvan een deel van de bodem gecompacteerd was. Er werd aangenomen dat de er een lineaire toename was in bladoppervlak door de groei van zaailingen (van 0 naar 1.2 m²/m² in een jaar), wat een toename in verdamping tot gevolg had. Tegelijkertijd speelt bodemverdamping een veel grotere rol dan onder bos. De totale evapotranspiratie is direct na het kappen ongeveer 25% van de neerslag (bestaande uit bodemverdamping) en neemt toe tot 37% (met een afname in bodemverdamping en toename in transpiratie). De evapotranspiratie flux wordt op de open plek veel meer bepaald door het bodemvocht alleen dan onder bos en varieert tussen de 0 en 5 mm/dag. De percolatie neemt direct na het kappen toe van 40% (onder bos) naar 70% van de neerslag, terwijl na een jaar de percolatie nog 60% bedraagt. De toename in percolatie is niet gerelateerd aan een vergroting van de dagelijkse flux, die ongeveer gelijk is aan die onder bos, en die bepaald wordt door de bodemeigenschappen. Door de afwezigheid van transpiratie is de bodem op een open plek echter het hele jaar boven veldcapaciteit, waardoor de percolatie in het droge seizoen doorgaat terwijl hij onder bos stopt. De toename in percolatie door het kappen vindt dus vooral plaats in het droge seizoen. Simulaties van een periode van twee jaar met een toename in bladoppervlak tot 2.7 m²/m² (gebaseerd op een studie in Costa Rica van Parker, 1985), dat de waterbalans zich gedeeltelijk herstelt. Al bij

een toename tot $1.0 \text{ m}^2/\text{m}^2$ is de evapotranspiratie op 75% van het bos. Daarna herstellen de verhoudingen in percolatie/evapotranspiratie zich erg langzaam. Dit duidt aan dat een lichte bedekking met planten al erg stabiliserend werkt.

Een klein stroomgebied van 6.18 hectare, bestaande uit DEF op ARa (80%) en MF op ARo en FRh (20%) werd gekapt met een intensiteit van $21 \text{ m}^3/\text{ha}$. De verstoorde gebieden zijn evenredig verdeeld over het toegankelijke deel van het stroomgebied (de waterscheiding en de toppen van de hellingen). Ongeveer 23% van het gebied werd aangetast door de zware machines, de steile hellingen en de dalbodem bleven ongestoord. Theoretisch zou een toename in percolatie een verhoging van het grondwaterpeil, en hierdoor een toename in afvoer moeten veroorzaken. Deze veranderingen werden echter niet waargenomen. De verschillen voor en na het kappen waren kleiner dan de nauwkeurigheid van de waarnemingen die over het algemeen wordt aangenomen bij dit soort experimenten. Het duurt ongeveer 60 dagen voordat de neerslag die op de waterscheiding valt, als afvoer het gebied verlaat. Hierdoor werden de effecten van het kappen gemaskeerd door de vertraagde seizoensfluctuaties. Ook omdat driekwart van het gebied nog ongestoord was, werden de eventuele veranderingen op de open plekken gebufferd door het omringende bos. Omdat de steile hellingen niet gekapt werden was er geen toename in oppervlakkige afstroming en piekafvoer in de beek. Hieruit blijkt dat een intensiteit van $21 \text{ m}^3/\text{ha}$ geen meetbare invloed heeft op de waterbalans van het stroomgebied. Dit wordt deels veroorzaakt doordat de bodems zeer doorlatend zijn en de grondwaterspiegel zich ver beneden het oppervlak bevindt. Daardoor kunnen deze resultaten niet geëxtrapoleerd worden naar een ander type gebied.

REFERENCES

- Abrahams D.A., Parsons A.J. and Hirsch, P.J. (1992). Field and laboratory studies of resistance to interrill overland flow on semi-arid hillslopes, southern Arizona. pp 1-24 in: Overland Flow, Hydraulics and Erosion Mechanics, eds. A.J. Parsons and D.A. Abrahams. Chapman and Hall, New York.
- Ahmad, N. (1989). Acid sandy soils of the tropics with particular reference to the Guyanas. in: Farming systems for low fertility acid sandy soils, CARDI conference Georgetown 1988, ed D. Walmsley. CTA, Ede-wageningen, The Netherlands.
- Allen, L.H. and Lemon, E.R. (1976). Carbon dioxide exchange and turbulence in a Costa Rican tropical rain forest. pp265-308 in: Vegetation and the Atmosphere Vol 2, ed J.L. Monteith. Academic Press, London.
- Allen, L.H., Lemon, E.R. and Müller, L. (1976). Carbon dioxide exchange and turbulence in a Costa Rican tropical rain forest. *Ecology* 53: 102-111.
- Barron, C.N. (1986). The geological map of Guyana. Guyana Geology and Mines Commission, Georgetown.
- Basnet, K. (1992). Effect of topography on the pattern of trees in Tabonuco (*Dacryodes excelsa*) dominated rain forest in Puerto Rico. *Biotropica* 24(1): 31-42.
- Beasley, D.B., Huggins, L.F. and Monke, E.J. (1980). AMSWERS: a model for watershed planning. American Society of Agricultural Engineers, Transactions of ASAE Vol.23, no. 4, 938-944.
- Belbin, L. and McDonald, C. (1993). Comparing three classification strategies for use in ecology. *Journal of Vegetation Science* 4: 341-348.
- Beusekom, C.F. van, Goor, C.P. van, Schmidt, P. (1987). Tropenbos: wise utilization of tropical rain forest lands. Tropenbos Scientific Series 1.
- Bezdek, J.C. (1981). Pattern recognition with Fuzzy Objective Function Algorithms. Plenum Press NY.
- Bonell, M., Gilmour, D.A. and Sinclair, D.F. (1981). Soil hydraulic properties and their effect on surface and subsurface water transfer in a tropical rain forest catchment. *Hydrological Sciences Bulletin* 26(1)/3: 1-18.
- Bonell, M., Cassels, D.S. and Gilmour, D.A. (1982). Vertical and lateral soil water movement in a tropical rain forest catchment. The 1st nat. symp. on Forest Hydrology, Melbourne: 30-38.
- Bonell, M., Gilmour, D.A., Cassels, D.S. (1983). Runoff generation in tropical rainforests of northeast Queensland, Australia, and the implications for land use management. Hydrology of the humid tropical regions with particular reference to the hydrological effects of agriculture and forestry practice. Proceedings of the Hamburg symposium, IAHS 140.
- Bouten, W. (1992). Monitoring and modelling forest hydrological processes in support of acidification research. PhD thesis, Laboratory of Physical Geography and Soil Science, University of Amsterdam, The Netherlands.
- Brinkman, R. (1979). Ferolysis: a soil forming process in hydromorphic conditions. PhD thesis Agricultural University Wageningen, The Netherlands.
- Brinkman, W.L.F. (1989). Hydrology. Chapter 5 in: Tropical rainforest ecosystems, biogeographical and ecological studies, eds H. Lieth and M.J.A. Werger. Ecosystems of the world 14B. Elsevier, Amsterdam, The Netherlands.
- Brunschot, J.van and De Lange, K. (1992). The impact of selective logging on the micro climate and the nutrient balance in two gaps of different size in tropical rain forest in Guyana. MSc thesis, Dept. of Physical Geography, University of Utrecht, Tropenbos internal report.
- Bruijnzeel, L.A. (1983). Hydrological and biochemical aspects of manmade forests in South-central Java, Indonesia. PhD thesis, Faculty of Earth Sciences, Free University, Amsterdam, The Netherlands.
- Bruijnzeel, L.A. (1989). Nutrient cycling in moist tropical forests: the hydrological framework. pp383-415, in: Mineral nutrients in tropical forest and savannah ecosystems. ed. J. Proctor. Blackwell Scientific Press., Oxford.
- Bruijnzeel, L.A. Wiersum, K.F. (1987). Rainfall interception by young acacia auriculiformis (A.Cunn) plantation forest in West Java (Indonesia): application of Gash's analytical model. *Hydrological Processes* 1: 309-317.

- Bruijnzeel, L.A. (1990). Hydrology of moist tropical forests and effects of conversion: a state of knowledge review. Faculty of Earth Sciences, Free University, Amsterdam, The Netherlands.
- Brus, D.J. (1993). Incorporating models of spatial variation in sampling strategies for soil. PhD thesis, DLO Staring Centre, Agricultural University of Wageningen, The Netherlands.
- Burrough, P.A. (1986). Principles of Geographical Information Systems for natural resource analysis, Oxford University Press, Oxford.
- Burrough, P.A. (1989) Fuzzy mathematical methods for soil survey and land evaluation, *Journal of Soil Science* **40**: 477-492.
- Burrough, P.A., MacMillan, R.A. and Deursen, W. van (1992). Fuzzy classification methods for determining land suitability from soil profile observations and topography. *Journal of Soil Science* **43**: 193-210.
- Burrough, P.A., Brown, L. and Morris, E.C. (1977). Variations in vegetation and soil pattern across the Hawkesbury Sandstone Plateau from Barren Grounds to Fitzroy Falls, N.S.W. *Australian Journal of Ecology* **2**: 137-159.
- Campbell, G.S. (1988). Soil Physics with Basic, transport models for soil-plant systems. *Developments in Soil Science* 14, Elsevier Science Publ., New York.
- Chow, V.T., Maidment, D.R. and Mays, L.W. (1988). *Applied Hydrology*. McGraw-Hill, London.
- Daniel, J.R.K. and Hons, B.A. (1984). Geomorphology of Guyana, an integrated study of natural environments. Occasional Paper no. 6. Dept. of Geography, University of Guyana, Georgetown.
- Davis, J.C. (1986). Statistical and data analysis in geology. John Wiley and Sons inc., New York.
- De Roo, A.P.J., Wesseling, C.G., Cremers, N.H.D.T., Offermans, R.J.E., Ritsema, C.J., Oostindie, K. van (1994). LISM: A physically based hydrological and soil erosion model incorporated in a GIS. Proceedings of the European Conference on GIS, EGIS, Paris.
- De Roo, A.P.J. (1992). Modelling surface runoff and soil erosion in catchments using Geographical Information Systems. PhD thesis, Faculty of Geographical Sciences, University of Utrecht. *Netherlands Geographical Studies* 157.
- DeWalle, D.R. and Paulsell, L.K. (1969). Canopy interception, stemflow and streamflow on a small drainage in the Missouri Ozarks. *Research Bulletin University of Missouri - Columbia College of Agriculture*, **951**.
- Dias, A.C.C.P. and Nortcliff, S. (1985). Effects of tractor passes on the physical properties of an Oxisol in the Brazilian Amazon. *Tropical Agriculture Trinidad* **62**(2): 137-142.
- Diekkrüger, B. (1992). Standort- und Gebietsmodelle zur Simulation der Wasserbewegung in Agrarökosystemen. *Landschaftsökologie und Umweltforschung*, Vol. 19. PhD thesis, Technical University Braunschweig, Germany.
- Dolman, A.J. 1987, Predicting evapotranspiration from an oak forest. Dissertation, Groningen University.
- Draaiers, G. (1993). The variability of atmospheric deposition to forests, the effects of canopy structure and forest edges. PhD thesis, Faculty of Geographical Sciences, University of Utrecht. *Netherlands Geographical Studies* 156.
- Driessen, P.M. and Dudal, R. (1989). Lecture notes on the geography, formation, properties and use of the Major Soils of the world. Agricultural University Wageningen and Katholieke Universiteit Leuven, ISRIC Wageningen, The Netherlands.
- Dunne, T. and Leopold, L.B. (1972). *Water in environmental planning*. W.H. Freeman, New York.
- Eernisse, N. (1991). A soil hydrological study of the Mabura Hill area, Guyana. Tropenbos internal report.
- Emmett, W.W. (1970). The hydraulics of overland flow on hillslopes. Dynamic and descriptive studies of hillslopes. Geological survey professional paper 662-A
- FAO (1966). Report on the soil survey project of British Guyana - Volume III Reconnaissance soil survey, FAO nr. MR/28627 Rome.
- FAO (1977). Guidelines for soil description.
- FAO/UNESCO (1988). Soil map of the world. Revised legend. World soil resources report 60, Rome.
- Feddes, R.A. Kabat, P., Bakel, P.J.T. van, Bronswijk, J.J.B. and Halbertsma, J. (1988). Modelling soil water dynamics in the unsaturated zone - state of the art. *Journal of Hydrology* **100**: 69-111.
- Feddes, R.A., Kowalik, P.J. and Zaradny, H. (1978). Simulation of field water use and crop yield. Pudoc, Wageningen, The Netherlands.

- Ford, E.D. and Deans, J.D. (1978). The effects of canopy structure on stemflow, throughfall and interception loss in a young Sitka spruce plantation, *Journal of Applied Ecology* **15**: 905-917.
- Fritsch, J.M. (1990). Les effets du defrichement de la foret Amazonienne et de la mise en culture sur l'hydrologie de petits bassins versants. Operation ECEREX en Guyane Fracaise. PhD thesis, Univerité de Montpellier.
- Gaans, P.F.M. van and Burrough, P.A. (1993). The use of fuzzy logic and continuous classification in GIS applications: a review. EGIS conference 1993.
- Gash, J.H.C. (1979). An analytical model of rainfall interception of forests. *Quarterly Journal of the Royal Meteorological Society* **105**: 43-55.
- Gash, J.H.C. and Morton, A.J. (1978). An application of the Rutter model to the estimation of the interception loss from Thetford forest. *Journal of Hydrology* **38**: 49-58.
- Gash, J.H.C., Wright, I.R. and Lloyd, C.R. (1980). Comparative estimates of interception loss from three coniferous forests in Great Britain. *Journal of Hydrology* **48**: 89-105.
- Genuchten, M.Th van (1980). A closed form equation for predicting the hydraulic conductivity of unsaturated soils. *Soil Science Society of America Journal* **44**: 892-898.
- Genuchten, M.Th van (1987). A numerical model for water and solute movement in and below the root zone. Research report 121, USDA, Agricultural research service, US salinity laboratory, Riverside, California, USA.
- Germann, P.F. and Beven, K.J. (1981). Water flow in soil macropores: I. an experimental approach. *Journal of soil science* **32**: 1-13.
- Germann, P.F. (1986). Rapid drainage respons to precipitation. *Hydrologiual processes* **1**: 3-13.
- Gilley, J.E. Flanagan, D.C., Kottwitz, E.R. and Weltz, M.A. (1992). Darcy-Weisbach roughness coefficients for overland flow. pp 25-52 in: *Overland Flow, Hydraulics and Erosion Mechanics*, eds. A.J. Parsons and D.A. Abrahams. Chapman and Hall, New York.
- Goudriaan, J. (1977). Crop micrometeorology: a simulation study, *Simulation Monographs series*, Pudoc, Wageningen, The Netherlands.
- Groenewoud, H. (1992). The robustness of Correspondence, Detrended Correspondence and TWIN-SPAN analysis. *Journal of Vegetation Science* **3**, 239-246.
- Gruijter, J.J. de and McBratney, A.B. (1988). A modified fuzzy k-means method for predictive classification. pp 97-104 in: *Classification and related methods of data analysis*, ed. H.H. Bock, Elsevier.
- Gruijter, J.J. and ter Braak, C.J.F. (1990). Model free estimation from spatial samples: a reappraisal of classical sampling theory. *Mathematical Geology* **22**: 407-415.
- Hatheway, W.H. (1967)., Contingency table analysis of rain forest vegetation. In *Statistical Ecology, Volume 3: Populations, Ecosystems, and Systems Analysis*.
- Hendrickx, J.M.H. (1990). Determination of hydraulic soil properties. Chapter 3 in *Process studies in hillslope hydrology*, eds. Anderson, M.G. and Burt, T.P., Wiley & Sons, NY.
- Henrison, J. (1990). Damage-controlled logging in managed tropical rain forests in Surinam. PhD thesis, Agricultural University Wageningen, The Netherlands.
- Herwitz, S.R. (1985). Interception storage and capacities of tropical rainforest canopy trees. *Journal of Hydrology* **77**: 237-252.
- Heuvelink, G.B.M. (1993). Error propagation in quantitative spatial modelling, applications in GIS. PhD thesis, Faculty of Geographical Sciences, University of Utrecht. Netherlands Geographical Studies 163.
- Hill, M.O. (1979). DECORANA. A FORTRAN program for detrended correspondence analysis and reciprocal averaging. *Ecology and Sytematics*, Cornell University, Ithaca, New York.
- Hill, M.O. (1979). TWINSPLAN. A FORTRAN program for arranging multivariate data in an ordered two-way table by classification of the individuals and attributes. *Ecology and Sytematics*, Cornell University, Ithaca, New York.
- Hsia, Y.J and Koh, C.C. (1983). Water yield resulting from clearcutting a small hardwood basin in central Taiwan. *Hydrology of the humid tropical regions with particular reference to the hydrological effects of agriculture and forestry practice. Proceedings of the hamburg symposium*, IAHS 140.
- Isaaks, E.H. and Srivastava, R.M. (1989). *Applied Geostatistics*, Oxford University Press, Oxford
- Jackson, I.J. (1971), Problems of throughfall and interception assessment under tropical forest. *Journal of Hydrology* **12**: 234-254.

- Jackson, I.J. (1975). Relationships between rainfall parameters and interception by tropical forest. *Journal of Hydrology* 24: 215-238.
- Jetten, V.G., Riezebos, H.Th., Hoefsloot, F., and Van Rossum, J. (1993). Spatial Variation of Infiltration and related properties of tropical soils, *Earth Surface Processes and Landforms*, Vol 18.
- Jongman, R.H.G., Ter Braak, C.J.F. and Van Tongeren, O.F.R. (1987). *Data analysis in community and landscape ecology*, Pudoc Wageningen, The Netherlands.
- Jordan, C.F. and Heuvelink, J. (1981). The water budget of an Amazonian rain forest. *Acta Amazonica* 11(1): 87-92.
- Jordan, C.F. and Kline, J.R. (1977). Transpiration of trees in a tropical rain forest. *Journal of Applied Ecology* 14: 853-860.
- Journel, A.J. and Huijbregts, C.J. (1978). *Mining geostatistics*. Academic Press, London.
- Kamaruzaman, J. (1991). Effect of tracked and rubber-tyred logging machines on soil physical properties of the Berkelah Forest Reserve, Malaysia. *Pertanika* 14(3): 265-276.
- Keulen, H. van and Wolf, J. (1986). *Modelling of agricultural production: weather, soils and crops*. Pudoc Wageningen, The Netherlands.
- Khan, Z., Paul S., and Cummings, D. (1980). Mabura Hill, Upper Demerara Forestry Project. Soils Investigation report No.1, NARI, Mon Repos, Guyana.
- Khan, Z. and Jetten, V.G. (1993). A GIS based soil inventory of the Tropenbos Ecological Reserve, Mabura Hill. NARI/CARDI conference 1991, NARI Mon Repos, Guyana.
- Kekem, A.J. van (1993). Report of the second technical backstopping mission on land resources inventory for the Tropenbos programme, Guyana. Internal activities report 30, Staring Centre, Wageningen, The Netherlands.
- Kira, T. and Yoda, K. (1989). Vertical stratification in microclimate. Chapter 5 in: *Tropical rainforest ecosystems, structure and function*, ed F.B. Golley. *Ecosystems of the world 14B*. Elsevier, Amsterdam, The Netherlands.
- Klinge, H., Rodriugues, W.A., Brunig, E. and Fittkau, E.E. (1975). Biomass and structure in the central Amazonian rain forest. *Ecological Studies 11: Tropical Ecological Systems*. Eds. F. Golley and E. Medina.
- Lesack, L.F.W. (1993). Water balance and hydrologic characteristics of a rain forest catchment in the Central Amazon Basin. *Water Resources Research* 29(3): 759-773.
- Lima, J.L.M.P. de (1989). Overland flow under rainfall: some aspects related to modelling and conditioning factors. PhD thesis, Dept. of Hydrology, Agricultural University Wageningen, The Netherlands.
- Lloyd, C.R., Gash, J.H.C., Shuttleworth, W.J. and Marques F, A. de O. (1988). The measurement and modelling of rainfall interception by Amazonian rainforest. *Agricultural and Forest meteorology*: 43: 277-294.
- Lloyd, C.R. and Marques F, A. de O. (1988). Spatial variability of throughfall and stemflow measurements in Amazonian rainforest. *Agricultural and Forest meteorology* 42: 63-73.
- Luning, H.A. (1987). The need for tropical rain forests and their products. Chapter 2 in: *Tropenbos: wise utilization of tropical rain forest lands*. Tropenbos Scientific Series 1.
- Malmer, A. (1993). Dynamics of hydrology and nutrient losses as response to establishment of forest plantation, A case study on tropical rain forest land in Sabah, Malaysia. PhD thesis, Dept. of Forest Ecology, Swedish University of Agricultural Sciences, Umeå, Sweden.
- Marshall, A.G. and Swaine, M.D. (eds) (1992). *Tropical rain forest: disturbance and recovery*. Proc. of a Royal Society Discussion Meeting on September 1991. Royal Society, London.
- Massman, W.J. (1983). The derivation and validation of a new model for the interception of rainfall by forests. *Agricultural Meteorology* 28: 261-286.
- McBratney, A.B. and Gruijter, J.J. de (1992). A continuum approach to soil classification by modified fuzzy k-means with extragrades. *Journal of Soil Science* 43: 159-176.
- McWilliam, A.L.C., Roberts, J.M., Cabral, O.M., Leitao, M.V., Costa, A.C. de, Zamparoni, C.A. (1993). Leaf area index and above-ground biomass of terra firme forest and adjacent clearings in Amazonia. *Functional Ecology* 7: 310-317.
- Medina, E. (1983). Adaptions of tropical trees to moisture stress. Chapter 14 in: *Tropical rainforest ecosystems, structure and function*, ed F.B. Golley. *Ecosystems of the world 14B*. Elsevier, Amsterdam, The Netherlands.

- Molz, F.J. (1981). Models of water transport in the soil-plant system: a review. *Water Resources Research* 17(5): 1245-1260.
- Moore, I.D. and Larson, C.L. (1979). Estimating micro-relief surface storage from point data. *Transactions of ASAE* 20:1073-1077.
- Moraczewski, I.R. (1993). Fuzzy logic for Phytosociology: I. Syntaxa as vague concepts. *Vegetatio* 106, 1-11.
- Mualem, Y. (1976). A new model for predicting the hydraulic conductivity of unsaturated porous media. *Water Resources Research* 12(3): 513-522.
- Murphy, C.E. and Knoerr, K.R. (1975). The evaporation of intercepted rainfall from a forest stand: analysis by simulation. *Water Resources Research*, 11(2): 273-280.
- Neuman, S.P., Feddes, R.A. and Bresler, E. (1974). Finite Element simulation of flow in saturated-unsaturated soils considering water uptake by plants. Development of methods, tools and solutions for unsaturated flow, 3rd annual report (part 1). Israel Institute of Technology.
- Noij, I.G.A.M., Janssen B.H., Wesseling, I.G. and Van Grinsven, J.J.M. (1993). Modelling nutrient and moisture cycling in tropical forests. Tropenbos series 4.
- Northcliff, S. and Thornes, J.B. (1981). Seasonal variations in the hydrology of a small forested catchment near Manaus, Amazonas, and the implications for its management. pp 37-57 in: *Tropical Agricultural Hydrology*, eds. R., Lal and E.W. Russell. John Wiley and Sons, New York.
- Odeh, I.O.A., McBratney, A.B. and Chittleborough, D.J. (1990). Design of optimal sampling spacings for mapping soil using fuzzy k-means and regional variable theory. *Geoderma* 47: 93-122.
- Odeh, I.O.A., McBratney, A.B. and Chittleborough, D.J. (1992a). Soil pattern recognition with fuzzy c-means: application to classification and soil landform interrelationships. *Soil Science Society of America Journal* 56: 505-516.
- Oldeman, R.A.A. (1987). Tropical forest: the ecosystems. Chapter 4 in: *Tropenbos: wise utilization of tropical rain forest lands*. Tropenbos Scientific Series 1.
- Oliver, M.A. and Webster, R. (1986). Combining nested and linear sampling for determining the scale and form of spatial variation of regionalized variables. *Geographical Analysis* 18(3): 227-242.
- Parker, G.G. (1985). The effects of disturbance on water and solute budgets of hillslope tropical rainforest in northeastern Costa Rica. PhD thesis. University of Georgia, Athens, Georgia, USA.
- Pearce, A.J., Rowe, L.K. and Stewart, J.B. (1980). Nighttime, wet canopy evaporation rates and the water balance of an evergreen mixed forest. *Water Resources Research* 16(5): 955-959.
- Pearce, A.J. and Rowe, L.K. (1982). Rainfall interception in a multistoried evergreen mixed forest: estimates using Gash's analytical model. *Journal of Hydrology* 49: 341-353.
- Pearcy, R.W., Ehleringer, J., Mooney, H.A. and Rundil, P.W. (1989). *Plant physiological ecology: field methods and instrumentation*. Chapman and Hall, New York.
- Pinder, G.F. and Gray, W.G. (1977). *Finite Element simulation in surface and subsurface hydrology*. Academic Press, New York.
- Pinker, R.T., Thompson, O.E. and Eck, T.F. (1980). The albedo of tropical evergreen forest. *Quarterly Journal of the Royal Meteorological Society* 106: 551-558.
- Plas, M.C. van der and Bruijnzeel, L.A. (1993). Impact of mechanized selective logging of rainforest on topsoil infiltrability in the Upper Segama area, Sabah, Malaysia. *Hydrology of warm humid regions*, Proceedings of the Yokohama symp. 1993, IAHS 216.
- Poels, R. (1987). Soils, water and nutrients in a forest ecosystem in Suriname. PhD thesis, Agricultural University Wageningen, The Netherlands.
- Pook, P.H., Moore, P.H.R. and Hall, T. (1991) Rainfall Interception by Trees of *Pinus radiata* and *Eucalyptus viminalis* in a 1300 mm Rainfall Area of Southeastern New South Wales: I. Gross Losses and their Variability. *Hydrological Processes*, 5(2), 127-141.
- Pook, P.H., Moore, P.H.R. and Hall, T. 1991, 'Rainfall Interception by Trees of *Pinus radiata* and *Eucalyptus viminalis* in a 1300 mm Rainfall Area of Southeastern New South Wales: II. Influence of Wind Borne Precipitation. *Hydrological Processes* 5(2): 142-155.
- Prinsen, H.A.M. and Straatsma, J. (1992). Decomposition of leaf litter and other tropical rain forests in Guyana. MSc thesis, Dept. of Physical Geography, University of Utrecht. Tropenbos internal report.

- Proctor, J. (1987). Nutrient cycling in primary and old secondary rain forests. *Applied Geography* 7: 135-152.
- Riha, S.J. (1993). GAPS - A general all purpose simulator for the soil-plant-atmosphere system. Dept. of Soil, Crop and Atmospheric Sciences, Cornell University, Ithaca, USA.
- Richter, J. (1990). Models for processes in the soil, programs and exercises. Catena Verlag, Germany.
- Riezebos, H.Th. (1989). Application of nested analysis of variance in mapping procedures for land evaluation. *Soil use and management* 5: 25-30.
- Riezebos, H.Th. (1983). Geomorphology, soils and vegetation differentiation in a tropical rain forest environment in Suriname. *Geologie en Mijnbouw* 62: 669-675.
- Riezebos, H.Th. (1979). Geomorphology and savannisation in the Upper Sipalawini River basin (S. Suriname). *Zetschrift fur Geomorphologie* 28(3): 265-284.
- Roberts, J., Cabral, O.M.R. and Aguiar, L.F. de (1990). Stomatal and boundary-layer conductances in an Amazonian Terra Firme rain forest. *Journal of Applied Ecology* 27: 336-353.
- Roberts, J., Cabral, O.M.R., Fisch, G. Molion, L.C.B., Moore, C.J. and Shuttleworth, W.J. (1993). Transpiration from an Amazonian rain forest calculated from stomatal conductance measurements. *Agricultural and Forest Meteorology*, in press.
- Rompaaij, R. van (1993). Forests of SE Liberia and SW Cote d'Ivoire. PhD thesis Agricultural University Wageningen, The Netherlands.
- Ross, J. (1976). Radiative transfer in plant communities. Chapter 2 in *Vegetation and the atmosphere*, vol I. ed J.L. Monteith. Academic Press, London.
- Rotmans, A. (1993). Overland flow under natural tropical rain forest. MSc thesis, Dept. of Physical Geography, University of Utrecht. Tropenbos internal report.
- Rutter, A.J., Kershaw, K.A., Robins, P.C. and Morton, J. (1971). A predictive model of rainfall interception in forests: I. Derivation of the model from observations in a plantation of Corsican pine. *Agricultural Meteorology* 9: 367-384.
- Rutter, A.J., Morton, A.J. and Robins, P.C. (1975). A predictive model of rainfall interception in forests: II. Generalization of the model and comparison with observations in some coniferous and hardwood stands. *Journal of Applied Ecology* 12: 367-380.
- Rutter, A. and Morton, A.J. (1977). A predictive model of rainfall interception in forests: III. Sensitivity of the model to stand parameters and meteorological variables. *Journal of Applied Ecology* 14: 567-588.
- Rutter, A.J. (1976). The hydrological cycle in vegetation. Chapter 4 in: *Vegetation and the Atmosphere*, Vol. I ed J.L. Monteith, Academic Press, London.
- Shuttleworth, W.J., Gash, J.H.C., Lloyd, C.R., Moore, C.J., Roberts, J., Marques, F.A.O. de, Fisch, G., Filho, V.P.S. de, Ribeiro, M.N.G. de, Molion, L.C.B., Abreu Sa, L.D. de, Nobre, J.C.A., Cabral, O.M.R., Patel, S.R., Moraes, J.C. de (1984). Eddy correlation measurements of energy partition for Amazonian forest. *Quarterly Journal of the Royal Meteorological Society* 110: 1163-1169.
- Shuttleworth, W.J. (1984). Observations of radiation exchange above and below Amazonian forest. *Quarterly Journal of the Royal Meteorological Society* 110: 1143-1162.
- Sellers, P.J. and Lockwood, J.G. (1981). A computer simulation of the effects of differing crop types on the water balance of small catchments over long time periods. *Quarterly Journal of the Royal Meteorological Society* 107: 395-414.
- Singh, B and Szeicz, G. (1979). The effect of intercepted rainfall on the water balance of a hardwood forest. *Water Resources Research* 15(1): 131-138.
- Slack, D.C. and Larson, C.L. (1981). Modelling infiltration: the key process in water management, runoff and erosion. pp 434-450 in: *Tropical Agricultural hydrology*, eds R.Lal and E.W. Russell. John Wiley and Sons, New York.
- Spaans, E.J.A., Baltissen, G.A.M, Bouma, J., Miedema, R. and Lansu, A.L.E. (1989). Changes in physical properties of young and old volcanic surface soils in Costa Rica after clearing of Tropical rain forest. *Hydrological Processes* 3: 383-392.
- Stoorvogel, J.J. (1994). Gross inputs and outputs of nutrients in undisturbed forest Taï region, Côte d'Ivoire. Tropenbos Scientific series 5. The Tropenbos Foundation, Wageningen, The Netherlands.
- Sánchez, P.A. (1976). Properties and management of soils in the tropics. Wiley, New York.

- Ter Steege, H. (1994). HEMIPHOT: a programme to analyze vegetation Indices, light and light quality from hemispherical photographs. Tropenbos Documents 3. The Tropenbos Foundation, Wageningen, The Netherlands.
- Ter Steege, H., Jetten, V., Polak, M. and Werger, M. 1993, 'Tropical rainforest types and soils of a watershed in Guyana, South America. *Journal of Vegetation Science* 4: 705-716.
- Ter Steege, H. ter (1993). Patterns in Tropical Rain Forest in Guyana. PhD thesis, Faculty of Biology, Utrecht University. Tropenbos Series 3, Tropenbos Foundation, Wageningen, The Netherlands.
- Ter Steege, H. and Persaud, C.A. (1991). The phenology of Guyanese timber species: a compilation of a century of observations. *Vegetatio* 95: 177-198.
- Thom, A.S. (1976). Momentum, mass and heat exchange of plant communities. Chapter 3 in: *Vegetation and the Atmosphere*, Vol 1, ed J.L. Monteith, Academic Press London.
- Triantafyllis, J. and McBratney, A.B. (1993). Application of continuous methods of soil classification and land suitability assessment in the lower Namoi Valley. Dept. of Agricultural Chemistry and Soil Science, University of Sidney, Australia.
- Tropenbos (1990). Annual Report 1990. The Tropenbos Foundation, Wageningen, The Netherlands.
- Vriend, S.P. and Gaans, P.F.M. van (1984). FUZNLM, A programme for fuzzy c-means clustering and non linear mapping. Modified from a program by Bezdek, J.C., Erlich, R. and Full, W.. Dept. of Physical Geography, University of Utrecht.
- Vriend, S.P., Gaans, P.F.M. van, Middelburg, J. and Nijs, A. de (1988). The application of fuzzy c-means clustering analysis and non-linear mapping to geochemical datasets: examples from Portugal. *Applied Geochemistry*, Vol 3, 213-224.
- Weert, R. van der (1974). Influence of mechanical clearing on soil moisture conditions and the resulting effects on root growth. *Tropical Agriculture trinidad* 51(2):325-331.
- Webster, R. and Oliver, M.A. (1990). Statistical methods in soil and land resource survey, Spatial information systems, Oxford University Press, Oxford.
- Wesseling, C., Deursen W. van, and Pebesma, E.J. (1993). PCRASTER. Dept. of Physical Geography, University of Utrecht, The Netherlands.
- Williams, W.T., Lance, G.N., Webb, L.J., Tracey, J.G. and Connel, J.H. (1986). Studies in the numerical analysis of complex rain-forest communities: IV. Method for the elucidation of small-scale forest pattern. CSIRO, Australia.
- Walker, J., Bullen, F. and Williams, B.G. (1993). Ecohydrological changes in the Murray-Darling Basin. I. The number of trees cleared over two centuries. *Journal of Applied Ecology* 30, 265-273.
- Ward, R.C. and Robinson, M. (1990). Principles of hydrology. McGraw-Hill, London.
- Werger, M.J.A. (1992). De aantasting van het tropisch regenwoud. In: *Tropisch regenwoud. Schatkamer van biodiversiteit*, eds. M.S. Hoogmoed and R. de Jong, Nationaal Natuurhistorisch Museum Leiden, The Netherlands.
- Whitmore, T.C. (1990). Introduction to tropical rain forests. Clarendon Press, Oxford.
- Wilson, G.V., Jardine, P.M., Luxmoore, R.J. and Jones, J.R. (1990). Hydrology of a forested hillslope during storm events. *Geoderma* 46: 119-138.
- IJssel, W.J. and Sombroek, W.G. (1987). Spatial variability of tropical forests and forest lands. Chapter 5 in: *Tropenbos: wise utilization of tropical rain forest lands*. Tropenbos Scientific Series 1.
- Zadeh, L.A. (1965). Fuzzy sets. *Information and control* 8: 338-353.

CURRICULUM VITAE

Victor Jetten werd geboren op 10 januari 1962 te Veghel. In 1980 behaalde hij zijn OVWO diploma aan het Kruissheren Kollege te Uden. Een jaar later begon hij zijn studie Fysische Geografie aan de Universiteit Utrecht. Tijdens zijn studie volgde hij de bijvakken Bodemkunde aan de Universiteit Utrecht en Irrigatie Techniek aan de Landbouw Universiteit van Wageningen. Voor zijn doctoraalscriptie onderzocht hij de landgeschiktheid voor extensieve akkerbouw en veeteelt in zuid Botswana (Afrika), gebruik makend van Geografische Informatie Systemen (GIS) en modellering van de stikstofbalans voor de voorspelling van grasproductie. Tevens assisteerde hij de lokale overheid met het in kaart brengen van waterbronnen en de dorpsontwikkeling.

In Augustus 1988 begon hij als toegevoegd onderzoeker bij de vakgroep Fysische Geografie en voerde opdrachten uit voor verschillende ingenieursburo's. Tijdens het eerste jaar onderzocht hij in opdracht van Rijkswaterstaat de mogelijkheden van het gebruik van remote sensing en GIS voor waterkwaliteitsbeheer van het IJsselmeergebied. Tevens verzorgde hij inleidende cursussen GIS voor buitenlandse gasten. Sinds September 1989 werkt hij in opdracht van de Stichting Tropenbos aan het onderzoek dat leidde tot dit proefschrift.